Chapter 3
Thermal Evaluation

TABLE OF CONTENTS

LIST OF TABLES

LIST OF FIGURES

Chapter 3
Thermal Evaluation

NOTE: References in this Chapter are shown as [1], [2], etc. and refer to the reference list in Section 3.5.

This chapter presents the thermal evaluations which demonstrate that the TN-LC transport cask meets thermal requirements of 10CFR71 [1] for transportation of commercial or research reactor spent fuel as described in Chapter 1, Section 1.2.2. The thermal analysis of the TN-LC package considers transportation within and without an ISO container to evalaue the worst conditions during NCT and HAC.

The maximum heat load per shipment allowed for transportation in TN-LC transport cask varies for the different basket types from 0.39 kW to 3.0 kW. The table below summarizes the maximum heat load per shipment for transportation.

FA Types and Decay Heat Loads for NCT

FA Type	Heat Load (kW)	Heat Load (Btu/hr)
PWR	3.00	10237
BWR	2.00	6825
MTR	1.50	5118
TRIGA	1.50	5118
NRU/NRX	0.39	1331
PWR/BWR/EPR/MOX Fuel Pins	3.00	10237

Thermal performance of the TN-LC transport cask is evaluated based on finite element analyses using ANSYS computer code [9].

This evaluation demonstrates that packaging component temperatures are within material temperature limits and fuel cladding temperatures meet the thermal requirements of ISG-11 [2], where applicable.

3.1 Description of Thermal Design Criteria

The TN-LC transport cask is designed to passively reject decay heat under Normal Conditions of Transport (NCT) and Hypothetical Accident Conditions (HAC) while maintaining packaging temperatures and pressures within specified limits. Objectives of the thermal analyses performed for this evaluation include:

(a) Determination of maximum component temperatures with respect to cask materials limits to ensure components perform their intended safety functions,

(b) Determination of temperature distributions to support the calculation of thermal stresses,

(c) Determination of the cask cavity gas temperature to support containment pressure calculations, and

(d) Determination of the maximum fuel cladding temperature.

Chapter 1 presents the principal design bases for the TN-LC transport cask.

Several thermal design criteria are established for the TN-LC transport cask to ensure that the package meets all its functional and safety requirements. These are:

- Maximum fuel cladding temperature limits of 752°F (400°C) for NCT and 1,058°F (570°C) for HAC are considered for the LWR fuel assemblies and pins with an inert cover gas as concluded in ISG-11 [2].

- For research reactor fuel assemblies with aluminum cladding loaded in the TN-LC-NRUX/MTR/TRIGA basket, the cladding temperature shall not exceed 204°C (400°F) during NCT. This criterion is considered conservative to ensure the integrity of the aluminum cladding for NCT. The lowest melting point of aluminum alloys 1100 and 6063 (1140°F [5]) is considered as the cladding temperature limit for research reactor fuels.

- Containment of radioactive material and gases is a major design requirement. Seal temperatures must be maintained within specified limits to satisfy the leak-tight containment requirement. A maximum steady state temperature limit of 400°F (204°C) and 482°F (250°C) for short-term exposure for the Fluorocarbon seals in the containment vessel ([6] and [7]) for NCT and HAC are used. A study in [28] shows that the floruocarbon seals are leak tight (no leakage above 1.0×10^{-7} ref cc/sec) at 470°F (243°C) for 10 hours, and at 500°F (260°C) for 3 hours.

- To maintain the stability of the neutron shield resin, a maximum allowable temperature of 320°F (160°C) is considered for the neutron shield [33] for NCT.

- To prevent melting of the gamma shield (lead) under NCT, an allowable maximum temperature of 621°F (327°C – melting point of lead) is considered for the gamma shield [5].

- A temperature limit of 320°F (160°C) is considered for wood to prevent excessive reduction in structural properties at elevated temperatures [8].

- In accordance with 10CFR71.43(g) [1] the maximum temperature of the accessible packaging surfaces in the shade is limited to 185°F (85°C).

- The NCT ambient temperature range is –20°F to 100°F (-29°C to 38°C) per 10CFR71.71(b) [1]. In general, all the thermal criteria are associated with maximum temperature limits and not minimum temperatures. All materials can be subjected to the minimum environment temperature of -40°F (-40°C) without adverse effects as required by 10CFR71.71(c)(2) [1].

- The bounding TN-LC cavity internal pressures are summarized below:

Operating Condition	Calculated Pressure	Values used for Structural Evaluation in Chapter 2
Normal Conditions of Transport (NCT) (3% rods ruptured) (MNOP)	16.9 psig	30 psig
Hypothetical Accident Conditions (HAC) (100% rods ruptured)	91 psig	120 psig

3.1.1 Design Features

3.1.1.1 TN-LC Transport Cask

The TN-LC cask consists of multiple shells which conduct the decay heat to the cask outer surface. The other thermal design feature of the cask is the conduction path created by the aluminum boxes that contain the neutron shielding material as shown in Figure 3-3. The neutron shielding material is provided by a resin compound cast into long slender aluminum boxes placed around the outer shell and enclosed within a steel shell (shield shell). The aluminum boxes are designed to fit tightly against the steel shell surfaces, thus improving the heat transfer across the neutron shield.

Heat dissipates from the packaging outer surfaces via natural convection and radiation to the ambient when the cask is transported without the ISO container. When the cask is inside the ISO container, heat is dissipated from the cask surface via natural convection and radiation to walls of the ISO container, thereby dissipating to the ambient.

The steel-encased wood impact limiters are shown Figure 3-4. These components are included in the thermal analysis because of their contribution as a thermal insulator. The impact limiters provide protection to the lid and bottom regions from the external heat input due to fire during the HAC thermal event.

The TN-LC cask does not require a personnel barrier when transported without the ISO container. The ISO container encloses the cask body and impact limiters and prevents access to the outer surfaces of the cask when the cask is transported with the ISO container.

The gaps considered in the thermal model of TN-LC cask are shown in Figure 3-5.

The fuel baskets are designed to accommodate the irradiated fuel contents listed in Chapter 1, Section 1.2.2, conduct the decay heat in the fuel region through basket components to the TN-LC cask components, and dissipate heat from the cask outer surface or the ISO container via natural convection and radiation to the ambient.

The heat removal from the fuel basket fuel region to the TN-LC cask inner shell includes radiation, conduction and convection. No convection heat transfer is considered in the basket model for conservatism. Radiation heat transfer within the homogenized fuel region is considered implicitly between the fuel rods and the fuel compartment in calculation of transverse effective fuel conductivity. The TN-LC cask models are shown in Figure 3-1 through Figure 3-3.

The main design features of the fuel baskets are described in the sections that follow.

3.1.1.2 TN-LC-NRUX Basket

The structure of the TN-LC-NRUX basket is described in Appendix 1.4.2. The stainless steel tubes provide the necessary heat conduction path from the fuel assemblies to the perimeter of tube subassemblies. The guid plate supports provide additional conduction path between the guide plates and the basket shell. For conservatism, the guide plate supports are not included in the 2D TN-LC-NRUX basket model. Radiation heat transfer between spaces among tubes, wrap plates, guide plates, basket shell and the cask inner shell are considered in the TN-LC-NRUX basket model. The bounding NRX effective fuel conductivity is used in the model.

3.1.1.3 TN-LC-MTR Basket

The structure of the TN-LC-MTR basket is described in Appendix 1.4.3. The bucket assemblies, in combination with the basket plates and solid aluminum rails, provide the necessary heat conduction path from the fuel assemblies to the perimeter of the TN-LC cask. Radiation between basket rail and the cask inner shell gap is considered in the TN-LC-MTR basket model.

3.1.1.4 TN-LC-TRIGA Basket

The structure of the TN-LC-TRIGA basket is described in Appendix 1.4.4. The heat conduction path from the fuel assemblies to the basket rails is provided by the fuel compartment assemblies and the poison plates, which are sandwiched between the fuel compartments. The heat conduction path from the fuel compartment assemblies to the perimeter of the cask inner shell is provided by aluminum rails. Radiation between basket rail and the cask inner shell is considered in the TN-LC-TRIGA basket model.

3.1.1.5 TN-LC-1FA Basket

The structure of the 1FA basket is described in Appendix 1.4.5. The heat conduction path from the fuel assembly to the perimeter of the TN-LC cask inner shell is provided by the fuel compartment in combination with poison plates around the fuel compartment, the BWR sleeve (only for BWR fuel assemblies), and the aluminum basket rails assembly. The heat conduction path from the fuel rods to the perimeter of the pin-can assembly is provided by the tubes containing the fuel rods and the pin-can side wall. Radiation heat transfer between the basket rails and the cask inner shell space is considered in the TN-LC-1FA basket model with one PWR fuel assembly. Radiation heat transfer between the sleeve and basket frame is also considered in the TN-LC-1FA basket model with one BWR fuel assembly. Radiation heat transfer between the sleeve and the 25-pin can is added in the TN-LC-1FA basket model with the 25-pin-can assembly. The bounding effective fuel conductivity for the PWR, BWR, and 25-pin-can assembly are used in the model.

3.1.2 Contents Decay Heat

The design basis decay heat loading for the irradiated fuel to be transported within the TN-LC cask is a function of the irradiation history and the cooling time since discharge. Chapter 1, Section 1.2.2, provides details of the fuel elements to be transported. For the purposes of this evaluation, the design basis decay heat loadings are as shown the in the following table.

Basket Type	No. of Elements/ Assemblies in Basket	Heat Load per Element/Assembly (W)	Maximum Allowable Heat Load (kW)
TN-LC-NRUX	26 NRU/NRX Assemblies	15/Assembly	0.39
TN-LC-MTR	54 Elements	30/Element	1.50
TN-LC-TRIGA	180 Elements	8.33/Elements	1.50
TN-LC-1FA (BWR)	1 BWR Assembly	2000/Assembly	2.00
TN-LC-1FA (PWR)	1 PWR Assembly	3000/Assembly	3.00
TN-LC-1FA	9 Fuel Pins [1]	200/Pin	1.80
TN-LC-1FA	25 Fuel Pins	120/Pin	3.00

Notes
1. The thermal evalaution considers 13 fuel pin with the 220 W per pin, which consercatively bounds the above 9 fuel pin configuration.

3.1.3 Summary Tables of Temperatures

The maximum and minimum TN-LC cask and basket component temperatures for NCT are summarized in Table 3-1, Table 3-2 and Table 3-3. The component temperatures remain within the allowable range for NCT.

The maximum TN-LC cask and basket component temperatures for cold conditions at -20°F and -40°F ambient without insolation are presented in Table 3-4 and Table 3-5. These temperatures are used for the structural evaluation of TN-LC cask and baskets.

The maximum accessible surface temperature without an ISO container with the maximum decay heat load of 3 kW, ambient temperature of 100°F and no insolation is 169°F (76°C).

For the TN-LC cask with an ISO container, the maximum temperature of the accessible surface, that is, the outer surface of the ISO container is 147°F (64°C) with the maximum decay heat load of 3 kW, ambient temperature of 100°F (38°C), and insolation. The maximum temperature of the ISO container surface would be lower when the cask is in a shade without insolation.

These temperatures are below the maximum temperature of 185°F (85°C) specified in [1] for the outer surfaces of the package under shade and, therefore, no personnel barrier is needed.

The maximum transient temperatures of the TN-LC cask components and the time at which they occur are summarized in Table 3-6 and Table 3-7 for HAC. The resins and wood are assumed to

be decomposed or charred after fire accident. Therefore, the maximum temperatures for these components are irrelevant for HAC. The maximum fuel cladding, gamma shield and seal temperatures remain below the allowable limits and ensure the appropriate integrity of the fuel cladding and the containment boundary for HAC.

3.1.4 Summary Tables of Maximum Pressures

The maximum internal pressures inside the TN-LC cask cavity are calculated in Section 3.3.3 for NCT and Section 3.4.3 for HAC. The maximum internal pressures of the TN-LC cavity are summarized in Table 3-8. Based on an assumed fill gas temperature of 70°F, the maximum pressure rise under NCT is 16.9 psig, while the pressure rise under HAC conditions is 90.9 psig. The maximum normal operating pressure (MNOP) is 16.9 psig. These pressures are below the pressures of 30 psig and 120 psog for NCT and HAC respectively considered for the structural evaluation.

3.2 Material Properties and Component Specifications

3.2.1 Material Properties

The following tables provide the thermal properties of materials used in the analysis of the TN-LC cask.

1. Uranium Zirconium Alloy (UZrH) Thermal Conductivity [3]

Temperature		Thermal Conductivity	
(°F)	(°C)	(W/m-K)	(Btu/hr-in.-°F)
50	10	17.66	0.85
100	38	17.86	0.86
200	93	18.28	0.88
300	149	18.70	0.90
400	204	19.11	0.92
500	260	19.53	0.94
600	316	19.95	0.96
700	371	20.36	0.98
800	427	20.78	1.00
900	482	21.20	1.02
1,000	538	21.61	1.04

The above data is calculated based on the following equation given in [3],

$k_{UZrH} = 0.0075\ T + 17.58$, with k_{UZrH} in (W/m-K) and T in (°C).

2. Uranium-Aluminum (U-Al) Thermal Conductivity

Fuel Type	Weight Fraction of Uranium, W_U	Thermal Conductivity [14]
		(Btu/hr-in.-°F)
NRX	0.28	6.73
NRU	0.21	7.66

The above data is calculated based on the following equation given in Section 3.3 of [14], $k_{U\text{-}Al} = 2.17 - 2.76 \times W_U$, with $k_{U\text{-}Al}$ in (W/cm-K).

3. Irradiated UO_2 Thermal Conductivity

Temperature		Thermal Conductivity [13] [1]	
(K)	(°F)	(W/m-K)	(Btu/hr-in.-°F)
300	80	2.95	0.142
400	260	2.79	0.134
500	440	2.63	0.127
600	620	2.47	0.119
700	800	2.33	0.112
800	980	2.2	0.106
900	1160	2.08	0.100
1000	1340	1.98	0.095

Notes

2. The thermal conductivity values of irradiated UO_2 are conservatively based on the maximum burnup of 92 GWd/MTU from Table 4 of [13].

4. Zircaloy Thermal Conductivity [Eq.B-2.3 of Reference 12]

Temperature	Thermal Conductivity	Thermal Conductivity
(°F)	(Btu/min-in.-°F)	(Btu/hr-in.-°F)
200	0.0109	0.654
300	0.0115	0.690
400	0.0121	0.726
500	0.0126	0.756
600	0.0131	0.786
800	0.0142	0.852

5. SA-240, Type 304 and SA-182, F304 Stainless Steel Properties [11]

Temperature	Thermal Conductivity	Specific Heat	Density
(°F)	(Btu/hr-in-°F)	(Btu/lbm-°F)	(lbm/in.^{3})
70	0.717	0.116	0.284
100	0.725	0.117	
200	0.775	0.121	
300	0.817	0.125	
400	0.867	0.128	
500	0.908	0.131	
600	0.942	0.132	
700	0.983	0.134	
800	1.025	0.136	
900	1.058	0.137	
1000	1.092	0.138	

6. SA-240, Type XM-19/SA-182, Grade FXM-19 Stainless Steel Properties [11]

Temperature	Thermal Conductivity		Specific Heat	Density
(°F)	(Btu/hr-ft-°F)	(Btu/hr-in.-°F)	(Btu/lbm-°F)	(lbm/in.^{3})
70	6.400	0.533	0.113	0.284
100	6.600	0.550	0.116	
200	7.100	0.592	0.120	
300	7.700	0.642	0.125	
400	8.200	0.683	0.127	
500	8.800	0.733	0.130	
600	9.300	0.775	0.133	
700	9.900	0.825	0.135	
800	10.400	0.867	0.137	
900	10.900	0.908	0.138	
1000	11.400	0.950	0.139	

7. SA-182, Grade F6NM Martensitic Stainless Steel Properties [11]

Temperature	Thermal Conductivity		Specific Heat	Density
(°F)	(Btu/hr-ft-°F)	(Btu/hr-in.-°F)	(Btu/lbm-°F)	(lbm/in.^{3})
70	14.2	1.183	0.105	0.284
100	14.2	1.183	0.107	
200	14.3	1.192	0.112	
300	14.4	1.200	0.117	
400	14.5	1.208	0.122	
500	14.5	1.208	0.128	
600	14.6	1.217	0.135	
700	14.6	1.217	0.142	
800	14.7	1.225	0.150	
900	14.7	1.225	0.157	
1000	14.7	1.225	0.166	

8. Aluminum 6061 Properties [11]

Temperature	Thermal Conductivity	Specific Heat	Density
(°F)	(Btu/hr-in.-°F)	(Btu/lbm-°F)	(lbm/in.^{3})
70	8.008	0.213	0.098
100	8.075	0.215	
150	8.167	0.218	
200	8.250	0.221	
250	8.317	0.223	
300	8.383	0.226	
350	8.442	0.228	
400	8.492	0.230	

9. Aluminum 6063 Properties [11]

Temperature	Thermal Conductivity		Specific Heat[1]	Density
(°F)	(Btu/hr-ft-°F)	(Btu/hr-in.-°F)	(Btu/lbm-°F)	(lbm/in.^{3})
70	120.8	10.067	0.213	0.098
100	120.3	10.025	0.215	
150	119.7	9.975	0.218	
200	119.0	9.917	0.221	
250	118.5	9.875	0.223	
300	118.1	9.842	0.226	
350	118.0	9.833	0.228	
400	117.6	9.800	0.230	

Notes:
1. Specific heat of 6061 aluminum were assumed for 6063 aluminum.

10. Lead Properties [16]

Temperature		Thermal Conductivity		Specific Heat		Density	
(K)	(°F)	(W/m-K)	(Btu/hr-in.-°F)	(kJ/kg-K)	(Btu/lbm-°F)	(kg/m^3)	(lbm/in.^{3})
200	-100	36.7	1.767	0.125	0.030	11,430	0.413
250	-10	36.0	1.733	0.127	0.030	11,380	0.411
300	80	35.3	1.700	0.129	0.031	11,330	0.409
400	260	34.0	1.637	0.132	0.032	11,230	0.406
500	440	32.8	1.579	0.137	0.033	11,130	0.402
600	620	31.4	1.512	0.142	0.034	11,010	0.398

11. Neutron Shield Resin (Vyal B) Properties

Temperature		Specific Heat [33]		Density [33]		Minimum Thermal Conductivity
(°C)	(°F)	(J/g-C)	(Btu/lbm-°F)	(g/cm^3)	(lbm/in.^{3})	(Btu/hr-in.-°F)
40	104	1.07	0.256	1.75	0.06	0.039
60	140	1.09	0.260			
80	176	1.18	0.282			
100	212	1.26	0.301			
140	284	1.5	0.358			
160	320	1.59	0.380			

Minimum conductivity of VYAL B is taken from [33]. Thermal conductivity for Vyal B bounds Resin F based on the Table 7 of [34].

12. Wood Properties

Minimum conductivity, k_{min} = 0.0019 Btu/hr-in.-°F [1] for cool-down period		
Maximum conductivity, k_{max} = 0.0378 Btu/hr-in.-°F [1] during fire period		
Thermal diffusivity, α = 2.5E-4 in.^{2}/ s =0.90 in.^{2}/hr [8], Page 3-17		
Temperature (°C)	Specific Heat [8], Page 3-17 (Btu/lbm-°F)	Density[2] (lbm/in.^{3})
100	0.312	0.007
200	0.363	0.006
300	0.414	0.005
400	0.466	0.005
500	0.517	0.004
600	0.568	0.004

Notes:

1. Minimum and Maximum conductivities of wood are listed in Section 3.2, Item 8, of Reference 21. Minimum conductivity of wood is used for NCT and post-fire conditions to decrease the heat dissipated to environment, whereas maximum conductivity is used during HAC to increase heat input into the cask during fire accident.
2. The wood density is calculated based on thermal diffusivity using $\alpha = \frac{k}{\rho c_p}$ with

   k = conductivity =0.0019 (Btu/hr-in.-°F),
   ρ = density (lbm/in.^{3}), and
   c_p = specific heat (Btu/lbm-°F).

13. Air Thermal Properties

Temperature		**Thermal conductivity**	
(K)	(°F)	(W/m-K)	(Btu/hr-in.-°F)
200	-100	0.01822	0.0009
250	-10	0.02228	0.0011
300	80	0.02607	0.0013
400	260	0.03304	0.0016
500	440	0.03948	0.0019
600	620	0.04557	0.0022
800	980	0.05698	0.0027
1000	1340	0.06721	0.0032

The above data is calculated based on the following polynomial function from [10],
$k = \sum C_i T_i$ for conductivity in (W/m-K) and T in (K).

For 250 < T < 1050 K	
C0	-2.2765010E-03
C1	1.2598485E-04
C2	-1.4815235E-07
C3	1.7355064E-10
C4	-1.0666570E-13
C5	2.4766304E-17

Specific heat, dynamic viscosity, density and Prandtl number of air are used to calculate heat transfer coefficients described in Section 3.3.1.1based on the following data from [10].

$c_p = \sum A_i T_i$ for specific heat in (kJ/kg-K) and T in (K).

For 250 < T < 1050 K	
A0	0.103409E+1
A1	-0.2848870E-3
A2	0.7816818E-6
A3	-0.4970786E-9
A4	0.1077024E-12

$\mu = \sum B_i T_i$ for viscosity $(N\text{-}s/m^2)\times 10^6$ and T in (K).

For 250 < T < 600 K		For 600 < T < 1050 K	
B0	-9.8601E-1	B0	4.8856745
B1	9.080125E-2	B1	5.43232E-2
B2	-1.17635575E-4	B2	-2.4261775E-5
B3	1.2349703E-7	B3	7.9306E-9
B4	-5.7971299E-11	B4	-1.10398E-12

$\rho = P / RT$ for density (kg/m^3) with P = 101.3 kPa; R = 0.287040 kJ/kg-K; T = air temperature in (K).

$Pr = c_p \mu / k$ Prandtl number.

14. Helium Thermal Conductivity [10]

Temperature		Thermal Conductivity	
(K)	(°F)	(W/m-K)	(Btu/hr-in.-°F)
300	80	0.1499	0.0072
400	260	0.1795	0.0086
500	440	0.2115	0.0102
600	620	0.2466	0.0119
800	980	0.3073	0.0148
1000	1340	0.3622	0.0174
1050	1430	0.3757	0.0181

The above data is calculated based on the following polynomial function from [10], $k = \sum C_i T_i$ for conductivity in (W/m-K) and T in (K).

For 300 < T < 500 K		For 500< T < 1050 K	
C0	-7.761491E-03	C0	-9.0656E-02
C1	8.66192033E-04	C1	9.37593087E-04
C2	-1.5559338E-06	C2	-9.13347535E-07
C3	1.40150565E-09	C3	5.55037072E-10
C4	0.0E+00	C4	-1.26457196E-13

15. Fuel Effective Thermal Conductivities of TN-LC Contents

Calculation of the effective properties for homogenized fuel is discussed in Appendix 3.6.6. The bounding effective properties for each fuel type are listed below.

Fuel Effective Transverse Thermal Conductivities

MTR		**TRIGA**		**NRU**		**NRX**	
Tavg	k_{eff}	Tavg	k_{eff}	Tavg	k_{eff}	Tavg	k_{eff}
(°F)	(Btu/hr-in.-°F)	(°F)	(Btu/hr-in.-°F)	(°F)	(Btu/hr-in.-°F)	(°F)	(Btu/hr-in.-°F)
105	0.0361	114	0.0375	102	7.457E-03	103	5.560E-03
204	0.0431	212	0.0445	202	8.321E-03	202	6.304E-03
304	0.0516	310	0.0531	301	9.273E-03	302	7.132E-03
403	0.0616	409	0.0632	401	1.030E-02	402	8.047E-03
503	0.0731	507	0.0750	501	1.142E-02	502	9.082E-03
602	0.0860	606	0.0885	601	1.263E-02	601	1.016E-02
702	0.1003	705	0.1033	701	1.373E-02	701	1.125E-02
802	0.1159	804	0.1199	801	1.496E-02	801	1.239E-02
1FA (25 Fuel Pins)		1FA (9 Fuel Pins) (1)		1FA (PWR)		1FA (BWR)	
Tavg	k_{eff}	Tavg	k_{eff}	Tavg	k_{eff}	Tavg	k_{eff}
(°F)	(Btu/hr-in.-°F)	(°F)	(Btu/hr-in.-°F)	(°F)	(Btu/hr-in.-°F)	(°F)	(Btu/hr-in.-°F)
158	0.0453	192	0.0271	178	0.0159	200	0.0157
253	0.0496	284	0.0296	267	0.0186	300	0.0181
348	0.0542	377	0.0324	357	0.0218	400	0.0210
444	0.0592	471	0.0353	448	0.0259	500	0.0245
541	0.0642	565	0.0382	541	0.0307	600	0.0282
638	0.0694	660	0.0412	635	0.0361	700	0.0324
735	0.0747	756	0.0444	730	0.0422	800	0.0369
833	0.0800	852	0.0475	826	0.0488		

Notes

(1) The thermal evalaution considers 13 fuel pin with the 220 W per pin to bound the 9 fuel pin configuration.

Fuel Effective Axial Thermal Conductivities, Effective Fuel Density and Specific Heat used for Transient Analysis of TN-LC Cask

Tavg	**k_axial**	**ρ**	**Tavg**	**Cp**
(°F)	(Btu/hr-in.-°F)	(lbm/in.^{3})	(°F)	(Btu/lbm-°F)
200	0.0456	0.1114	80	0.05924
300	0.0481		260	0.06538
400	0.0506		692	0.07255
500	0.0527		1502	0.07779
600	0.0548			
800	0.0594			

16. Effective Conductivity for Top and Bottom Gamma Shielding

(See Section 3.3.1.3 for calculation of effective properties)

Temperature		k_{plate}	k_{air}		k_{eff_axial}
(°F)	(K)	(Btu/hr-in.-°F)	(W/m-K)	(Btu/hr-in.-°F)	(Btu/hr-in.-°F)
-100	200.0	1.767	0.0182	0.0009	0.028
-10	250.0	1.733	0.0223	0.0011	0.035
80	300.0	1.700	0.0261	0.0013	0.040
260	400.0	1.637	0.0330	0.0016	0.051
440	500.0	1.579	0.0395	0.0019	0.060
620	600.0	1.512	0.0456	0.0022	0.069
Temperature		k_{plate}	k_{air}		k_{eff_radial}
(°F)	(K)	(Btu/hr-in.-°F)	(W/m-K)	(Btu/hr-in.-°F)	(Btu/hr-in.-°F)
-100	200.0	1.767	0.0182	0.0009	1.713
-10	250.0	1.733	0.0223	0.0011	1.681
80	300.0	1.700	0.0261	0.0013	1.649
260	400.0	1.637	0.0330	0.0016	1.587
440	500.0	1.579	0.0395	0.0019	1.531
620	600.0	1.512	0.0456	0.0022	1.466

17. Effective Conductivity for Air in ISO Container "Region 3"

(See Section 3.3.1.3 for calculation of effective properties)

T_i	T_o	T_{avg}	T_{avg}	k	β	μ	ρ	C_p	Pr	Ra_b	Nu	k_eff	k_eff
(°F)	(°F)	(°F)	(K)	(W/m-K)	(1/K)	(kg/m-s)	(kg/m^3)	(J/kg-K)	(---)	(---)	(---)	(W/m-K)	(Btu/hr-in-°F)
130	100	115	319	0.0275	3.13E-03	1.94E-05	1.11E+00	1008	0.71	4.97E+08	29.99	0.82	0.0397
140	110	125	325	0.0279	3.08E-03	1.97E-05	1.09E+00	1008	0.71	4.60E+08	29.41	0.82	0.0395
150	120	135	330	0.0283	3.03E-03	1.99E-05	1.07E+00	1009	0.71	4.26E+08	28.84	0.81	0.0392
160	130	145	336	0.0287	2.98E-03	2.02E-05	1.05E+00	1009	0.71	3.94E+08	28.29	0.81	0.0390
170	140	155	341	0.0290	2.93E-03	2.04E-05	1.03E+00	1010	0.71	3.66E+08	27.77	0.81	0.0388
180	150	165	347	0.0294	2.88E-03	2.07E-05	1.02E+00	1010	0.71	3.40E+08	27.26	0.80	0.0386
190	160	175	353	0.0298	2.84E-03	2.09E-05	1.00E+00	1011	0.71	3.17E+08	26.77	0.80	0.0384
200	170	185	358	0.0302	2.79E-03	2.12E-05	9.86E-01	1011	0.71	2.95E+08	26.30	0.79	0.0383

18. Effective Conductivity for Air in ISO Container "Region 2"

(See Section 3.3.1.3 for calculation of effective properties)

T_i	T_o	T_{avg}	T_{avg}	k	β	μ	ρ	C_p	Pr	Ra_b	Nu	k_eff	k_eff
(°F)	(°F)	(°F)	(K)	(W/m-K)	(1/K)	(kg/m-s)	(kg/m^3)	(J/kg-K)	(---)	(---)	(---)	(W/m-K)	(Btu/hr-in-°F)
130	125	128	326	0.0280	3.07E-03	1.97E-05	1.08E+00	1008	0.71	6.10E+06	8.01	0.22	0.0108
140	135	138	332	0.0284	3.01E-03	2.00E-05	1.06E+00	1009	0.71	5.65E+06	7.86	0.22	0.0107
150	145	148	337	0.0288	2.96E-03	2.02E-05	1.05E+00	1009	0.71	5.24E+06	7.71	0.22	0.0107
160	155	158	343	0.0291	2.92E-03	2.05E-05	1.03E+00	1010	0.71	4.86E+06	7.57	0.22	0.0106
170	165	168	348	0.0295	2.87E-03	2.07E-05	1.01E+00	1010	0.71	4.52E+06	7.43	0.22	0.0106
180	175	178	354	0.0299	2.82E-03	2.10E-05	9.97E-01	1011	0.71	4.21E+06	7.30	0.22	0.0105
190	185	188	360	0.0303	2.78E-03	2.12E-05	9.82E-01	1011	0.71	3.92E+06	7.17	0.22	0.0105
200	195	198	365	0.0307	2.74E-03	2.15E-05	9.67E-01	1012	0.71	3.66E+06	7.05	0.22	0.0104

19. Effective Conductivity for Poison Plate

(See Section 3.3.1.5 for calculation of effective properties)

Basket Type	Helium Gap	Poison	Poison + 0.02 in. Helium Gap	
	K	K	K_eff_cross	Keff_along
	(Btu/hr-in.-°F)	(Btu/hr-in.-°F)	(Btu/hr-in.-°F)	(Btu/hr-in.-°F)
TN-LC-1FA	0.0072	3.513	0.088	3.233
TN-LC-TRIGA			0.109	3.287

20. Effective Conductivity for Basket Plates

(See Section 3.3.1.5 for calculation of effective properties)

	Helium Gap	SA-240 Type 304	Outer Plate + 0.01in. Gap (TN-LC-MTR Basket)		Wrap Plate + 0.02 Helium Gap (TN-LC-TRIGA Basket)	
Temp	K	K	K_eff_cross	Keff_along	K_eff_cross	Keff_along
(°F)	(Btu/hr-in-°F)	(Btu/hr-in-°F)	(Btu/hr-in-°F)	(Btu/hr-in-°F)	(Btu/hr-in-°F)	(Btu/hr-in-°F)
100	0.0074	0.725	0.318	0.716	0.044	0.610
200	0.0082	0.775	0.347	0.765	0.048	0.652
300	0.0090	0.817	0.374	0.806	0.053	0.687
400	0.0098	0.867	0.404	0.855	0.058	0.730
500	0.0107	0.908	0.433	0.897	0.063	0.765
600	0.0117	0.942	0.460	0.929	0.069	0.793
700	0.0125	0.983	0.487	0.971	0.073	0.828
800	0.0133	1.025	0.513	1.012	0.078	0.863
1000	0.0149	1.092	0.560	1.077		

21. Effective Conductivity for Air in Thermal Shield

(See Section 3.3.1.3 for calculation of effective properties)

Temperature (°F)	SS304, ASME 2004 [11] k_{steel} (Btu/hr-in.-°F)	k_{eff} (Btu/hr-in.-°F)
70	0.717	0.0387
100	0.725	0.0391
200	0.775	0.0418
300	0.817	0.0441
400	0.867	0.0468
500	0.908	0.0490
600	0.942	0.0508
700	0.983	0.0530
800	1.025	0.0553
900	1.058	0.0571
1000	1.092	0.0589

22. Emissivities and Absorptivities

Calculations to determine the effective fuel properties and thermal radiation exchange within the baskets for the TN-LC cask assume an emissivity of 0.3 for stainless steel based on the report in [17]. An emissivity of 0.1 is used for aluminum fuel cladding and aluminum rails in the cask baskets based on [10]. An emissivity of 0.8 is used for Zircaloy based on Table B-3.11 of [12].

For NCT calculations, the emissivity of the cask rolled stainless steel plates is taken as 0.587 as reported in [20]. An emissivity of 0.001 is used for symmetry planes. Solar absorptance values of 0.39 and 0.47 are given in [19] for rolled and machined stainless steel plates, respectively. For conservatism, it is assumed that the solar absorptivity of stainless steel is equal to emissivity. Solar absorptivity and emissivity of 0.587 [20] is used for the uncoated stainless steel outer surfaces of the impact limiter shell and neutron shield shells for NCT analysis.

Thermal radiation at the external surfaces of the ISO container is considered for the TN-LC cask thermal evaluation. The surfaces of ISO containers are commonly painted. Reference [18] gives an emissivity between 0.92 and 0.96 for oil paints of all colors. To account for dust and dirt and to bound the problem, the NCT thermal analysis uses an emissivity of 0.9 for the surfaces of the ISO container. The analysis also assumes a solar absorptivity of 0.5 corrsponding to light paints as specified in [18] to cover a wide range of paint absoptivities commonly used for ISO conatiners.

For the initial conditions before the HAC fire, NCT surface properties are used. During the HAC fire, a conservative fire emissivity of 1.0 is used. An emissivity of 0.8 is assumed for all surfaces exposed to the fire as required by 10CFR71.73 [1]. For post fire conditions, it is assumed that all external surfaces are covered with soot. The solar absorptivity of soot is 0.95 [18]. To bound the problem, the thermal evaluation uses a solar absorptivity of 1.0 and an emissivity of 0.9 for the packaging outer surfaces during the cooldown period.

3.2.2 Component Specifications

The components for which thermal technical specification are necessary are the TN-LC cask containment seals and the poison plates used in the baskets.

3.2.2.1 TN-LC Cask

The seals used in the packaging are the Fluorocarbon seals (Viton O-rings). The seals will have a minimum and maximum steady state temperature rating of -40°F and 400°F, respectively. The short term maximum temperature limit is 482°F.

3.2.2.2 TN-LC Fuel Baskets

The 1FA and TRIGA basket designs allow the use of neutron absorber materials such as Borated Aluminum, Metal Matrix Composite (MMC) or Boral®.

The neutron absorber materials in the baskets are subjected the following minimum thermal conductivity, which is used in the basket thermal analyses. The minimum conductivity of 3.513 Btu/hr-in.-°F (73 W/m-K) considered for poison plates is based on 95 percent of the conductivity of Boral® plate core (B_4C) given in [32]. The poison plate thicknesses considered in the thermal analyses are 0.25 in. in the TN-LC-1FA basket and 0.31 in. in the TN-LC-TRIGA basket.

Temperature	k	k
(°F)	(Btu/hr-in.-°F)	(W/m-K)
All Range	3.513	73

The poison plates may be replaced with a thinner plate that meets the minimum B10 areal density requirement as specified in Appendices 1.4.4 and 1.4.5 and the balance of the thickness can be made up with a sheet of aluminum to compensate the minimum thermal conductivity requirement. The sum of the thicknesses shall be equal to the design thickness specified in drawing in Appendix 1.4.1. The following equation can be used to determine the minimum thermal conductivity, k_2, for the thinner poison plate.

$$k_2 = \frac{k_1 t_1 - k_3 t_3}{t_2}$$

Where:
k_1 = minimum thermal conductivity of poison plate at design thickness (73 W/m-K),
t_1 = poison plate design thickness (0.25 in. in the TN-LC-1FA basket and 0.31 in. in the TN-LC-TRIGA basket),
k_2 = minimum thermal conductivity of the thinner poison plate (W/m-K),
t_2 = thickness of the thinner poison plate (in.),
k_3 = thermal conductivity of aluminum (W/m-K), and
t_3 = thickness of the aluminum sheet (in.).

3.3 Thermal Evaluation under Normal Conditions of Transport

The NCT ambient conditions are used for the determination of the maximum fuel cladding temperature, the maximum TN-LC cask temperatures, the containment pressure, and the thermal stresses. These steady state environmental conditions correspond to maximum daily averaged ambient temperature of 100°F and to 10CFR71.71(c)(1) [1] insolation averaged over a 24-hour period.

Ambient conditions for NCT are taken from 10CFR71 [1] and applied to the boundaries of the cask model. These conditions are listed in the following table.

Normal Conditions of Transport

Case #	Ambient Temperature (°F)	Insolation	Purpose
1	100	Yes	Maximum Component Temperatures
2	-20	No	Cold conditions for Structural Analysis
3	-40	No	Maximum Thermal Stress
4	100	No	Maximum Accessible Surface Temperature

The maximum heat loads allowed for the various contents of the TN-LC cask are shown in Section 3.1.2. For conservatism, heat loads of 1.85 kW and 0.5 kW are evaluated for the TN-LC cask with MTR and NRU/NRX fuel, respectively, to provide the bounding inner shell temperature profile to determine the maximum fuel cladding and component temperatures. The heat loads considered for the thermal analysis of the cask are listed in Table 3-14.

3.3.1 Thermal Models

The thermal performance of the TN-LC cask, loaded with the above load cases (with and without the ISO container), 3D finite element models were developed using the ANSYS computer code [9]. ANSYS is capable of solving steady state and transient thermal analysis problems in one, two, or three dimensions. Heat transfer via a combination of conduction, radiation, and convection can be modeled by ANSYS [9].

Two finite element models were developed for analyses of the TN-LC cask with and without the ISO container.

(a) A half-symmetric, three-dimensional finite element model of the TN-LC cask is used to analyze the thermal performance of the TN-LC cask without an ISO container. The model contains the inner shell, gamma shield, outer shield, cask bottom flange, lid, impact limiters, neutron shield within the neutron shield boxes and neutron shield shell. All the dimensions in the model correspond to the nominal dimensions shown in the Chapter 1, Appendix 1.4.1 drawings. SOLID70 elements are used to model the components including the gaseous gaps. Impact limiter gussets are modeled using SHELL57 elements. Surface elements SURF152 are used for applying the insolation boundary conditions.

(b) A 90° three-dimensional model finite element model of the TN-LC cask is used to analyze the thermal performance of the TN-LC cask with an ISO container. The above 3D finite element model of the TN-LC cask without the ISO container is modified to include the ISO container and the air between the cask outer surfaces and the ISO container. The ISO container is modeled using SHELL57 elements. To model the radiation heat exchange between the outer surface of the transport cask and the inner surface of the ISO container, SHELL57 elements are overlaid on the external surfaces to create a radiation super-element. Thermal radiation between the TN-LC transport cask and ISO container is modeled using AUX12 processor.

To analyze the thermal performance of the fuel baskets for the hot and cold NCT cases described above, half-symmetric 2D finite element models of the fuel baskets, including the homogenized fuel, basket components and the cask inner shell wall, were developed using the ANSYS computer code. All dimensions in the model correspond to nominal dimensions. For the cold environment condition with ambient temperature of -20°F, the maximum fuel cladding and component temperatures are bounded by design load case #1 in the table above, and the maximum thermal stresses are bounded by design case #3. Therefore, no thermal analysis was needed for the baskets at ambient temperature of -20°F.

The heat loads considered for the thermal analysis of the basket are listed in Table 3-14.

The heat load is applied as a uniform volumetric heat generation within a homogenized fuel region. Only radial heat transfer is considered in the fuel basket models. The bounding effective thermal conductivities for the homogenized fuel regions inside the fuel baskets are presented in Section 3.2.1 and account for radiation and conduction within the fuel regions.

The basket components, including the gaseous gaps, were modeled using PLANE55 elements. Radiation between the adjacent surfaces is modeled using the radiation super-element processor (AUX12). LINK32 elements are used in modeling radiating surfaces to create the radiation super-element. The LINK32 elements were unselected prior to the solution of the model.

3.3.1.1 TN-LC Transport Cask Model

The following assumptions are used in the TN-LC transport cask model:

For the TN-LC transport cask, heat load is simulated by heat flux distributed uniformly over the active fuel length of each fuel assembly on the radial inner surface of the inner shell. The active fuel length for PWR, MTR, and NRU/NRX fuel assemblies considered in the cask model are 144 in., 176 in., and 121 in., respectively.

For the TN-LC transport cask with a PWR fuel assembly, the active fuel length of 144 in. is used to model the heat flux which is much shorter than the basket length of 181 in. This is conservative since the solid aluminum rails dissipate heat along the entire length of the basket and, therefore, applying the heat flux only on the active fuel length of 144 in. maximizes the peak temperatures. Furthermore, this bounds any uncertainties due to the lengths of the different PWR fuel assemblies.

No convection is considered within the cask cavity.

No heat transfer is considered within the shear key slot.

The following gaps are considered in the TN-LC transport cask model:

(a) 0.0625 in. gap is considered on either side of the top and bottom gamma shieldings.

(b) 0.0625 in. radial gap is considered between the gamma shielding and the top lid / bottom flange.

(c) 0.125 in. radial gap is considered between the top lid and the top flange.

(d) 0.06 in. axial gap is considered between the top lid and the top flange.

(e) 0.019 in. radial gap between gamma shield and cask outer shell.

(f) 0.01 in. radial gaps between neutron shield boxes and surrounding shells.

(g) 0.01 in. axial gap between the top lid/bottom flange and impact limiter shell.

The 0.0625 in. axial gaps on either side of the top and bottom gamma shieldings and the 0.0625 in. radial gap considered between the gamma shieldings and the top lid / bottom flange maximize the radial heat transfer through inner shell toward the cask to bound the maximum component temperatures conservatively.

The 0.125 in. radial gap considered between the top lid and the top flange and the 0.06 in. axial gap considered between the top lid and the top flange are equal to the nominal cold gaps. These gaps are conservative since the hot gaps at thermal equilibrium would be smaller.

The 0.01 in. radial gaps between the neutron shield boxes and the surrounding shells is based on assumptions as shown in Section 3.4.1.1 of the MP197 SAR [21].

An axial gap of 0.01 in. is considered between the impact limiter spacers and the cask top or bottom end surfaces. This gap accounts for the thermal resistance among the bolted components.

For the TN-LC cask transported without an ISO container, the transport operation occurs in the horizontal position. Therefore, the lower halves of the cask cylindrical surfaces are not exposed to insolation. No solar heat flux is considered over these surfaces. To remove any uncertainty about the solar impact on the vertical surfaces, the entire surface areas of vertical surfaces are considered for application of the solar heat flux.

For the TN-LC cask transported within an ISO container, all the surfaces of the ISO container are considered to be exposed to solar heat flux. This assumption is conservative as it increases the total amount of solar heat input into the model.

For the thermal evaluation of the TN-LC cask within an ISO container, the inner surfaces of the ISO container are modeled using SHELL57 elements. The below table presents the inner dimensions of the ISO container assumed for this analysis.

Dimensions of ISO Container

Dimension	[in.]
Length	234
Width	91
Height	87

The thickness of the bottom gamma shielding considered in the ANSYS thermal models of the TN-LC cask is 4.0 in. However, the correct thickness of the TN-LC cask bottom gamma shielding is 3.50 in. This change in the thickness of the bottom gamma shielding has a negligible effect on the peak temperatures of the TN-LC cask components and is not considered in this evaluation. The 0° orientation is located at the top of the horizontal transport cask as shown in the drawings contained in Chapter 1, Appendix 1.4.1.

Decay heat load is applied as a uniform heat flux over the inner surface of the inner shell. The various heat loads used in this analysis are shown below and are computed as follows:

$$q'' = \frac{Q}{\pi D_i L_b}$$

q" = decay heat flux (Btu/hr-in.^{2}),

Q = decay heat load (Btu/hr),

D_i = inner shell diameter = 18 in.,

L_b = Basket / Active Fuel length (in.).

Decay Heat Flux

Fuel Assembly Type	Heat Load (kW)	Heat Load (Btu/hr)	Bounding Heat Load Case	L_b (in.)	Decay Heat Flux (Btu/hr-in.^{2})
PWR	3.0	10237	PWR	144	1.257
BWR	2.0	6825	PWR	144	0.838
MTR	1.85	6313	MTR	176	0.634
TRIGA	1.5	5118	MTR	156.25	0.579
NRU/NRX	0.5	1706	NRUX	121	0.249
Fuel Pins (PWR/BWR/EPR/MOX)	3.0	10237	PWR	144	1.257

A comparison of the total heat load and the decay heat flux presented above for the PWR, BWR, TRIGA, and MTR fuel elements / assemblies show that the maximum heat load/heat flux specified for the BWR fuel assembly and TRIGA fuel assemblies within the TN-LC transport cask are bounded by PWR and MTR fuel assemblies, respectively. Therefore no further analysis is performed for the TN-LC transport cask with BWR and TRIGA fuel assemblies and the

temperature profiles determined for the PWR fuel assemblies and MTR fuel elements are used to determine the peak temperature of BWR and TRIGA basket components, respectively.

The insolation values taken from 10CFR71 [1] are averaged over 24 hours and multiplied by the surface absorptivity factor to calculate the solar heat flux applied in the TN-LC cask model. The solar heat flux values used in the model are summarized below.

Solar Heat Flux

Surface Material	**Shape**	**Insolation over 12 hrs [1] (gcal/cm^2)**	**Solar Absorptivity** [1]	**Total solar heat flux averaged over 24 hrs (Btu/hr-in.^{2})**
Stainless Steel (Cask Outer Surface)	Curved	400	0.587 (2)	0.2505
	Flat Vertical	200	0.587 (2)	0.1252
Paint (ISO Container)	Flat Vertical	200	0.50	0.1067
	Flat Horizontal	800	0.50	0.4267

Notes:
1. See Section 3.2.1 for surface properties.
2. Solar absorptivity of stainless steel is taken equal to its emissivity.

Convection and radiation heat transfer from the outer surfaces of the TN-LC transport cask and the ISO container are combined together as total heat transfer coefficients. The total heat transfer coefficients are calculated using free convection correlations from [10] and are incorporated in the model using ANSYS macros. These correlations are described below. The ANSYS macros used in this calculation are listed in Appendix 3.6.1.

Total heat transfer coefficient, h_t, is used to combine the convection and radiation heat transfer together.

$$h_t = h_r + h_c$$

Where:

h_r = radiation heat transfer coefficient (Btu/hr-in.^{2}-°F),

h_c = free convection heat transfer coefficient (Btu/hr-in.^{2}-°F).

The radiation heat transfer coefficient, h_r, is given by the equation:

$$h_r = \varepsilon F_{w\infty} \left[\frac{\sigma(T_w^4 - T_{amb}^4)}{T_w - T_{amb}} \right] \text{ Btu/hr-in.}^2\text{-°F}$$

Where:
ε = surface emissivity,

$F_{w\infty}$ = view factor from surface 1 to ambient = 1,

$\sigma = 0.1714 \times 10^{-8}$ Btu/hr-ft^2-°R^4,

T_w = surface temperature (°R),

T_{amb} = ambient temperature (°R).

Surface emissivity values are listed in Section 3.2.

The following equations from [10] are used to calculate the free convection coefficients.

For horizontal cylinders:

$$Ra = Gr\,Pr \quad ; \quad Gr = \frac{g\beta(T_w - T_\infty)D^3}{\nu^2}$$

$$Nu_l = \frac{2f}{\ln(1 + 2f / Nu^T)} \text{ with}$$

$$Nu^T = 0.772\,\overline{C}_l\,Ra^{1/4} \quad ; \; f = 1 - \frac{0.13}{(Nu^T)^{0.16}}; \text{with } \overline{C}_l = 0.515 \text{ for gases [10].}$$

$$Nu_t = \overline{C}_t\,Ra^{1/3}$$

$\overline{C}_t = 0.103$ for air with $Pr \approx 0.71$ [10].

$$Nu = \left[(Nu_l)^m + (Nu_t)^m\right]^{1/m} \quad \text{with} \quad m = 10 \quad \text{for} \quad 10^{-10} < Ra < 10^7.$$

$$h_c = \frac{Nu\,k}{D} \times 0.1761/144$$

For vertical flat surfaces:

$$Ra = Gr\,Pr \quad ; \quad Gr = \frac{g\beta(T_w - T_\infty)L^3}{\nu^2}$$

$$Nu_l = \frac{2.0}{\ln(1 + 2.0 / Nu^T)} \text{ with}$$

$$Nu^T = \overline{C}_l\,Ra^{1/4} \quad \text{with } \overline{C}_l = 0.515 \quad \text{for gases [10].}$$

$$Nu_t = C_t^V \, f \, Ra^{1/3} / \left(1 + 1.4 \times 10^9 \, Pr/Ra\right) \qquad \text{with}$$

$$C_t^V = \frac{0.13 Pr^{0.22}}{(1 + 0.61 Pr^{0.81})^{0.42}} \qquad f = 1.0 + 0.078 \left(\frac{T_w}{T_\infty} - 1 \right).$$

$$Nu = \left[(Nu_l)^m + (Nu_t)^m \right]^{1/m} \qquad \text{with} \quad m = 6 \quad \text{for} \quad 1 < Ra < 10^{12}.$$

$$h_c = \frac{Nu \, k}{L}$$

For horizontal flat surfaces facing upwards:

The following correlations are used only for the upper surface of the ISO container.

$$Ra = Gr \, Pr \quad ; \quad Gr = \frac{g \beta (T_w - T_\infty)(L^*)^3}{\nu^2} \quad .$$

$$Nu_l = \frac{1.4}{\ln(1 + 1.4 / Nu^T)} \qquad \text{with}$$

$$Nu^T = 0.835 \, \overline{C}_l \, Ra^{1/4} \text{ with } \overline{C}_l = 0.515 \qquad \text{for gases [10],}$$

$$Nu_t = C_t^u \, Ra^{1/3} \qquad \text{with } C_t^u = 0.140 \qquad \text{for gases [10],}$$

$$Nu = \left[(Nu_l)^m + (Nu_t)^m \right]^{1/m} \qquad \text{with} \quad m = 10 \quad \text{for} \quad 1 < Ra < 10^{10}.$$

$$h_c = \frac{Nu \, k}{L^*}$$

Where:

g = gravitational constant =9.81 m/s^2,

β = expansion coefficient = 1/T (1/K),

T = absolute temperature (K),

ν = kinematic viscosity (m^2/s),

D = diameter of the horizontal cylinder (m),

L = height of the vertical flat surface (m),

$$L^* = \frac{A}{p} = \frac{\text{heated area}}{\text{heated perimeter}},$$

k = air conductivity (W/m-K).

The above correlations are incorporated in ANSYS model via macro "HTOT_HCL.MAC" for horizontal cylinders, "HTOT_VPL.MAC" for vertical flat surfaces and "HC_ROOF.MAC" for horizontal flat surfaces facing upwards. These macros are shown in Appendix 3.6.1. Air properties are taken from [10] and listed in Section 3.2.

To simplify the model, the assumed 0.0625 in. gaps around the top and bottom gamma shieldings are integrated into the model using effective conductivity properties. The effective conductivity of the top and bottom gamma shieldings with 0.0625–in. gaps around them are calculated in Section 3.3.1.3.

When the TN-LC cask is transported within an ISO container, heat is dissipated from the cask surface by natural convection that exists inside the ISO container cavity and by radiation between surfaces. The radiation heat exchange between the surfaces is modeled using the AUX12 processor and the MATRIX50 super element.

To model the natural convection that exists inside the ISO container cavity, the entire length is divided into three regions. "Region 1" includes the space between the ISO container and the end impact limiter outer surfaces of the TN-LC transport cask. "Region 2" includes the area between the radial impact limiter outer surface and the ISO container. "Region 3" includes the area around the neutron shield between the impact limiter inner surfaces and the ISO container. These regions are shown in Figure 3-2.

For "Region 1," any effects of natural convection are ignored and only gaseous conduction due to the presence of air is considered. For "Region 2" and "Region 3," the effects of natural convection are implemented using an effective conductivity calculated using empirical correlations for heat transfer across gap between two horizontal cylinders from [22]. The effective conductivity calculation is shown in Section 3.3.1.3.

The material properties used in the transport cask model are listed in Section 3.2.

The geometry of the model and its mesh density are shown in Figure 3-1 through Figure 3-5. Mesh sensitivity of the model is evaluated in Appendix 3.6.2.

Typical boundary conditions for the transport cask model are shown in Figure 3-6 and Figure 3-7.

The seal O-rings are not explicitly considered in the model. The maximum seal temperatures are retrieved from the models by selecting the nodes at the locations of the corresponding seal O-rings.

3.3.1.2 Calculation of Maximum Accessible Surface Temperature

An ISO container will be used to ship the cask and transport skid, however, the transport cask is evaluated with and without an ISO container. There are no openings in the ISO container.

When the cask is transported without the ISO container, heat dissipates from the packaging outer surfaces via natural convection and radiation to the ambient. The two transport cask models

described in Section 3.3.1.1 are run without insolation to determine the accessible surface temperature of the cask in the shade. A heat load of 3 kW and boundary conditions at 100°F and no insolation are considered in the cask model to bound the maximum accessible surface temperature under shade. The maximum accessible surface temperature of the cask outer surface without the ISO container is 169°F on the neutron shield shell.

When the cask is transported inside the ISO container, heat is dissipated from the cask surface via natural convection and radiation to the walls of the ISO container, thereby subsequently dissipating to the ambient. A heat load of 3 kW and boundary conditions at 100°F and insolation are considered in the cask model to bound the maximum accessible surface temperature under shade. The maximum accessible surface temperature of the ISO container is 147°F.

3.3.1.3 Effective Thermal Properties in TN-LC Transport Cask Model

1. Effective Heat Transfer Coefficient for Top and Bottom Gamma Shieldings

Air gaps of 0.0625 in. are considered between the gamma shielding and the top lid /bottom flange. These gaps account for contact resistance and fabrication imperfections between adjacent plates.

For simplification of the model, the axial and radial air gaps of 0.0625 in. are integrated into the gamma shielding using effective conductivities in both radial and axial directions.

The gaps and the plates built up serial thermal resistances in the axial direction and parallel resistances in the radial direction. The conductivity values are taken from Section 3.2.1.

The effective conductivity in the axial (serial) direction is:

$$k_{eff\_axial} = \frac{t_{plate} + n * t_{gap}}{\frac{t_{plate}}{k_{plate}} + \frac{n * t_{gap}}{k_{air}}}$$

The effective conductivity in the radial (parallel) direction is:

$$k_{eff\_radial} = \frac{k_{plate} * t_{plate} + k_{air} * n * t_{gap}}{t_{plate} + n * t_{gap}}$$

Where:

k_{eff_axial} = effective conductivity in axial direction (Btu/hr-in.-°F),

k_{eff_radial} = effective conductivity in radial direction (Btu/hr-in.-°F),

t_{plate} = thickness of gamma shielding = 4 in.,

t_{gap} = 0.0625 in. between the gamma shielding and the top lid /bottom flange,

k_{plate} = conductivity of gamma shielding,

k_{air} = conductivity of air (Btu/hr-in.-°F),

n = number of gaps,

= 2 for gaps between gamma shielding and the top lid /bottom flange.

The results for the effective heat transfer coefficients are summarized in Section 3.2.1, material 16.

2. Effective Conductivity for Air in ISO Container

Decay heat from the TN-LC transport cask is transferred across the air filled gap between the transport cask and the ISO container by natural convection and radiation. The natural convection that occurs across the gap is modeled using an effective conductivity. The effective conductivity for heat transfer across gap between two horizontal concentric cylinders is [22]:

$$\frac{k_{eff}}{k_{air}} = 0.386\left[\frac{\ln(D_o/D_i)}{b^{3/4}(1/D_i^{3/5}+1/D_o^{3/5})^{5/4}}\right]\left(\frac{Pr}{0.861+Pr}\right)^{1/4} Ra_b^{1/4},$$

$$2b = D_o - D_i,$$

$$Ra_b = \frac{g*\beta*\Delta T*b^3*\rho^2*C_p}{k*\mu},$$

Where:

k_{air} = Conductivity of air (W/m-K),

D_o = Outer Diameter = Height of the ISO container = 87 in.

D_i= Inner Diameter

= Outer Diameter of the Neutron Shield Shell for "Region 3" (See Figure 3-2) = 38.50 in.

= Outer Diameter of the Impact Limiter Shell for "Region 2" (See Figure 3-2) = 66.00 in.

g = gravitational constant =9.81 m/s^2,

T_i = Temperature of the transport cask surface,

T_o = Temperature of the ISO container,

ΔT = $T_i - T_o$ (K),

$T_{avg} = (T_i + T_o)/2$ (K),

β = expansion coefficient = 1/ T_{avg} (1/K),

μ = dynamic viscosity (kg-m/s),

ρ = density (kg/m^3),

C_p = specific heat (J/kg-K),

Pr = $\mu * C_p / k_{air}$.

The effective conductivity values for "Region 2" and "Region 3" are listed in Section 3.2.1 materials 17 and 18.

3. Effective Conductivity for Air Thermal Shield Area

A stainless steel thermal shield is welded inside of the shear block to protect the cask shell from direct exposure to fire in this area. The thermal shield is shown schematically below and consists of a 0.25 in. stainless steel plate supported by two long blocks with a 0.25 in. x 0.125 in. cross section. The long blocks provide an air gap of 0.125–in. gap between the cask outer shell and the thermal shield plate. A cross-sectional view of the region between the thermal shield and cask outer shell is shown below.

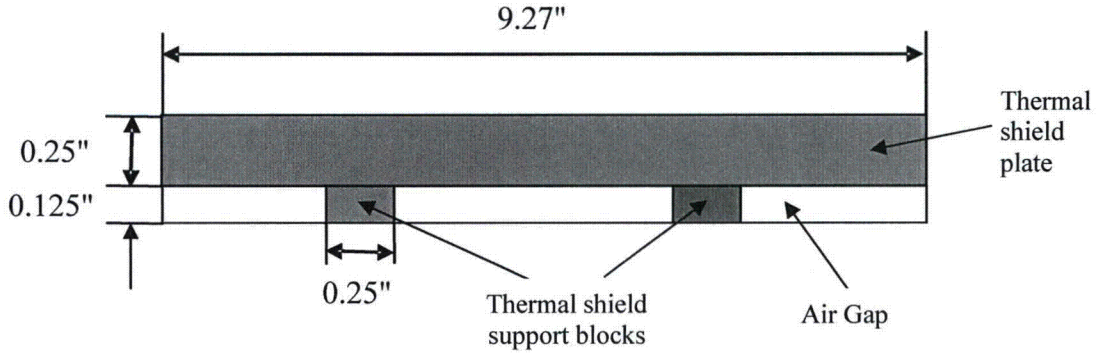

The effective thermal conductivity of the region between the thermal shield and cask outer shell across the 0.125–in. height gap can be calculated as follows when neglecting the thermal conductivity of the air:

$k_{eff} = (k_{steel} * A_2) / (\text{Total Area})$

Where:

k_{eff} = effective conductivity across the gap,

k_{steel} = thermal conductivity of the stainless steel,

Total Area = Area of the region = 9.27 in. × 0.125 in. = 1.15875 $in.^2$,

A_2 = Area of the stainless steel blocks = 2 × 0.25 ×.0.125 = 0.0625 $in.^2$.

The planar thermal conductivity of the gap, which is perpendicular to the gap height, is assumed to be that of air. Heat capacity for this region is conservatively ignored. Further, radiation between the inner surface of the shield plate and the outer surface of the cask is modeled using the AUX12 processor. The effective conductivity values across the gap between the thermal shield plate and cask outer shell are listed in Section 3.2.1, material 21.

3.3.1.4 TN-LC Fuel Basket Model

The following assumptions and conservatism are considered for the fuel basket model:

Commercial fuel assemblies (PWR, BWR or Fuel Pins) loaded in the TN-LC-1FA basket shall have a calculated maximum fuel cladding temperature in accordance with the guidance in ISG-11, Rev. 3, [2]. For NCT, the cladding temperature shall not exceed 400°C (752°F).

Research reactor fuel assemblies with aluminum cladding loaded in the TN-LC-NRUX/MTR/TRIGA basket shall have a maximum calculated cladding temperature less than 204°C (400°F) during NCT as specified in Section 3.1. This criterion is conservatively established to ensure the integrity of the aluminum cladding for NCT.

No convection is considered within the basket models.

The maximum inner shell temperatures resulting from the TN-LC transport cask model within an ISO container described in Section 3.3.1.1 are conservatively applied as uniform temperature boundary conditions in the fuel basket models.

The nominal cold radial gap of 0.25 in. between basket rail/shell and the cask inner shell is assumed conservatively for the hot conditions in the fuel basket models.

For the TN-LC-MTR basket model, a helium gap of 0.01 in. is considered between the basket rail and the outer plate to calculate effective conductivities of the outer plate in the cross section of the basket.

For the TN-LC-TRIGA basket model, 0.01 in. gaps on either side of the poison plates and wrap plates, and between any two adjacent plates are considered to calculate effective conductivities for these components in the cross section of the basket.

For the TN-LC-1FA basket models (including 1 PWR, 1 BWR and Pin-Can Types), 0.01 in. gaps on either side of the poison plates and between the basket rail and the frame plate are considered to calculate effective conductivities for these components in the cross-section of the basket.

The gaps between adjacent components are related only to the flatness and roughness tolerances of the plates. The micro gaps related to these tolerances are non-uniform and provide interference contact at some areas and gaps on the other areas as shown schematically in Figure 3-10.

For the purpose of thermal evaluation, surfaces of intermittent contact between adjacent components are conservatively modeled as a uniform gap of 0.01 in. Based on the MP197 SAR, Appendix A, Section A.3.6.7.4 [21], the assumed gap size of 0.01 in. is approximately two times larger than the contact resistances between the adjacent components and is therefore conservative.

Heat loads considered for the thermal analysis of the TN-LC fuel baskets, i.e., TN-LC-NRUX, TN-LC-MTR, TN-LC-1FA (Pin-Can), as listed in Table 3-14 are higher than the maximum allowable heat loads for the these baskets listed in Section 3.1.2. No axial heat transfer is considered through the basket to provide additional conservatism in calculation of the maximum fuel cladding and maximum component temperatures. This assumption includes additional conservatism in evaluation of the maximum temperature gradients through the basket.

For the TN-LC-1FA basket model, the fuel effective conductivity is selected based on the irradiated UO_2 fuel conductivity. The small differences between the irradiated UO_2, MOX, and EPR fuel conductivities have an insignificant impact on thermal evaluation of the TN-LC-1FA basket as shown in Appendix 3.6.7.

All other dimensions are based on nominal dimensions of TN-LC fuel baskets.

The thermal evaluation of the TN-LC transport cask determined that the maximum temperature of the cask inner shell during transportation with an ISO container is higher than that without an ISO container. The bounding maximum cask inner shell temperatures are rounded up to provide additional margin for conservatism. The resulting values are applied as uniform temperature boundary conditions to the fuel basket models. The uniform temperature boundary conditions used for the basket models are summarized in Table 3-15. The maximum cask inner shell temperature resulting for the TN-LC-MTR basket is used to evaluate TN-LC-TRIGA basket. Similarly, the maximum cask inner shell temperature resulting for TN-LC-IFA with PWR fuel assemblies is used to evaluate TN-LC-IFA with BWR or fuel pins. This approach is conservative as discussed in Section 3.3.1.1. The TN-LC-1FA pin-can basket with 3 kW heat load shows the largest maximum basket temperature gradient among all fuel baskets during hot NCT. Therefore, to bound the maximum basket temperature gradients for the TN-LC transport cask during cold NCT, the TN-LC-1FA pin-can basket for cold NCT with -40°F ambient and no insolation for 3 kW heat load is evaluated.

Decay heat load is applied as a uniform heat generation within a homogenized fuel region. The various heat loads used in this analysis are shown in the table below and are computed as follows:

$$q''' = \frac{Q}{A \times L_{Fuel}} \times PF$$

Where:

q''' = uniform heat generation rate (Btu/hr-in.^{3}),

Q = decay heat load per fuel element/assembly (Btu/hr),

A = area per fuel compartment (in.^{2}),

L_{Fuel} = active fuel length per fuel element/assembly (in.),

PF = peaking factor.

Heat Generation in Fuel Basket Model

Basket Type	Total Heat Load Per Basket (kW)	Heat Load per Element/Assembly (W)	Peaking Factor	Active Fuel Length per Element/Assembly (in.)	Heat Generation (Btu/hr-in.^{3})
TN-LC-NRUX	0.39	15/Assembly	1.0	96.0	0.135
TN-LC-MTR	1.62	30/Element	1.0	22.0 (1)	0.384
TN-LC-TRIGA	1.5	4x8.33/Element	1.0	14.0	0.671
TN-LC-1FA (BWR)	2.0	2000/Assembly	1.2	144.0	1.580
TN-LC-1FA (PWR)	3.0	3000/Assembly	1.1	144.0	0.993
TN-LC-1FA (Pin-Can)	3.0	3000/Can	1.1	144.0 (2)	3.128

Notes:
1. The shortest active fuel length is considered to bound all design basis MTR fuels listed in Chapter 1.
2. The active fuel length of 144 in. is typical for PWR and BWR fule rods and bounds the active fuel length for MOX and EPR fuel rods.

The material properties used in the basket models are listed in Section 3.2.1. Effective conductivity for basket plates is calculated in Section 3.3.1.5.

Except for the contact gaps described above in this section, all the other gaps considered in the fuel basket model are based on cold nominal gaps. The geometry of the models and their mesh densities are shown in Figure 3-11 and Figure 3-12. Mesh sensitivities of the basket models are discussed in Appendix 3.6.4.

Typical boundary conditions for the fuel basket model are shown in Figure 3-13.

3.3.1.5 Effective Thermal Properties for Basket Components

1. Effective Conductivity for Basket Poison, Wrap and Outer Plates

A helium gap of 0.01 in. is assumed between any two adjacent plates to account for contact resistance and fabrication imperfections between the plates.

The gaps in the plates build up serial thermal resistances through the thickness of the plates and parallel thermal resistances perpendicular to the thickness of the plates.

For conservatism in the calculation of the effective conductivity for the poison plates, the conductivity value of helium is based on the bounding value at 70°F (= 0.0072 Btu/hr-in.-°F). The conductivity value of the poison plate is based on 95 percent of the Boral core thermal conductivity at 500°F (=3.513 Btu/hr-in.-°F). No credit is taken for the conductivity through the aluminum cladding of the Boral plate.

The conductivities for the basket wrap (TN-LC-MTR basket) and outer plates (TN-LC-TRIGA basket) are taken from Section 3.2.1 based on stainless steel, SA-240 Type 304.

The effective conductivity in the transverse direction is:

$$k_{eff\_cross} = \frac{t_{plate} + n \times t_{gap}}{\frac{t_{plate}}{k_{plate}} + \frac{n \times t_{gap}}{k_{he}}}$$

The effective conductivity in the direction parallel to the plates is:

$$k_{eff\_along} = \frac{k_{plate} \times t_{plate} + k_{he} \times n \times t_{gap}}{t_{plate} + n \times t_{gap}}$$

Where:

k_{eff_cross} = effective conductivity in the transverse (cross) direction (Btu/hr-in.-°F),

k_{eff_along} = effective conductivity in the parallel (along) direction (Btu/hr-in.-°F),

t_{plate} = thickness of the plate (in.),

t_{gap} = 0.01 in. gap thickness between the two adjacent plates,

k_{plate} = conductivity of the plate (Btu/hr-in.-°F),

k_{he} = conductivity of helium at 80°F = 0.0072 Btu/hr-in.-°F,

n = number of gaps

= 1 for one side gap of the plate,

2 for two side gaps of the plate.

Effective conductivities for the poison plates and basket plates in the fuel basket models are listed in Section 3.2.1, materials 19 and 20.

3.3.2 Heat and Cold

The maximum component temperatures of the TN-LC transport cask for various heat loads without the ISO container for hot NCT for an ambient temperature of 100°F with insolation are listed in Table 3-9.

Based on the results presented in Table 3-9, the TN-LC transport cask with a 3 kW heat load bounds the maximum component temperatures. Therefore, for the TN-LC cask transported within an ISO container, only the TN-LC cask with 3 kW heat load is considered for analysis. The maximum component temperatures for hot NCT with 100°F ambient and insolation for the TN-LC cask within an ISO container with 3 kW heat load are listed in Table 3-10.

As shown in Section 3.3.1 and calculated in Section 3.3.1.2, the maximum accessible surface temperature without an ISO container with the maximum decay heat load of 3 kW, ambient temperature of 100°F and no insolation is 169°F.

For the TN-LC transport cask within an ISO container, the maximum temperature of the accessible surface, that is, the outer surface of the ISO container, is 147°F with the maximum decay heat load of 3 kW, ambient temperature of 100°F, and insolation.

These temperatures (169°F and 147°F) are below the maximum temperature of 185°F specified in [1] for the outer surfaces of the package under shade and, therefore, no personnel barrier is needed.

For the TN-LC transport cask with 3 kW heat load, the maximum temperature increase of cask components is 36°F (for the neutron shield resin) when the cask is transported within an ISO container compared to the cask transported without the ISO container. To bound the maximum component temperatures for the TN-LC transport cask with lower heat loads, the same temperature increase of 36°F is conservatively considered for all the components. Based on the results presented in Table 3-10, the maximum temperatures still remain below their respective temperature limits with the TN-LC cask transported in an ISO container with heat loads up to 3 kW.

For the TN-LC transport cask, the maximum temperature gradients occur when the cask is directly exposed to cold conditions. Therefore, the maximum temperature gradients for the cold conditions are based on the TN-LC transport cask without an ISO container.

As shown in Section 3.2.1, materials 17 and 18, a ΔT of 30°F and 5°F are assumed for the calculation of "Region 3" and "Region 2" effective conductivities, respectively. The temperature difference calculated between the average inner and outer surface of "Region 3" is significantly greater than the assumed 30°F. The assumed temperature differences are conservative since a lower temperature difference decreases the effective conductivity, thereby maximizing the peak temperatures.

The results presented in Table 3-9 indicate that the TN-LC cask with a 3 kW heat load bounds the maximum component temperatures. The maximum temperature gradients are also expected to be bounded by this heat load. Therefore, the TN-LC transport cask with 3 kW heat load case is selected to determine the maximum temperature gradients through the cask. The maximum component temperatures for cold NCT at -20°F and -40°F ambient temperatures without insolation are listed in Table 3-4.

The maximum temperatures of the major TN-LC cask components, summarized from Table 3-9, Table 3-10 and Appendix 3.6.3, are shown in Table 3-1. The effect of the inner/outer shell and top/bottom flange material change on the ANSYS thermal model and the results are evaluated in the Appendix 3.6.3. Based on the results of the sensitivity analysis presented in Appendix 3.6.3, 1°F was conservatively added to all maximum component temperatures shown in Table 3-1.

Table 3-1 shows that the maximum calculated temperatures of the TN-LC cask components for NCT are lower than the allowable limits.

The seal O-rings are not explicitly considered in the models. The maximum seal temperatures are retrieved from the models by selecting the nodes at the locations of the corresponding seal O-rings. The maximum seal temperature of 205°F (96°C) for NCT is below the long-term limit of 400°F (204°C) specified for continued seal function.

The maximum neutron shield temperature calculated is 216°F (102°C) for NCT, which is below the long-term limit of 320°F (160°C). No degradation of the neutron shielding is expected.

The maximum temperature of the gamma shielding is 237°F (114°C) for NCT which is well below the melting point of lead, 621°F (327°C).

The predicted maximum aluminum fuel cladding temperature of 266°F (130°C) with the maximum heat load of 3 kW is well within the allowable fuel temperature limit of 400°F (204°C) for NCT.

The predicted maximum zircaloy fuel cladding temperature of 542°F (283°C) with the maximum heat load of 3kW is well within the allowable fuel temperature limit of 752°F (400°C) for NCT.

The temperature distributions for NCT with 100°F ambient and insolation are shown in Figure 3-8 and Figure 3-9.

Under the minimum ambient temperature of -40°F (-40°C), the resulting packaging component temperatures will approach -40°F if no credit is taken for the decay heat load. Since the package materials, including containment structures and the seals, continue to function at this temperature, the minimum temperature condition has no adverse effect on the performance of the TN-LC transport cask.

The maximum component temperatures for ambient temperatures of -40°F and -20°F with maximum decay heat of 3 kW and no insolation are calculated for the TN-LC transport cask to use for structural evaluations. These temperatures are listed in Table 3-4.

The average temperatures of helium gas in the cask cavity and the average temperatures of fuel assemblies and helium within the TN-LC cask cavity for NCT are listed in Table 3-11. These temperatures are used to evaluate the maximum internal pressures within the TN-LC transpoprt cask.

Thermal stresses for the TN-LC transport cask loaded with the various payloads are discussed in Chapter 2. The maximum normal operating pressure for the TN-LC transport cask is discussed in Section 3.3.3. The performance of the TN-LC transport cask loaded with the various payloads during HAC is discussed in Section 3.4.

The maximum temperatures for fuel cladding and fuel basket components with the ISO container for hot NCT (ambient temperature of 100°F with insolation) are listed in Table 3-16. A summary of these temperatures is shown in Table 3-2.

Typical temperature distributions for fuel baskets are shown in Figure 3-14 and Figure 3-15.

Table 3-17 lists the maximum basket temperature gradients during hot NCT.

The resulting maximum temperatures for the fuel basket and fuel cladding, and maximum basket temperature gradient (ΔT_{basket}) based on TN-LC-1FA pin-can basket for cold conditions (-40°F ambient and no insolation), are listed in Table 3-18.

Table 3-17 shows that the maximum basket temperature gradient (ΔT_{basket}) for hot NCT is 139°F for the TN-LC-1FA pin-can basket and 56°F for other fuel baskets. However, the worst case condition for the bounding maximum basket temperature gradient is cold NCT with -40°F ambient. As can be seen from Table 3-18, the bounding maximum basket temperature gradient (ΔT_{basket}) during the worst case condition (cold NCT, -40°F ambient) is 181°F for the TN-LC-1FA 25-pin-can basket. The maximum basket temperature gradient difference between hot and cold NCT (181°F-139°F=42°F) for the TN-LC-1FA pin-can basket combined with the bounding maximum basket temperature gradient (ΔT_{basket}) for other fuel baskets during the worst case condition (cold NCT, -40°F ambient) is calculated as 98°F (56°F+42°F). The conservative basket temperature gradient limit with additional margins ($\Delta T_{basket, limit}$) used for fuel basket maximum stress evaluation is summarized in Table 3-5.

The minimum temperatures for fuel cladding and fuel basket components during NCT are bounded by a daily average ambient temperature of -40°F based on assuming no credit for decay heat for fuel contents in fuel baskets.

The maximum fuel cladding temperatures calculated for the TN-LC-NRUX/MTR/TRIGA basket in TN-LC transport cask for NCT and shown in Table 3-2, are lower than the allowable limit of 400°F. The maximum fuel cladding temperatures calculated for the TN-LC-1FA basket loaded with a PWR/BWR/Pin-Can in the TN-LC transport cask for NCT are lower than the allowable limit of 752°F.

The minimum temperatures for fuel cladding and basket components are based on assuming no credit for decay heat for cold NCT and are summarized Table 3-3.

The maximum fuel cladding and basket component temperatures for cold NCT at -20°F ambient are bounded by those for hot NCT with 100°F shown in Table 3-2.

The maximum temperatures for fuel cladding and basket components for cold conditions at -40°F ambient are summarized in Table 3-5. The maximum basket temperature gradient for cold NCT at -40°F ambient conditions shown in Table 3-5 bounds that for cold NCT at -20°F ambient conditions.

All materials can be subjected to a minimum environment temperature of -40°F (-40°C) without any adverse effects.

3.3.3 Maximum Normal Operating Pressure

The maximum internal pressure for the TN-LC cask for NCT and HAC is determined based on the maximum allowable heat load of 3 kW and a maximum burnup of 70,000 MWD/MTU. The limiting fuel assembly type considered in this evaluation is the B&W 15x15 assembly.

The calculations account for the cask cavity free volume, the quantities of backfill gas, fuel rod fill gas, fission products and the average cask cavity gas temperature. The ideal gas law is then used to determine the amount of gasses in the cask cavity and the internal cask cavity pressure.

The quantities of helium backfill in the cask cavity and gases released from fuel rods, including fission products and helium fill gas contained in the fuel rods, are determined using the ideal gas law.

The resulting cask cavity pressure during NCT is then determined using the quantities of gases calculated, the cask cavity free volume, and the average cavity gas temperature.

The following assumptions are considered to determine the maximum pressures within the cask during NCT loaded with the various payloads.

- All dimensions used in calculating the maximum pressures are nominal.
- 98 percent of the cask cavity free volume is conservatively used in calculating the maximum pressures.
- The initial temperature of helium backfill in the cask cavity is assumed to be 70°F.
- The maximum initial pressure of the helium backfill in the cask cavity is 3.5 psig.
- The TN-LC cask is capable of transporting PWR, BWR, fuel pins, NRX/NRU, MTR and TRIGA fuel assemblies (FAs) in various types of baskets such as TN-LC-1FA, TN-LC-NRUX, TN-LC-MTR and TN-LC-TRIGA. Thermal analysis of the various baskets presented in this Chapter shows that both the maximum heat load as well as the maximum temperatures are bounded by the TN-LC-1FA basket. The maximum fuel cladding temperature and the maximum average helium temperature within the TN-LC cask cavity occur when the basket is loaded with fuel pins at 3.0 kW. However, the maximum pressure within the TN-LC cask cavity occurs when the cask is loaded with a PWR FA since this has the highest number of fuel rods with the largest amount of fission/fill gases. Therefore, the maximum pressures for the TN-LC cask are computed for the TN-LC cask with 1 PWR FA.
- Based on the analysis presented in Appendix M, Section M.4.4.4.1 of [25] B&W 15x15 has the bounding characteristics for calculating the maximum internal pressures and is used as the bounding PWR FA.
- The maximum burnup for the FA/fuel pins is limited to 62,500 MWd/MTU. However the maximum pressure for NCT are calculated assuming a burnup of 70,000 MWd/MTU. This is a conservative assumption since it increases the amount of fission gases.

The total free gas in a fuel rod, which includes fuel rod fill gas and gases released because of irradiation for bounding B&W 15x15 FA, is provided in Table 7-14 of [23] for a maximum burnup of 55000 MWd/MTU as shown in the table below. The volume of gas has been linearly extrapolated to the maximum burnup of 70,000 MWd/MTU considered for the PWR FA in a TN-LC transport cask.

Amount of Gas Released from Fuel Rods (B&W 15x15 FA)

Burnup, MWd/MTU	Total Free Gas at STP, cm^3
55,000	1400 [23]
70,000	1782 (Extrapolated)

The bounding volume of 5,935 $in.^3$ computed for 1 B&W 15x15 FA with control components (CC) calculated in Appendix M, Section M.4.4.4.2 of [25] is used.

The bounding maximum average temperature for the helium within the TN-LC cask cavity for NCT is 282°F and the maximum average fuel temperature shown in Table 3-11 is 455°F at the hottest cask cross-section.

The bounding maximum average helium temperature calculated in Section 3.4 for the TN-LC cask cavity for HAC is 480°F and the maximum average fuel temperature shown in Table 3-11 is 617°F at the hottest TN-LC cask cross-section.

The TN-LC cask cavity internal pressure is calculated for the most limiting normal and accident cases. For these cases, 3 percent and 100 percent of the fuel rods are assumed to rupture. Also, 100 percent of the fuel rod helium fill gas and 30 percent of the fission gases are assumed to be released into the cask cavity [24].

1. Cask Cavity Free Volume

The free volume of the TN-LC cask cavity, $V_{free,cavity}$, is calculated as:

$$V_{free,cavity} = (V_{cavity} - V_{basket} - V_{FA}) * 0.98$$

$$= (\frac{\pi}{4} ID_{Cask}{}^2 * L_{TC} - V_{basket} - V_{FA}) * 0.98$$

$$= (\frac{\pi}{4} 18^2 * 182.50 - 28{,}843 - 5935) * 0.98$$

$$= 11{,}429 \text{ in.}^3.$$

Where:

ID_{Cask} = Inner diameter of the cask inner shell = 18 in.,

L_{TC} = TN-LC cask cavity length = 182.50 in.,

V_{cavity} = Volume of TN-LC cask cavity,

V_{basket} = Volume of TN-LC-1FA basket for 1 PWR FA = 28,843 $in.^3$ (from Chapter 2),

V_{FA} = Bounding volume of 1 B&W 15x15 FA with CC = 5935 $in.^3$ [25].

2. Average Helium Temperature for NCT and HAC

The average volumetric helium temperature in the cask cavity is calculated based on average temperatures of the fuel and the helium elements at the hottest cross section of the basket from Section 3.3.1.4 and the volume of the helium within the fuel compartment and also the volume of the helium outside the fuel compartment. The following equation is used to calculate the average helium temperatures in the cask cavity and the computed values are summarized in the Table 3-11:

$$T_{avg,he} = \frac{T_{FA} * V_{he\_FA} + T_{he} * V_{he\_cavity}}{V_{free,cavity}}$$

$$= \frac{T_{FA} * (a_{comp}{}^2 * L_{TC} - V_{FA}) + T_{he} * [V_{free,cavity} - (a_{comp}{}^2 * L_{TC} - V_{FA})]}{V_{free,cavity}}.$$

3. Quantity of Helium Fill Gas in the Cask Cavity

The TN-LC cask cavity free volume is assumed to be filled with $P_{initial}$ = 3.5 psig (18.2 psia) of helium. The helium average initial temperature of 70°F is used to estimate the amount of helium in the cask cavity. Using the ideal gas law,

$PV = nRT,$

$n = PV / RT,$

The number of moles of helium in the cask cavity is:

$$n_{he,Initial} = \frac{P_{initial} * (6894.8\ Pa/psi) * V_{free,cavity} * (1.6387 * 10^{-5}\ m^3/in.^3)}{R * T_{avg,He}(5/9\ K/°R)}$$

$$= \frac{18.2\ psia * (6894.8\ Pa/psi) * 11{,}429\ in.^3 * (1.6387 * 10^{-5}\ m^3/in.^3)}{8.314\ J/(mol-K) * 530°R\ (5/9\ K/°R)}$$

$$= 9.6\ g-moles.$$

Where:

$n_{he,initial}$ = number of moles of helium in TN-LC cask cavity, g – moles,

$T_{avg,He}$ = Initial average temperature of helium = 70°F (530°R),

R = Universal gas constant, 8.314 J/(mol – K),

$V_{free,cavity}$ = Free volume of TN-LC cask cavity = 11,429 $in.^3$.

4. Release of Helium Fill/Fission Gas from Fuel Assembly

The maximum total volume of the fission gases released from a fuel rod is assumed to be 1,782 cm^3 at STP and there are a maximum of 208 fuel rods for the bounding B&W 15x15 FA. Per the ideal gas law, the quantity of fission gases released from 208 fuel rods in 1 PWR FA ($n_{free\text{-}FA}$) is:

$$n_{free-FA} = \frac{P_{STP} * (6894.8\ Pa/psi) * V_{fill,gas} * (0.061\ in.^3/cm^3)(1.6387 * 10^{-5}\ m^3/in.^3)}{R * T_{STP}(5/9\ K/°R)} * 208$$

$$n_{free-FA} = \frac{14.7\ psia * (6894.8\ Pa/psi) * 1782\ cm^3 * (0.061\ in.^3/cm^3)(1.6387 * 10^{-5}\ m^3/in.^3)}{8.314\ J/(mol-K) * 492°R * (5/9\ K/°R)} * 208$$

$$n_{free-FA} = 16.52\ g-moles.$$

Where:

P_{STP} = Standard pressure = 14.7 psia,

T_{STP} = Standard temperature = 273.15 K = 32°F (492°R),

R = Universal gas constant, $8.314\ J/(mol-K)$,

$V_{fill,gas}$ = Volume of fill gas per FA = 1,782 cm^3.

Based on the maximum fraction of the fuel rods assumed to rupture for normal (3 percent) and accident conditions (100 percent), Table 3-12 summarizes the total amount of fuel rod fill gases released into the TN-LC cask cavity for normal and accident conditions of transport.

5. Release of Helium Fill Gas from Control Components (CCs)

The TN-LC transport cask may include CCs. The evaluation of gas quantities for CCs is based on the B&W15x15 FAs documented in [25]. For 1 FA a total of 2.24 g-moles of gas could be released to the TN-LC cask cavity assuming 100 percent cladding rupture (based on 53.8 g-mol for 24 FAs in the 24P DSC, from [25] Appendix J, Section J.4.4). Table 3-13 summarizes the total amount of fuel rod fill gases released into the TN-LC cask cavity from the CCs for normal conditions.

6. Maximum Normal Operating Pressure Calculation

The total amount of gas in the TN-LC cask cavity for NCT, $n_{he,NCT}$, is calculated as follows:

$$n_{he,NCT} = n_{he,initial} + n_{Free-FA,NCT} + n_{CC-NCT}$$
$$= 9.6 + 0.50 + 0.07$$
$$= 10.17\ g-moles.$$

Where:

$n_{he,initial}$ = number of moles of helium fill gas in cask cavity, g-moles,

$n_{Free-FA,NCT}$ = number moles of fuel rod fill/fission gas released for NCT, g-moles,

n_{CC-NCT} = number of moles of fill gas released from CCs for NCT, g-moles.

The maximum pressure in the cask cavity for NCT, P_{NCT}, is calculated as:

$$P_{NCT} = \frac{\left(1.4504*10^{-4}\ \frac{psia}{Pa}\right)*(n_{he,NCT})*R*T_{avg,he,NCT}*(5/9\ K/^{\circ}R)}{V_{free,cavity}*(1.6387*10^{-5}\ m^3/in.^3)}$$

$$= \frac{\left(1.4504*10^{-4}\ \frac{psia}{Pa}\right)*(10.17\ g-moles)*(8.314\ J/mol-K)*(870^{\circ}R)*(5/9\ K/^{\circ}R)}{(11{,}429\ in.^3)*(1.6387*10^{-5}\ m^3/in.^3)}$$

$$= 31.6\ psia = 16.9\ psig.$$

Where:

$T_{avg,he,NCT}$ = Average Temperature of Helium in TN-LC cask cavity for NCT = 410°F (870°R) (See Table 3-11).

The maximum pressure for NCT is shown in Table 3-8. The maximum internal pressure in the TN-LC cask for the bounding payload is lower than the pressure used in structural evaluation in Chapter 2.

3.3.4 Thermal Evaluation for Loading/Unloading Operations

The loading operations for PWR/BWR fuel assemblies occur inside the pool when the TN-LC cask is in vertical orientation. Vacuum drying is considered as a normal condition for wet loading operations. The loading operations for PWR/BWR fuel pins and research reactor fuel elements occur in a dry environment while the TN-LC cask is in vertical or horizontal orientation.

Except for the fuel pins, the unloading operations occur inside a pool with the cask in the vertical orientation. The bounding wet unloading operation is the reflood of the TN-LC cask with water. Unloading the fuel pins occurs in a dry environment inside a hot cell with the cask most likely in a horizontal orientation.

This section evaluates the loading/unloading operations described above and selects the bounding conditions to determine the maximum component temperatures including the maximum fuel cladding temperature.

3.3.4.1 Wet Loading/Unloading

The operations for wet loading of PWR/BWR fuel assemblies occur when the TN-LC cask is located vertically inside the spent fuel pool. The fuel assembly is always submerged in free-flowing pool water permitting heat dissipation. After completion of fuel loading, the TN-LC cask is removed from the pool and drained, dried, sealed and backfilled with helium. Helium is used as the medium either to replace air during draining or to force the water out of the cask cavity. The subsequent vacuum drying occurs with a helium environment in the cask cavity. The vacuum drying operation does not reduce the pressure sufficiently to reduce the thermal conductivity of the helium in the cavity ([25], Appendix T, Section T.4).

The bounding operation for wet loading is the vacuum drying when the TN-LC cask is out of the spent fuel pool. During vacuum drying, no impact limiter is attached to the cask and the cask body upper and lower segments beyond the neutron shield are open to the environment for heat dissipation. With helium being present during vacuum drying operations and larger heat dissipation areas, the maximum cask component temperatures and, consequently, the maximum basket and fuel cladding temperatures are bounded by those calculated for NCT in Section 3.3. Therefore, no additional thermal evaluation is needed for wet loading operations.

The presence of helium during blowdown and vacuum drying operations eliminates the thermal cycling of fuel cladding during helium backfilling of the cask cavity subsequent to vacuum drying. Therefore, the thermal cycling limit of 65°C (117°F) for short-term operations set by ISG-11 [2] is satisfied for vacuum drying operation in the TN-LC transport cask.

The bounding wet unloading operation considered is the reflood of the cask cavity with water. For wet unloading operations, the cask is filled with the spent fuel pool water through its drain port. During this filling operation, the cask vent port is maintained open with effluents routed to the plant's off-gas monitoring system.

The maximum fuel cladding temperature during the reflooding event is significantly less than the vacuum drying condition owing to the presence of water/steam in the cask cavity. Based on the above rationale, the maximum cladding temperature during the unloading operation is bounded by the maximum fuel cladding temperature for the vacuum drying operation.

Initially, the pool water is added to the cask cavity containing hot fuel and basket components; some of the water will flash to steam causing internal cavity pressure to rise. This steam pressure is released through the vent port. The procedures specify that the flow rate of the reflood water be controlled such that the internal pressure in the cask cavity does not exceed the maximum pressure specified for reflooding operations. This is assured by monitoring the maximum internal pressure in the cask cavity during the reflood event. The reflood for the TN-LC cask is considered as a Service Level D event and the cask cavity pressures used for structural evaluation are well above the specified reflood pressure. Therefore, there is sufficient margin in the cask internal pressure during the reflooding event to assure that the TN-LC cask will not be over pressurized.

3.3.4.2 Dry Loading/Unloading

During dry loading/unloading, the impact limiters are detached from the TN-LC cask and the cask body upper and lower segments beyond the neutron shield are open to environment for heat dissipation. In addition, the loading/unloading operations occur within a building which protects the cask from direct solar impact. Therefore, the ambient boundary conditions specified for NCT in Section 3.3 remain bounding for the dry loading/unloading operations.

The TN-LC transport cask model for NCT described in Section 3.3.1.1 does not include the baskets and applies the heat load as a uniform heat flux on the inner surface of the inner shell of the cask. Since this model does not include the basket and the helium backfill, the boundary conditions considered for the TN-LC transport cask model are bounding for dry loading/unloading operations and the resulting cask temperatures for NCT in Section 3.3.2 bound those for dry loading/unloading conditions.

Based on the above discussion, the cask inner shell temperatures resulting from the TN-LC transport cask model without the ISO container can be used conservatively to determine the maximum basket component and fuel cladding temperatures for dry loading/unloading conditions. The maximum cask inner shell temperatures for NCT conditions without the ISO container are 204°F and 166°F for 3 kW and 1.85 kW heat loads, respectively, as reported in Table 3-9. For conservatism, cask inner shell temperatures of 210°F and 170°F are used in this calculation for evaluation of the TN-LC-1FA pin-can and TN-LC-MTR baskets under dry loading/unloading conditions.

The TN-LC-1FA fuel pin basket and TN-LC-MTR basket models described in Section 3.3.1.4 are used in this calculation to determine the bounding maximum basket component and fuel cladding temperatures for fuel pins and research reactor fuels under dry loading/unloading conditions. The properties of backfill gas in these models are changed from helium to air in order to simulate the dry loading/unloading conditions. The effective fuel conductivities in these basket models were calculated in Appendix 3.6.6 considering helium as backfill gas. For evaluation of the dry loading/unloading conditions, the effective conductivities of fuel pins and MTR fuel elements are recalculated considering air as backfill gas. The fuel assembly models described in Appendix 3.6.6 are used for recalculation of the effective fuel conductivities for dry loading/unloading conditions. The same methodology as described in Appendix 3.6.6 is used in this section to determine the effective fuel conductivities.

Steady state conditions are considered for dry loading/unloading conditions. Therefore, no time limits are applicable for these operations.

The following temperature limits are considered as design criteria for the evaluation of loading/unloading conditions:

- For commercial fuel assemblies (PWR, BWR or Fuel Pins) loaded in the TN-LC-1FA basket, the fuel cladding temperature is limited to 400°C (752°F). For short-term operations, such as vacuum drying, temperature differences greater than 65°C (117°F) are not permitted for repeated cycling of fuel cladding temperature during drying and backfilling operations in accordance with guidance provided by ISG-11, Rev 3 [2].

- For research reactor fuel assemblies with aluminum cladding loaded in the TN-LC-NRUX/MTR/TRIGA basket, the cladding temperature shall not exceed 204°C (400°F). This criterion is considered conservatively to ensure the integrity of the aluminum cladding for loading/unloading conditions.

An average ambient temperature of 100°F is considered for dry loading/unloading conditions, which is consistent with the maximum hot temperature considered for NCT in Section 3.3.

The maximum allowable heat load of 3 kW is considered for the evaluation of commercial fuels, PWR, BWR, and fuel pins for loading/unloading conditions. Based on Table 3-9, the bounding (highest) heat load for research reactor fuels resulting in the highest maximum cask component temperatures belongs to the MTR basket. The results of the basket analysis reported in Table 3-2 also shows that the maximum basket component temperatures are bounded by the TN-LC-MTR basket. Although, the maximum fuel cladding temperature reported in Table 3-2 is for the TRIGA fuel elements, among all the research reactor fuels, the maximum temperature of the MTR fuel is only 4°F lower and the difference is not significant. Therefore, the TN-LC transport cask with the MTR basket is considered in this calculation to determine the bounding maximum basket component and fuel cladding temperatures for research reactor fuels under loading/unloading conditions. The maximum heat load of 1.85 kW was considered conservatively for the TN-LC-MTR basket in the TN-LC transport cask model described in Section 3.3.1.1. The maximum heat load of 1.62 kW was considered in the basket model described in Section 3.3.1.4. The same heat loads are considered in this evaluation for calculation of the maximum basket and fuel cladding temperatures for the TN-LC-MTR basket for conservatism. The maximum allowable heat load for TN-LC-MTR basket is 1.50 kW.

Material properties used in this calculation are the same as those used for the TN-LC transport cask, TN-LC-1FA basket, and TN-LC-MTR basket except that air properties are used instead of helium for the backfill gas. The effective conductivities for the poison and wrap plates are calculated assuming air gaps instead of helium gaps using the same methodologies described in Section 3.3.1.5 and material properties from Section 3.2.1. The resulting values of these effective conductivities are listed in the tables below.

Effective Conductivity for Poison Plates in TN-LC-1FA Basket

For TN-LC-1FA Basket	**Air Gap**	**Poison**	**Poison + 0.02 in. Air Gap**	
Temperature (°F)	K (Btu/hr-in.-°F)	K (Btu/hr-in.-°F)	K_eff_cross (Btu/hr-in.-°F)	Keff_along (Btu/hr-in.-°F)
All Ranges	0.0013	3.513	0.016	3.232

Effective Conductivity for Outer Plates in TN-LC-MTR Basket

For TN-LC-MTR Basket	Air Gap	SA-240 Type 304	Outer Plate + 0.01 in. Gap	
Temperature (°F)	K (Btu/hr-in.-°F)	K (Btu/hr-in.-°F)	K_eff_cross (Btu/hr-in.-°F)	Keff_along (Btu/hr-in.-°F)
100	0.0013	0.725	0.087	0.715
200	0.0015	0.775	0.098	0.765
300	0.0017	0.817	0.109	0.806
400	0.0018	0.867	0.120	0.855
500	0.0020	0.908	0.130	0.896
600	0.0022	0.942	0.140	0.929
700	0.0023	0.983	0.150	0.970
800	0.0025	1.025	0.159	1.012
1000	0.0028	1.092	0.177	1.077

Since the dry loading/unloading is assumed to occur in air, the transverse effective conductivities of fuel assemblies for fuel pins and MTR fuel elements are determined with air conductivity in this calculation using the same methodologies described in Appendix 3.6.6. The calculated transverse fuel effective thermal conductivity of MTR fuel elements and fuel pins with air as backfill gas are listed the table below.

Transverse Effective Fuel Conductivities in Air

MTR		1FA (Fuel Pins)	
T_{avg}	k_{eff}	T_{avg}	k_{eff}
(°F)	(Btu/hr-in.-°F)	(°F)	(Btu/hr-in-°F)
114	0.0135	273	0.0144
210	0.0186	351	0.0165
308	0.0252	433	0.0187
406	0.0334	518	0.0212
504	0.0433	605	0.0238
603	0.0548	694	0.0266
703	0.0681	784	0.0296
802	0.0830	876	0.0326

The maximum component temperatures of the bounding cases for dry loading/unloading conditions are listed in Table 3-19. Table 3-20 shows a comparison between the maximum fuel cladding temperatures from Table 3-19 and the corresponding values resulting for NCT with helium backfill from Table 3-2.

As shown in Table 3-20, the maximum fuel cladding temperatures for commercial fuels increases by 177°F during dry loading/unloading operations when the fuel is transferred from the low temperature under helium backfill gas to the high temperature under air or vice versa. Since

this change in temperature occurs only once during loading/unloading steps, this change is not considered as repeated cycling of fuel cladding temperature and, therefore, the thermal cycling limit of 65°C (117°F) for short-term operations set by ISG-11 [2] is satisfied.

Typical temperature distributions for the TN-LC-MTR and TN-LC-1FA (Pin-Can) baskets for dry loading/unloading conditions are shown in Figure 3-16.

As discussed above, the maximum cask component, basket component, and fuel cladding temperatures for wet loading operations are bounded by those calculated for NCT in Section 3.3. Therefore, no additional thermal evaluation is needed for wet loading operations. The bounding wet unloading operation is the reflood of the cask cavity with water. For this operation, procedural controls assure that the cask will not be over pressurized. The maximum fuel cladding temperature during wet unloading operation remains bounded by the maximum fuel cladding temperature for NCT.

The maximum cask component temperatures for dry loading/unloading conditions are bounded by the NCT as discussed above.

The maximum fuel cladding and basket component temperatures resulting from the bounding cases discussed for dry loading/unloading conditions are listed in Table 3-19.

3.4 Thermal Evaluation under Hypothetical Accident Conditions

The thermal performance of the TN-LC transport cask loaded with the bounding payload of a PWR fuel assembly with a heat load up to 3 kW, is evaluated in this section under the HAC described in 10CFR71.73 [1]. This evaluation is performed primarily to demonstrate the containment integrity of the TN-LC transport cask for HAC. This is assured by demonstrating that the long-term and short-term O-ring seal temperature in the cask lid and cask bottom forging remain below 400°F (204°C) and 482°F (250°C), respectively, the gamma shielding remains below 621°F (327.5°C), melting point of lead, and the cask cavity pressure is less than the pressure used in structural evaluation as specified in Section 3.1.

The finite element model of the TN-LC transport cask developed in Section 3.3.1.1 is modified in this evaluation to determine the maximum component temperatures for HAC. For the transient runs considering HAC conditions, the model includes a homogenized basket, fuel region, thermal shield and basket-to-inner shell gap. SOLID70 elements are used to model the homogenized region. The elements for other components are the same as those described in Section 3.3.1.1.

Since the ISO container prevents the fire from direct access to the cask, the TN-LC cask without ISO container is considered for HAC analysis to bound the maximum temperatures.

Ambient conditions for HAC are based on 10CFR71 [1] requirements and are applied on the boundaries of the cask model. These conditions are listed below.

Hypothetical Accident Condition for TN-LC Transport Cask

Period	Ambient Temperature (°F)	Insolation	Duration (hr)
Initial Conditions	100	Yes	N/A
Fire	1475	No	0.5
Cool-Down	100	Yes	N/A

The assumptions and conservatism considered in evaluation for HAC are described in Sections 3.4.1 and 3.4.2.

3.4.1 Initial Conditions

The initial temperatures for the TN-LC transport cask transient model before the fire accident are determined using the same boundary conditions for NCT (100°F ambient with insolation) described in Section 3.3.1.1. For normal conditions of transport, the maximum temperature for the TN-LC transport cask without an ISO container occurs when the cask is loaded with a PWR fuel assembly and a maximum heat load of 3 kW. These conditions are reanalyzed with a homogenized basket and the resulting temperatures are used as initial conditions in this analysis to bound the maximum temperatures of the cask for HAC. The decay heat load is applied as a uniform heat generation rate over the homogenized basket for the transient runs.

$$q''' = \frac{Q}{(\pi/4)\, D_i^2\, L_b} = 0.279 \text{ Btu/hr-in.}^3,$$

Where:

q''' = decay heat generation rate (Btu/hr-in.^{3}),

Q = decay heat load, 3.0 kW = 10237 Btu/hr,

D_i = inner shell diameter = 18 in.,

L_b = active fuel length = 144 in.

All the assumptions and conservatism described in Section 3.3.1.1 for the TN-LC transport cask model are valid for determination of initial conditions.

3.4.2 Fire Test Conditions

No fire test is performed. Instead, the fire conditions are simulated using the finite element model of the TN-LC transport cask. The geometry of the model and its mesh density are shown in Figure 3-17. Typical boundary conditions for the model are shown in Figure 3-18 and Figure 3-19.

Based on the requirements in 10CFR71.73 [1], a fire temperature of 1,475°F, fire emissivity of 0.9 and a period of 30 minutes are required to be used for the fire conditions, however, and emissivity of 1.0 is conservatively used in the evaluation. A bounding forced convection coefficient of 4.5 Btu/hr-ft^2-°F is used during the burning period based on data from reference [27]. Surface emissivity of 0.8 is used for the packaging surfaces exposed to the fire based on 10CFR71.73 [1]. During the cool-down period, an emissivity of 0.9 is used for the transport cask external surfaces, as justified in Section 3.2.1, Material 22.

The total heat transfer coefficient during the fire is determined using the following equations.

$$h_{t,fire} = h_{r,fire} + h_{c,fire}$$

Where:

$h_{r,fire}$ = fire radiation heat transfer coefficient (Btu/hr-in.^{2}-°F)

$h_{c,fire}$ = forced convection heat transfer coefficient during fire = 4.5 Btu/hr-ft^2-°F

The radiation heat transfer coefficient, $h_{r,fire}$, is given by the equation:

$$h_{r,fire} = \varepsilon_w F_{wf} \left[\frac{\sigma(\varepsilon_f T_f^4 - T_w^4)}{T_f - T_w} \right] \quad \text{Btu/hr-in.}^2\text{-°F}$$

Where:

ε_w = transport cask outer surface emissivity = 0.8 [1]

ε_f = fire emissivity = 1.0

F_{wf} = view factor from transport cask surface to fire = 1.0

$\sigma = 0.1714 \times 10^{-8}$ Btu/hr-ft^2-°R^4

T_w = surface temperature (°R)

T_f = fire temperature = 1475°F = 1,935°R

The following modifications to the ANSYS model used for NCT were made to maximize the heat input from the fire toward the cask during the fire period to bound the maximum temperatures during the cool-down period.

- The thermal properties of the gaps used for initial conditions are changed to the properties for one of the adjacent components. The thermal properties of these gaps are restored after the fire during the cool-down period. These gaps are listed in Table 3-21.

- The neutron shield resin remains intact during the fire period. After the fire, the neutron shield is decomposed and charred but for conservatism air (conduction only) was substituted for the neutron shield resin material in the ANSYS model during the cool-down period.

The impact limiters of the TN-LC transport cask model are modified to reflect deformation due to the drop accidents. The crush depths of the impact limiters are determined in Chapter 2 based on end, side, corner, and slap down accident drops. The minimum distances between the cask and the surface of the damaged impact limiters are recalculated based on the crush depths given in Chapter 2 and are as follows:

- The minimum axial thickness of the impact limiter from the top lid/bottom flange after the HAC drop is 7.0 in..

- The minimum radial thickness of the impact limiter after the HAC drop is 5.5 in.

Since the impact limiter deformations are considered uniformly in all directions, the thermal model conservatively bounds the deformations determined in Chapter 2.

Although the impact limiters are locally deformed during the drop accident, they remain attached to the cask. Since the impact limiter shell welds do not break, the wood within the impact limiter shell cannot access air and would char but not burn during the hypothetical fire accident. Hence, the steel encased wood impact limiters still protect the bottom plate and the lid of the cask from the external heat input caused by the fire.

Although unlikely, the worst-case assumed damage due to a hypothetical puncture condition based on 10CFR71.73 [1] may result in the outer steel skin of the impact limiter being torn off, wood being crushed out of the damaged area, and exposure of the partially contained wood to the hypothetical fire conditions.

Based on the standard fire test (ASTM E119, 1988) reported in [26], if a thick piece of wood is exposed to fire temperatures between 815°C and 1,038°C (1,500°F and 1,900°F), the outermost layer of wood is charred. At a depth of 13 mm (~0.5 in.) from the active char zone, the wood is

only 105°C (220°F). This behavior is due to the low conductivity of wood and fire retardant characteristics of the char.

It is also shown that the char forming rate under high temperature fire conditions is between 37 mm/hr for soft woods and 55 mm/hr for hard woods. Redwood has a char rate of 46 mm/hr [26]. However, a conservative char rate of 55 mm/hr is considered for redwood.

Based on the shortest distance considered between the cask and the impact limiters in the axial direction, the thickness of redwood at the central segment of the impact limiter is approximately 5 in. (127 mm) in the model. Assuming the redwood is compressed after the drop accident, a char rate of 55 mm/hr can be considered for the wood in the central segment of the impact limiter. The time interval for the charring, until it reaches 13 mm above the inner surface of the center cover plate, can be calculated as follows.

$$\text{(Redwood thickness -13) / char rate} = \frac{(127-13)}{55} = 2.1 \text{ hr}$$

At this moment the maximum char temperature would be imposed at the impact limiter inner surface. It takes another 14 minutes until the last 13 mm of Redwood is charred.

$$\text{(Thickness of last portion of hot Redwood) / char rate} = \frac{13}{55} = 0.24 \text{ hr} = 14.2 \text{ min}$$

During the last 14 minutes, the inner surface of the impact limiter is exposed to the high temperature of the charring wood. The impact of the charring wood on the cask is maximized if charring occurs immediately after fire for 14 minutes.

Considering the maximum seal temperatures for the TN-LC cask are at the top of the cask for NCT, it is assumed that the entire 360° segment of the wood between the impact limiter gussets is torn due to the puncture accident. The torn segment of the impact limiter is shown in Figure 3-19 with the wood smoldering temperature applied over the region.

To bound the problem and remain conservative, the inner surface of the impact limiter inner cover is exposed to the char wood temperature for 30 minutes immediately after the end of fire. A char wood temperature of 900°F is directly applied over the exposed surface of the impact limiter inner skin as shown in Figure 3-19 for these conditions. The char wood temperature of 900°F is approximately the average of the maximum and minimum char wood temperatures given in [26].

No heat dissipation is considered for the open surface of the torn segment after this period. It is conservatively assumed that this surface is entirely covered with a thin layer of low conductivity wood char.

Transient runs, which consider the worst damaged cases due to the drop and puncture accidents, are performed for 20 hours after the fire. The results of the transient runs discussed in Section 3.4.3 show that the maximum temperatures of cask components are declining so that the

maximum cask component temperatures at 20 hours after the fire accident bound the maximum temperatures for the steady state conditions.

Transient runs for HAC were made with the TN-LC cask basket with a PWR fuel assembly and the basket-to-cask inner shell gap homogenized. The effective thermal properties calculation and results for the homogenized basket are shown in Appendix 3.6.5.

SOLID70 elements are used to model the TN-LC homogenized basket and gap region. The elements for other components are the same as those described in Section 3.3.1 for NCT.

Ambient conditions for HAC are based on 10CFR71 [1] requirements and are applied on the boundaries of the transport cask model. These conditions are listed in the table below.

Design Load Cases for HAC

Period	Ambient temperature (°F)	Insolation	Duration (hr)
Initial Conditions	100	Yes	N/A
Fire	1475	No	0.5
Wood Smoldering	100	Yes	0.5
Cool-Down	100	Yes	N/A

Insolation is applied as a heat flux over the transport cask outer surfaces using average insolation values from 10CFR71 [1]. The insolation values are averaged over 24 hours and multiplied by the surface absorptivity factor to calculate the solar heat flux. The solar heat flux values used in the TN-LC transport cask model for HAC are summarized in the table below.

Solar Heat Flux for Cool-Down Period

Surface Material	Shape	Insolation over 12 hrs [1] (gcal/cm^2)	Solar Absorptivity	Total solar heat flux averaged over 24 hrs (Btu/hr-in.^{2})
All materials	Curved	400	1.0	0.4267
	Flat vertical	200	1.0	0.2133

Convection and radiation heat transfer from the transport cask outer surfaces are combined together as total heat transfer coefficients using the same methodology described in Section 3.3.1.

The highest peak temperature of the cask inner shell resulting from the transient TN-LC transport cask model was used as a steady-state, uniform boundary condition for a two-dimensional model of the TN-LC-1FA pin-can basket. The 2D model of the TN-LC-1FA pin-can basket is the same model described in Section 3.3.1.4 for evaluating NCT. A heat load of 3.0 kW is used in the model and the cask inner shell temperature and the heat generating rates are applied on the TN-LC-1FA pin-can basket model for HAC using the same methodology as was used for NCT.

The transient thermal evaluation of the TN-LC transport cask showed that the highest peak temperature of the cask inner shell during HAC is 445°F, as shown in Table 3-6. For conservatism, a steady-state, uniform cask inner shell temperature of 450°F is applied as the boundary conditions on the nodes representing the inner surface of the cask inner shell in the TN-LC-1FA pin-can basket model for HAC evaluation.

The TN-LC-1FA pin-can basket with 3.0 kW heat load provides the highest maximum temperatures for the fuel cladding among all fuel baskets for NCT. Since a steady-state model of the basket is used to determine the maximum fuel cladding temperature, the same behavior is assumed for HAC. Therefore, the maximum fuel cladding temperature determined using the 2D model of the TN-LC-1FA pin-can basket is the bounding cladding temperature for other fuel baskets loaded into the TN-LC cask.

3.4.3 Maximum Temperatures and Pressure

Temperature distributions for the TN-LC transport cask under HAC are shown in Figure 3-20 and the time temperature histories are shown in Figure 3-21 through Figure 3-23. Typical temperature distribution of the fuel basket components for HAC is shown in Figure 3-24.

The maximum component temperatures for transient runs are listed in Table 3-6. The calculated maximum temperatures of the TN-LC cask components for HAC are lower than the allowable limits.

The seal O-rings are not explicitly considered in the models. The maximum seal temperatures are retrieved from the models by selecting the nodes at the locations of the corresponding seal O-rings.

The maximum long-term temperature of 275°F (135°C) calculated for the Viton fluorocarbon seals is for the top cavity port seal during steady state cool-down conditions.

As seen in Table 3-6, the maximum Viton fluorocarbon seal temperatures are below the long-term limit of 400°F (204°C), except for the top lid seal.

The length of the time intervals, in which the seal temperatures are above the long-term limit of 400°F, are extracted from the data based on the transient runs and listed in Table 3-22. The maximum short-term seal temperature is 449°F (232°C) for the top lid seal, which remains at most for one hour at an elevated temperature. This short-term temperature is well below the specified short-term limit of 482°F (250°C) for the Viton fluorocarbon seals.

The maximum temperature of gamma shielding (lead) is 558°F (292°C), which is well below the lead melting point of 621°F (327°C).

The resins and wood are assumed to be decomposed or charred after fire accident. Therefore, the maximum temperatures for these components are irrelevant for HAC.

The maximum temperatures for fuel cladding and fuel basket components for HAC are listed in Table 3-7. The maximum fuel cladding temperature of 694°F (368°C) calculated for fuel pins in the TN-LC-1FA pin-can basket with 3.0 kW heat load is the bounding fuel cladding temperature for all other fuel types in the TN-LC-NRUX, MTR, TRIGA and 1FA baskets.

The maximum fuel cladding temperatures calculated for the TN-LC-1FA pin-can basket in the TN-LC transport cask for HAC is lower than the allowable limit of 1,058°F (570°C) for LWR fuel. This bounding maximum calculated fuel cladding temperature of 694°F is lower than the lowest melting point of aluminum alloys 1100 and 6063 (1140°F/616°C [5]).

The maximum pressure in the cask cavity for HAC is calculated using the same methodology described in Section 3.3.3.

1. TN-LC Cask Cavity HAC Pressure

The maximum cask cavity pressure in the TN-LC transport cask for HAC is calculated using the same methodology and assumptions as described for NCT in Section 3.3.3. The methodology and assumptions used are defined in Section 3.3.3.

The total amount of gas in the TN-LC cask cavity for HAC, $n_{he,HAC}$, is calculated as follows:

$$n_{he,HAC} = n_{he,initial} + n_{Free-FA,HAC} + n_{CC-HAC}$$
$$= 9.6 + 16.52 + 2.24$$
$$= 28.36 \text{ g} - \text{moles.}$$

Where:

$n_{he,initial}$ = number of moles of helium fill gas in cask cavity = 9.6 g-moles (Section 3.3.3),

$n_{Free-FA,HAC}$ = number of moles of fuel rod fill/fission gas released for HAC = 16.52 g-moles (Table 3-11),

n_{CC-HAC} = number of moles of fill gas released from CCs for HAC = 2.24 g-moles (Table 3-12),

The maximum pressure in the cask cavity for HAC, P_{HAC}, is calculated as:

$$P_{HAC} = \frac{\left(1.4504 * 10^{-4} \frac{\text{psia}}{\text{Pa}}\right) * (n_{he,HAC}) * R * T_{avg,he,HAC} * (5/9 \text{ K}/^{\circ}\text{R})}{V_{free,cavity} * (1.6387 * 10^{-5} \text{ m}^3/\text{in.}^3)}$$
$$= \frac{\left(1.4504 * 10^{-4} \frac{\text{psia}}{\text{Pa}}\right) * (28.36 \text{ g} - \text{moles}) * (8.314 \text{ J/mol} - \text{K}) * (1041^{\circ}\text{R}) * (5/9 \text{ K}/^{\circ}\text{R})}{(11{,}429 \text{ in}^3) * (1.6387 * 10^{-5} \text{ m}^3/\text{in.}^3)}$$
$$= 105.6 \text{ psia} = 90.9 \text{ psig.}$$

Where:

$T_{avg,he,HAC}$ = Average Temperature of Helium in TN-LC cask cavity for HAC = 581°F (1041°R) (See Table 3-11),

$V_{free,cavity}$ = Free volume of the TN-LC cask cavity = 11,429 in.^{3}.

3.4.4 Maximum Thermal Stresses

Thermal stresses for the TN-LC transport cask loaded with the different loaded baskets are discussed in Chapter 2.

3.4.5 Accident Conditions for Fissile Material Packages for Air Transport

The TN-LC transport cask is not designed for air transportation. Therefore, the accident conditions for air transport are irrelevant.

3.5 References

1. U.S. Code of Federal Regulations, Part 71, Title 10, "Packaging and Transportation of Radioactive Material."
2. U.S. NRC, Spent Fuel Project Office, Interim Staff Guidance, ISG-11, Rev 3, "Cladding Considerations for the Transportation and Storage of Spent Fuel."
3. Mesquita, A. M., "Experimental Heat Transfer Analysis of the IPR-R1 TRIGA Reactor," International Atomic Energy Agency Publications, 2007.
4. Incropera, F.P., DeWitt, D.P., "Fundamentals of Heat and Mass Transfer," 3rd Edition, Wiley, 1990.
5. Perry, Chilton, "Chemical Engineers' Handbook," 5th Edition, 1973.
6. Parker O-ring Handbook 5700, Y2000 Edition, 1999.
7. Parker O-ring Division, Material Report Number KJ0835, 1989.
8. U.S. Department of Agriculture, Forest Service, Wood Handbook: Wood as an Engineering Material, March 1999.
9. ANSYS computer code and On-Line User's Manuals, Version 10.0A1.
10. Roshenow, W. M., J. P. Hartnett, and Y. I. Cho, "Handbook of Heat Transfer," 3rd Edition, 1998.
11. ASME Boiler and Pressure Vessel Code, Section II, Part D, Materials Properties, 2004 with 2006 Addenda.
12. NUREG/CR-0497, "A Handbook of Materials Properties for Use in the Analysis of Light Water Reactor Fuel Rod Behavior," MATPRO - Version 11 (Revision 2), EG&G Idaho, Inc., TREE-1280, August 1981.
13. C. Ronchi et al., "Effect of Burn-up on the Thermal Conductivity of Uranium Dioxide up to 100,000 $MWdt^{-1}$," Journal of Nuclear Materials 327 (2004) 58-76.
14. IAEA Report, "Research Reactor Core Conversion Guidebook," IAEA-TECDOC-643, Volume 4: Fuels (Appendices I-K).
15. Updated Final Safety Analysis Report for NUHOMS® HD Horizontal Modular Storage System for Irradiated Nuclear Fuel, Rev. 2, including Amendment 1.
16. Roshanow, Hartnett, Ganic, "Handbook of Heat Transfer Fundamentals," 2nd Edition, 1985.
17. Paloposki T., Leidquist L., "Steel Emissivity for Higher Temperatures," Nordic Innovation Centre, NT Technical Report #570, 2006.
18. Siegel, Howell, "Thermal Radiation Heat Transfer," 4th Edition, 2002.
19. Henninger, J. H., "Solar Absorptance and Thermal Emittance of Some Common Spacecraft Thermal-Control Coatings," NASA Scientific and Technical Information Branch, NASA Reference Publication 1121, 1984.

20. Bucholz, J., "Scoping Design Analysis for Optimized Shipping Casks Containing 1-, 2-, 3-, 5-, 7-, or 10-Year old PWR Spent Fuel," Oak Ridge National Laboratory, January, 1983, ORNL/CSD/TM-149.

21. Safety Analysis Report for NUHOMS®-MP197 Transport Packaging, including application for Revision to CoC No. 9302, Docket No. 71-9302, dated April 14, 2009, plus supplemental submittals on June 22, 2009, April 20, 2010, July 15, 2010, and March 29, 2011.

22. Kreith, Frank, Principles of Heat Transfer, 3rd Edition, 1973, and 4th Edition 1986.

23. Plannel, et al., "Topical Report, Extended Fuel Burnup Demonstration Program. Transport Considerations for Transnuclear Casks," Project 1014, DOE/ET 34014-11, TN-E-4226.Transnuclear Inc., 1983.

24. U.S. Nuclear Regulatory Commission, Standard Review Plan for Transportation Packages for Spent Nuclear Fuel, Final Report, NUREG-1617, January 2000.

25. Updated Final Safety Analysis Report for the Standardized NUHOMS® Horizontal Modular Storage System for Irradiated Nuclear Fuel, NUH-003, Revision 11.

26. Mitchell S. Sweet, "Fire Performance of Wood: Test Methods and Fire Retardant Treatments, Fire Safety of Wood Products," USDA Forest Service, http://www.fpl.fs.fed.us/documnts/pdf1993/sweet93a.pdf

27. Gregory, et al., "Thermal Measurements in a Series of Long Pool Fires," SANDIA Report, SAND 85-0196, TTC-0659, 1987.

28. T. Eric Skidmore, "Performance Evaluation of O-Ring Seals in Model 9975 Packaging Assemblies (U)," Savannah River Technology Center, WSRC-TR-98-00439, December 1998.

29. SAND90-2406, Sanders, T.L., et al., "A Method for Determining the Spent Fuel Contribution to Transport Cask Containment Requirements," TTC-1019, UC-820, November 1992.

30. Mixed Oxide Fresh Fuel Package, SAR, Volume 1, Revision 4, January 2007, Docket 71-9295.

31. Popov S. G., Carbajo J. J., Ivanov V. K., Yoder G. L., Thermophysical Properties of MOX and UO_2 Fuels including the Effect of Irradiation, ORNL/TM-2000/351.

32. AAR Brooks & Perkins, Advanced Structural Division, "Boral® The Neutron Absorber," Product Performance Report 624.

33. Test Report, Properties to be Considered for Safety for Resin Vyal B, Transnuclear International, Report No. DI/RI-A-1-5-02, Rev. 1, 2006.

34. Rapport De Qualification De La Resine Vyal B, NTC-06-00025736, Revision 0.

35. Safety Analysis Report for the Standardized NUHOMS® Horizontal Modular Storage System for Irradiated Nuclear Fuel, Application for Amendment 13, Docket 72-1004.

3.6 Appendices

3.6.1 Macros for Heat Transfer Coefficient

Proprietary Information on pages 3-58 through 3-63
Withheld Pursuant to 10 CFR 2.390

3.6.2 TN-LC Cask Mesh Sensitivity

A slice of the TN-LC transport cask model is recreated for mesh sensitivity analysis. The length of the TN-LC cask slice model is 21.3 in. and includes the inner shell, gamma shield, outer shell, neutron shield, neutron shield boxes, and neutron shield shell. The mesh density of this model is the same as the mesh density of the geometry model used in Section 3.3.1.1 from z=67.626 in. to z=88.908 in. The slice model contains 11,052 elements and 12,150 nodes.

For mesh sensitivity analysis, the mesh density of the slice model is increased to approximately nine times of its original value so that the number of elements and nodes are increased to 37,575 elements and 38,848 nodes, respectively.

Ambient temperature of 100°F with insolation and a decay heat of 3 kW are considered as boundary conditions for both the TN-LC cask slice models with coarse and fine meshes. The boundary conditions are applied using the same methodology as described in Section 3.3.1.1. The maximum temperatures are retrieved from results and listed in the table below for comparison.

Mesh sensitivity analysis is performed to determine the adequacy of the finite element mesh used for the thermal analysis and the material change for the inner/outer shell and top/bottom flange as noted in Appendix 3.6.3 does not affect this analysis.

Maximum Temperatures for Coarse and Fine Model of TN-LC Transport Cask

Mesh Type	**Fine**	**Coarse**	**Difference**
Component	T_{max} (°F)	T_{max} (°F)	$(T_{Fine} - T_{Coarse})$ (°F)
Inner Shell	201.12	201.16	-0.04
Gamma Shield	199.75	199.79	-0.04
Neutron Shield	184.47	184.48	-0.01
Neutron Shield Shell	175.73	175.74	-0.01
Outer Shell	189.33	189.34	-0.01

As seen in the table above, the differences between the maximum temperature for coarse and fine mesh models are less than 1°F. Therefore, it can be concluded that the transport cask model used is mesh insensitive and the results reported are adequately accurate for the evaluation.

3.6.3 Sensitivity Analysis for Material Properties

The materials for the inner/outer shell and top/bottom flange for the TN-LC cask are SA-240, Type XM-19 and SA-182 Type FXM-19 nitrogen strengthened austenitic stainless steels, respectively. However, the material properties used for the TN-LC cask inner/outer shell and top/bottom flange in the ANSYS thermal model are considered as SA-240 Type 304 and SA-182 Type F304 austenitic stainless steel, respectively.

A sensitivity analysis is performed to evaluate the effect of this change on the maximum component temperatures reported in Section 3.3.2. To evaluate the effect of the material change, an ANSYS run used to obtain the reported results was rerun with the correct material properties. The maximum component temperatures from the sensitivity analysis are summarized in the table below and compared to the corresponding values reported in Table 3-9.

Comparison of TN-LC Cask Maximum Temperatures for Different Shell/Flange Material (NCT, 100°F, Insolation, without ISO Container)

Heat Load (kW)	**3.00**		
FA Type	**PWR**		
	F304	**FXM-19**	
	Temperature [°F]	**Temperature [°F]**	**Difference, ΔT (°F)**
Inner Shell	204	205	1
Gamma Shield	203	203	0
Gamma Shield (Top and Bottom)	170	170	0
Outer Shell	192	192	0
Neutron Shield Boxes	186	187	1
Neutron Shield Resin[1]	179	180	1
Neutron Shield Shell	177	177	0
Cask Lid	171	170	-1
Cask Bottom Flange	156	156	0
Cask Top Flange	173	174	1
Wood in Impact Limiter	169	169	0
Bottom Drain Seal	156	156	0
Bottom Plug Seal	155	154	-1
Bottom Test Seal	155	154	-1
Top Cavity Port Seal	169	169	0
Top Lid Seal	172	172	0
Top Test Port Seal	173	173	0

Notes:
1. For the neutron shield resin, the volumetric average temperature at the hottest cross-section of the resin is considered.

As seen in the table above, for the rerun of the TN-LC transport cask ANSYS thermal model, the temperature change is within 1°F for the maximum temperatures. This shows that the change in the shell/flange materials has an insignificant effect on the thermal performance of the TN-LC transport cask. However, when used in this report, 1°F is conservatively added to the maximum TN-LC cask temperatures resulting from the model and then reported in Table 3-1 to bound the maximum temperatures.

3.6.4 Mesh Sensitivity of Fuel Basket Models

The thermal results listed in the table below are based on mesh size of 0.5 in. for fuel basket models. For mesh sensitivity analysis for the fuel basket models, the mesh size is refined from 0.5 in. to 0.25 in. The table below summarizes the number of elements and nodes in the design basis and fine meshed models.

Summary of Element and Node Numbers in the Fuel Basket Models

Design Basis Model		**NRUX**	**MTR**	**TRIGA**	**1FA-PWR**	**1FA-BWR**	**1FA-PIN**
Elem No.	PLANE55	1328	942	887	708	708	708
	MATRIX50	4	1	1	1	2	3
	Total	1332	943	888	709	710	711
Node No.		1306	995	938	754	754	754
Fine Meshed Model		**NRUX**	**MTR**	**TRIGA**	**1FA-PWR**	**1FA-BWR**	**1FA-PIN**
Elem No.	PLANE55	3120	2348	2357	2358	2358	2358
	MATRIX50	4	1	1	1	2	3
	Total	3124	2349	2358	2359	2360	2361
Node No.		3136	2438	2454	2450	2450	2450

The resulting maximum temperatures for hot NCT with insolation using design basis and fine meshed models are listed in the table below.

Maximum/Average Temperatures of Fuel Basket Component for Hot NCT

Heat Load (kW)	**0.390**			**1.62**			**1.5**		
Basket Type	**TN-LC-NRUX**			**TN-LC-MTR**			**TN-LC-TRIGA**		
Mesh Type	Coarse	Fine		Coarse	Fine		Coarse	Fine	
Maximum Temperature	T_{max} (°F)	T_{max} (°F)	ΔT (°F)	T_{max} (°F)	T_{max} (°F)	ΔT (°F)	T_{max} (°F)	T_{max} (°F)	ΔT (°F)
Basket Shell/Rail	178	178	+0	220	220	+0	231	231	+0
Guide Plate (Side, Center and A Plates)	191	192	+1	--	--	--	--	--	--
Tube Wrap/Outer Plate (Compartment)	193	193	+0	250	250	+0	239	239	+0
Poison Plate	--	--	--	--	--	--	255	257	+2
Tube/Bucket	199	200	+1	256	256	+0	255	257	+2
Fuel Cladding	205	205	+0	262	262	+0	266	268	+2
Average Temperature	T_{avg} (°F)	T_{avg} (°F)	ΔT (°F)	T_{avg} (°F)	T_{avg} (°F)	ΔT (°F)	T_{avg} (°F)	T_{avg} (°F)	ΔT (°F)
Helium	182	182	+0	220	220	+0	217	217	+0
Fuel Cladding	196	196	+0	245	245	+0	250	251	+1

Heat Load (kW)	**2.0**			**3.0**			**3.0**		
Basket Type	**TN-LC-1FA (BWR)**			**TN-LC-1FA (PWR)**			**TN-LC-1FA (Pin-Can)**		
Mesh Type	Coarse	Fine		Coarse	Fine		Coarse	Fine	
Maximum Temperature	T_{max} (°F)	T_{max} (°F)	ΔT (°F)	T_{max} (°F)	T_{max} (°F)	ΔT (°F)	T_{max} (°F)	T_{max} (°F)	ΔT (°F)
Basket Rail	261	261	+0	268	268	+0	268	268	+0
Poison Plate	265	265	+0	275	275	+0	274	274	+0
Frame	267	267	+0	278	279	+1	277	277	+0
Sleeve Wall	298	298	+0	--	--	--	318	318	+0
Pin Can Wall	--	--	--	--	--	--	379	380	+1
Fuel Cladding	497	496	-1	520	519	+1	543	542	+1
Average Temperature	T_{avg} (°F)	T_{avg} (°F)	ΔT (°F)	T_{avg} (°F)	T_{avg} (°F)	ΔT (°F)	T_{avg} (°F)	T_{avg} (°F)	ΔT (°F)
Helium	260	260	+0	256	256	+0	282	282	+0
Fuel Cladding	396	396	+0	401	401	+0	455	456	+1

Based on the results presented in the table above, there is an insignificant effect on maximum temperatures for fuel cladding and basket components (within 2°F) by refining mesh size from

0.5 in. to 0.25 in. Therefore, the fuel basket models based on mesh size of 0.5 in. is applicable to predict thermal results for fuel baskets.

3.6.5 Effective Properties for the Homogenized TN-LC-1FA Basket with PWR Fuel Assembly

The TN-LC-1FA basket effective density, thermal conductivity and specific heat with PWR fuel assembly are calculated for use in the transient analyses. The calculation of these effective thermal properties is based on the major dimensions listed in the following table.

Major Dimensions of the TN-LC-1FA Basket

Basket Radius, (in.)	D_{basket}	17.50
Length of the Basket, (in.)	L_{basket}	181
Width of Fuel Compartment Opening, (in.)	W_{comp}	8.875
Height of Fuel Compartment Opening, (in.)	H_{comp}	8.875
Width of Stainless Steel Plates, (in.)	$W_{ss\text{-}plate}$	1
Height of Stainless Steel Plates, (in.)	$H_{ss\text{-}plate}$	10.875

The specific heat and density of TN-LC-1FA basket components are listed in the following table.

Specific Heat and Density of TN-LC-1FA Basket Components

Density of Aluminum, (lb/in.^{3}) [11]	$\rho_{aluminum}$	0.098
Specific Heat of Aluminum, (Btu/lbm-°F) [11]	$C_{p\ aluminum}$	0.213
Density of Stainless Steel, (lb/in.^{3}) [5]	ρ_{steel}	0.290
Specific Heat of Stainless Steel, (Btu/lbm-°F) [11]	$C_{p\ steel}$	0.116
Specific Heat of Fuel, (Btu/lbm-°F)	$C_{p\ fuel}$	0.5924

The following assumptions are used in the calculation of the basket effective density and specific heat calculation:

- A constant specific heat is conservatively used for the fuel, aluminum and stainless steel components.
- Conservatively, poison material and helium are not included in density and specific heat calculation.

3.6.5.1 Effective Density and Specific Heat

The basket effective density $\rho_{eff\ basket}$, and specific heat $c_{p\ eff\ basket}$ are calculated, respectively using equations listed below.

$$\rho_{eff\ basket} = \frac{\sum W_i}{V_{basket}} = \frac{W_{fuel} + W_{rail} + W_{ss-plate}}{L_{basket} \cdot \pi \cdot D_{basket}^{\ 2} / 4},$$

$$c_{p\,eff\ basket} = \frac{\sum W_i \cdot c_{pi}}{\sum W_i} = \frac{W_{fuel} \cdot c_{p\,fuel} + W_{rail} \cdot c_{p\ rail} + W_{ss-plate} \cdot c_{p\ ss-plate}}{W_{fuel} + W_{rail} + W_{ss-plate}}$$

Where:

W_i = weight of basket components,

V_{basket} = total volume of basket in FE model,

L_{basket} = basket length (see the dimensional table above),

D_{basket} = basket OD (see the dimensional table above),

$c_{p\,i}$ = specific heat of basket materials.

Calculation of Effective Density for Fuel Basket

Components	**Material**	**Total Weight (lbm)**
Fuel Assembly	Composite	1,715
Fuel Compartment	SS304	2,073(2)
Rail	Aluminum	2,169(2)
Total		5,957
D_{basket} (in)	17.50	
L_{basket} (in)	181	
V_{basket} (in^3)	43.536	
$\rho_{eff\ basket}$(1) (lbm/in^3)	0.130	

Notes:
1. Only 95 percent of the effective density (0.95 * 0.137 lbm/in.^{3} = 0.130 lbm/in.^{3}) is considered in the analysis.
2. Weight of fuel compartment and rail are calculated based on the dimensions and properties shown on the previous page.

Calculation of Effective Specific Heat for Fuel Basket

Components	Weight	Heat Capacity ($m*C_p$)
	(lbm)	(Btu/°F)
Fuel Assembly	1,715	1016
Fuel Compartment	2,073	240
Rail	2,169	213
$C_{p\ eff\ basket}$ (1)		0.274 Btu/lbm-°F

Notes:
1. Only 95 percent of the effective specific heat (0.95 * 0.288 Btu/lbm-°F = 0.274 Btu/lbm-°F) is considered in analysis.

3.6.5.2 Axial Effective Thermal Conductivity

The axial effective thermal conductivity for the TN-LC-1FA basket with PWR FA is calculated as area average and is listed in the Table below:

$$k_{eff,axial} = \frac{k_{fuel} * A_{fuel} + k_{ss-plate} * A_{ss-plate} + k_{rail} * A_{rail}}{A_{Basket}}$$

Where:

k_{fuel}, $k_{ss\text{-}plate}$, k_{rail} = thermal conductivity of fuel, stainless steel compartment plates and aluminum basket rails, respectively, (Btu/hr-in-°F),

A_{fuel}, $A_{ss\text{-}plate}$, A_{rail} = Area of fuel, stainless steel compartment plates and aluminum basket rails, respectively, (in^2),

$k_{eff,axial}$ = effective axial thermal conductivity of TN-LC-1FA basket, (Btu/hr-in-°F).

Effective Axial Conductivity for TN-LC-1FA Basket

Temperature (°F)	k_{SS304} (Btu/hr-in.-°F)	$k_{Al\ 6061}$ (Btu/hr-in.-°F)	k_{fuel} (Btu/hr-in.-°F)	$k_{eff,\ axial}$ (95%) (Btu/hr-in.-°F)
70	0.717	8.008	0.04235	3.99
100	0.725	8.075	0.0431	4.03
200	0.775	8.25	0.0456	4.12
300	0.817	8.383	0.0481	4.19
400	0.867	8.492	0.0506	4.25
500	0.908	8.492	0.0527	4.26
600	0.942	8.492	0.0548	4.26
700	0.983	8.492	0.0571	4.27
800	1.025	8.492	0.0594	4.28
900	1.058	8.492	0.0640	4.29
1000	1.092	8.492	0.0663	4.29

3.6.5.3 Radial Effective Thermal Conductivity

The 2D model of the TN-LC-1FA basket with PWR FA from Section 3.3.1.1 is used to calculate the transverse effective conductivity of the basket. For this purpose, constant temperature boundary conditions are applied on the outermost nodes of the 2D model and heat generating conditions are applied over the fuel element.

The following equation is given in [22] for long solid cylinders with uniformly distributed heat sources:

$$T = T_o + \frac{\dot{q}\, r_o^2}{4k}\left[1 - \left(\frac{r}{r_o}\right)^2\right] \qquad \text{(A.1)}$$

With T_o = Temperature at the outer surface of the cylinder (°F),

T = Maximum temperature of cylinder (°F),

$\dot{q}$ = Heat generation rate (Btu/hr-in.^{3}),

r_o = Outer radius = D_{basket} /2 = 8.75 in.,

r = Inner radius = 0 for slice model,

k = Thermal conductivity (Btu/hr in.-°F).

Equation (A.1) is rearranged to calculate the transverse effective conductivity of the basket as follows:

$$\dot{q} = \frac{Q_{rad}}{V} \qquad (A.2)$$

$$k_{eff,\,radial} = \frac{Q_{rad} \cdot r_0^2}{4 \cdot V \cdot \Delta T} \times 0.95 = \frac{0.95\, Q_{rad}}{2\pi \cdot L \cdot \Delta T}$$

With $Q_{rad} = Q_{react}$ = Amount of heat leaving the periphery of the 2D model and reaction solution of the outermost nodes (Btu/hr),

L = Length of the slice model = 1 in. for 2D Model,

V = Volume of the half-symmetrical slice model = $(\pi r_0^2 L)/2$,

$\Delta T = (T_{max} - T_o)$,

= Difference between maximum and the outer surface temperatures (°F).

In determining the temperature dependent transverse effective conductivities, an average temperature, equal to $(T_{max} + T_o)/2$, is used for the basket temperature.

Only 95 percent of the estimated radial effective conductivity is considered for conservatism.

The transverse effective conductivities of TN-LC-1FA basket are listed in the table below.

Effective Transverse Conductivity for TN-LC-1FA Basket

T_{shell}	T_{max}	T_{avg}	$k_{eff\ radial}$	$k_{eff\ radial}$ (95%)
[°F]	[°F]	[°F]	[Btu/hr-in.-°F]	[Btu/hr-in.-°F]
100	438	269	0.0184	0.0175
200	495	348	0.0211	0.0200
300	556	428	0.0243	0.0231
400	622	511	0.0281	0.0267
500	692	596	0.0324	0.0308
600	767	684	0.0372	0.0353
700	847	773	0.0424	0.0403
800	937	868	0.0455	0.0432
900	1035	968	0.0460	0.0437
1000	1134	1067	0.0464	0.0441
Q_{react}	39.099	Btu/hr		

3.6.6 Effective Thermal Properties of the PWR and BWR Fuel Assemblies

The purpose of this appendix is to determine the effective thermal conductivity, specific heat and density for the fuel assemblies within the fuel basket assemblies for use in the analysis of the thermal performance of the TN-LC transport package. The TN–LC transport package is designed to accommodate the contents described in Chapter 1. The general fuel descriptions are:

- Fuel pins: UO_2, MOX, and EPR,
- PWR or BWR fuel assemblies,
- NRU and NRX fuel assemblies,
- MTR fuel elements,
- TRIGA fuel elements.

The characteristics of the design basis fuel assemblies/elements selected for calculation of effective fuel properties are listed in table below:

Characteristics of Design Basis Contents in TN-LC Transport Package

Fuel Basket Type	1FA (25-Pin-Can)	1FA (9-Pin-Can)	NRUX	MTR (ORR#1)	TRIGA (Al Clad)
Decay Heat, W	120/Pin	220/Pin	10/Element	33/Element	15/Element
Fuel Compartment Open Size, in.	5.0 x 5.0		Φ 2.245	3.48 x 3.48	3.48 x 3.48
Active Fuel Length, in.	144		107.9 (NRU) / 96 (NRX)	22/Element	14/Element
Active Fuel Cross Section Size, in.	Φ 0.3088		Φ 0.216 (NRU)/ Φ 0.250 (NRX)	2.5 x 0.02	Φ1.41
Cladding Thickness, in.	0.0225		0.03 (NRU) 0.045 (NRX)	0.014	0.03

The fuel pin sizes are based on the minimum dimensions for the allowable fuel pins to maximize the gaps and bound the lowest effective conductivity.

The following assumptions were made:

(a) Fuel elements or fuel rods are centered in the fuel compartment.

(b) Heat generation is uniformly distributed along active fuel region. Decay heat load has negligible effect on the transverse effective thermal conductivities.

(c) The fuel compartment opening size for the PWR FA in the TN-LC-1FA basket is identical to the compartment opening size of the 24PTH basket. The bounding effective fuel properties for PWR fuel assemblies in the 24PTH basket are evaluated in Appendix P, Section P.4.8 of [25]. Evaluations in Appendix P, Section P.4.8 of [25] are based on unirradiated UO_2 properties. The evaluation in Chapter 4, Section 4.8.6 of [15] shows that

the transverse effective fuel conductivity decreases by approximately 3 percent due to effect of irradiation of UO_2 pellets. The transverse effective thermal conductivity of unirradiated PWR fuel taken from Appendix P, Section P.4.2 of [25] is reduced by 5 percent in this evaluation, to conservatively bound the effect of fuel irradiation.

(d) The fuel compartment opening size for BWR FA in the TN-LC-1FA basket is identical to the compartment opening size of the 61BTH basket. The bounding effective fuel properties for BWR fuel assemblies in the 61BTH basket based on the FANP 9x9-2 fuel assembly are evaluated in Appendix T, Section T.4.8.1 of [25]. Evaluations in Appendix Y, Section Y.4.9.5 of [35] include the effect of irradiated UO_2 properties on the transverse effective fuel conductivity and shows that the effect of irradiated UO_2 conductivity on effective conductivity for BWR fuel assemblies is small (approximately 2 percent lower than the one with unirradiated UO_2 conductivity for fuel temperature at 800 °F).

(e) For an irradiated fuel pin in the TN-LC-1FA basket, the irradiated UO_2 fuel properties are used to calculate the bounding transverse effective fuel conductivity among UO_2, MOX and EPR fuels. This assumption is justified in Appendix 3.6.7.

(f) Due to small nominal fuel component dimensions, its thermal expansion has negligible effect on the geometry and on the effective thermal properties of fuel assemblies/elements.

(g) Convection is conservatively ignored within the fuel assembly/element model. Heat transfer from the fuel rods/elements to the compartment walls is only through conduction and radiation.

(h) It is assumed that the conductivity of a MOX fuel pellet reduces by the same amount as a UO_2 fuel pellet due to irradiation effects. This assumption is verified Appendix 3.6.7.

The fuel properties for PWR and BWR fuel assemblies are taken from the evaluations performed for the 24PTH basket and 61BTH basket in [25]. The transverse effective thermal conductivity of unirradiated PWR fuel taken from [25] is reduced by 5 percent to consider the effect of fuel irradiation.

The transverse fuel effective conductivity for other fuel assemblies/elements is determined by creating a two-dimensional finite element model of fuel assembly/element centered within a fuel compartment using the ANSYS computer code [9]. The outer surfaces representing the fuel compartment/tube walls are held at a constant temperature and a heat generating boundary condition is applied to the fuel pellets within the model. The maximum fuel assembly temperature is then determined.

Two-dimensional finite element models of the fuel pins, NRU and NRX fuel assemblies, TRIGA fuel elements, and MTR fuel elements were modeled separately within ANSYS. The components were modeled using PLANE55 elements. No convection was considered within the fuel assembly models. Heat transfer from the fuel rods to the compartment walls is only through conduction and radiation.

Radiation between the fuel rods, fuel elements, and compartment walls is modeled using the radiation super-element processor AUX12. LINK32 elements are used in modeling radiating

surfaces to create the radiation super-element. The LINK32 elements were unselected prior to the solution of the model. The model was run with a series of isothermal boundary conditions applied to the outermost nodes representing fuel compartment walls. The conductivity of helium is used for the back fill gas.

The finite element models of TN-LC contents are shown in Figure 3-25.

The isotropic effective thermal conductivity of a heat generating square, such as the fuel pins in the TN-LC-1FA basket, can be calculated as described in [29]:

$$k_{eff} = 0.29469 \times \frac{Q}{4 \times L \times (T_c - T_a)} = 0.29469 \times \frac{Q_{react}}{4 \times (T_c - T_a)}$$

Where:

Q = decay heat load per fuel assembly (Btu/hr)

Q_{react} = reaction solution in the model =Q/L (Btu/hr-in.)

L = active fuel length (in.)

T_c = maximum temperature of fuel assembly (°F)

T_a = compartment wall temperature (°F)

The isotropic effective thermal conductivity of a heat generating cylinder such as the fuel assembly in TN-LC-NRUX basket tubes can be calculated as described in [4]:

$$k_{eff} = \frac{Q}{4 \times \pi \times L \times (T_c - T_a)} = \frac{Q_{react}}{4 \times \pi \times (T_c - T_a)}$$

In determining the temperature dependent effective fuel conductivities an average temperature, equal to $(T_c + T_o)/2$, is used for the fuel temperature.

Section 3.2.1, Material 15 provides the calculated fuel effective thermal conductivities. Effective fuel density, specific heat and axial fuel thermal conductivity used for transient thermal analysis of the TN-LC cask are based on the TN-LC-1FA basket loaded with one PWR fuel assembly. The bounding values for a PWR fuel assembly are taken from the 24PTH analysis in Appendix P.4, Section P.4 of [25].

Figure 3-26 shows typical temperature plots for the TN-LC payload fuel assemblies with 800°F applied to the compartment walls.

Figure 3-27 shows a comparison plot of fuel transverse effective thermal conductivities for the TN-LC contents.

3.6.7 Bounding Transverse Fuel Effective Thermal Conductivity for UO_2, MOX, and EPR Irradiated Fuels

3.6.7.1 UO_2 and MOX Irradiated Fuel Assembly Thermal Conductivity Evaluation

The effect of using MOX fuel instead of UO_2 fuel on the transverse fuel effective thermal conductivity is evaluated based on a sensitivity analysis of a WE 14x14 FA. As shown in Appendix M, Section M.4.8.1 of [25], the WE 14x14 FA model provides the bounding (lowest) transverse effective conductivity among PWR FAs. The WE 14x14 FA model developed in Appendix M, Section M.4.8.1 of [25] is used for the sensitivity analysis in this calculation.

The characteristics of the WE 14x14 model used for the sensitivity analysis are listed in the table below.

Characteristics of Design Basis FAs and Surface Properties

Design Basis FA Type	WE 14x14
Decay Heat, kW	0.75
Fuel Compartment Open Size, in.	8.7 x 8.7
Active Fuel Length, in.	144
Emissivity of Zircaloy	0.8
Emissivity of Stainless Steel Wall	0.46
Emissivity of Al/Poison Wall	0.85
Emissivity of Symmetry Plane	0.001

In the sensitivity analysis, the transverse fuel effective conductivities are calculated once using the irradiated conductivity of UO_2 for the fuel pellets. The conductivity of the fuel pellet is then replaced by the conductivity of irradiated MOX.

Effect of irradiation on thermal conductivity for UO_2 fuel is calculated as

$k_{UO2\ irr} / k_{UO2\ un\text{-}irr}$

It is assumed that this effect can also be used to calculate the irradiated MOX fuel thermal conductivity:

$k_{MOX\ irr} = k_{MOX\ un\text{-}irr} * k_{UO2\ irr} / k_{UO2\ un\text{-}irr}$.

The results of irradiated MOX fuel thermal conductivity are shown in the table below.

Calculation of Irradiated MOX Fuel Thermal Conductivity

T	$k_{UO2\ un\text{-}irr}$ [12]	$k_{UO2\ irr}$ [13]	$k_{UO2\ irr}$ / $k_{UO2\ un\text{-}irr}$	$k_{MOX\ un\text{-}irr}$ [30]	$k_{MOX\ irr}$	$k_{MOX\ irr}$ [31]
°F	Btu/hr-in.-°F	Btu/hr-in.-°F		Btu/hr-in.-°F	Btu/hr-in.-°F	Btu/hr-in.-°F
200	3.322E-01	1.813E-01	54.6%	2.354E-01	1.285E-01	-
300	3.023E-01	1.735E-01	57.4%	2.204E-01	1.265E-01	-
400	2.773E-01	1.657E-01	59.76%	2.078E-01	1.242E-01	-
500	2.562E-01	1.579E-01	61.6%	1.967E-01	1.212E-01	-
600	2.381E-01	1.501E-01	63.0%	1.866E-01	1.176E-01	-
700	2.224E-01	1.434E-01	64.5%	1.785E-01	1.151E-01	-
800	2.087E-01	1.369E-01	65.6%	1.709E-01	1.121E-01	1.248E-01

The irradiated conductivity of a MOX fuel is 1.248E-01 Btu/hr-in.-°F for 4 percent enrichment and ~5 percent PuO_2 in MOX (UO_2 - PuO_2) fuel pellet as reported in [31]. As shown in the table above, the conductivity of irradiated MOX fuel pellet at 800°F (1.121E-01 Btu/hr-in.-°F) calculated based on the above assumption is lower than the conductivity of irradiated MOX fuel pellet reported in [31]. Therefore, the assumption that the conductivity of a MOX fuel pellet reduces by the same amount as a UO_2 fuel pellet due to irradiation effect is conservative and can be used for calculation of the irradiated MOX fuel thermal conductivities.

The computed transverse fuel effective conductivities of UO_2 and MOX FAs as function of temperature are tabulated in the table below.

Transverse Fuel Effective Conductivity of WE14x14 FA

	MOX FA (WE 14x14) Appendix Z, Section Z.9.1 of [35]	**UO_2 FA (WE 14x14) Appendix Z, Section Z.9.1 of [35]**	
T_{avg}	$k_{MOX\ FA}$	$k_{UO2\ FA}$	$k_{MOX\ FA}$/
(°F)	(Btu/hr-in.-°F)	(Btu/hr-in.-°F)	$k_{UO2\ FA}$
200	0.0186	0.0190	0.98
300	0.0221	0.0227	0.98
400	0.0267	0.0273	0.97
500	0.0320	0.0329	0.97
600	0.0381	0.0392	0.97
700	0.0449	0.0463	0.97
800	0.0525	0.0543	0.97

As seen in the table above, the bounding transverse fuel effective conductivities for a MOX FA (based on WE 14x14 FA) are approximately 3 percent lower than those for a UO_2 FA (based on WE 14x14 FA). However, as shown in Appendix Z, Section Z.4.9 of [35], this small decrease in effective conductivity for a FA has negligible effect (less than 1°F) on the maximum temperatures. Therefore, the effective thermal conductivity calculated for a UO_2-based fuel assembly can be used for a MOX fuel assembly.

3.6.7.2 UO_2 and EPR Irradiated Fuels Evaluation

The parameters of EPR and UO_2 fuel rods are shown in the table below.

Irradiated PWR and EPR Fuel Rod Parameters

Parameter	PWR UO_2 rod	EPR UO_2 rod
Active length	4,300 mm for 1,300 MWe 3,700 mm for 900 MWe	4,551 mm
Pellets Diameter:	Min.: 8.04 mm Max.: 8.30 mm	8.192 ±0.012 mm
Cladding	Alloy containing at least 95% Zirconium	M5
External diameter of cladding	Max. 9.70 mm Min. 9.36 mm	9.500 ±0.040 mm
Cladding thickness	Max.: 0.68 mm Min.: 0.52 mm	0.570 mm nominal 0.535 mm minimal

The design of the EPR and UO_2 fuel assembly is similar as seen from the parameters shown in the table above.

As seen in the table above, fuel rods for PWR and EPR FAs have the same UO_2 fuel. They have similar geometry with close pellet and cladding dimension. Further M5 has a higher thermal conductivity than zircaloy [30]. Therefore, FA effective thermal conductivity calculated for a PWR fuel pin-can be used for an EPR fuel pin.

Table 3-1
Maximum and Minimum Temperatures of TN-LC Cask Components for NCT

Ambient Condition	**100°F with Insolation**	**-40°F without Insolation[2]**	
	Temperature	Temperature	Temperature Limit
	[°F]	[°F]	[°F]
Inner Shell	239	-40	
Gamma Shield	237	-40	621 [5]
Outer Shell	226	-40	
Neutron Shield Boxes	221	-40	
Neutron Shield Resin[1]	216	-40	320 [33]
Neutron Shield Shell	211	-40	
Cask Lid	203	-40	
Cask Bottom Flange	186	-40	
Cask Top Flange	206	-40	
Wood in Impact Limiter	201	-40	320 [8]
ISO Container	147	-40	
Seals	205	-40	400 [6]

Notes:
1. The resin temperature is the volumetric average temperature at the hottest cross-section.
2. These temperatures are based on assuming no credit for decay heat and a daily average ambient temperature of -40°F.

Table 3-2
Maximum Temperatures of Fuel Basket Components for NCT

Fuel Basket Type	**NRUX**	**MTR**	**TRIGA**	**Limit**	**1FA**	**Limit**
	T_{max}	T_{max}	T_{max}	T_{limit}	T_{max}	T_{limit}
Component	(°F)	(°F)	(°F)	(°F)	(°F)	(°F)
Basket Shell/Rail	178	220	231	--	268	--
Guide Plates	191	--	--	--	--	--
Tube Wrap/Outer Plate (Compartment)	193	250	239	--	277	--
Poison Plate	--	--	255	--	275	--
Sleeve Wall	--	--	--	--	318	--
Tube/Bucket/Pin Can	199	256	255	--	379	--
Fuel Cladding	205	262	266	400	542	752 [2]

Table 3-3
Minimum Temperatures of Fuel Basket Components for NCT

Fuel Basket Type	**All**	
Component	T_{min} (°F)	$T_{min, limit}$ (°F)
Basket Component	-40	-40
Fuel Cladding	-40	-40

Table 3-4
Maximum Temperatures of TN-LC Cask Components for Cold NCT

Ambient Temperature	**-20°F**	**-40°F**
	Temperature	Temperature
	[°F]	[°F]
Inner Shell	88	70
Gamma Shield	87	69
Gamma Shield (Top and Bottom)	52	34
Outer Shell	73	55
Neutron Shield Boxes	68	50
Neutron Shield Resin(1)	63	44
Neutron Shield Shell	63	45
Cask Lid	52	34
Cask Bottom Flange	36	18
Cask Top Flange	55	37
Wood in Impact Limiter	51	33

Notes:
1. The resin temperature is the volumetric average temperature at the hottest cross-section.

Table 3-5
Maximum Fuel Basket/Fuel Cladding Temperature and
Maximum Fuel Basket Temperature Gradient for Cold NCT

Fuel Basket Type	**1FA (Pin-Can)**	**Others Except 1FA (Pin-Can)**
$T_{max, Fuel}$ (°F)	432	
$T_{max, basket}$ (°F)	250	
ΔT_{basket} (°F)	190	100

Table 3-6
Maximum Temperatures of TN-LC Cask Components for HAC

	Time	**T_{max} (Transient)**	**T_{∞} [2] (Steady state, after fire)**	**Temperature Limit**
Component	(hr)	(°F)	(°F)	(°F)
Inner Shell	1.11	445	253	--
Gamma Shield	0.50	558	252	621 [5]
Gamma Shield (Top and Bottom)	1.74	378	275	621 [5]
Outer Shell	0.50	809	250	--
Neutron Shield Boxes	0.50	1200	229	--
Neutron Shield Shell	0.50	1215	231	--
Cask Lid	1.00	596	275	--
Cask Bottom Flange	0.50	353	229	--
Cask Top Flange	1.00	624	259	--
Bottom Drain Seal	3.44	293	223	400 [6] / 482 [6,28] [1]
Bottom Plug Seal	6.17	283	229	400 [6] / 482 [6, 28] [1]
Bottom Test Seal	6.17	285	229	400 [6] / 482 [6, 28] [1]
Top Cavity Port Seal	1.74	372	275	400 [6] / 482 [6, 28] [1]
Top Lid Seal	1.11	449	271	400 [6] / 482 [6, 28] [1]
Top Test Port Seal	3.44	369	253	400 [6] / 482 [6, 28] [1]

Notes:
1. For the Fluorocarbon seals, the temperature limit of 400°F is for long-term exposure under steady state conditions based on [6], and the temperature limit of 482°F is for short-term exposure during transient conditions based on [6] and verified in [28].
2. These values are retrieved from the transient model at 20 hr after the fire accident. Based on the time-temperature histories, the steady state temperatures are bounded by the temperatures at 20 hr transient after a 0.5 hr fire accident.

Table 3-7
Maximum Temperatures of Fuel Basket Components for HAC

Component	T_{max} (°F)	Limit (°F)
Basket Rail	469	--
Poison Plate	475	--
Frame	478	--
Sleeve Wall	507	--
Pin Can Wall	551	--
Fuel Cladding (1)	694	1058 [2]

Notes:
1. The calculated maximum temperature is bounding for NRU, NRX, MTR, and TRIGA fuels.

Table 3-8
Summary of Maximum Pressures

Condition	Cask Cavity Pressure
NCT (MNOP)	16.9 psi gauge
HAC	90.9 psi gauge

Table 3-9
TN-LC Cask Maximum Temperatures for Hot NCT (Without ISO Container)

Heat Load (kW)	**3.00**	**1.85**	**0.50**	
FA Type	**PWR**	**MTR**	**NRU/NRX**	
	Temperature	Temperature	Temperature	Temperature Limit
	[°F]	[°F]	[°F]	[°F]
Inner Shell	204	166	138	
Gamma Shield	203	166	137	621 [5]
Gamma Shield (Top and Bottom)	170	158	134	621 [5]
Outer Shell	192	160	136	
Neutron Shield Boxes	186	158	135	
Neutron Shield Resin[1]	179	152	131	320 [33]
Neutron Shield Shell	177	158	135	
Cask Lid	171	159	134	
Cask Bottom Flange	156	155	121	
Cask Top Flange	173	161	136	
Wood in Impact Limiter	169	157	134	320 [8]
Bottom Drain Seal	156	155	121	400 [6]
Bottom Plug Seal	155	153	120	400 [6]
Bottom Test Seal	155	154	120	400 [6]
Top Cavity Port Seal	169	157	133	400 [6]
Top Lid Seal	172	160	135	400 [6]
Top Test Port Seal	173	161	135	400 [6]

Notes:
1. For the neutron shield resin, the volumetric average temperature at the hottest cross-section of the resin is considered.

Table 3-10
Maximum Temperatures for Hot NCT TN-LC Transport Cask with and without ISO Container

Heat Load (kW) Loading Condition	**3.00 Temperature** [°F] With ISO Container	**3.00 Temperature** [°F] Without ISO Container (From Table 3-9)	**Temperature Limit** [°F]
Inner Shell	238	204	
Gamma Shield	236	203	621 [5]
Gamma Shield (Top and Bottom)	202	170	621 [5]
Outer Shell	225	192	
Neutron Shield Boxes	220	186	
Neutron Shield Resin[1]	215	179	320 [33]
Neutron Shield Shell	210	177	
Cask Lid	202	171	
Cask Bottom Flange	185	156	
Cask Top Flange	205	173	
Wood in Impact Limiter	200	169	320 [8]
ISO Container	146	--	
Bottom Drain Seal	184	156	400 [6]
Bottom Plug Seal	183	155	400 [6]
Bottom Test Seal	183	155	400 [6]
Top Cavity Port Seal	200	169	400 [6]
Top Lid Seal	204	172	400 [6]
Top Test Port Seal	204	173	400 [6]

Notes:
1. For the neutron shield resin, the volumetric average temperature at the hottest cross-section of the resin is considered.

Table 3-11
Average Helium Temperature in Cask Cavity

		NCT	HAC
Free Volume of Cask Cavity, $V_{free,cavity}$	$in.^3$	11,429	
FA Compartment Width, a_{comp}	in.	8.875	
Helium Volume in Fuel Compartment V_{he_FA}	$in.^3$	8,440	
Helium Volume outside Fuel Compartment, $V_{he\ cavity}$	$in.^3$	2,990	
Average Temperature of Fuel, T_{FA}	°F	455	617
Average Temperature of Helium outside Fuel Compartment, T_{he}	°F	282	480
Volumetric Average Helium Temperature in cask cavity, $T_{avg,he}$	°F	410	581

Table 3-12
Fuel Assembly Helium Fill/Fission Gas Release

Operating conditions	**Moles of fill/fission gases released from fuel assembly, *g-moles***
NCT (3% rod rupture)	0.50
HAC (100% rod rupture)	16.52

Table 3-13
Control Components Helium Fill Gas Release

Operating conditions	**Moles of fill gases released from CCs, *g-moles***
NCT (3% rod rupture)	0.07
HAC (100% rod rupture)	2.24

Table 3-14
Basket Types and Heat Loads Used in Thermal Calculations for TN-LC Transport Cask

Basket Type	No. of Elements/ Assemblies in Basket	Heat Load per Element/Assembly (W)	Peaking Factor	Total Heat Load Considered in Basket Model (kW)	Heat Load Considered in Cask Model (kW)
TN-LC-NRUX	26 NRU/NRX Assemblies	15/Assembly	1.0	0.390	0.5
TN-LC-MTR	54 Elements	30/Element	1.0	1.62	1.85
TN-LC-TRIGA	180 Elements	8.33/Elements	1.0	1.5	1.5
TN-LC-1FA (BWR)	1 BWR Assembly	2000/Assembly	1.2	2.0	2.0
TN-LC-1FA (PWR)	1 PWR Assembly	3000/Assembly	1.1	3.0	3.0
TN-LC-1FA	9 Fuel Pins (1)	220/Pin	1.1	2.86	3.0
(Pin-Can)	25 Fuel Pins	120/Pin	1.1	3.0	3.0

Notes:
1. The thermal model considers 13 fuel pins with heat load of 220 W per pin, which is bounding for the 9 fuel pin configuration.

Table 3-15
Temperature Boundary Conditions for Fuel Basket Models

Basket Type	Ambient Temperature (°F)	Uniform Cask Inner Shell Temperature in Fuel Basket Model (°F)
TN-LC-NRUX	100	170
TN-LC-MTR	100	200
TN-LC-TRIGA	100	200
TN-LC-1FA (PWR)	100	240
TN-LC-1FA (BWR)	100	240
TN-LC-1FA	100	240
(Pin-Can)	-40	69

Table 3-16
Maximum/Average Temperatures of Fuel Basket Component for Hot NCT

Basket Type	TN-LC-NRUX	TN-LC-MTR	TN-LC-TRIGA
Maximum Temperature	T_{max} (°F)	T_{max} (°F)	T_{max} (°F)
Basket Shell/Rail	178	220	231
Guide Plate (Side, Center and A Plates)	191	--	--
Tube Wrap/Outer Plate (Compartment)	193	250	239
Poison Plate	--	--	255
Tube/Bucket	199	256	255
Fuel Cladding	205	262	266
Average Temperature	T_{avg} (°F)	T_{avg} (°F)	T_{avg} (°F)
Helium	182	220	217
Fuel Cladding	196	245	250

Basket Type	TN-LC-1FA (BWR)	TN-LC-1FA (PWR)	TN-LC-1FA (Pin-Can)
Maximum Temperature	T_{max} (°F)	T_{max} (°F)	T_{max} (°F)
Basket Rail	261	268	268
Poison Plate	265	275	274
Frame	267	278	277
Sleeve Wall	298	--	318
Pin Can Wall	--	--	379
Fuel Cladding	497	520	543
Average Temperature	T_{avg} (°F)	T_{avg} (°F)	T_{avg} (°F)
Helium	260	256	282
Fuel Cladding	396	401	455

Table 3-17
Maximum Basket Temperature Gradients Calculation for Hot NCT

Fuel Basket Type	1FA (Pin-Can)	1FA (PWR)	1FA (BWR)	TRIGA	MTR	NRUX
T_{amb} (°F)	100	100	100	100	100	100
$T_{max, basket}$ (°F)	379	278	298	255	256	199
$T_{Inner Shell}$ (°F)	240	240	240	200	200	178
ΔT_{basket} (°F)	139	38	58	55	56	21

Table 3-18
Maximum Basket/Fuel Cladding Temperature and
Maximum Basket Temperature Gradient for Cold NCT (-40°F Ambient)

Fuel Basket Type	1FA (Pin-Can)
T_{amb} (°F)	-40
$T_{max, Fuel}$ (°F)	432
$T_{max, basket}$ (°F)	250
$T_{Inner Shell}$ (°F)	69
ΔT_{basket} (°F)	181
$T_{avg, Fuel}$ (°°F)	335
$T_{avg, Helium}$ (°F)	125

Table 3-19
Maximum Fuel Cladding and Basket Component Temperatures
for Dry Loading/Unloading Conditions

TN-LC with NRU/NRX/MTR/TRIGA Fuels		
Component	**Maximum Temperature (°F)**	**Temperature Limit (°F)**
Basket Shell/Rail	225	---
Basket Plate	281	---
Tube/Bucket	309	---
Fuel Cladding	320	400
TN-LC with PWR/BWR Fuel Assemblies / Fuel Pins		
Component	**Maximum Temperature (°F)**	**Temperature Limit (°F)**
Basket Rail	274	---
Poison Plate	306	---
Frame	309	---
Sleeve Wall	383	---
Pin Can Wall	476	---
Fuel Cladding	720	752

Table 3-20
Comparison of Maximum Fuel Cladding Temperatures

TN-LC-MTR Basket			
Component	Dry Loading/Unloading T_{max} (°F)	NCT (Table 3-2) T_{max} (°F)	ΔT (°F)
Fuel Cladding	320	262	+58
TN-LC-1FA (Pin-Can) Basket			
Component	Dry Loading/Unloading T_{max} (°F)	NCT (Table 3-2) T_{max} (°F)	ΔT (°F)
Fuel Cladding	720	543	+177

Table 3-21
Gaps and Thermal Properties for HAC Analysis

	Gap Size (in.)	Location	Initial / Cool-down Properties	Properties during Fire
1	0.0625	Axial gaps on either sides of the top and bottom gamma shieldings	Air [1]	ASTM B29 Copper Lead (Gamma shield)
2	0.0625	Radial gap between the gamma shieldings and the top lid/ bottom flange	Air [1]	ASTM B29 Copper Lead (Gamma shield)
3	0.125	Radial gap between the top lid and top flange	Air	SA-182 F304 (Top Lid)
4	0.06	Axial gap between the top lid and top flange	Air	SA-182 F304 (Top Lid)
5	0.019	Radial gap between gamma shield and cask outer shell	Air	ASTM B-29 Copper Lead (Gamma shield)
6	0.01	Radial gaps between neutron shield boxes and surrounding shells	Air	Al 6063 (Neutron shield boxes)
7	0.01	Axial gap between impact limiter inner cover plate and top lid / bottom flange	Air	SA-182-F304/SA-182-FXM-19 (Top Lid / Bottom Flange)

Notes:
1. These gaps are incorporated into corresponding plates as effective conductivities.

Table 3-22
Time Intervals for Short-Term Exposure of Seals to High Temperatures

Conditions	Top Lid Seal	
	Time (hr)	Temperature (°F)
HAC, Top Impact Limiter Punctured	.83	364
	.92	400
	1.00	431
	1.11	449
	1.74	403
	1.91	400
	3.44	372
Approximate Short-term Exposure Time (hr)	1	

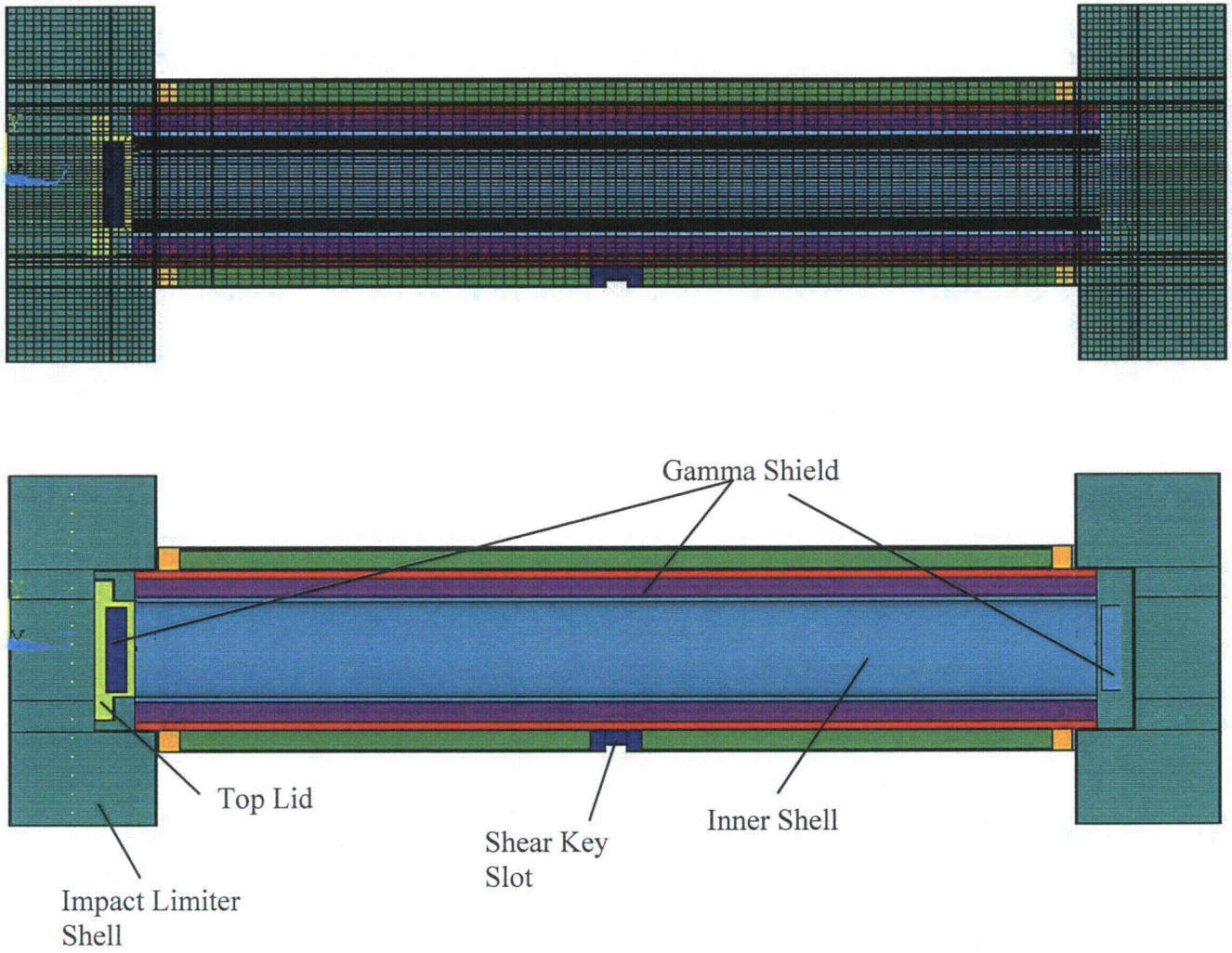

Figure 3-1
Finite Element Model of TN-LC Cask Without ISO Container, Longitudinal Section

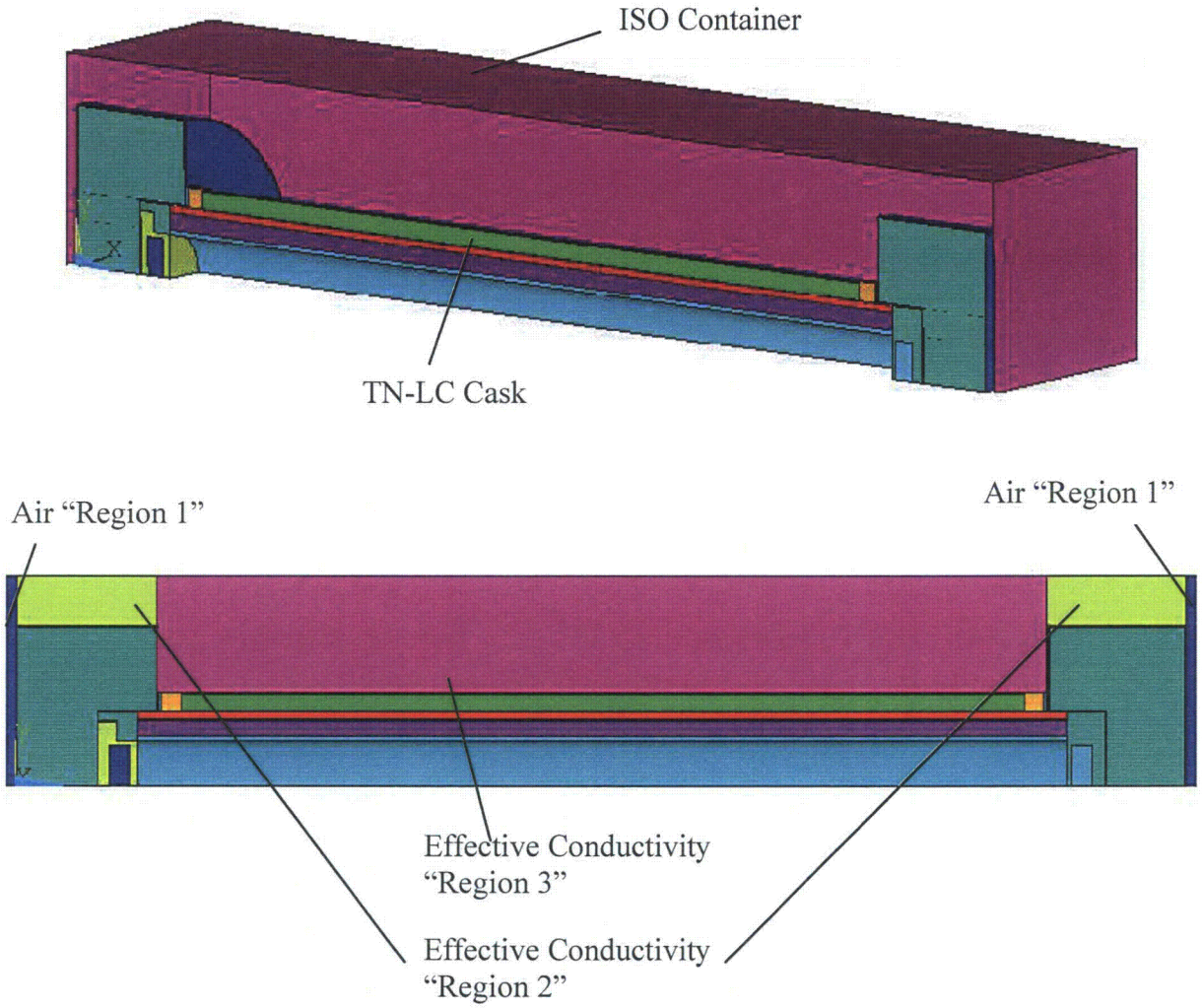

Figure 3-2
Finite Element Model of TN-LC Transport Cask within ISO Container, Longitudinal Section

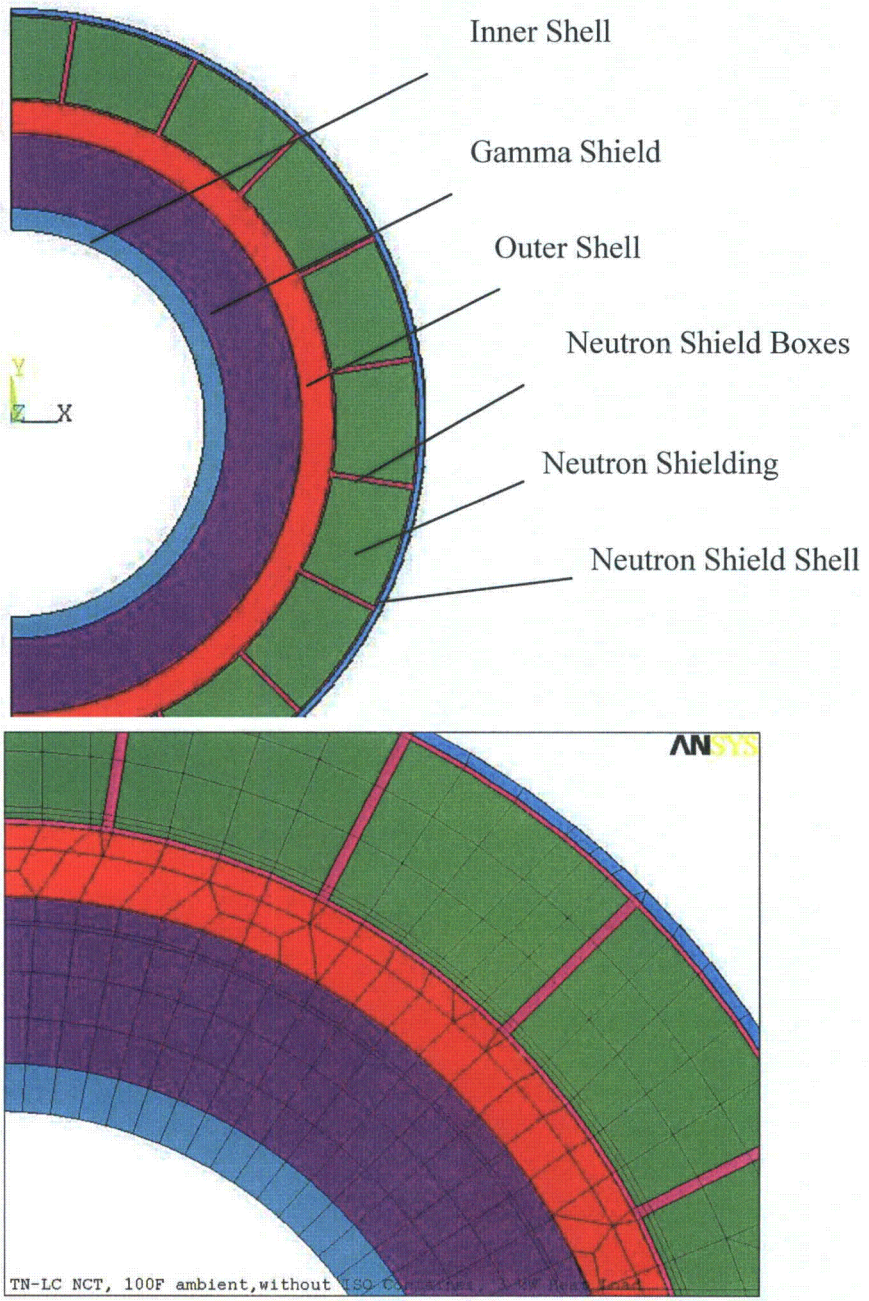

Figure 3-3
Finite Element Model of TN-LC Transport Cask, Cross Section

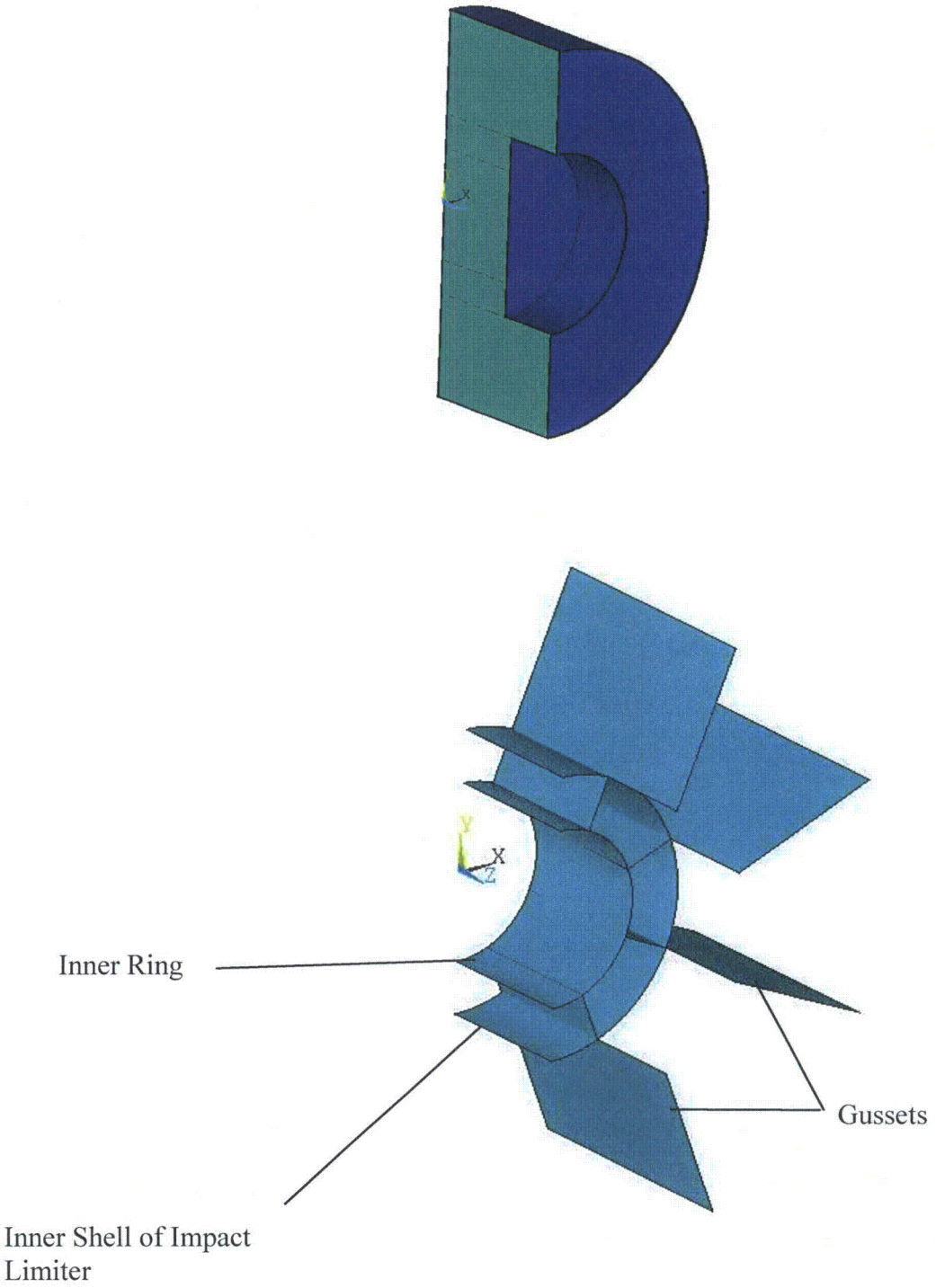

Figure 3-4
Finite Element Model of TN-LC Transport Cask, Impact Limiter Components

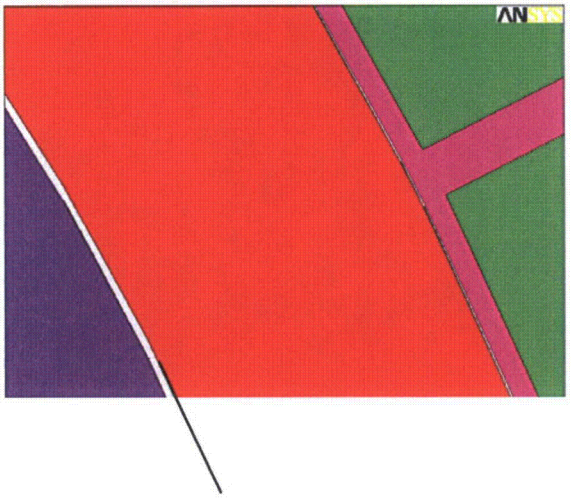

0. 019" gap between gamma shield and outer shell

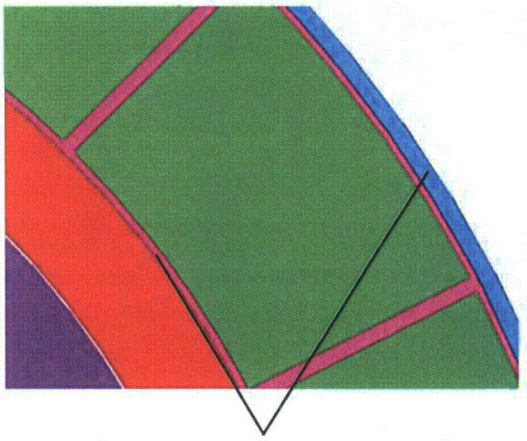

0.01" gap between neutron shield boxes and outer / neutron shield shell

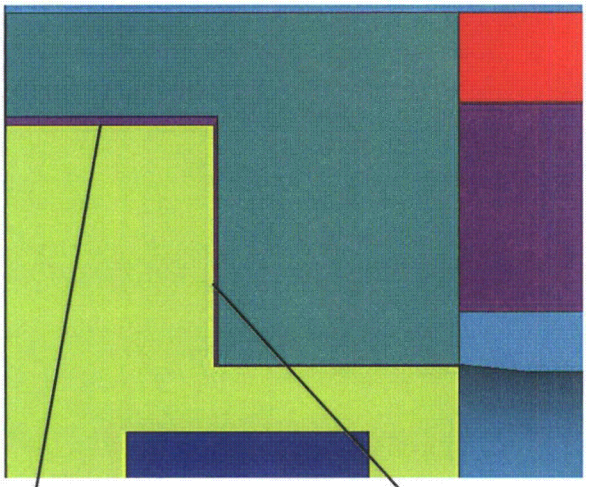

0.125" radial gap between top lid and top flange

0.06" axial gap between top lid and top flange

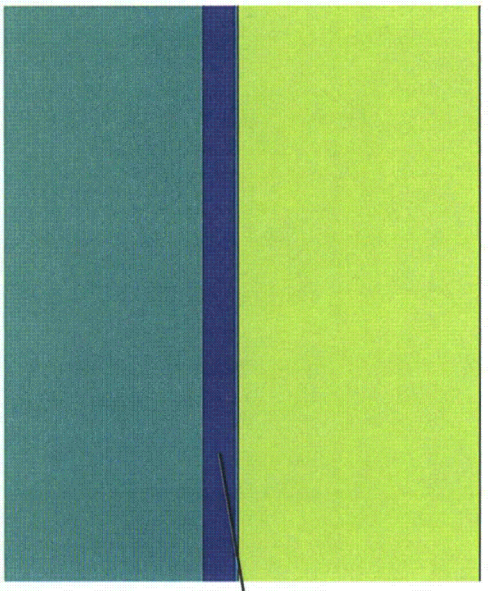

0.01" axial gap between top lid / bottom flange lid and impact limiter surface

Figure 3-5
Gaps in Finite Element Model of TN-LC Cask

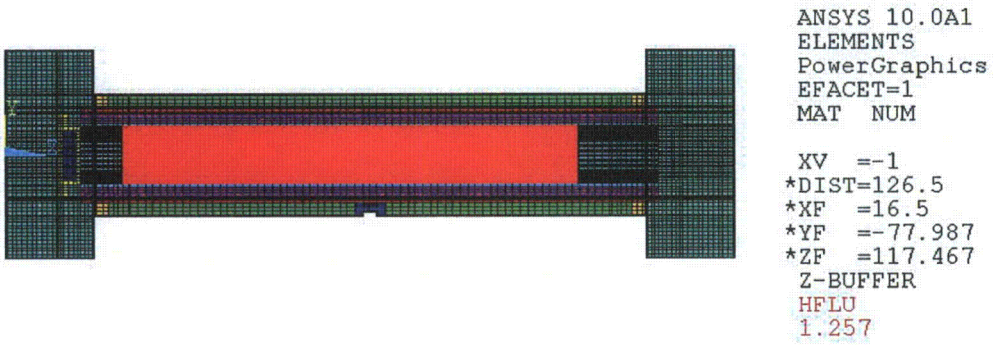

Decay Heat Flux

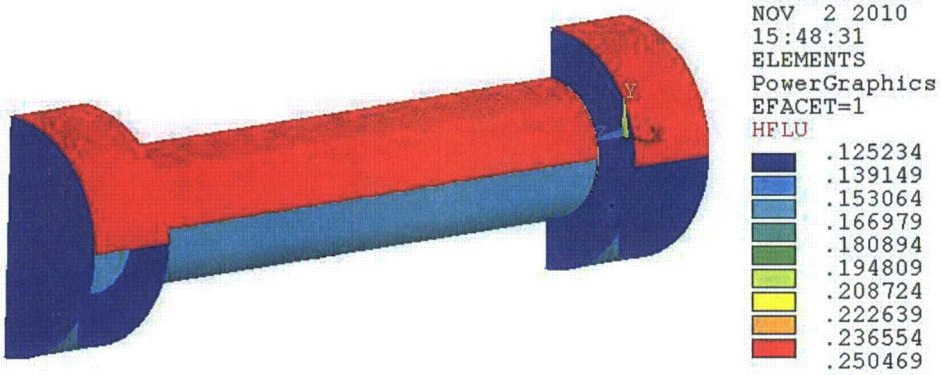

Solar Heat Flux

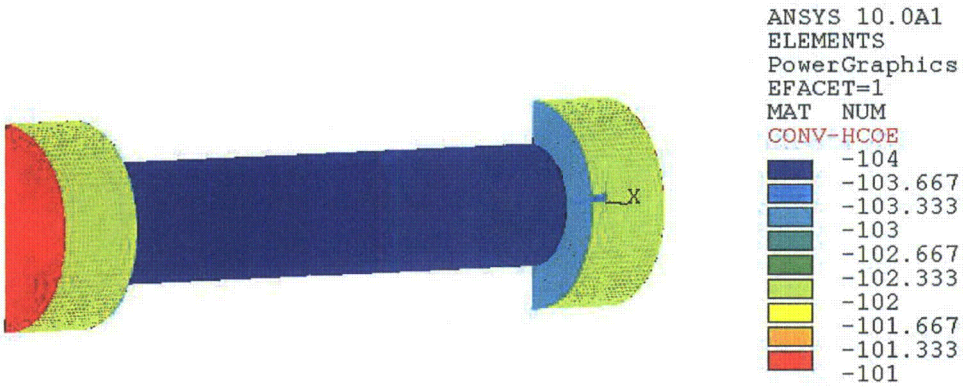

Convection from TN-LC Transport Cask to ambient

Figure 3-6
Typical Boundary Conditions for TN-LC Transport Cask without ISO Container

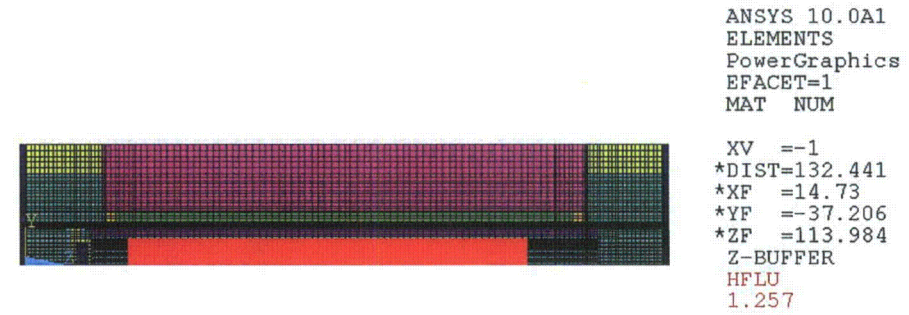

Decay Heat Flux

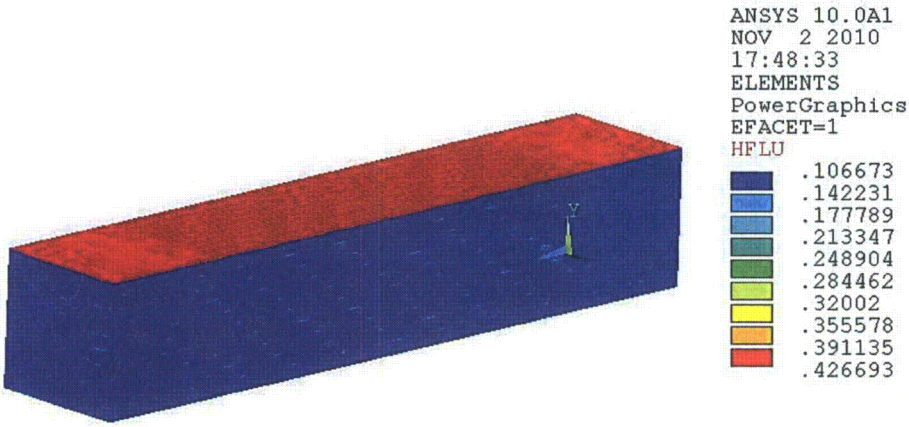

Solar Heat Flux

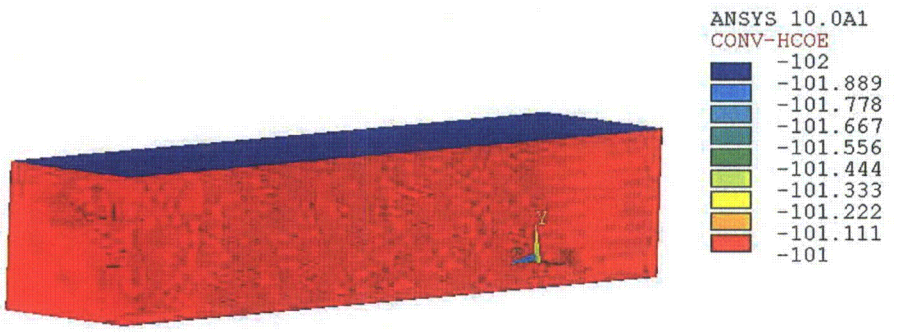

Convection from ISO container to ambient

Figure 3-7
Typical Boundary Conditions for TN-LC Transport Cask model within ISO Container

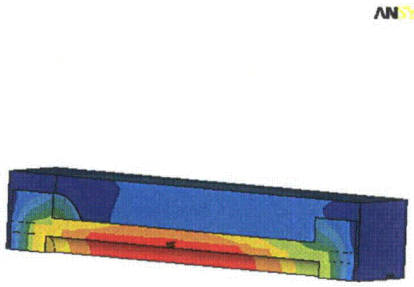

TN-LC Transport Cask with ISO Container

TN-LC Cask Body

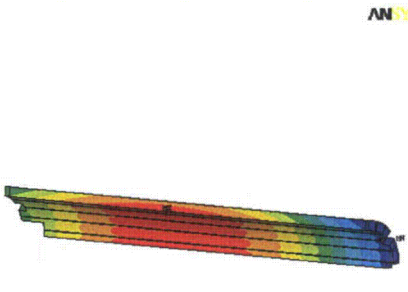

TN-LC Cask Neutron Shield

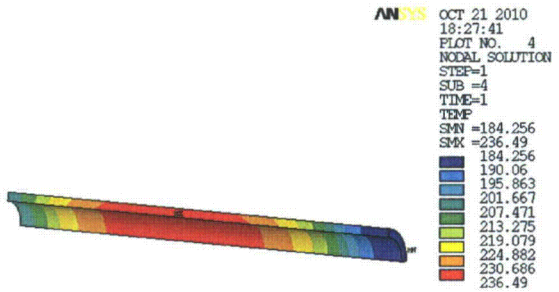

TN-LC Cask Structural Shell

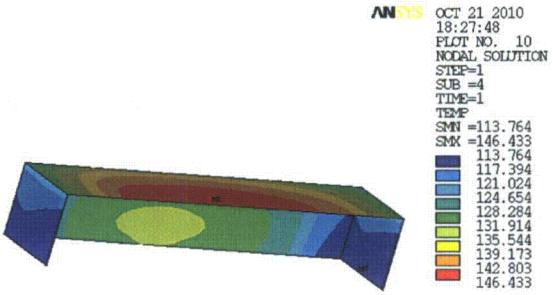

ISO Container

Figure 3-8
Temperature Distribution of TN-LC Transport Cask within ISO Container for Hot NCT, 100°F Ambient with Insolation

(Part 1 of 2)

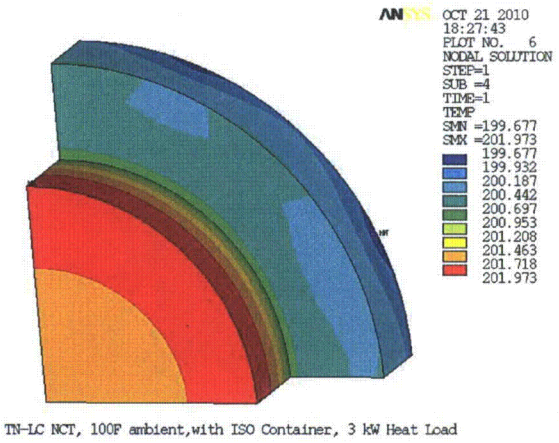

TN-LC Cask Lid

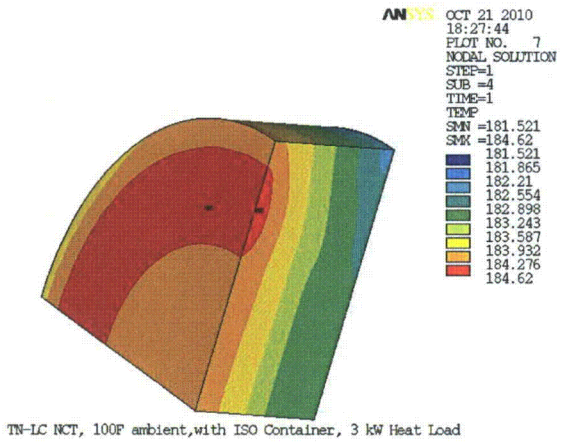

TN-LC Bottom Flange and Gamma Shielding

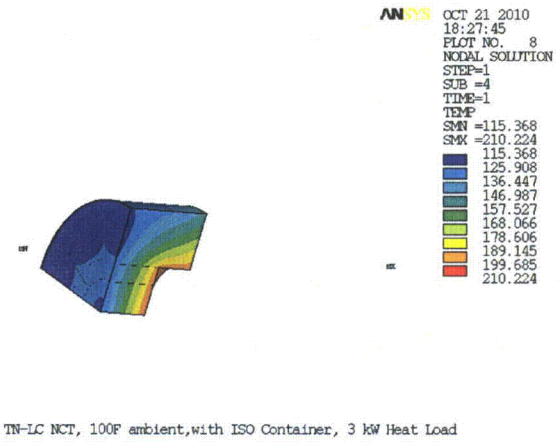

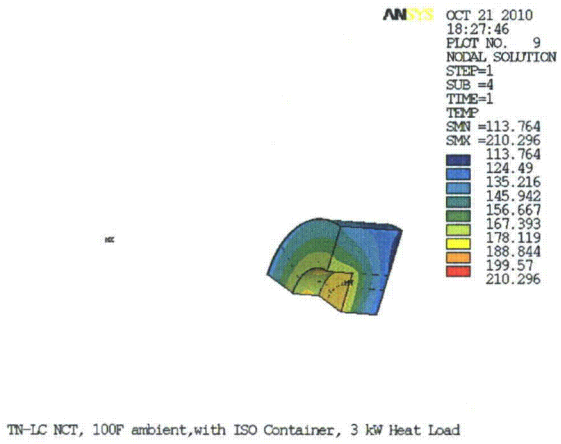

TN-LC Cask Top and Bottom Impact Limiters

Figure 3-8
Temperature Distribution of TN-LC Transport Cask within ISO Container for Hot NCT, 100°F Ambient with Insolation

(Part 2 of 2)

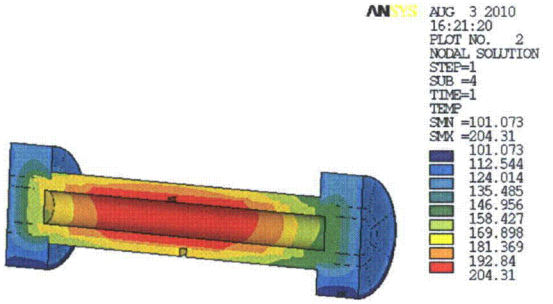

TN-LC NCT, 100F ambient,without ISO Container, 3 kW Heat Load, PWR FA

TN-LC Transport Cask without ISO Container

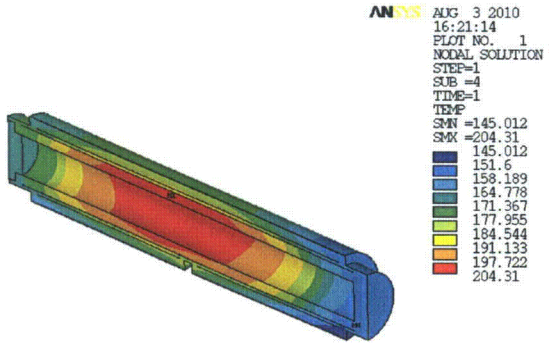

TN-LC NCT, 100F ambient,without ISO Container, 3 kW Heat Load, PWR FA

TN-LC Cask Body

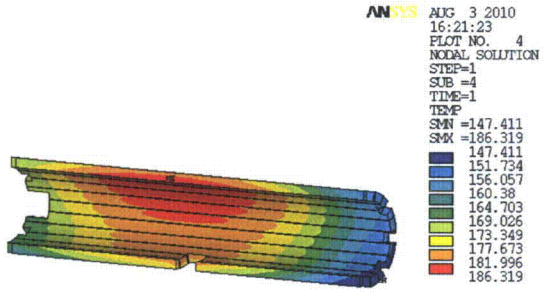

TN-LC NCT, 100F ambient,without ISO Container, 3 kW Heat Load, PWR FA

TN-LC Cask Neutron Shield

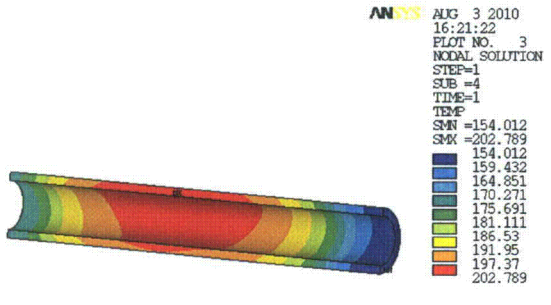

TN-LC NCT, 100F ambient,without ISO Container, 3 kW Heat Load, PWR FA

TN-LC Cask Structural Shell

Figure 3-9
Temperature Distribution of TN-LC Transport Cask without ISO Container for Hot NCT, 100°F Ambient with Insolation

(Part 1 of 2)

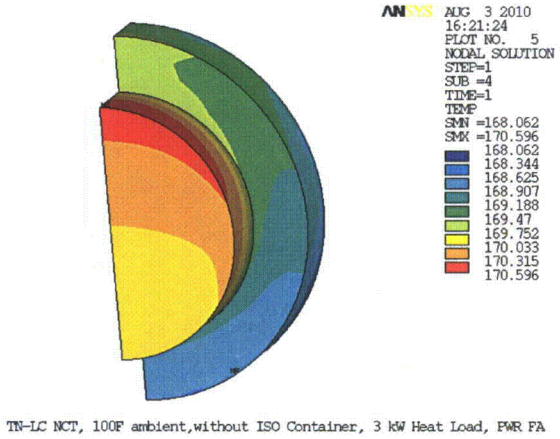

TN-LC Cask Lid

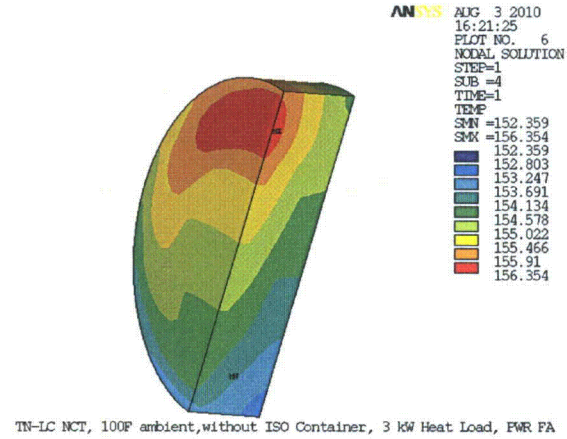

TN-LC Bottom Flange and Gamma Shielding

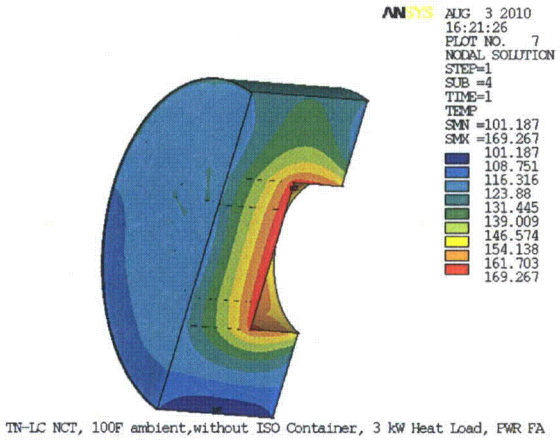

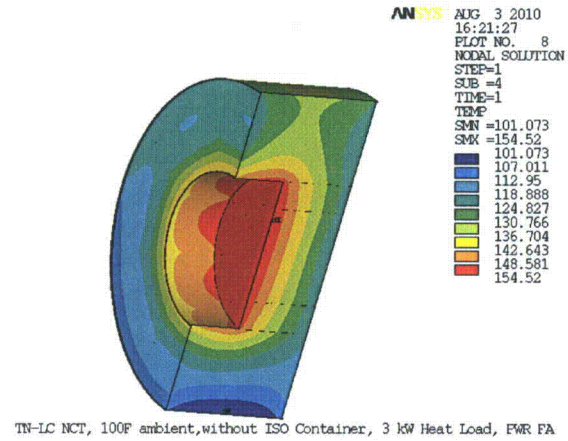

TN-LC Cask Top and Bottom Impact Limiters

Figure 3-9
Temperature Distribution of TN-LC Transport Cask without ISO Container for Hot NCT, 100°F Ambient with Insolation

(Part 2 of 2)

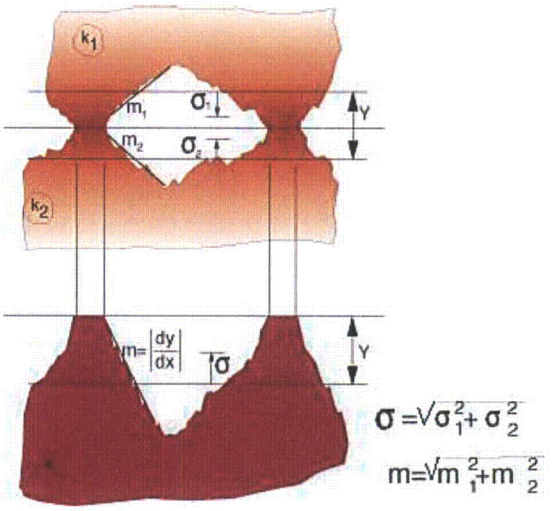

Figure 3-10
Conforming Rough Surfaces

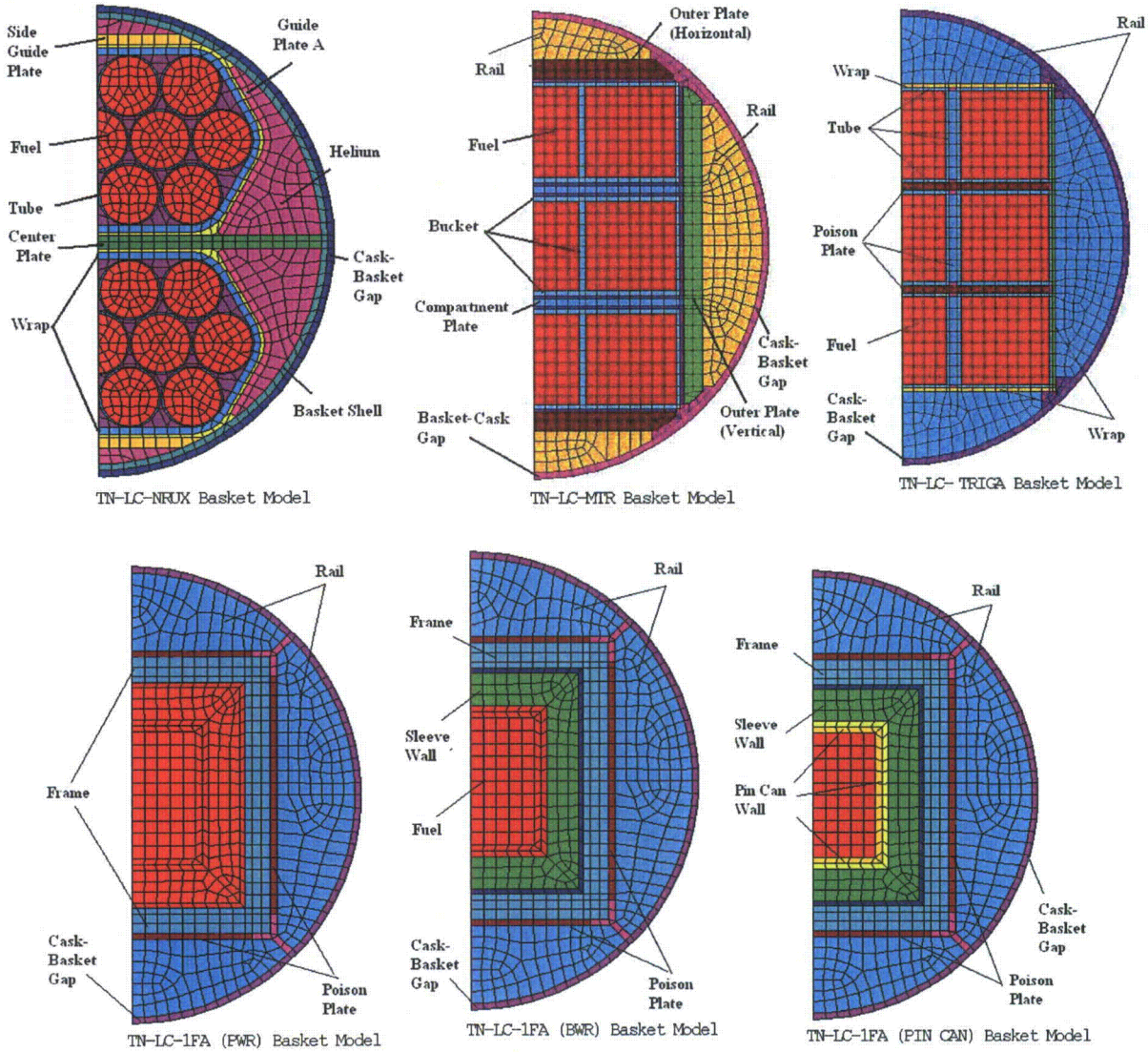

Figure 3-11
2D Finite Element Model of Fuel Baskets, Cross Section

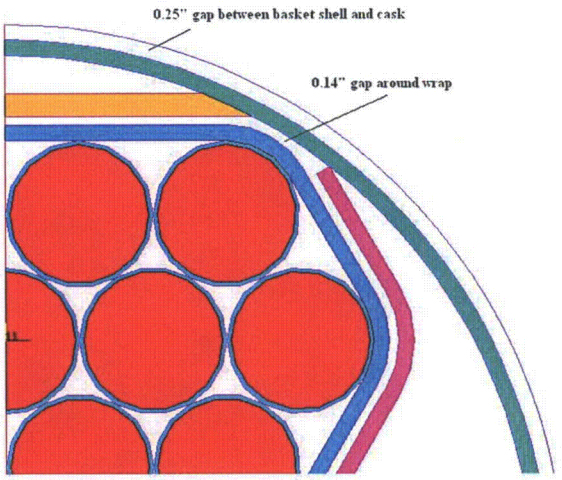

(1) TN-LC-NRUX Basket

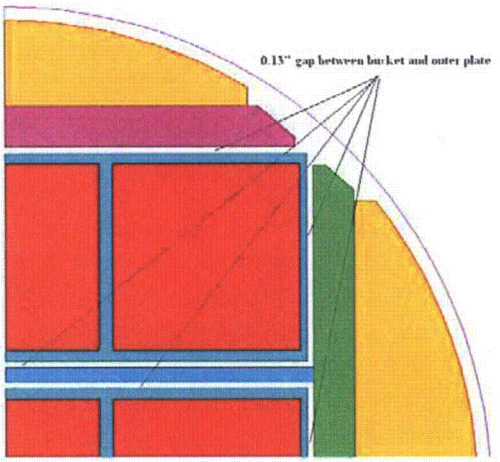

(2) TN-LC-MTR Basket

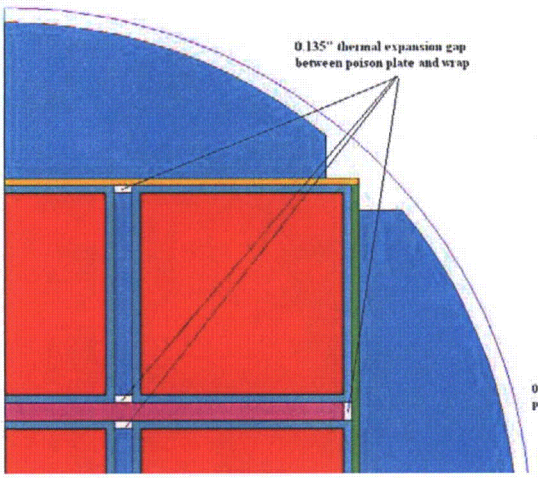

(3) TN-LC-TRIGA Basket

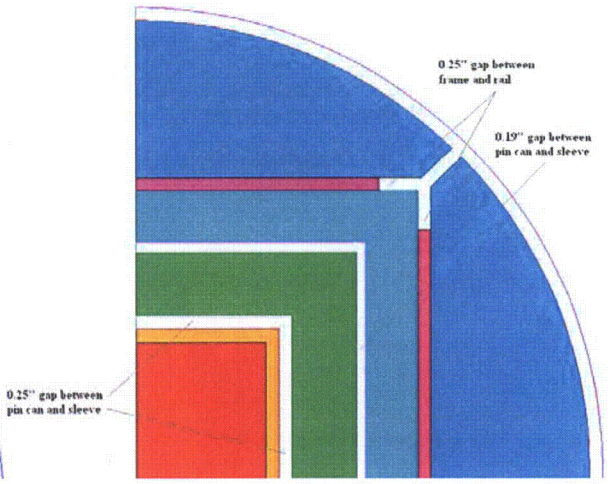

(4) TN-LC-1FA Basket

Figure 3-12
Typical Gaps in Finite Element Model of Fuel Baskets

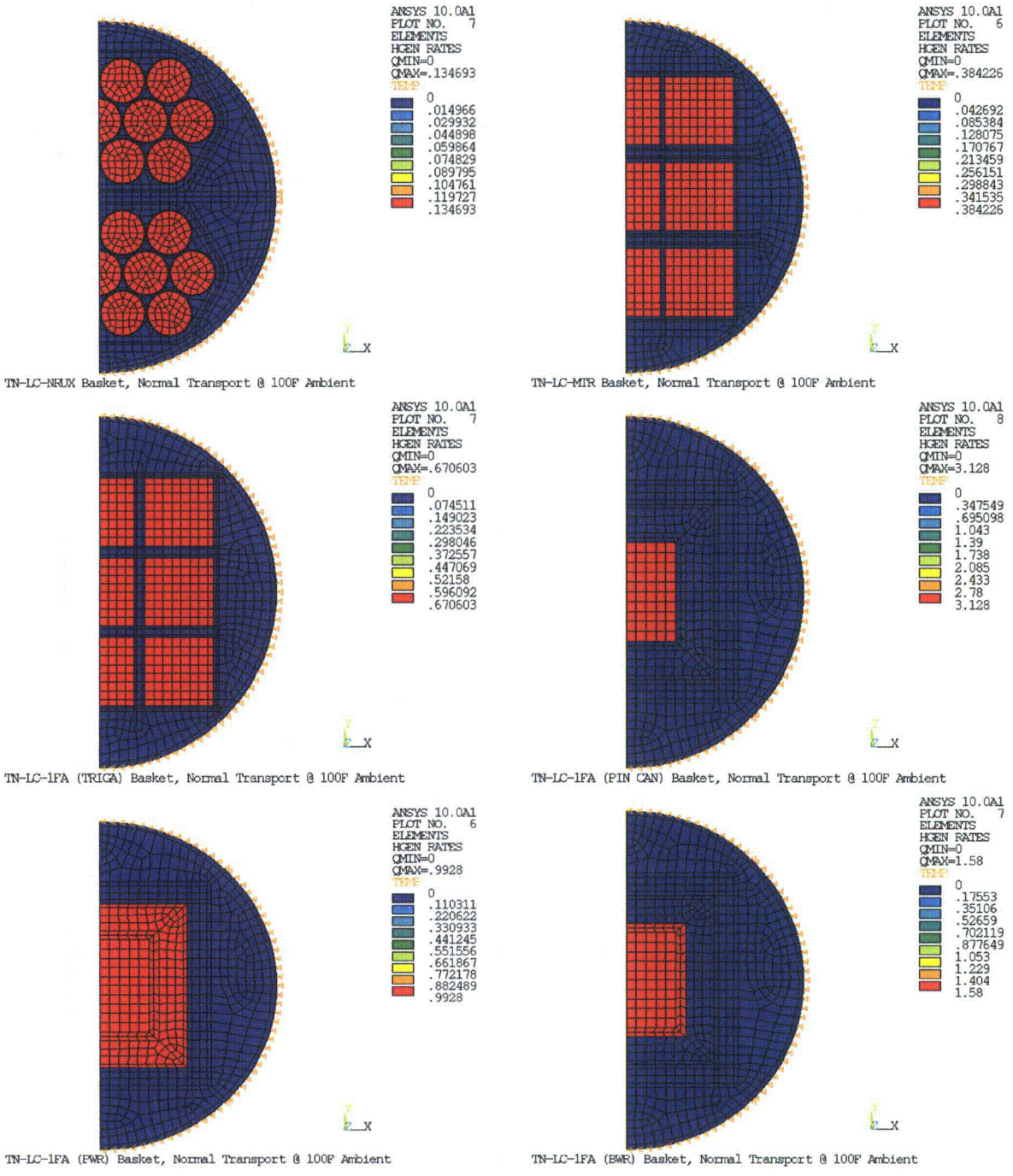

Figure 3-13
Typical Boundary Conditions for Fuel Baskets

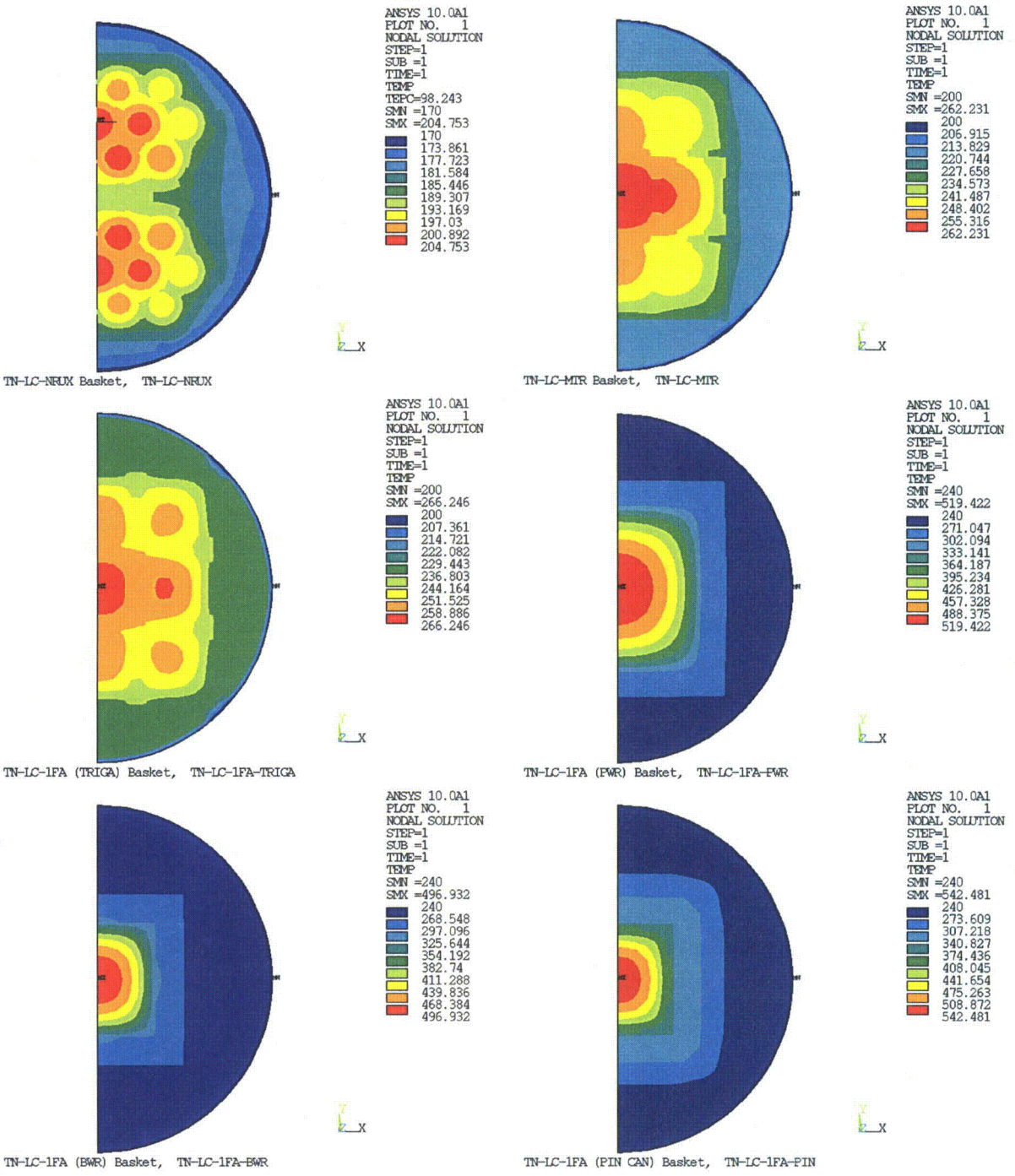

Figure 3-14
Temperature Distribution of Fuel Basket in TN-LC Transport Cask inside ISO Container for Hot NCT, 100°F Ambient with Insolation

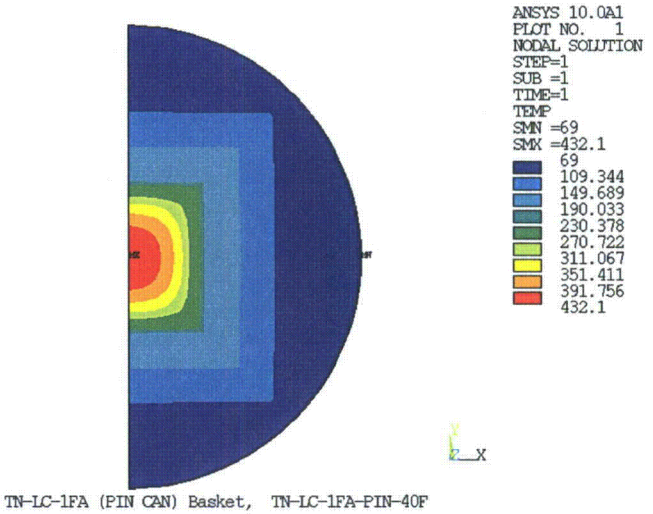

Figure 3-15
Temperature Distribution of Fuel Basket in TN-LC Transport Cask without ISO Container for Cold NCT, -40°F Ambient without Insolation

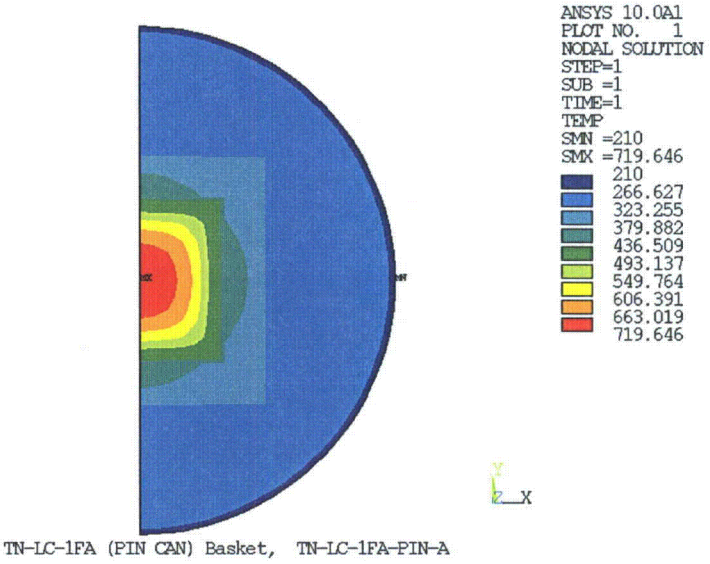

TN-LC-1FA with Fuel Pin Basket

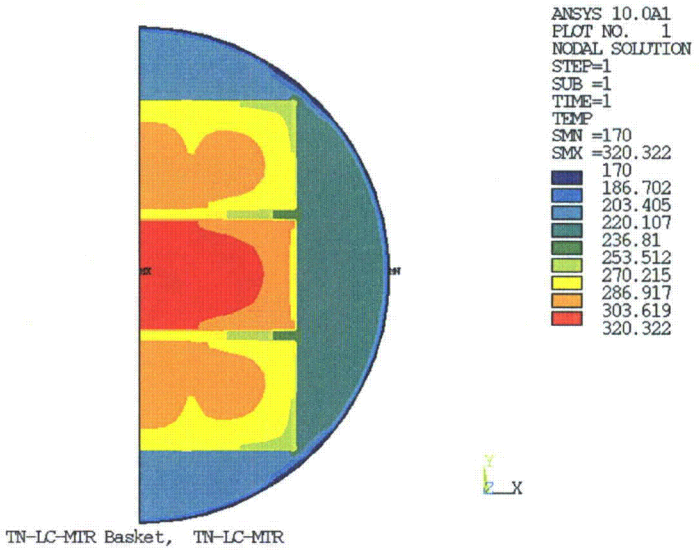

TN-LC-MTR Basket

Figure 3-16
Temperature Distribution of Fuel Baskets for
Dry Loading/Unloading Conditions

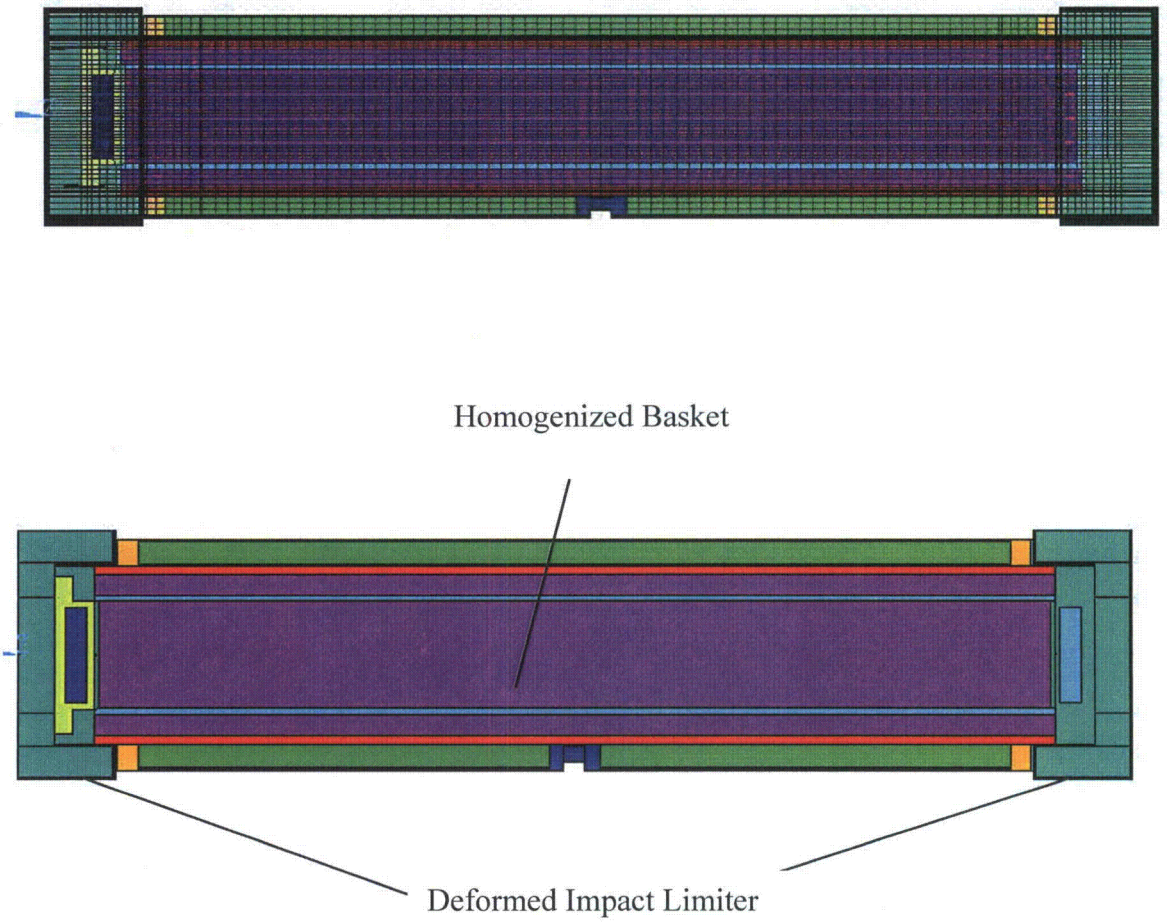

Figure 3-17
TN-LC Transport Cask Model for HAC Thermal Analysis

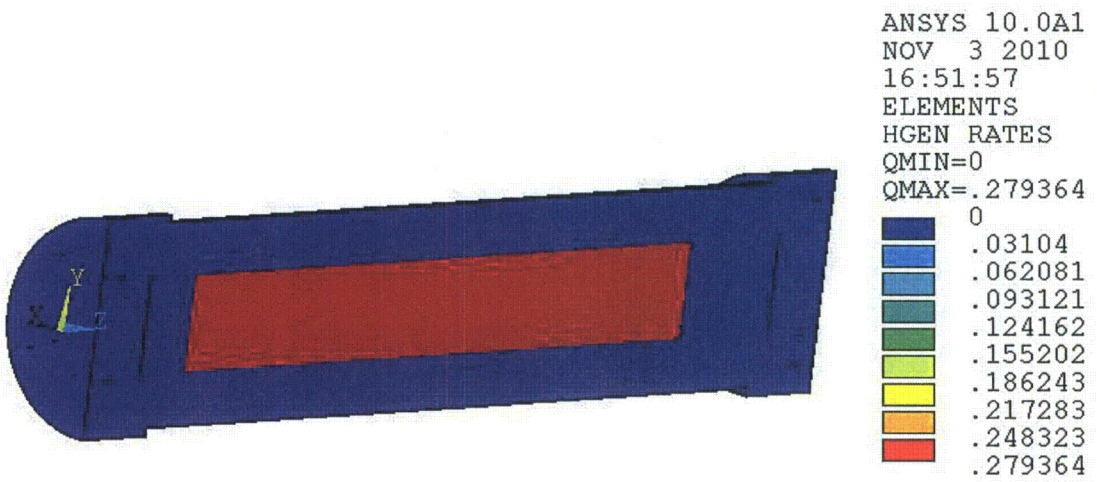

Heat Generation

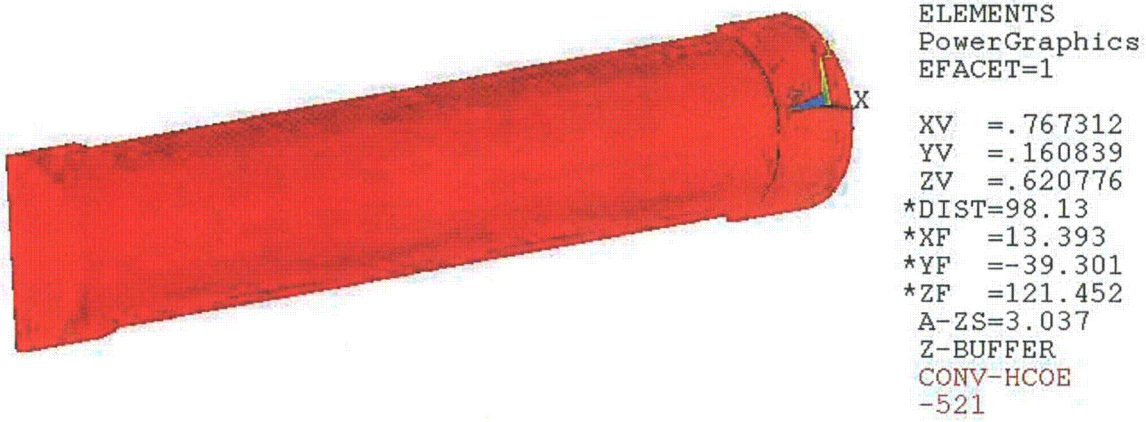

Fire Boundary Condition Applied over the Entire Exterior Surface of the Cask

Figure 3-18
Typical Boundary Conditions During Fire Conditions

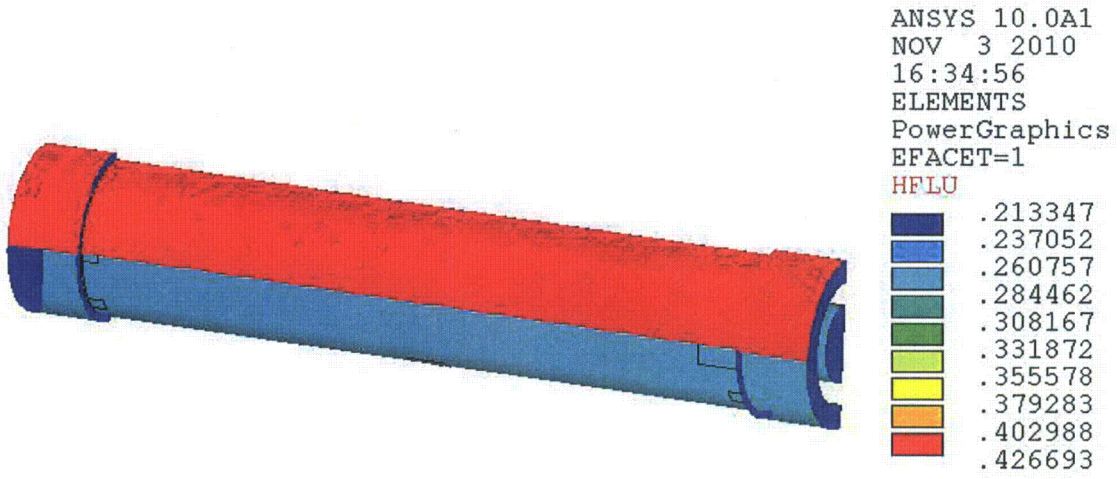

Solar Heat Flux Boundary Conditions During Smoldering/Post-Fire Conditions

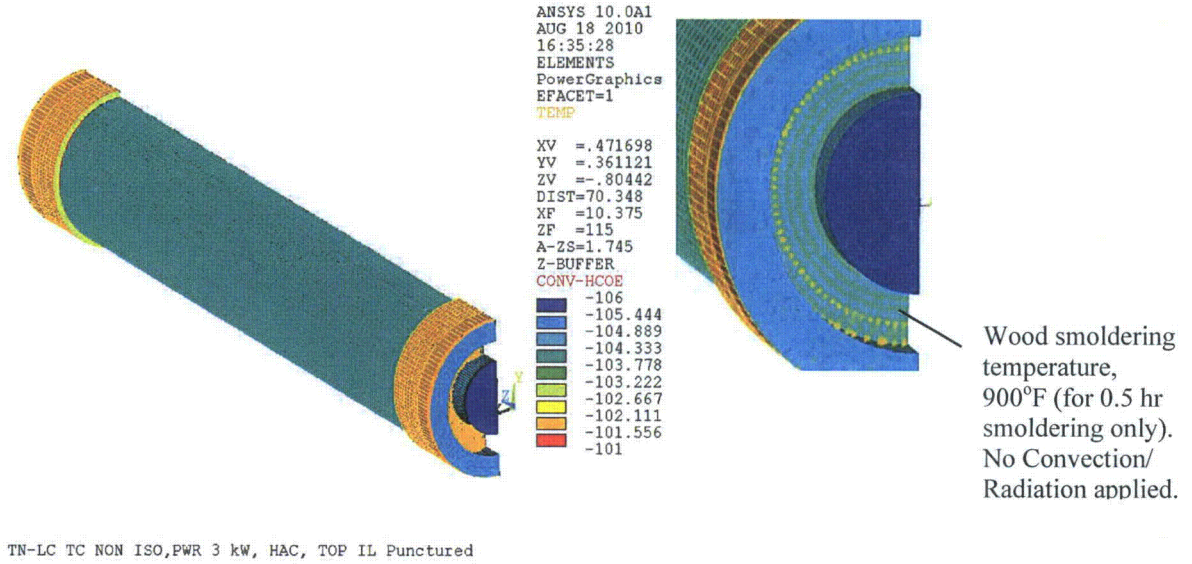

Convection Boundary Smoldering Conditions During /Cool Down Conditions

Figure 3-19
Typical Boundary Conditions for Smoldering/Cool Down Periods

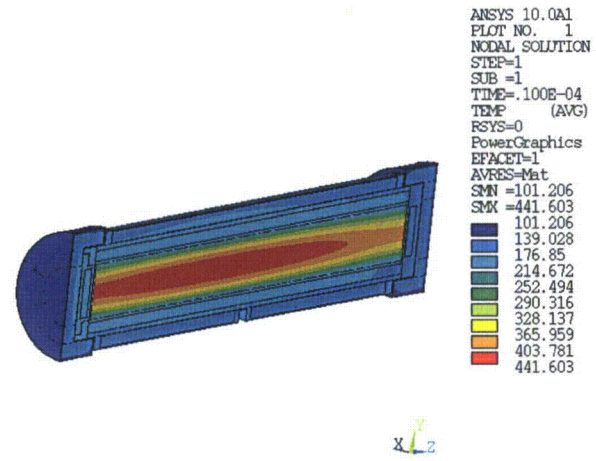

TN-LC TC, PWR 3 kW, NON-ISO, HAC Initial Temperatures

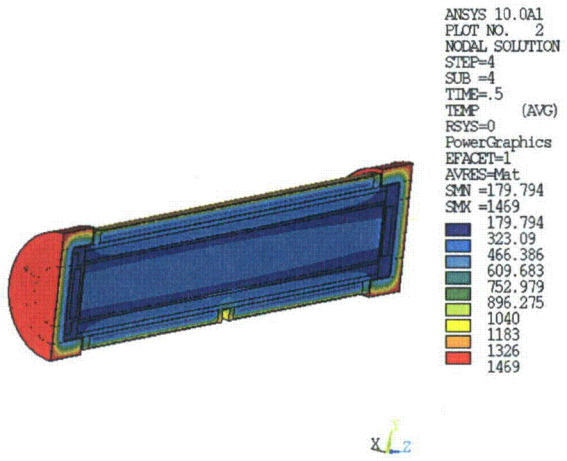

TN-LC TC, PWR 3 kW, NON-ISO, End of Fire

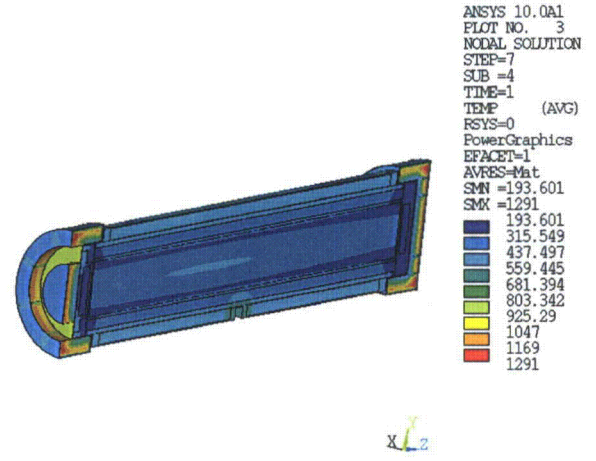

TN-LC TC, PWR 3 kW, NON-ISO, Smoldering Wood after Fire

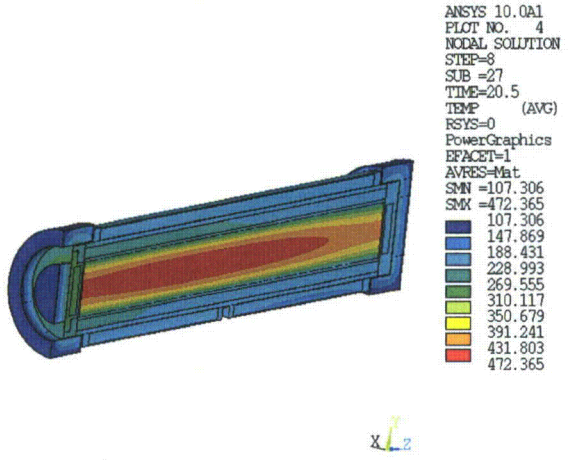

TN-LC TC, PWR 3 kW, NON-ISO, Puncture top IL, 20 hrs after Fire

Figure 3-20
Temperature Profiles for TN-LC Transpor Cask with 3 kW Heat Load under HAC

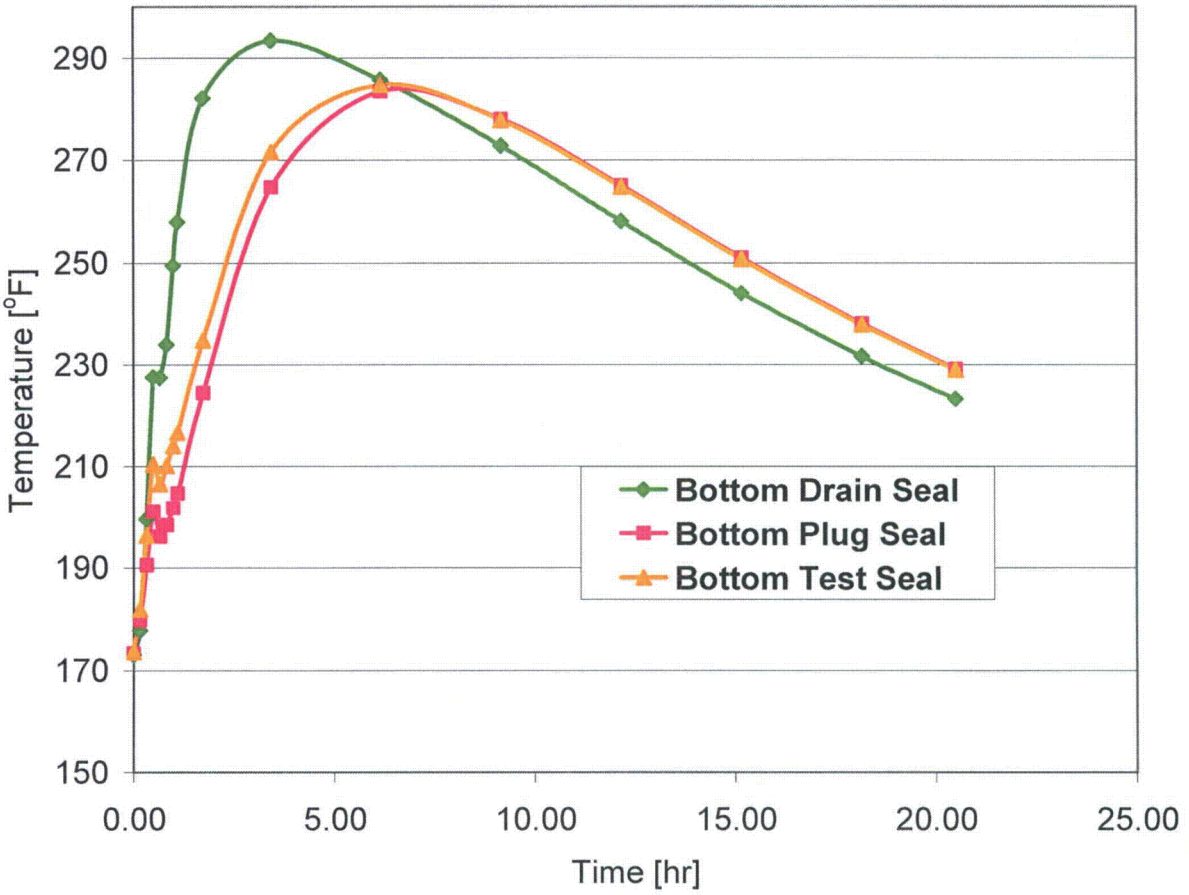

Figure 3-21
Temperature History for Seals at Bottom of TN-LC Transport Cask with 3 kW Heat Load under HAC

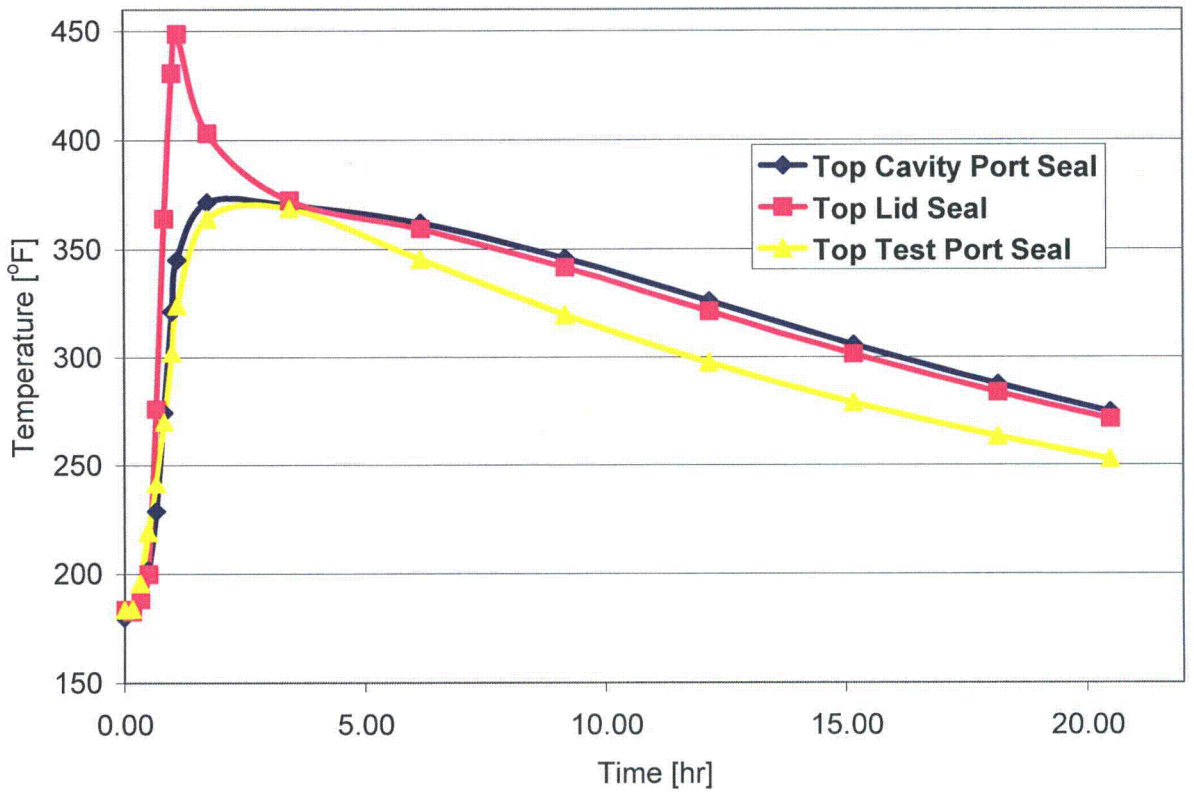

Figure 3-22
Temperature History for Seals at Top of TN-LC ransport Cask with 3 kW Heat Load under HAC

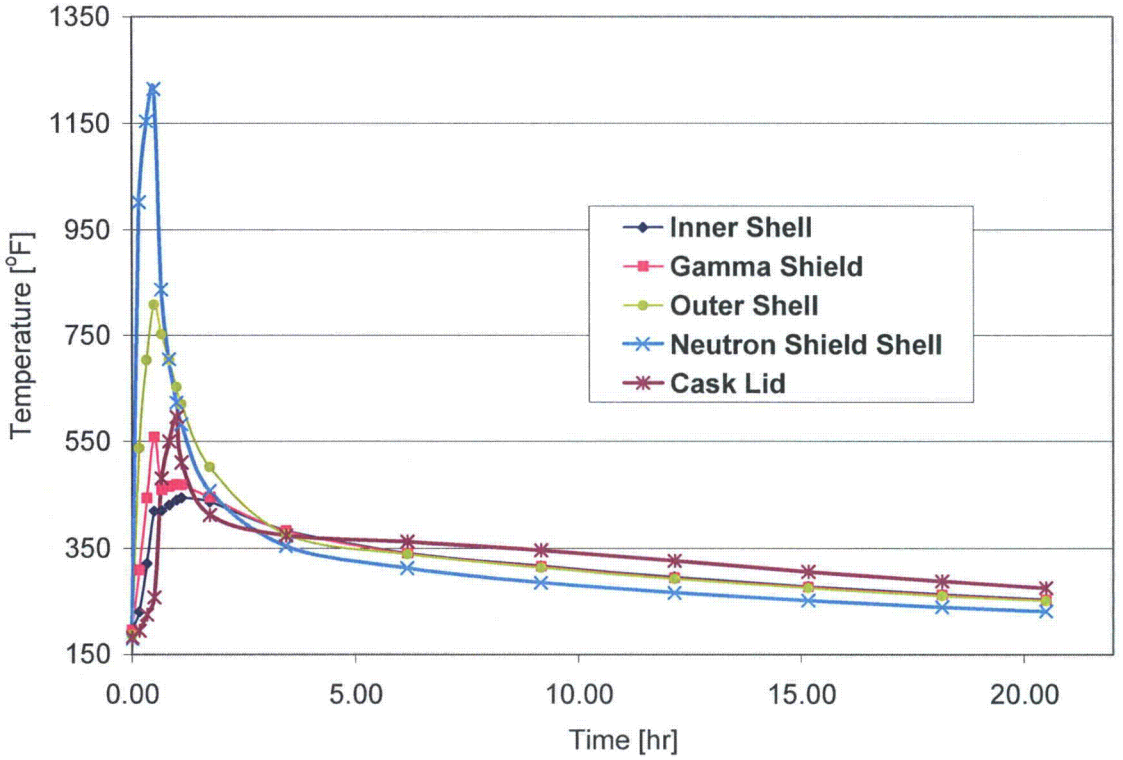

Figure 3-23
Temperature History for Components of TN-LC Transport Cask with 3 kW Heat Load under HAC

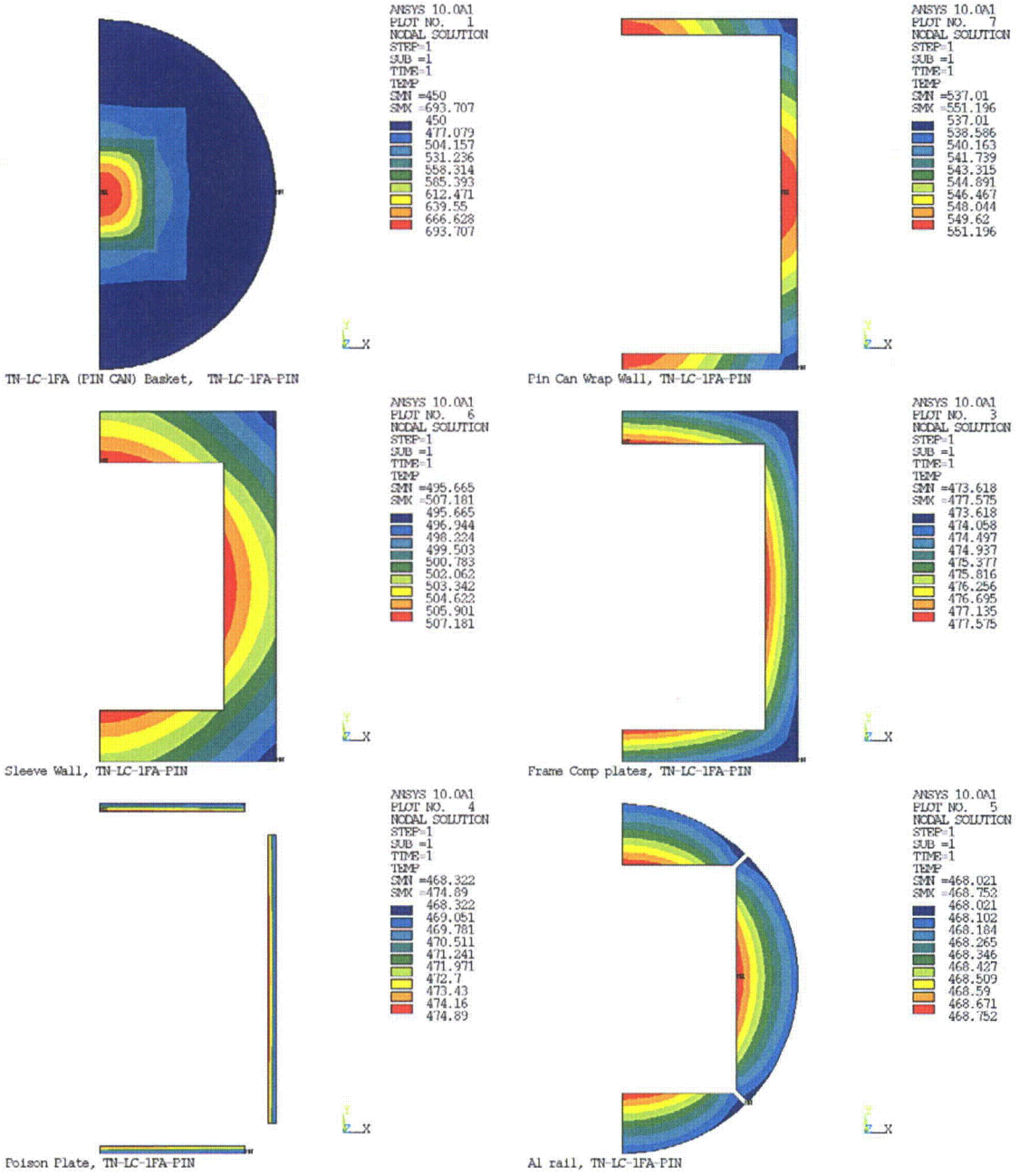

Figure 3-24
Typical Temperature Distribution of Fuel Basket Components for HAC

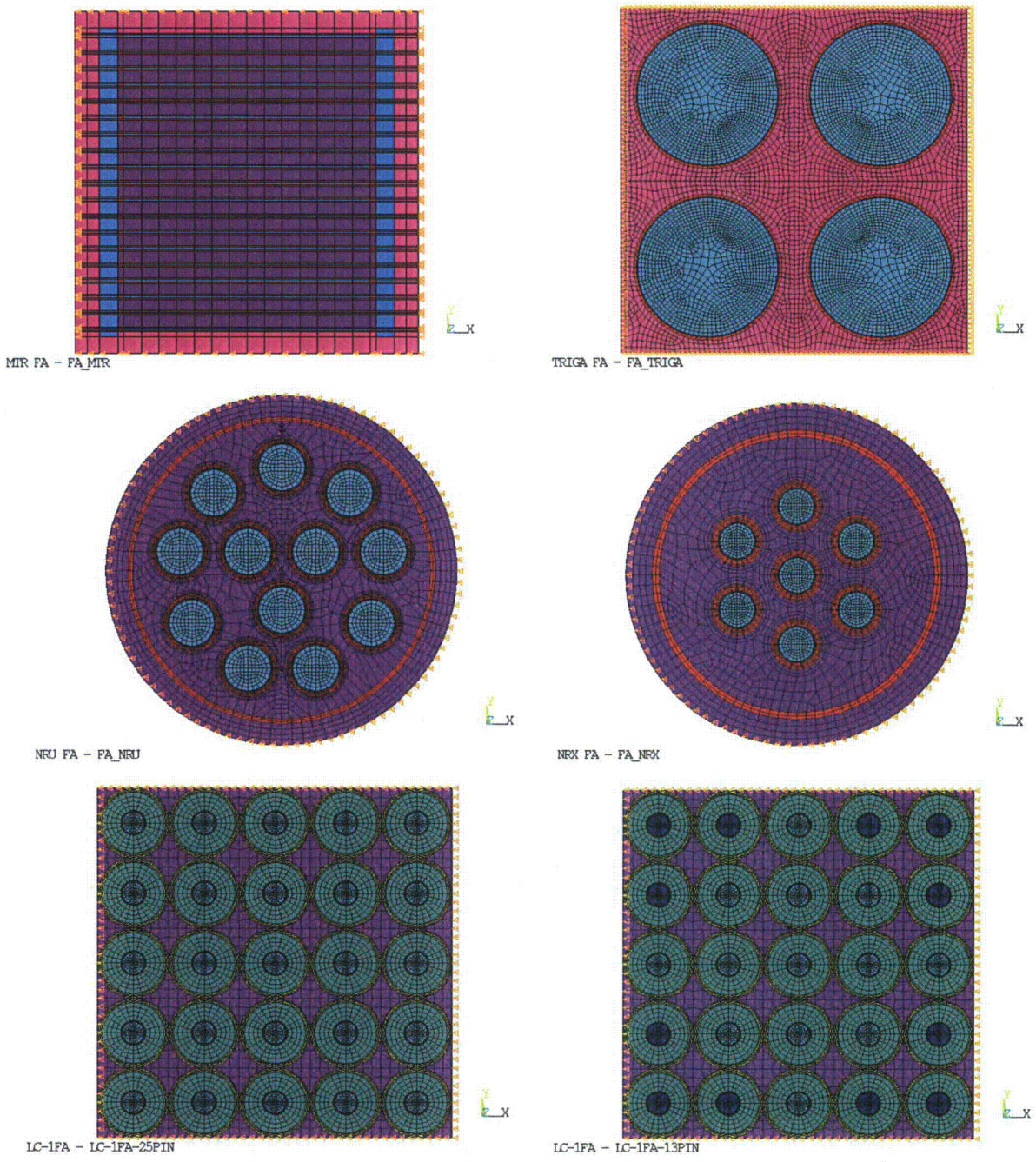

Figure 3-25
Two-Dimensional Finite Element Models of TN-LC Contents

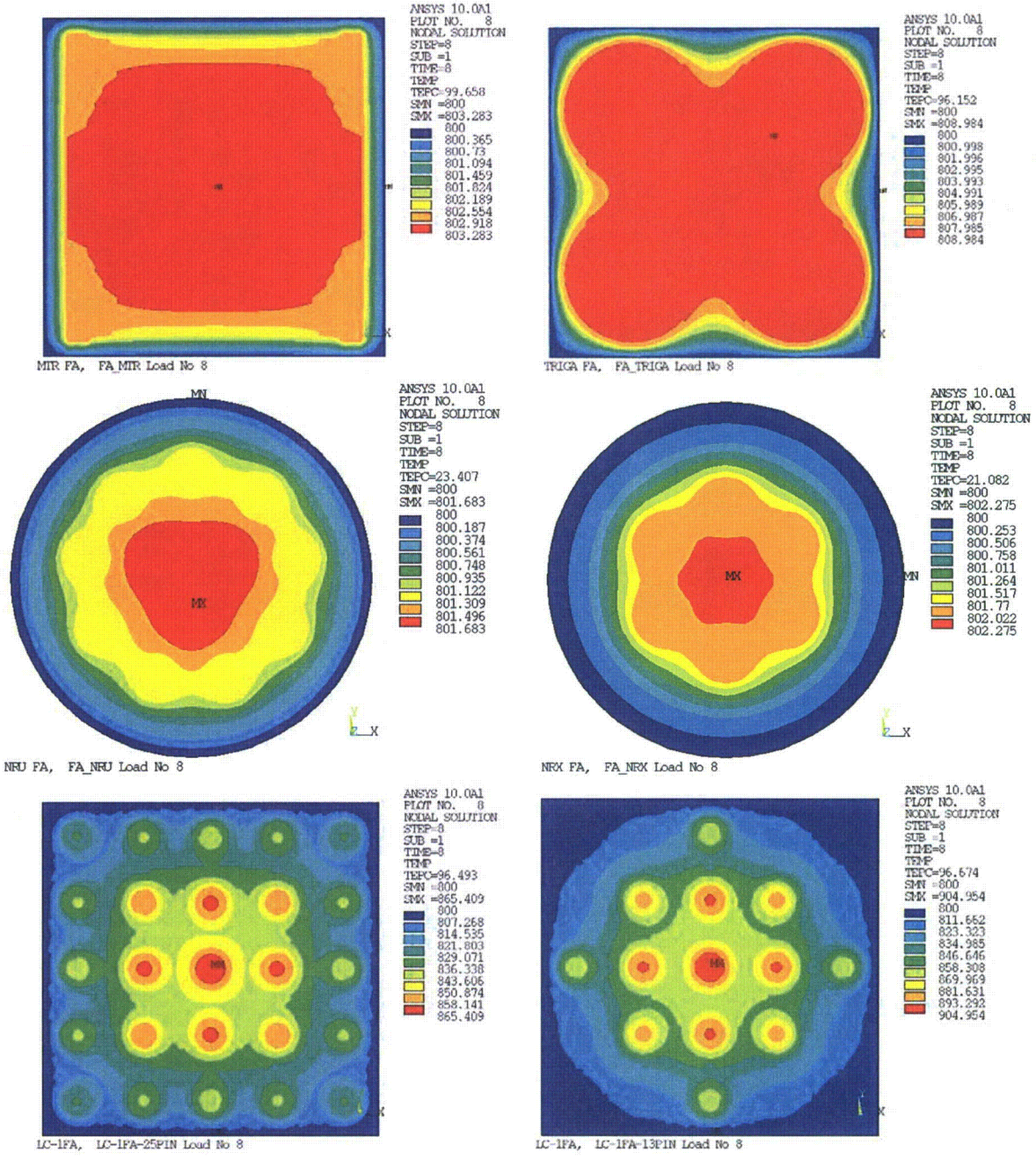

Figure 3-26
Temperature Plots for TN-LC FAs

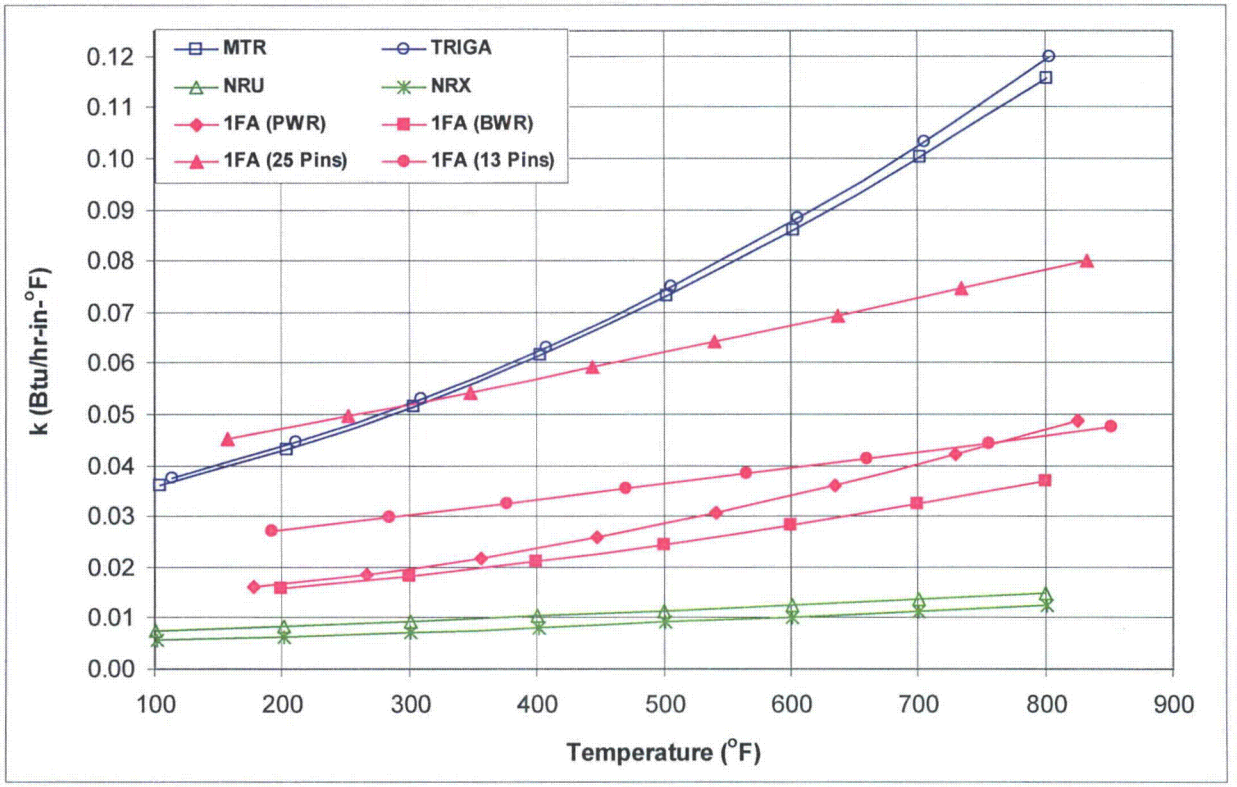

Figure 3-27
Transverse Fuel Effective Thermal Conductivity of TN-LC FAs

Chapter 4
Containment

TABLE OF CONTENTS

LIST OF FIGURES

Chapter 4
Containment

NOTE: References in this Chapter are shown as [1], [2], etc. and refer to the reference list in Section 4.5.

4.1 Description of Containment System

4.1.1 Containment Boundary

The containment boundary for the TN-LC cask consists of the inner shell, the bottom flange, the bottom plug, the bottom plug O-ring, the top flange, the lid, the lid inner O-ring seal and vent and drain port plug bolts and seals. The containment boundary is shown in Figure 4-1. The construction of the containment boundary is shown on the drawings provided in Chapter 1, Appendix 1.4.1. The containment vessel prevents leakage of radioactive material from the cask cavity. It also maintains an inert atmosphere (helium) in the cask cavity.

Helium assists in heat removal and provides a non-reactive environment to protect fuel assemblies against fuel cladding degradation which might otherwise lead to gross rupture.

4.1.1.1 Containment Vessel

The TN-LC packaging containment vessel consists of the 1.00-inch thick inner shell, a massive bottom end forging, bottom plug, a top end massive forging, a top lid cover assembly forging with lid bolts, vent and drain port closure bolts and seals, and the inner O-ring seals for the lid and bottom plug. An 18.00 inch diameter by 182.50 inch long cavity is provided.

The inner shell is SA-240 Type XM19 nitrogen-strengthened austenitic stainless steel, and the top and bottom flange forging materials are SA-182 Grade FXM19. The lid is constructed from SA-182 Grade F304 austenitic stainless steel. The TN-LC packaging containment vessel is designed, fabricated, examined and tested in accordance with the requirements of Subsection NB of the ASME Boiler and Pressure Vessel (BP&V) Code [1] to the maximum practical extent. In addition, the design meets the requirements of Regulatory Guides 7.6 [2] and 7.8 [3]. Alternatives to the ASME Code are discussed in Section 2.1.4 and Appendix 2.13.13. The design of the containment boundary is discussed in Chapter 2.

The TN-LC packaging design, fabrication and testing are performed under Transnuclear's (TN) Quality Assurance Program which conforms to the criteria in Subpart H of 10CFR71.

The materials of construction meet the requirements of Section III, Subsection NB-2000 and Section II, material specifications or the corresponding ASTM Specifications. The containment vessel is designed to the ASME BP&V Code, Section III, Subsection NB, Article 3200.

The containment vessel is fabricated and examined in accordance with NB-2500, NB-4000 and NB-5000. Also, weld materials conform to NB-2400 and the material specification requirements of Section II, Part C of the ASME BP&V Code.

The containment vessel is hydrostatically tested in accordance with the requirements of the ASME B&PV Code, Section III, Article NB-6200.

Even though the Code is not strictly applicable to transport casks, it is the intent to follow Section III, Subsection NB of the Code as closely as possible for design and construction of the containment vessel. The casks may, however, be fabricated by other than N-stamp holders and materials may be supplied by other than ASME Certificate Holders. Thus the requirements of NCA are not imposed. TN's quality assurance requirements, which are based on 10CFR71 Subpart H and NQA-1, are imposed in lieu of the requirements of NCA-3850. This SAR is prepared in place of the ASME design and stress reports. Surveillances are performed by TN and other personnel rather than by an Authorized Nuclear Inspector (ANI).

The materials of the TN-LC packaging will not result in any significant chemical, galvanic or other reaction as discussed in Chapter 2.

4.1.1.2 Containment Penetrations

The only penetrations through the containment boundary are the drain and vent ports, bottom plug plate (with or without gamma shielding) and the top closure plate (lid). Each penetration is designed to maintain a leak rate not to exceed 1.0×10^{-7} ref cm^3/s, defined as "leak tight" per ANSI N14.5 [4]. To obtain these seal requirements, each penetration has an O-ring face seal type closure. Additionally, the lid and bottom plug penetrations have double O-ring configurations.

4.1.1.3 Seals and Welds

All containment boundary welds are full penetration bevel or groove welds to ensure structural and sealing integrity. These full penetration welds are designed per ASME III Subsection NB and are fully examined by radiography or ultrasonic methods in accordance with Subsection NB.

Additionally, a liquid penetrant examination is performed on these welds.

Containment seals are located at the bottom plug plate, lid, the drain plug and the vent plug. The inner seal, when two seals are provided, is the primary containment seal. The outer, secondary seals, facilitate leak testing of the inner containment seal of the bottom plug and the lid. There are also test ports provided for these two closures. The test ports are not part of the containment boundary.

All the seals used in the TN-LC cask containment boundary are static face seals. The seal areas are designed such that no significant plastic deformation occurs under normal and accident loads as shown in Chapter 2. The bolts are torqued to maintain seal compression during all load conditions as shown in Appendix 2.13.2. The seals used for all of the penetrations are fluorocarbon elastomer O-rings. All seal contact surfaces are stainless steel and are machined to a 32 RMS or finer surface finish. The dovetail grooves in the cask lid and the bottom end plug cover plate are intended to retain the seals during installation. The volume of the grooves is controlled to allow the mating metal surfaces to contact under bolt loads, thereby providing uniform seal deformation in the final installation condition.

A fluorocarbon elastomeric seal was chosen for use on the TN-LC package because it has acceptable characteristics over a wide range of parameters. The fluorocarbon compound specified is VM835-75 or equivalent which meets the military rubber specification MIL-R-83485 [5]. (Note that this specification has been superseded by AMS-R-83485 [6]). Fluorocarbon O-rings are used in applications where temperatures are between -15°F and 400°F. The VM835-75 compound as listed on page 8-4 of the Parker O-ring Handbook [7] is specially formulated for use at temperatures as low as -40 °F while maintaining the upper temperature limit of 400°F. The selected seals remain leak tight (leak rate not exceeding 1.0×10^{-7} ref cm^3/s) at 482°F for accident conditions as shown in Parker O-Ring Handbook [7] and verified in the study documented in [8].

4.1.1.4 Closure

The containment vessel contains an integrally-welded bottom closure and a bolted and flanged top closure forging (lid). The lid forging is attached to the cask body with twenty (20), SA-540, Grade B23, Class 1, 1.0 inch diameter bolts and stainless steel washers. Closure of the bottom plug (with or without gamma shielding) is accomplished by eight (8), SA-540, Grade B23, Class 1, 0.5 inch diameter cap screws and stainless steel washers. The bolt torque required for the top lid and bottom plug are provided in Drawing 65200-71-01 in Chapter 1, Appendix 1.4.1. The closure bolt analysis is presented in Appendix 2.13.2.

Closure of each of the vent and drain ports is accomplished by a single 0.5 inch brass or ASTM A193, Grade B8 bolt with an elastomer seal under the head of the bolt.

4.2 Containment under Normal Conditions of Transport (Type B Packages)

4.2.1 Containment of Radioactive Material

As described earlier, the TN-LC cask is designed and tested for a leak rate of 1.0×10^{-7} ref cm^3/s, defined as "leak tight" per ANSI N14.5. Additionally, the structural and thermal analyses presented in Chapters 2 and 3, respectively, verify that there is no release of radioactive materials under any of the normal or accident conditions of transport.

4.2.2 Pressurization of Containment Vessel

The TN-LC cask contains one of four basket designs holding dry irradiated fuel and helium gas which is used to backfill the cask after drying. Therefore, the pressure in the TN-LC cask when loaded with fuel is from helium that has been backfilled into an evacuated cask cavity to a pressure of 2.5 ± 1 psig at the end of loading. If the TN-LC cask contains design basis fuel at thermal equilibrium, the cask cavity helium temperature with 100°F ambient air and maximum insolation is 282°F. The maximum normal operating pressure (MNOP) is calculated in Chapter 3 to be 16.9 psig. The analyses in Chapters 2 and 3 demonstrate that the TN-LC cask effectively maintains containment integrity with a cavity pressure of 30 psig.

4.2.3 Containment Criteria

The TN-LC cask is designed to be "leak tight." The acceptance criterion for fabrication verification and periodic verification leak tests of the TN-LC cask containment boundary shall be 1.0×10^{-7} ref cm^3/s. The test must have a sensitivity of at least one half the acceptance criterion, or 5.0×10^{-8} ref cm^3/s. The testing of the containment boundary is described in Chapter 8.

4.3 Containment under Hypothetical Accident Conditions (Type B Packages)

4.3.1 Fission Gas Products

There is no need to explicitly determine the source term available for release. As described earlier, the TN-LC cask is designed and tested for a leakage rate of 1.0×10^{-7} ref cm^3/s, defined as "leak tight" per ANSI N14.5.

4.3.2 Containment of Radioactive Material

The TN-LC cask is designed and tested to be "leak tight." The results of the structural and thermal analyses presented in Chapters 2 and 3, respectively, verify the package will meet the leakage criteria of 10CFR71.51 for the hypothetical accident scenario.

4.3.3 Containment Criterion

This package has been designed and is verified by leakage testing to meet the "leak-tight" criteria of ANSI N14.5. The results of the structural and thermal analyses presented in Chapters 2 and 3, respectively, verify the package will meet the leakage criteria of 10CFR71.51 for all the hypothetical accident conditions.

4.4 Special Requirements

The TN-LC package may contain plutonium in excess of 0.74 Tbq (20 Ci) per package as a consequence of irradiation of the reactor fuel. As such, the plutonium is in solid form within the fuel matrix and must remain in the solid form.

4.5 References

1. American Society of Mechanical Engineers, ASME Boiler and Pressure Vessel Code, Section III, Division 1 – Subsection NB, 2004 edition including 2006 Addenda.

2. USNRC Regulatory Guide 7.6, "Design Criteria for the Structural Analysis of Shipping Cask Containment Vessel," Rev. 1, March 1978.

3. USNRC Regulatory Guide 7.8, "Load Combinations for the Structural Analysis of Shipping Cask," Rev. 1, March 1989.

4. ANSI N14.5-1997, "American National Standard for Radioactive Material – Leakage Tests on Packages for Shipment," February 1998.

5. United States Air Force Military Specification MIL-R-83485, "Rubber, Fluorocarbon Elastomer, Improved Performance at Low Temperatures," December 8, 1976.

6. Society of Automotive Engineers (SAE) Aerospace Material Specification (AMS) AMS-R-83485, "Rubber, Fluorocarbon Elastomer, Improved Performance at Low Temperatures", May 1, 1998.

7. "Parker O-Ring Handbook," Publication No. ORD-5700, 2007 Edition, Parker Seals www.parkerorings.com.

8. Skidmore, T. Eric, "Performance Evaluation of O-Ring Seals in Model 9975 Packaging Assemblies (U)," Westinghouse Savannah River Company, Document No. WSRC-TR-98-00439, December 1998, http://sti.srs.gov/fulltext/1998/tr98439.pdf.

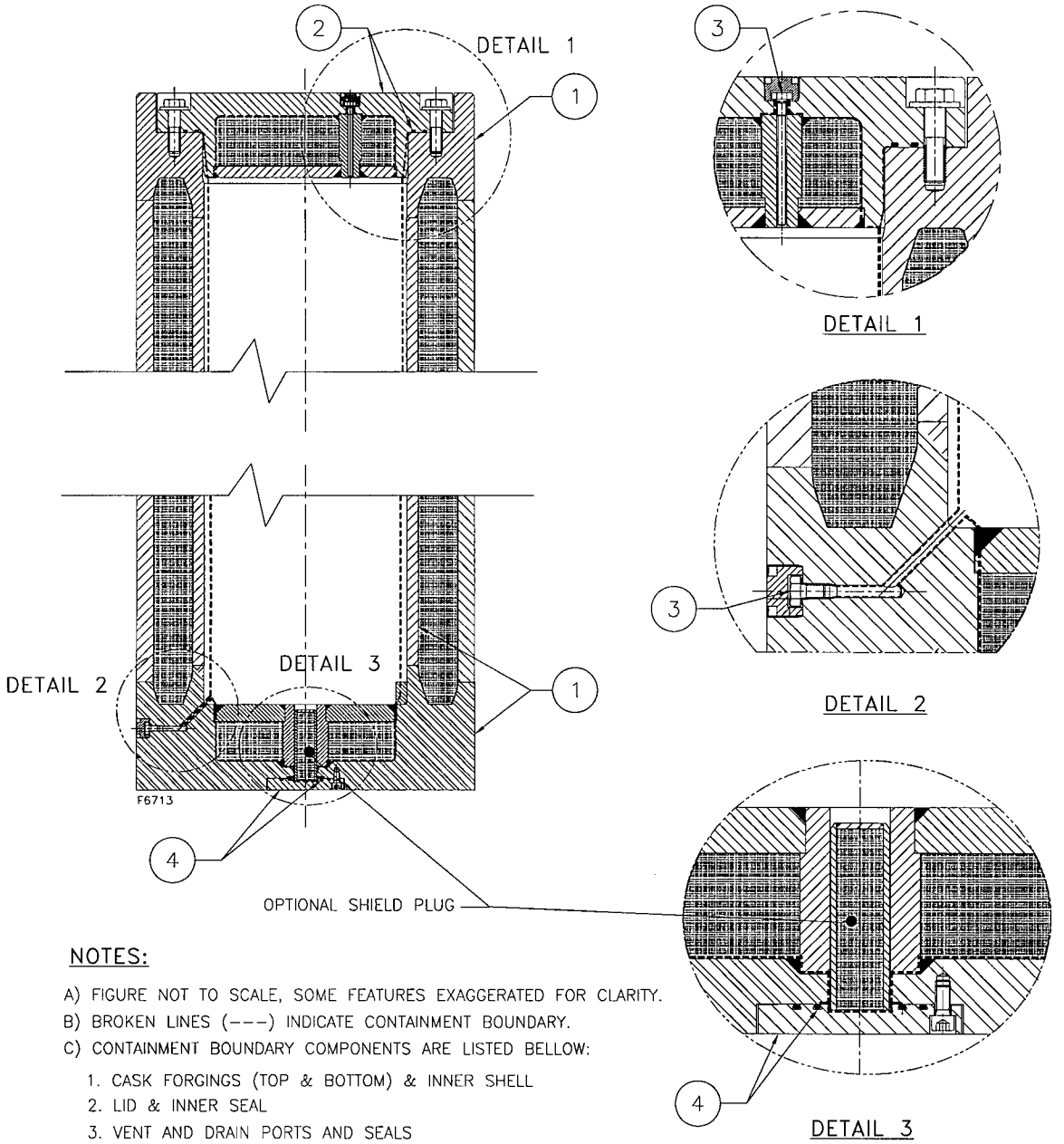

Figure 4-1
TN-LC Cask Containment

Chapter 5
Shielding Evaluation

TABLE OF CONTENTS

LIST OF TABLES

LIST OF FIGURES

Chapter 5
Shielding Evaluation

NOTE: References in this Chapter are shown as [1], [2], etc. and refer to the reference list in Section 5.5.

This chapter presents the shielding evaluation of the TN-LC transportation package. The dose rates are evaluated per the requirements of 10CFR71.47 and 71.51 for exclusive use transportation in a closed transport vehicle.

The dose rates are evaluated for the four basket types using MCNP5 v1.40 [1]. Information common to all analyses are summarized in the main body of this chapter. The details for each analysis are contained in a separate appendix. The list of appendices is as follows:

TN-LC-MTR Basket:	Appendix 5.6.1.
TN-LC-NRUX Basket:	Appendix 5.6.2.
TN-LC-TRIGA Basket:	Appendix 5.6.3.
TN-LC-1FA Basket:	Appendix 5.6.4.

5.1 Description of the Shielding Design

5.1.1 Design Features

The TN-LC cask is radially and axially shielded with steel and lead.

Proprietary Information Withheld Pursuant to 10 CFR 2.390.

The neutron shield may be either Resin-F or VYAL-B.

Proprietary information withheld pursuant to 10 CFR 2.390.

The description of the shielding design for the four basket types are contained in the individual appendices for each basket.

5.1.2 Summary Tables of Maximum Radiation Levels

Normal conditions of transport (NCT) dose rates are computed for exclusive use transport in a closed transport vehicle. These dose rate limits are as follows:

- Surface of the package: 1000 mrem/hr
- Surface of the transport vehicle: 200 mrem/hr
- 2 m from the surface of the transport vehicle: 10 mrem/hr

The transport vehicle is assumed to be 8 ft wide. Because the TN-LC is a long package, the ends of the transport vehicle are conservatively assumed to be at the ends of the impact limiters. The

underside (floor) of the vehicle is conservatively assumed to correspond to the radius of the impact limiters. The dose rates on the vehicle roof are not computed, as these dose rates are bounded by the dose rates on the underside of the vehicle.

Dose rates are computed 2 m from the sides and ends of the vehicle. The dose rates in an occupied location are estimated to correspond to 2 m from the ends of the vehicle. As these dose rates exceed the limit of 2 mrem/hr for some baskets, per 10CFR71.47(b)(4), the TN-LC shall be transported by private carrier, and personnel in occupied locations shall wear dosimetry devices. The NCT dose rates for each basket type are summarized in the following tables:

Table 5-1: Summary of TN-LC-MTR NCT Dose Rates

Table 5-2: Summary of TN-LC-NRUX NCT Dose Rates

Table 5-3: Summary of TN-LC-TRIGA NCT Dose Rates

Table 5-4: Summary of TN-LC-1FA NCT Dose Rates

Hypothetical accident condition (HAC) dose rates are computed for each basket. Under HAC, it is conservatively assumed that both the neutron shield and impact limiter wood is lost. Lead slump as a result of an accident is also included. Dose rates are computed 1 m from the surface of the cask body. The HAC dose rate limit is 1000 mrem/hr. The HAC dose rates for each basket type are summarized in the following tables:

Table 5-5: Summary of TN-LC-MTR HAC Dose Rates

Table 5-6: Summary of TN-LC-NRUX HAC Dose Rates

Table 5-7: Summary of TN-LC-TRIGA HAC Dose Rates

Table 5-8: Summary of TN-LC-1FA HAC Dose Rates

5.2 Source Specification

The TRITON module of the SCALE6 code package [2] is used to compute the gamma and neutron source terms for MTR, NRU/NRX, and TRIGA fuels. The SAS2H module of the SCALE4.4 code package [3] is used to compute the gamma and neutron source terms for BWR and PWR fuel assemblies and rods.

For each fuel type, a bounding source term is developed for NCT analysis. For MTR, NRU/NRX, and TRIGA fuels, the same source term may be used for NCT and HAC analysis This is because the contribution of neutron radiation sources to the total dose rate is either negligible (see, for example, Table 5-1 or Table 5-3), the total dose rate at some or all of the locations of interest are substantially lower than the regulatory limits (see Table 5-2), or both. For BWR/PWR fuel, the contribution of neutron radiation source to the total dose rate may be large, and separate HAC source terms are developed because the loss of the neutron shield increases the neutron contribution to the dose rate.

A detailed discussion of the source specification for each fuel type is contained in the individual appendices for each basket.

5.2.1 Crud Evaluation for Shielding

Proprietary Information Withheld Pursuant to 10 CFR 2.390

Proprietary Information Withheld Pursuant to 10 CFR 2.390

5.3 Shielding Model

5.3.1 Configuration of Source and Shielding

The fuel, basket, and cask are modeled explicitly in the MCNP computer program for all basket models. The cask model is common to all basket designs and is described in this section. The fuel and basket models are described in the individual appendices for each basket.

The cask is modeled explicitly. The key dimensions are provided in Table 5-9 for the cask and impact limiters. Cask and impact limiter dimensions are obtained from the drawings in Chapter 1. All important cask features are modeled, including the cavity test port penetration in the cask lid and the bottom plug assembly, both of which penetrate the lead at the ends of the cask. The lid leak test port, bottom leak test port, and drain port are not modeled because they are located in regions of the cask that would not result in appreciable streaming. An example of the overall model geometry (with the TN-LC-MTR basket illustrated) is shown in Figure 5-1 through Figure 5-4. The cask model for the other basket models is the same. The overall model geometry is illustrated in Figure 5-1. A close-up view of the model ends is illustrated in Figure 5-2. A view perpendicular to the cask axis is illustrated in Figure 5-3. A view through the impact limiter attachment blocks is illustrated in Figure 5-4.

In the neutron models, the trunnions, impact limiter attachment blocks, and the shear key are modeled explicitly because these items displace neutron shielding. The shear key is filled with steel because, in the transport condition, the shear key mates with a steel block attached to the transport vehicle. In the gamma models, these items are conservatively ignored and, hence, treated as neutron shielding material. All figures illustrate the neutron models because the neutron model geometry is more complex.

Proprietary Information Withheld Pursuant to 10 CFR 2.390

The impact limiters are modeled in a simplified manner as a 1/8 in. shell of steel filled with balsa without any other details because the impact limiters offer little shielding and are primarily filled with low-density material.

Under hypothetical accident conditions (HAC), the impact limiter wood and neutron shield resin are replaced with air. This bounds any postulated fire or crush damage. In addition, 1.2 in. of lead slump is modeled at both the top and bottom ends of the radial cask lead as a result of an end drop. This bounds the maximum lead slump value listed in Chapter 2. Radial lead slump of

0.2 in. is also modeled in the lead disks in the TN-LC-1FA (1FA acronym stands for the cask payload with one LWR assembly in the text that follows unless specified otherwise) model in the lid and bottom end as a result of a side drop. This bounds the maximum radial lead slump listed in Chapter 2. The structural evaluation in Chapter 2 demonstrates that the various basket geometries are maintained under HAC. Therefore, no changes are made to the basket geometries in the HAC shielding models. HAC dose rates are conservatively computed 1 m from the cask body surface for each basket.

5.3.2 Material properties

The material properties of all materials used in the basket and cask models are provided in this section. The SCALE standard composition [3] is employed for all materials except the neutron resin. Material properties for fuel materials are provided in the individual appendices.

Stainless steel used in the basket and cask models has a density of 7.94 g/cm^3 [3] and the composition provided in Table 5-10. The XM-19 stainless steel that comprises the inner shell, outer shell, and top and bottom forgings is modeled as 304 stainless steel for simplicity.

Cask lead is modeled as pure with a density of 11.35 g/cm^3 [3].

Aluminum used as basket rails and neutron resin casing is modeled as pure with a density of 2.7 g/cm^3 [3]. The poison plates in the TN-LC-TRIGA and TN-LC-1FA baskets are also modeled as pure aluminum (i.e., no boron is modeled).

Proprietary Information Withheld Pursuant to 10 CFR 2.390

The composition of air is provided in Table 5-12.

The composition of balsa wood is $C_6H_{10}O_5$ [3] and is used in the impact limiters. The minimum density of balsa is 7 lb/ft^3 per the drawings in Chapter 1, which is equivalent to a density of 0.112 g/cm^3.

5.3.3 Notes on VYAL-B Mixing and Installation

Proprietary Information Withheld Pursuant to 10 CFR 2.390

Proprietary Information Withheld Pursuant to 10 CFR 2.390

5.4 Shielding Evaluation

5.4.1 Methods

MCNP5 v1.40 is used for the shielding analysis [1]. MCNP5 is a standard, well-accepted shielding program utilized to compute dose rates for shielding licenses. A three-dimensional model is developed that captures all of the relevant design parameters of the cask and internals. Dose rates are calculated by tallying the neutron and gamma fluxes over surfaces of interest and converting these fluxes to dose rates using flux-to-dose rate conversion factors. Secondary gammas resulting from neutron capture are also tallied. Subcritical neutron multiplication is also performed by the program.

Separate models are developed for neutron and gamma source terms. Simple Russian roulette is used as a variance reduction technique for most tallies. The importance of the particles increases as the particles traverse the shielding materials. When necessary, DXTRAN spheres are used to accelerate program convergence above the vent port in the lid or below the bottom plug assembly.

5.4.2 Input and Output Data

Input and output data for the various basket models are discussed in the individual appendices.

5.4.3 Flux-to-Dose-Rate Conversion

ANSI/ANS-6.1.1-1977 flux-to-dose-rate conversion factors are utilized for both neutron and gamma radiation. These factors are obtained from the MCNP user's manual [4] and are provided in Table 5-13.

5.4.4 External Radiation Levels

Tally locations are selected to be consistent with exclusive use transportation in a closed transport vehicle. Therefore, the applicable NCT dose rate limits from 10CFR71.47(b)(1), (2) and (3) are:

- 1000 mrem/hr on the package surface. This includes the surface of the cask between the impact limiters, and the impact limiter surfaces.
- 200 mrem/hr on the vehicle surface. The vehicle has six surfaces (2 sides, 2 ends, roof, and underside). The two sides of the vehicle are assumed to be 8 ft apart with the package in the center. The underside (floor) of the vehicle is conservatively assumed to be at the impact limiter radius, and the dose rates at the underside of the vehicle bound the dose rates at the roof of the vehicle, which is farther away from the package. The ends of the vehicle are conservatively assumed to be at the impact limiter end surfaces.
- 10 mrem/hr 2 m from the vehicle surface. This dose rate does not apply 2 m from the roof of the vehicle or 2 m from the underside of the vehicle.

Circumferential tallies are placed around the packaging. Twenty-nine (29) axial locations are utilized, as illustrated in Figure 5-5. Locations 8 through 22 are utilized on the side of the cask between the impact limiters, Locations 6 through 24 are utilized on the side of the package at the

impact limiter radius (underside of vehicle) and the side of the vehicle, and Locations 1 through 29 are utilized 2 m from the side of the vehicle.

At the ends of the packaging, dose rates are tallied on the impact limiter surfaces and 2 m from the impact limiter surfaces. Eight radial locations are utilized for the surface tallies, as illustrated in Figure 5-6. Location 1 captures any streaming effects from the bottom plug assembly. An off-center tally is used directly over the lid port to capture any streaming effects on the top impact limiter surface. For the dose rates 2 m from the ends, five radial locations are utilized by combining Locations 1,2,3 and 4,5, as shown on Figure 5-6. The effect of end streaming through the lid port and bottom plug assembly is investigated only for the 1FA basket because this basket results in the highest dose rates through the ends of the package. The effects of streaming 2 m from the ends of the transport vehicle are shown to be small.

Because the basket designs are not circumferentially symmetric, the dose rate will vary around the perimeter of the package. This effect is most pronounced close to the package surface, and diminishes with distance. Close to the surface of the package, this variation is approximately 15 percent from the average in most cases. At 2 m from the surface of the vehicle, this variation is typically small (~5 percent). Because the dose rates near the radial surface of the cask are significantly below the dose rate limits, a detailed tally to capture these angular effects is not warranted. Therefore, circumferential average tallies are reported in the radial direction for most dose rate locations, and are supplemented with more detailed mesh tally results only when necessary.

However, because the impact limiter attachments and the shear key penetrate the neutron shield and displace neutron shielding material, there may be neutron streaming at these locations. This effect is captured explicitly using angular mesh tallies. The streaming effect is more pronounced at the location of the shear key because it is at the axial center of the cask. The impact limiter attachments are near the top and bottom of the cask where the neutron source is typically much smaller.

The shear key faces downward and results in a higher than average neutron dose rate on the surface of the package and the underside of the vehicle. For this reason, at these dose rate locations, the circumferential tally results are supplemented by neutron mesh tally results at the shear key. The shear key and impact limiter attachments do not result in gamma streaming because neutron shielding material is replaced with steel, which is a superior gamma shield. Therefore, these features are conservatively omitted in the gamma models.

Circumferential average dose rates are reported 2 m from the surface of the transport vehicle, which is the limiting location for dose rates. The cask pay load with 1 LWR fuel assembly, referred to as 1 FA through out this and other individual appendices, results in 2 meters from side of the cask radial dose rates that are bounding for those due to other payloads of the cask. Because of this, the circumferential averaged tallies are supplemented with mesh tallies at this location in the shielding analysis model of the cask with 1 LWR FA payload. It is demonstrated that at 2 m from the vehicle, the angular fluctuation of the dose rate is small (typically ~5 percent from the average value).

In the HAC models, the neutron shield resin and impact limiter wood is replaced with air, and the tally surfaces are located 1 m from the outer surfaces of the cask. Lead slump is modeled in the cask-body lead at both ends of the cask. Radial lead slump in the lead disks in the lid and

bottom ends are modeled in the 1FA models only, although the effect on the dose rates is negligible. The dose rates at the ends of the package are divided into three radial segments, and the dose rates at the side of the package are divided in 25 axial segments of equal width. The tally locations are shown on Figure 5-7.

The detailed results are provided in the individual appendices.

5.5 References

1. MCNP5, "MCNP – A General Monte Carlo N-Particle Transport Code, Version 5; Volume II: User's Guide," LA-CP-03-0245, Los Alamos National Laboratory, April 2003

2. SCALE: A Modular Code System for Performing Standardized Computer Analyses for Licensing Evaluations, ORNL/TM-2005/39, Version 6, Vols. I-III, January 2009

3. SCALE 4.4, "Modular Code System for Performing Standardized Computer Analyses for Licensing Evaluation for Workstations and Personal Computers," CCC-545, ORNL.

4. MCNP5, "MCNP – A General Monte Carlo N-Particle Transport Code, Version 5; Volume I: Overview and Theory," LA-UR-02-7162, Los Alamos National Laboratory, April 2003.

5. NUREG/CR-6487, "Containment Analysis for Type B Packages used to Transport Various Contents," Lawrence Livermore National Laboratory, 11/96.

5.6 Appendices

5.6.1 TN-LC-MTR Basket Shielding Evaluation

5.6.2 TN-LC-NRUX Basket Shielding Evaluation

5.6.3 TN-LC-TRIGA Basket Shielding Evaluation

5.6.4 TN-LC-1FA Basket Shielding Evaluation

Table 5-1
Summary of TN-LC-MTR NCT Dose Rates

(Exclusive Use Package for Transportation)

Package Surface (mrem/hr)				
	Top End	**Side**	**Bottom End**	
Gamma	82.5	65.5	32.3	
Neutron	1.98	5.89	0.922	
(n,g)	3.59E-02	8.48E-02	2.08E-02	
Total	84.5	71.5	33.3	
Limit	**1000**	**1000**	**1000**	
Vehicle Surface (mrem/hr)				
	Top End[1]	**Side**	**Bottom End [1]**	**Underside**
Gamma	82.5	21.2	32.3	46.6
Neutron	1.98	0.364	0.922	0.792
(n,g)	3.59E-02	1.51E-02	2.08E-02	2.71E-02
Total	84.5	21.6	33.3	47.5
Limit	**200**	**200**	**200**	
2 m from Vehicle Surface (mrem/hr)				
	Top End	**Side**	**Bottom End**	
Gamma	3.43	6.62	2.02	
Neutron	8.62E-02	0.119	4.86E-02	
(n,g)	1.64E-03	7.61E-3	1.11E-03	
Total	3.52	6.75	2.07	
Limit	**10**	**10**	**10**	

Note:
1) The vehicle surface is assumed to be the same as package surface.

Table 5-2
Summary of TN-LC-NRUX NCT Dose Rates

(Exclusive Use Package for Transportation)

Package Surface (mrem/hr)				
	Top End	**Side**	**Bottom End**	
Gamma	30.7	27.4	17.7	
Neutron	4.40	29.6	0.112	
(n,g)	7.46E-02	0.311	3.86E-03	
Total	35.2	57.3	18.8	
Limit	**1000**	**1000**	**1000**	
Vehicle Surface (mrem/hr)				
	Top End[(1)]	**Side**	**Bottom End [(1)]**	**Underside**
Gamma	30.7	9.61	17.7	12.2
Neutron	4.40	1.72	0.112	5.71
(n,g)	7.46E-02	0.109	3.86E-03	0.132
Total	35.2	11.4	18.8	18.0
Limit	**200**	**200**	**200**	
2 m from Vehicle Surface (mrem/hr)				
	Top End	**Side**	**Bottom End**	
Gamma	0.983	2.36	0.104	
Neutron	0.225	0.413	1.09E-02	
(n,g)	4.16E-03	2.03E-02	2.13E-04	
Total	1.21	2.79	0.115	
Limit	**10**	**10**	**10**	

Note:
1) The vehicle surface is assumed to be the same as package surface.

Table 5-3
Summary of TN-LC-TRIGA NCT Dose Rates

(Exclusive Use Package for Transportation)

Package Surface (mrem/hr)				
	Top End	**Side**	**Bottom End**	
Gamma	49.7	95.6	3.90	
Neutron	7.73E-02	0.182	4.36E-02	
(n,g)	1.93E-03	1.28E-02	1.78E-03	
Total	49.8	95.8	3.94	
Limit	**1000**	**1000**	**1000**	
Vehicle Surface (mrem/hr)				
	Top End[1]	**Side**	**Bottom End [1]**	**Underside**
Gamma	49.7	26.8	3.90	42.0
Neutron	7.73E-02	4.64E-02	4.36E-02	7.47E-02
(n,g)	1.93E-03	3.38E-03	1.78E-03	5.29E-03
Total	49.8	26.9	3.94	42.0
Limit	**200**	**200**	**200**	
2 m from Vehicle Surface (mrem/hr)				
	Top End	**Side**	**Bottom End**	
Gamma	2.63	8.25	0.415	
Neutron	4.26E-03	1.25E-02	1.69E-03	
(n,g)	1.06E-04	8.28E-04	1.37E-04	
Total	2.63	8.27	0.417	
Limit	**10**	**10**	**10**	

Note:
1) The vehicle surface is assumed to be the same as package surface.

Table 5-4
Summary of TN-LC-1FA NCT Dose Rates

(Exclusive Use Package for Transportation)

Package Surface (mrem/hr)				
	Top End	**Side**	**Bottom End**	
Gamma	106	1.43	137	
Neutron	0.753	573	1.87	
(n,g)	3.35E-02	7.25	8.69E-02	
Total	107	582	139	
Limit	**1000**	**1000**	**1000**	
Vehicle Surface (mrem/hr)				
	Top End[(1)]	**Side**	**Bottom End [(1)]**	**Underside**
Gamma	106	0.956	137	0.758
Neutron	0.753	31.1	1.87	121
(n,g)	3.35E-02	3.60	8.69E-02	5.29
Total	107	35.6	139	127
Limit	**200**	**200**	**200**	
2 m from Vehicle Surface (mrem/hr)				
	Top End	**Side**	**Bottom End**	
Gamma	5.44	3.54	6.73	
Neutron	4.74E-02	5.08	0.121	
(n,g)	2.50E-03	0.502	5.77E-03	
Total	5.49	9.12	6.86	
Limit	**10**	**10**	**10**	

Note:
1) The vehicle surface is assumed to be the same as package surface.

Table 5-5
Summary of TN-LC-MTR HAC Dose Rates

	1 m from Package Surface (mrem/hr)		
	Top End	**Side**	**Bottom End**
Gamma	18.8	146	10.8
Neutron	0.903	1.90	0.554
(n,g)	1.54E-03	2.92E-03	1.07E-03
Total	19.7	148	11.3
Limit	**1000**	**1000**	**1000**

Table 5-6
Summary of TN-LC-NRUX HAC Dose Rates

	1 m from Package Surface (mrem/hr)		
	Top End	**Side**	**Bottom End**
Gamma	4.92	18.8	1.02
Neutron	2.43	19.9	0.136
(n,g)	3.52E-03	2.08E-02	1.95E-04
Total	7.35	38.7	1.15
Limit	**1000**	**1000**	**1000**

Table 5-7
Summary of TN-LC-TRIGA HAC Dose Rates

	1 m from Package Surface (mrem/hr)		
	Top End	**Side**	**Bottom End**
Gamma	12.9	79.6	0.512
Neutron	4.65E-02	0.166	1.04E-02
(n,g)	1.61E-04	6.01E-04	2.94E-05
Total	13.0	79.8	0.523
Limit	**1000**	**1000**	**1000**

Table 5-8
Summary of TN-LC-1FA HAC Dose Rates

	1 m from Package Surface (mrem/hr)		
	Top End	**Side**	**Bottom End**
Gamma	6.63	0.893	0.316
Neutron	10.9	434	38.2
(n,g)	2.78E-02	0.938	0.115
Total	17.5	436	38.6
Limit	**1000**	**1000**	**1000**

Table 5-9
Important Packaging Model Dimensions

Proprietary Information Withheld Pursuant to 10 CFR 2.390

Table 5-10
Composition of Stainless Steel SS304

Component	Wt.%
C	0.08
Si	1.0
P	0.045
Cr	19.0
Mn	2.0
Fe	68.375
Ni	9.5
Density = 7.94 g/cm^3	

Table 5-11
Homogenized Resin-F Composition (130°F for 1 year)

Proprietary Information Withheld Pursuant to 10 CFR 2.390

Table 5-12
Composition of Air

Component	Wt.%
N	75.519
O	23.179
C	0.014
Ar	1.288
Density = 0.0012 g/cm^3	

Table 5-13
ANSI/ANS 1977 Flux-to-Dose-Rate Conversion Factors

E (MeV)	Neutron Factors (mrem/hr)/(n/cm^2/s)	E (MeV)	Neutron Factors (mrem/hr)/(n/cm^2/s)
2.50E-08	3.67E-03	0.5	9.26E-02
1.00E-07	3.67E-03	1.0	1.32E-01
1.00E-06	4.46E-03	2.5	1.25E-01
1.00E-05	4.54E-03	5.0	1.56E-01
1.00E-04	4.18E-03	7.0	1.47E-01
0.001	3.76E-03	10.0	1.47E-01
0.01	3.56E-03	14.0	2.08E-01
0.1	2.17E-02	20.0	2.27E-01
E (MeV)	**Gamma Factors (mrem/hr)/(γ/cm^2/s)**	**E (MeV)**	**Gamma Factors (mrem/hr)/(γ/cm^2/s)**
0.01	3.96E-03	1.4	2.51E-03
0.03	5.82E-04	1.8	2.99E-03
0.05	2.90E-04	2.2	3.42E-03
0.07	2.58E-04	2.6	3.82E-03
0.1	2.83E-04	2.8	4.01E-03
0.15	3.79E-04	3.25	4.41E-03
0.2	5.01E-04	3.75	4.83E-03
0.25	6.31E-04	4.25	5.23E-03
0.3	7.59E-04	4.75	5.60E-03
0.35	8.78E-04	5.0	5.80E-03
0.4	9.85E-04	5.25	6.01E-03
0.45	1.08E-03	5.75	6.37E-03
0.5	1.17E-03	6.25	6.74E-03
0.55	1.27E-03	6.75	7.11E-03
0.6	1.36E-03	7.5	7.66E-03
0.65	1.44E-03	9.0	8.77E-03
0.7	1.52E-03	11.0	1.03E-02
0.8	1.68E-03	13.0	1.18E-02
1.0	1.98E-03	15.0	1.33E-02

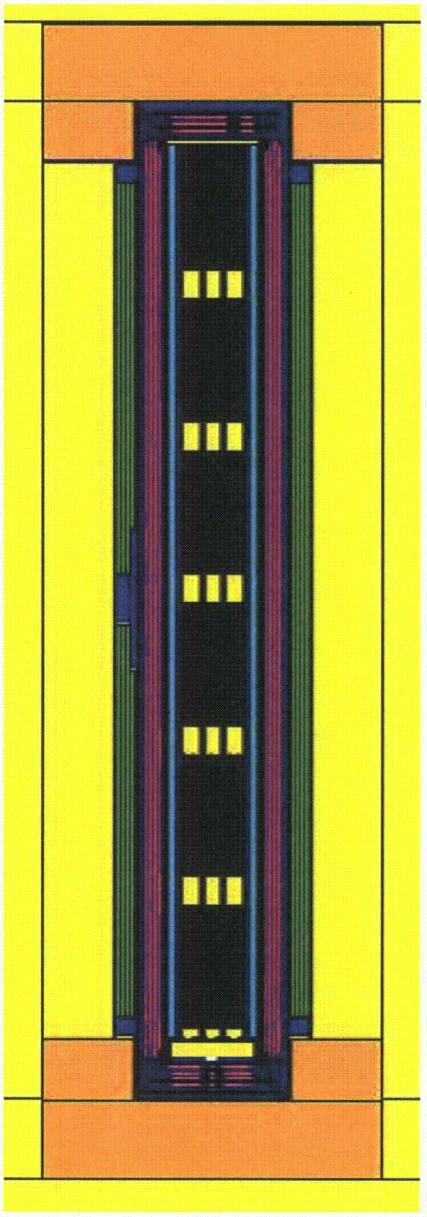

Figure 5-1
MCNP Model, Axial View (TN-LC-MTR Basket)

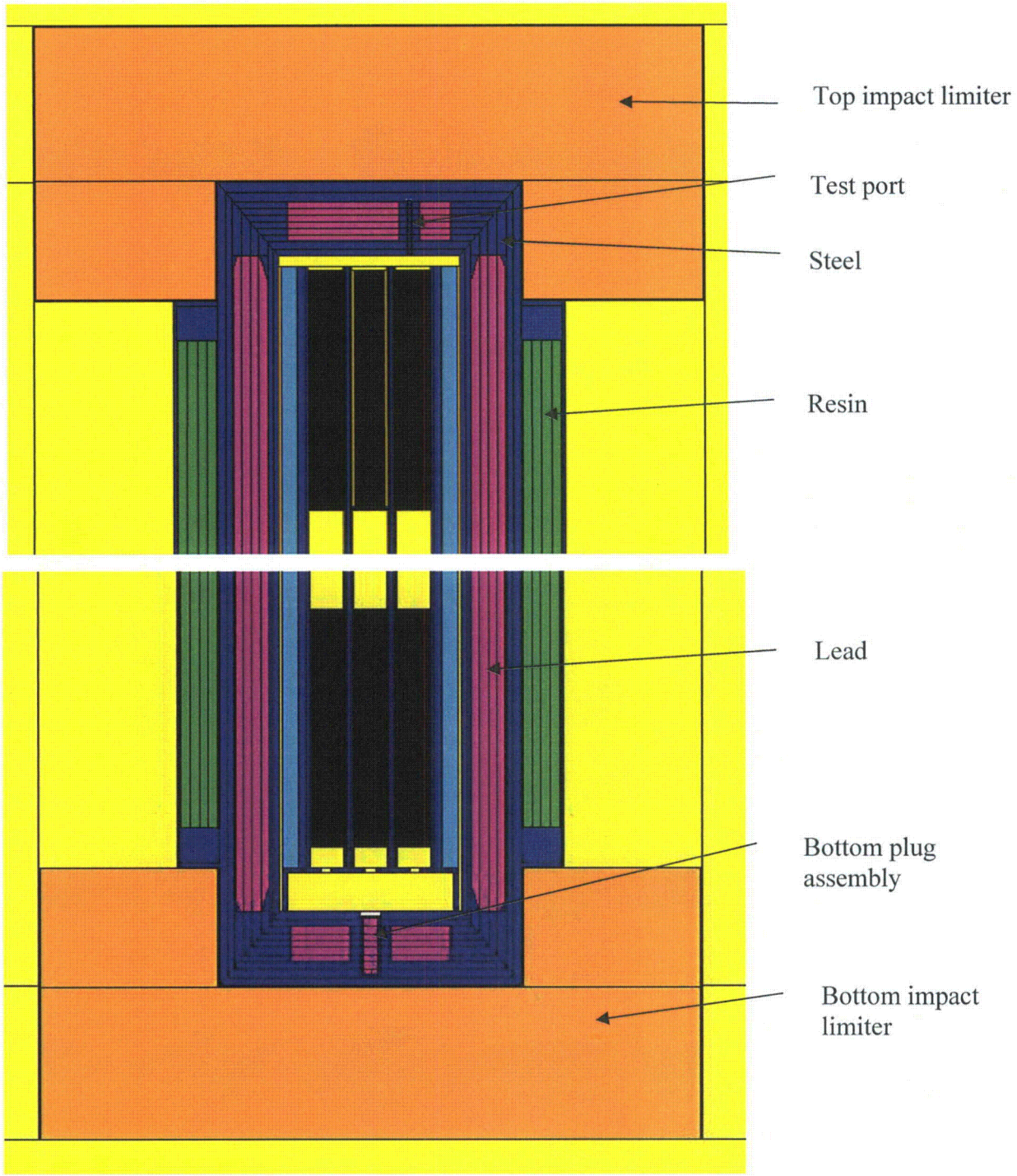

Figure 5-2
MCNP Model, Close-up Axial View (TN-LC-MTR Basket)

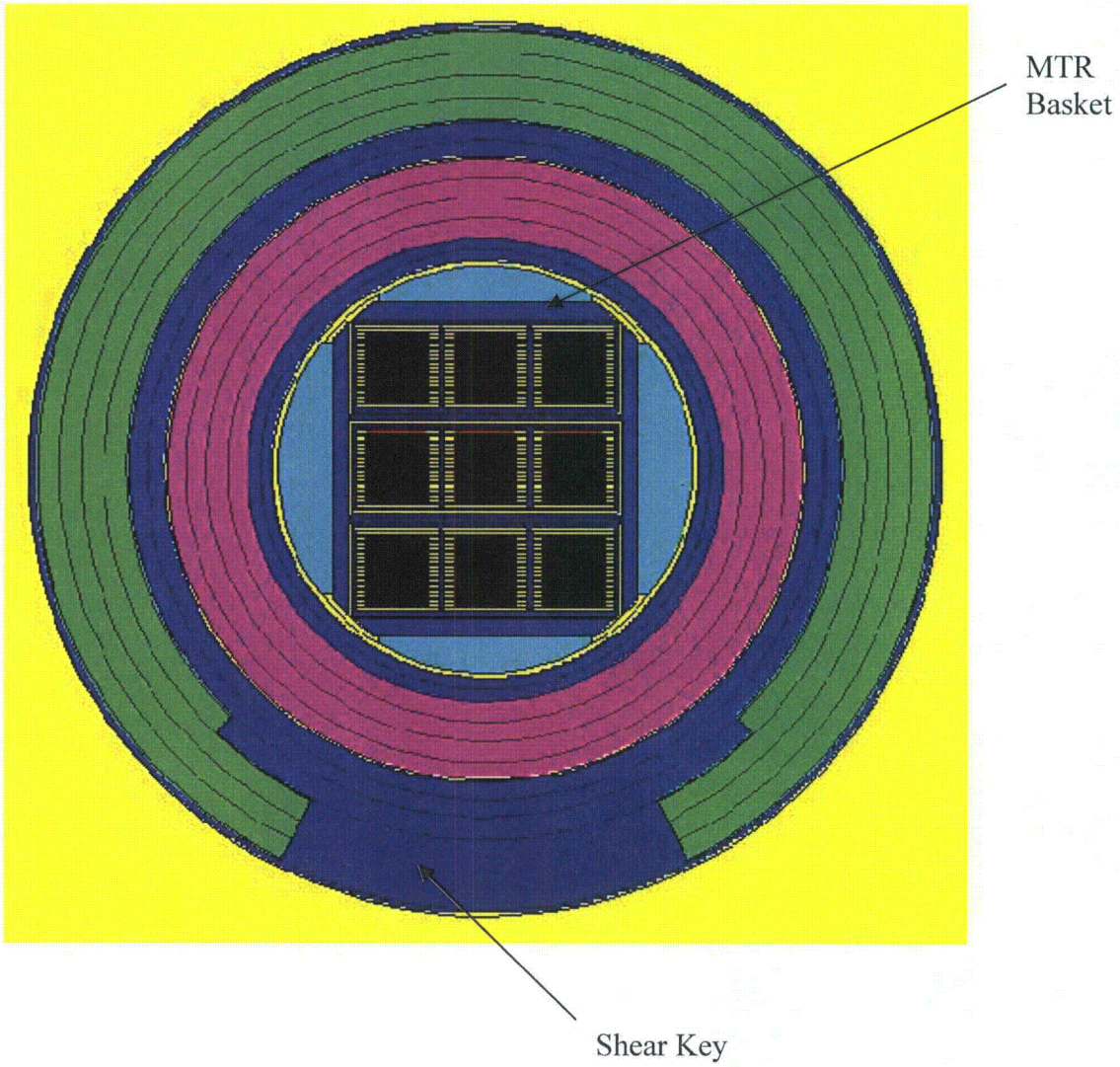

Figure 5-3
MCNP Model, View through Shear Key (TN-LC-MTR Basket)

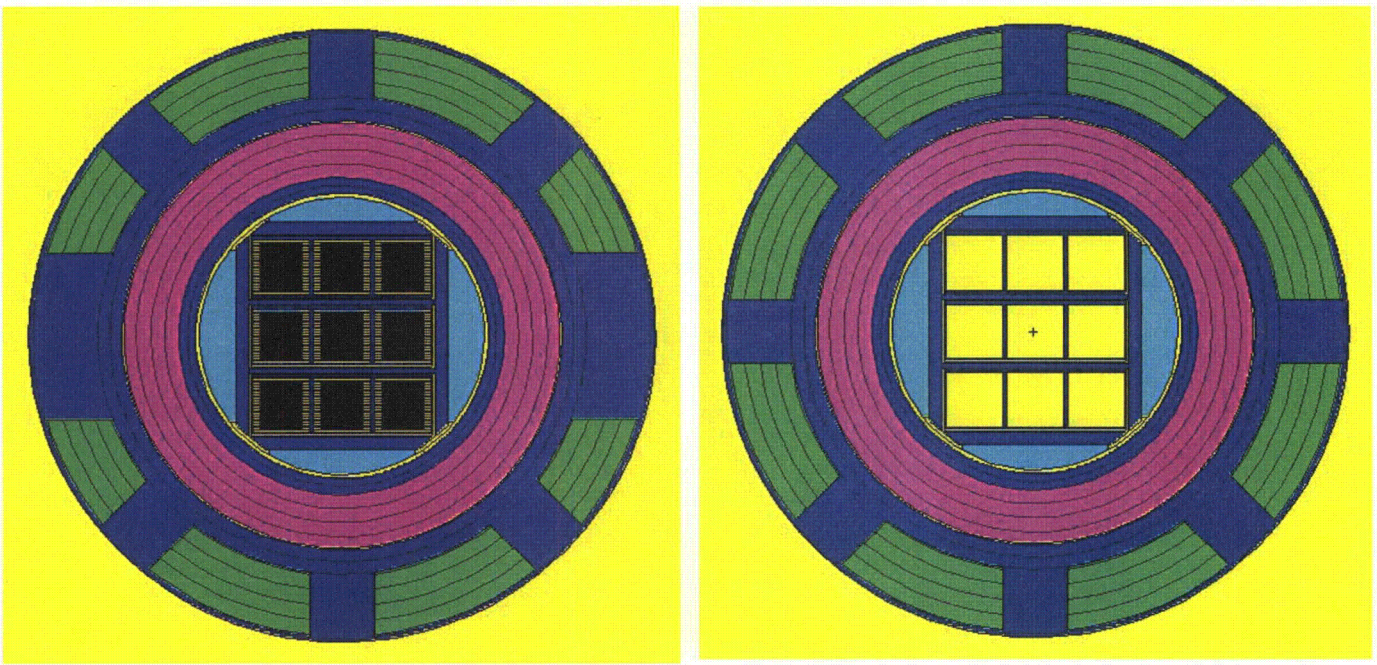

Top of Cask

Bottom of Cask

Figure 5-4
MCNP Model, View through Impact Limiter Attachment Blocks (TN-LC-MTR Basket)

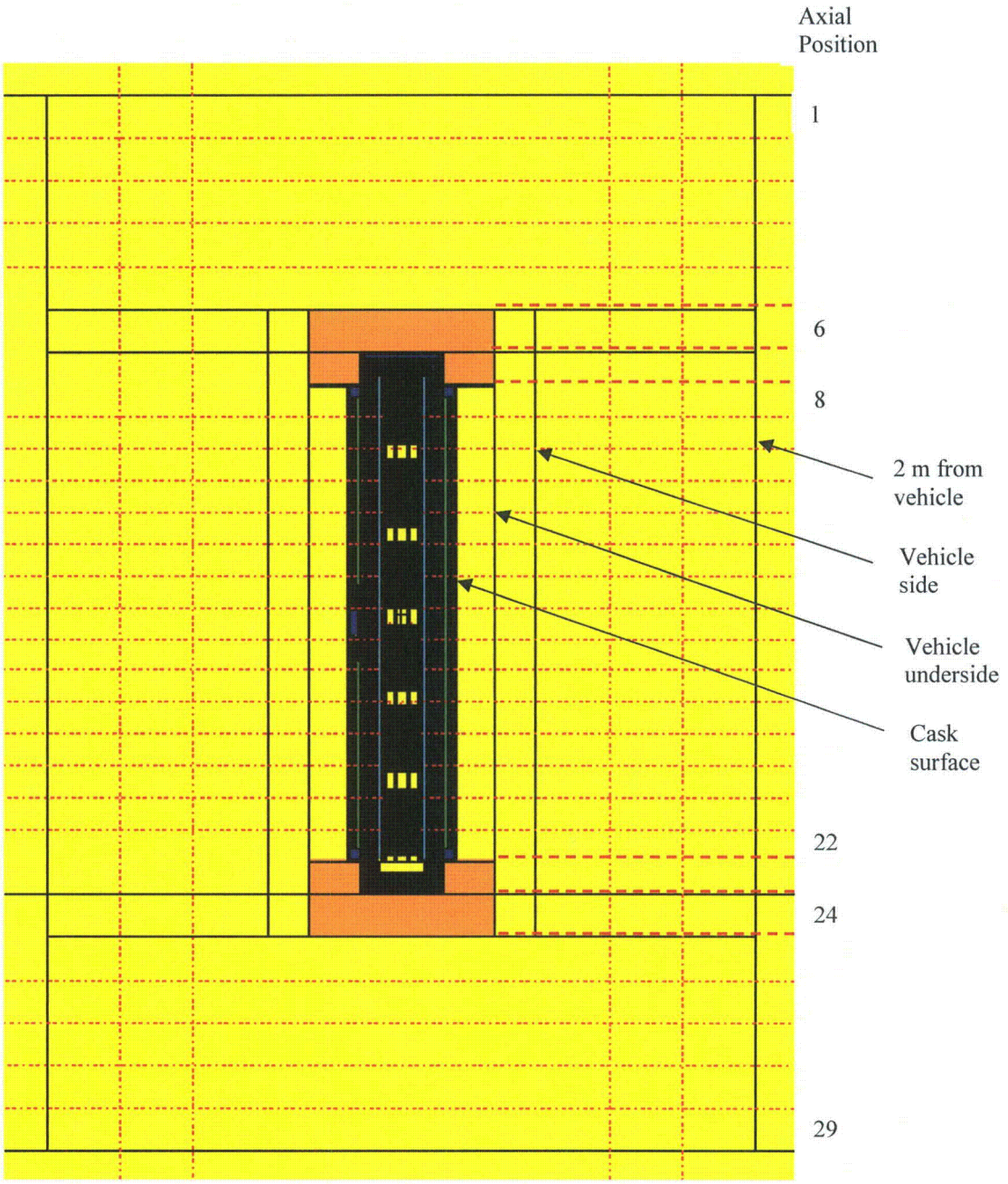

Figure 5-5
NCT Radial Surface Tallies (TN-LC-MTR Basket)

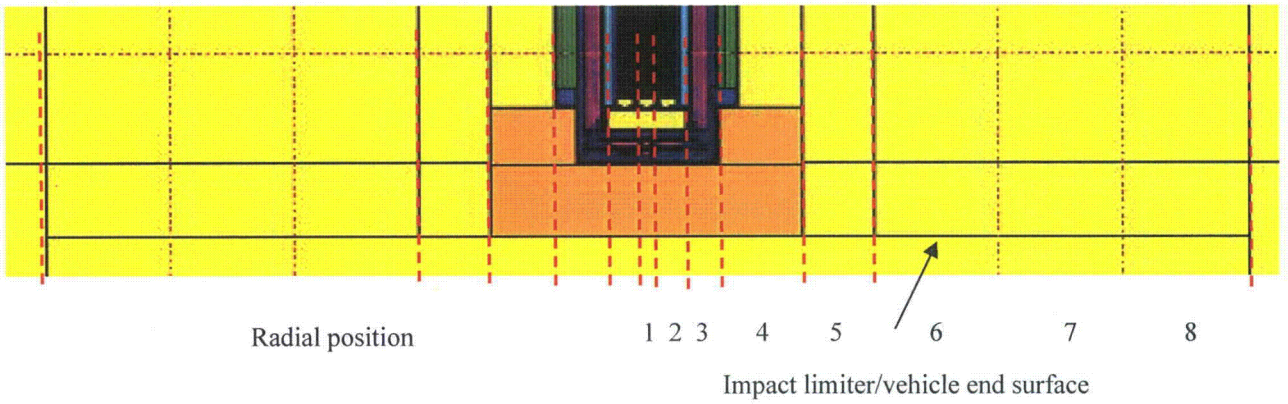

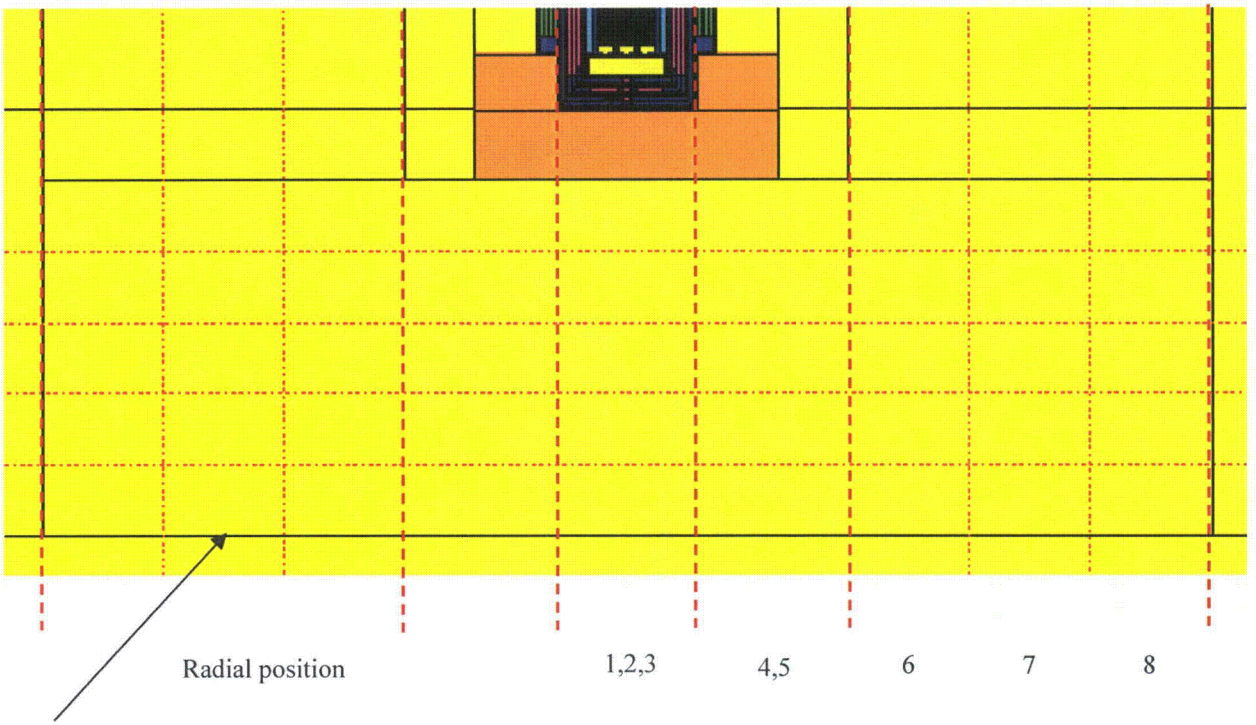

Figure 5-6
NCT End Surface Tallies (TN-LC-MTR Basket)

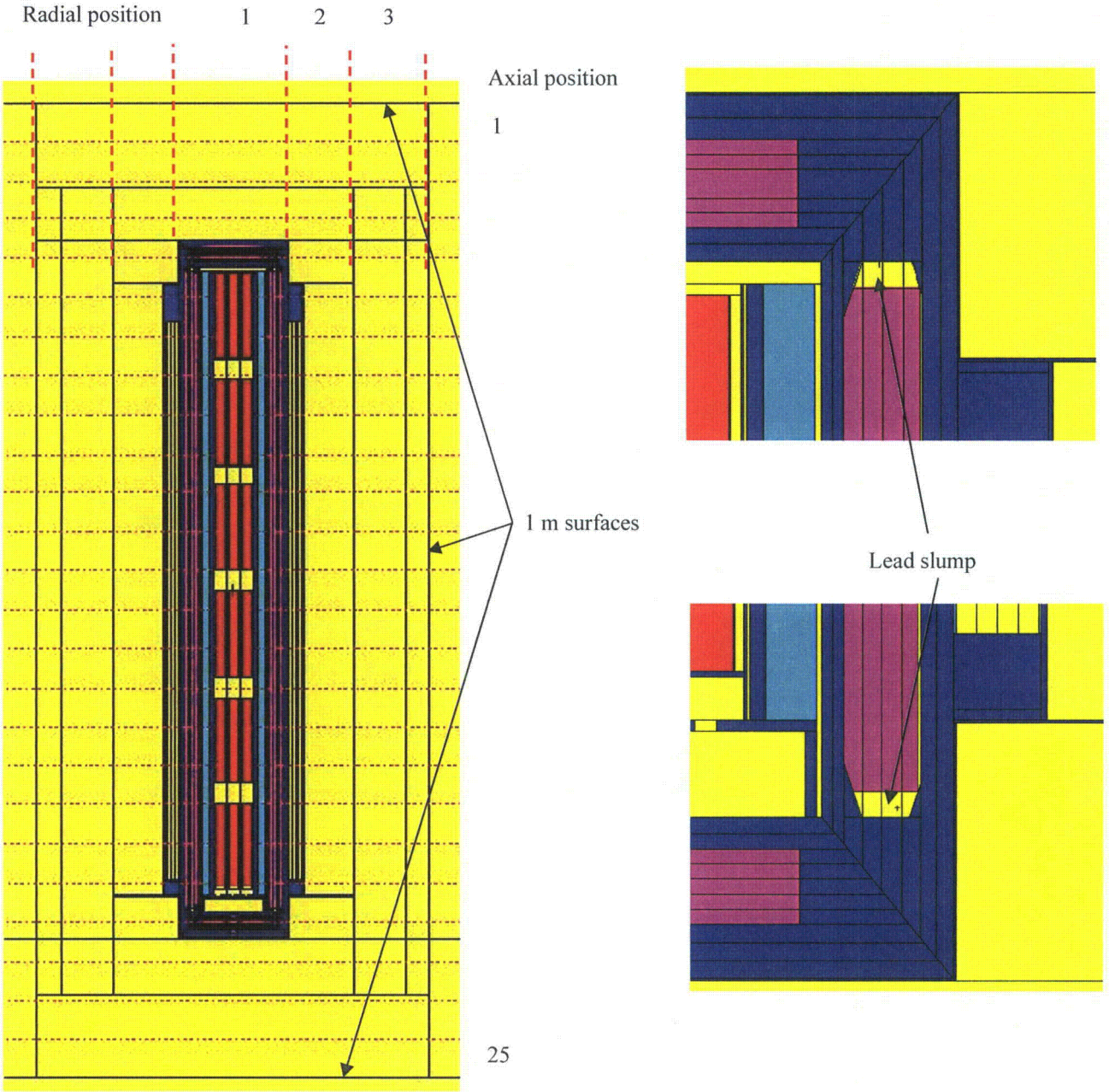

Figure 5-7
HAC 1 m Tallies (TN-LC-MTR Basket)

Appendix 5.6.1
TN-LC-MTR Basket Shielding Evaluation

TABLE OF CONTENTS

Proprietary Information Withheld Pursuant to 10 CFR 2.390.

LIST OF TABLES

LIST OF FIGURES

Appendix 5.6.1
TN-LC-MTR Basket Shielding Evaluation

NOTE: References in this Appendix are shown as [1], [2], etc. and refer to the reference list in Section 5.6.1.5.1.

This Appendix presents the shielding evaluation of the TN-LC transportation package containing the TN-LC-MTR basket. The MCNP computer program [1] is used to calculate the dose rates using a detailed three-dimensional model. The dose rates are evaluated per the requirements of 10CFR71.47 and 71.51 for exclusive use transportation in a closed transport vehicle.

5.6.1.1 Description of the Shielding Design

5.6.1.1.1 Design Features

The shielding design of the cask is described in Section 5.1.1. Shielding is also provided by the TN-LC-MTR basket.

Proprietary Information Withheld Pursuant to 10 CFR 2.390.

5.6.1.1.2 Summary Tables of Maximum Radiation Levels

Normal conditions of transport (NCT) dose rates are computed for exclusive use transport in a closed transport vehicle. These dose rate limits are as follows:

- Surface of the package: 1000 mrem/hr
- Surface of the transport vehicle: 200 mrem/hr
- 2 m from the surface of the transport vehicle: 10 mrem/hr

The transport vehicle is assumed to be 8 ft wide. Because the TN-LC is a long package, the ends of the transport vehicle are conservatively assumed to be at the ends of the impact limiters. The underside (floor) of the vehicle is conservatively assumed to correspond to the radius of the impact limiters. The dose rates on the vehicle roof are not computed as these dose rates are bounded by the dose rates on the underside of the vehicle. Dose rates are also computed 2 m from the sides and ends of the vehicle. The NCT dose rates for the TN-LC-MTR basket payload are summarized in Table 5.6.1-1.

The maximum package surface dose rate of 84.5 mrem/hr occurs on the top of the impact limiter above the port in the lid. This dose rate is less than the limit of 1000 mrem/hr on the package surface.

The maximum vehicle surface dose rate of 84.5 mrem/hr occurs at the top end of the vehicle (which also corresponds to the top surface of the impact limiter). This dose rate occurs over the port in the lid, and is less than the limit of 200 mrem/hr on the vehicle surface.

The maximum dose rate 2 m from the vehicle surface of 6.75 mrem/hr occurs at the side of the vehicle. This dose rate is less than the limit of 10 mrem/hr at 2 m from the vehicle surface.

Per 10CFR71.47(b)(4), dose rate limits in any normally occupied space do not apply if the carrier is private and exposed personnel wear dosimetry devices. If it is assumed that the normally occupied space is 2 m from the ends of the vehicle, then the dose rate limit of 2 mrem/hr is exceeded. Therefore, personnel in any normally occupied space shall wear dosimetry devices.

Hypothetical accident condition (HAC) dose rates are computed. Under HAC, it is conservatively assumed that both the neutron shield and impact limiter wood are replaced with air, and 1.2 in. of lead slump is modeled at both the top and bottom ends. Dose rates are computed 1 m from the surface of the cask body. The HAC dose rates for the TN-LC-MTR basket are summarized in Table 5.6.1-2. The maximum dose rate of 148 mrem/hr occurs at the side of the package, which is well below the limit of 1000 mrem/hr.

5.6.1.2 Source Specification

5.6.1.2.1 Gamma Source

The gamma source for MTR fuel is computed by the TRITON module of the SCALE6 code package [2]. TRITON allows for a two-dimensional representation of the fuel elements. Because the input is two dimensional, all input is for a basis of 1 metric ton of uranium (MTU). All TRITON output is also per 1 MTU, so the results must be scaled by the MTU of the fuel element.

MTR fuel assembly or element is not associated with a single reactor. The general characteristics of MTR type fuel are flat or curved plates with a fuel meat of uranium mixed with aluminum or silicon. Cladding is aluminum, and the plates are held in place in the fuel element by aluminum side plates.

The key characteristics of MTR fuel that defines the source at a given cooling time are the U-235 mass, enrichment, and burnup. A generic MTR fuel element is developed for the following four cases, (or enrichment types) which bound the MTR fuel element types listed in Chapter 1:

- High-enriched uranium (HEU) fuel type 1 (HEU1or Type A), U-235 mass = 380 g, minimum U-235 enrichment = 90 percent, maximum burnup = 660,000 MWD/MTU
- HEU fuel type 2 (HEU2 or Type B), U-235 mass = 460 g, minimum U-235 enrichment = 90 percent, maximum burnup = 577,500 MWD/MTU
- Medium-enriched uranium (MEU or Type C) fuel, U-235 mass = 380 g, minimum U-235 enrichment = 40 percent, maximum burnup = 293,300 MWD/MTU
- Low-enriched uranium (LEU or Type D) fuel, U-235 mass = 470 g, minimum U-235 enrichment = 19 percent, maximum burnup = 139,300 MWD/MTU

Any MTR fuel element with a U-235 mass, enrichment, and burnup bounded by the above values is eligible for shipment in the TN-LC. The burnup values are selected to result in a U-235 depletion of at least 80 percent. A full summary of the data used to develop the TRITON model is presented in Table 5.6.1-3.

A description of a generic MTR fuel assembly is presented in [3].

Proprietary Information Withheld Pursuant to 10 CFR 2.390.

The cooling times needed to meet decay heat and dose rate limits for the maximum burnup values listed above are long.

Proprietary Information Withheld Pursuant to 10 CFR 2.390.

Developing a bounding NCT source term involves the following methodology:

1. Run TRITON for the four generic MTR fuel types and five burnup values, a total of 20 TRITON runs. Save the TRITON "F71" output file for each case.

2. The limiting dose rate for transportation is usually the dose rate at a distance of 2 m from the side of the vehicle, which has a limit of 10 mrem/hr. The maximum burnup MEU source term with a decay time of 1940 days results in a 2 m dose rate of 7.19 mrem/hr, which provides a reasonable margin to the dose rate limit of 10 mrem/hr. This source term is selected as the design basis for shielding analysis, and the cooling times of the remaining fuel type/burnup combinations are selected to result in a smaller dose rate.

For these 20 cases, the decay times to meet dose rate limits, the final decay heat, as well as the NCT dose rate values used to select the bounding source, are provided in Table 5.6.1-4.

The dose rate calculations used to select the bounding source are performed using a "response function" developed by MCNP. To develop a response function, a fairly detailed MCNP model of the MTR fuel, basket, and TN-LC package is developed.

Proprietary Information Withheld Pursuant to 10 CFR 2.390.

The NCT gamma response function is provided in Table 5.6.1-5. The bounding gamma radiation source is provided in Table 5.6.1-6. The NCT neutron response function is developed in a similar manner and is discussed in Section 5.6.1.2.2.

Under HAC, the neutron shield is assumed to be lost. In general, the loss of the neutron shield will change the design basis source because the neutron component of the total dose rate increases much more than the gamma component. However, the neutron component of the total dose rate for MTR fuel is negligible compared to the gamma component, even under HAC (see the HAC dose rate results in Table 5.6.1-15). Therefore, the design basis NCT gamma source is also bounding for HAC analysis.

A sample TRITON input file and ORIGEN-S restart file are provided in Section 5.6.1.5.2.

5.6.1.2.2 Neutron Source

The neutron source is generated using the same TRITON models from which the gamma source is generated. The neutron source is comprised of both spontaneous fission and (α,n) reactions

with the aluminum in the fuel matrix. Like the gamma calculation, a neutron response function is also generated for NCT.

Proprietary Information Withheld Pursuant to 10 CFR 2.390.

The neutron NCT response functions are provided in Table 5.6.1-7. To determine the dose rate from an actual source, simply multiply the neutron source in each energy group for a single fuel element by the response function for that energy group, and sum the results. The results are for 54 fuel elements. The neutron source is provided in Table 5.6.1-8. The neutron source is for MEU fuel at maximum burnup. The same neutron source is bounding for NCT and HAC analysis because the neutron dose rate remains a small fraction of the gamma dose rate, even when the neutron shield is lost.

5.6.1.2.3 Fuel Qualification

The minimum cooling times required to meet the dose rate limit for each fuel category are provided in Table 5.6.1-4. In general, MTR fuel to be shipped will not correspond exactly to the enrichments, fuel loadings, and burnups listed in this table. Therefore, the following method is used in conjunction with Table 5.6.1-4 to determine the required cooling time for the fuel being shipped:

1. Determine the enrichment level of the fuel. Fuel with an enrichment ≥90 percent is HEU, 40 percent ≤ enrichment <90 percent is MEU, and 19 percent ≤ enrichment < 40 percent is considered LEU. Fuel with an enrichment <19 percent cannot be shipped.

2. Determine the U-235 mass for the fuel. For HEU, use category HEU1 if the U-235 mass ≤380 g, and use category HEU2 for 380 g < U-235 mass ≤ 460 g. The mass limit for MEU fuel is 380 g U-235, and the mass limit for LEU fuel is 470 g U-235. Fuel with a U-235 mass that exceeds these values cannot be shipped.

3. Determine the burnup level of the fuel. The minimum cooling time is based on the burnup level. Because only a limited number of burnup points are investigated, burnups may be either rounded up to the next higher burnup in Table 5.6.1-4, or linear interpolation may be used in conjunction with Table 5.6.1-4 and Table 5.6.1-16 to determine the minimum cooling time. Cooling time plots are provided in Figure 5.6.1-2 and Figure 5.6.1-3. Although the plots are reasonably linear after 1/4 of the maximum burnup, to ensure a conservative cooling time, add an additional 30 days to the linearly interpolated value. If the burnup is less than the minimum value shown in Table 5.6.1-4, use the cooling time listed for the minimum burnup. Fuel with a burnup value that exceeds the maximum values listed in Table 5.6.1-4 cannot be shipped.

Examples are provided to illustrate the method.

Example 1: An MTR fuel element has an enrichment of 25 percent U-235, U-235 mass of 300 g, and burnup of 75,000 GWD/MTU. Based on the enrichment, the fuel falls in the LEU category. The U-235 mass is less than the limit of 470 g U-235. Based on linear interpolation from the

data in Table 5.6.1-4, the minimum cooling time is 1605 days plus an additional 30 days, or 1635 days.

Example 2: An MTR fuel element has an enrichment of 95 percent U-235, U-235 mass of 350 g, and a burnup of 400,000 MWD/MTU. Based on the enrichment, the fuel falls in the HEU category. The U-235 mass is less than 380 g, so the fuel is HEU1. Based on linear interpolation from the data in Table 5.6.1-4, the minimum cooling time is 1542 days plus an additional 30 days, or 1572 days.

Example 3: An MTR fuel element has an enrichment of 40 percent U-235, U-235 mass of 320 g, and a burnup of 10,000 MWD/MTU. Based on the enrichment, the fuel falls in the MEU category. The U-235 mass is less than the limit of 380 g U-235. Because the burnup is below the minimum burnup in Table 5.6.1-4, the minimum cooling time corresponds to the minimum burnup MEU cooling time of 740 days.

5.6.1.3 Shielding Model

5.6.1.3.1 Configuration of Source and Shielding

The fuel, basket, and packaging are modeled explicitly in the MCNP computer program. The cask model is described in Section 5.3.1. The details of the model specific to the TN-LC-MTR basket are described in this section.

The generic 23 fuel plate element model is used for the source geometry. This geometry is described in Table 5.6.1-3. The TN-LC may transport a maximum of 54 MTR fuel elements. The maximum number is conservatively modeled in the dose rate analysis, which consists of six layers, and each layer contains nine fuel elements. Only the active fuel region of the MTR element is modeled. The source is evenly distributed throughout the fuel meat material, which is modeled with an active length 24 in. The end regions, if present, are aluminum and provide negligible source. Because the end regions, if present, would provide some shielding, it is conservative to neglect them. The side aluminum plates of the fuel element are also conservatively neglected, as these items would provide some self-shielding.

Important dimensions of the TN-LC-MTR basket model are summarized in Table 5.6.1-9. An example of the overall model geometry with the TN-LC-MTR basket is shown in Figure 5.6.1-4 through Figure 5.6.1-8. The overall model geometry is illustrated in Figure 5.6.1-4. A close-up view of the model ends is illustrated in Figure 5.6.1-5. A view perpendicular to the cask axis is illustrated in Figure 5.6.1-6. The model geometry of the fuel element is illustrated in Figure 5.6.1-7. A view through the impact limiter attachment blocks is illustrated in Figure 5.6.1-8.

The fuel is placed as close as possible to the ends of the cavity. At the bottom end, the bottom fuel bucket has a 1.5 in. spacer, the bottom of the bucket is 0.25 in. thick, and it is assumed the active fuel is at least 0.5 in. from the end of the fuel element. Therefore, the distance from the bottom of the active fuel to the top surface of the bottom spacer is 2.25 in. For simplicity, the bottom of the bucket is modeled as touching the active fuel in each of the six layers. Also, the spacer is modeled with a height of 4.0 in. rather than the actual height of 4.5 in., so the fuel is modeled slightly closer to the bottom of the cask, and slightly farther away from the top of the cask. The effect on the end dose rates is negligible. At the lid end, there is a 1 in. gap modeled between the end of the basket and the lid, and it is assumed the active fuel is at least 0.5 in. from the end of the fuel element. Therefore, the modeled distance from the lid to the top of the active fuel region is 1.5 in. The 0.25 in. thick steel tube cap plates on the top buckets are conservatively ignored. The remaining four layers of fuel are distributed so that the gaps between the six layers are equal.

Under hypothetical accident conditions (HAC), the impact limiter wood and neutron shield resin are replaced with air. This bounds any postulated fire or crush damage. In addition, 1.2 in. of lead slump is modeled at both the top and bottom ends of the cask as a result of an end drop. This bounds the maximum lead slump value of 1.129 in. from Appendix 2.13.3. The radial lead slump at the cask ends due to a side drop is negligible (<0.2 in.) and has been neglected. HAC dose rates are conservatively computed 1 m from the cask body surface.

5.6.1.3.2 Material properties

The material properties of the fuel are provided in Table 5.6.1-3. Material properties for the cask and basket structural materials are provided in Section 5.3.2. The 1/4 in. thick bucket bottom steel plate is modeled with a reduced density of 6.25 g/cm^3 because it has been homogenized with the bucket drainage holes.

5.6.1.4 Shielding Evaluation

5.6.1.4.1 Methods

MCNP5 v1.40 is used for the shielding analysis [1]. MCNP5 is a standard, well-accepted shielding program utilized to compute dose rates for shielding licenses. A three-dimensional model is developed that captures all of the relevant design parameters of the cask and internals. Dose rates are calculated by tallying the neutron and gamma fluxes over surfaces of interest and converting these fluxes to dose rates using flux-to-dose rate conversion factors. Secondary gammas resulting from neutron capture are also tallied. Subcritical neutron multiplication is also performed by the program.

Separate models are developed for neutron and gamma source terms. Geometry splitting and simple Russian roulette are used as a variance reduction technique for most tallies. The importance of the particles increases as the particles traverse the shielding materials. When necessary, DXTRAN spheres are used to accelerate program convergence above the lid port.

5.6.1.4.2 Input and Output Data

A number of input/output cases are used to generate the results. A sample input file is provided in Section 5.6.1.5.3. Some models are restarted to increase the run time to allow better convergence. Restart cases have a truncated filename.

Radiological sources are determined with TRITON\NEWT models.

MCNP models are used to calculate response function due to neutron and gamma radiation source as well as for a determination of radiation fields at various distances around the cask at NCT and HAC.

Convergence is good (<10 percent) for all total dose rates of interest. A separate gamma model is developed to compute the dose rate on the impact limiter surface over the lid port.

5.6.1.4.3 Flux-to-Dose-Rate Conversion

The flux-to-dose rate conversion factors are provided in Section 5.4.3.

5.6.1.4.4 External Radiation Levels

Tally locations are selected to be consistent with exclusive use transportation in a closed transport vehicle. Therefore, the applicable NCT dose rate limits from 10 CFR 71.47(b)(1), (2) and (3) are:

- 1000 mrem/hr on the package surface. This includes the surface of the cask between the impact limiters, and the impact limiter surfaces.
- 200 mrem/hr on the vehicle surface. The vehicle has six surfaces (2 sides, 2 ends, roof, and underside). The two sides of the vehicle are assumed to be 8 ft apart with the package in the center. The underside (floor) of the vehicle is conservatively assumed to be at the impact

limiter radius, and the dose rates at the underside of the vehicle bound the dose rates at the roof of the vehicle, which is farther away from the package. The ends of the vehicle are conservatively assumed to be at the impact limiter end surfaces.

- 10 mrem/hr 2 m from the vehicle surface. This dose rate does not apply 2 m from the roof of the vehicle or 2 m from the underside of the vehicle.

The dose rate limit of 2 mrem/hr in any normally occupied space does not apply if the TN-LC is transported by private carrier and exposed personnel wear radiation dosimetry devices. Exposed personnel shall wear radiation dosimetry devices so that this limit does not apply.

Circumferential tallies are placed around the packaging. Twenty-nine (29) axial locations are utilized, as illustrated in Figure 5.6.1-9. Locations 8 through 22 are utilized on the side of the cask between the impact limiters, Locations 6 though 24 are utilized on the side of the package at the impact limiter radius (underside of vehicle) and the side of the vehicle, and Locations 1 through 29 are utilized 2 m from the side of the vehicle.

At the ends of the packaging, dose rates are tallied on the impact limiter surfaces and 2 m from the impact limiter surfaces. Eight radial locations are utilized for the surface tallies, as illustrated in Figure 5.6.1-10. Location 1 captures any streaming effects from the bottom plug assembly. An off-center tally is used directly over the lid port to capture any streaming effects on the top impact limiter surface. For the dose rates 2 m from the ends, five radial locations are utilized by combining Locations 1,2,3 and 4,5, as shown on Figure 5.6.1-10. Any streaming effects are generally negligible 2 m from the ends and are not investigated for the TN-LC-MTR basket. Because the bounding end dose rates are for the 1FA basket, the end streaming effects at 2 m are examined in more detail in the 1FA shielding calculation (See Appendix 5.6.4).

Because the basket design is not circumferentially symmetric, the dose rate will vary around the perimeter of the package. This effect is most pronounced close to the package surface, and diminishes with distance. Close to the surface of the package, this variation is approximately 15 percent from the average in most cases. At 2 m from the surface of the vehicle, this variation is small (~5 percent). Because the dose rates are significantly below the dose rate limits, a detailed tally to capture these angular effects is not warranted. Therefore, circumferential average tallies are reported in the radial direction for most dose rate locations.

However, because the impact limiter attachments and the shear key penetrate the neutron shield and displace neutron shielding material, there will be neutron streaming at these locations. This effect is captured explicitly using angular mesh tallies. The axial heights of the mesh are chosen to correspond to the heights of the regions of interest. The mesh is 1 cm thick, and consists of 18 angular regions (20° each). For the case of MTR fuel, which has a very low neutron source, this streaming effect may be quantified, although it has little effect on the total dose rates.

The shear key faces downward and results in a higher than average neutron dose rate on the surface of the package and the underside of the vehicle because it displaces some amount of neutron shielding material there. Contrary, if considering a portion of gamma dose rate distribution around the cask that faces the sheer key and attachment blocks, the shear key and impact limiter attachments result in a "hole" in the dose rate distribution. This is because neutron shielding

material is replaced with steel, which is a superior gamma shield. For this reason, these features are conservatively ignored in the gamma models, and neutron mesh tally results for the upper impact limiter attachments are added to the average gamma results at axial Location 8, and likewise for the shear key results at axial Location 15. The mesh tally is used only at the cask surface and vehicle underside/impact limiter radius because any streaming effects will be essentially washed out beyond this distance, and also because it is not required to calculate dose rates 2 m from the underside of the vehicle. The reported dose rates 2 m from the side of the vehicle are circumferential tallies and, hence, include the contribution due to neutron streaming through the shear key.

Package surface: The NCT side surface dose rates are presented in Table 5.6.1-10. Dose rates on the side surfaces of the impact limiters are presented in Table 5.6.1-11 at axial locations 6, 7, 23, and 24. Dose rates on the external flat surfaces of the impact limiters are presented in Table 5.6.1-14. The maximum package surface dose rate occurs on the top of the impact limiter over the port with a dose rate of 84.5 mrem/hr. This dose rate is less than the limit of 1000 mrem/hr.

The maximum dose rate of 71.5 mrem/hr at the side surface of the package occurs near the upper impact limiter attachment, due to neutron streaming in this region. However, the neutron dose rate is relatively small.

Vehicle surface: The NCT vehicle underside/impact limiter radius dose rates are presented in Table 5.6.1-11. The maximum dose rate on the vehicle underside occurs at axial Location 7 near the top of the package with a dose rate of 47.5 mrem/hr. This maximum is likely due to gammas scattering around the top of the side lead as the fuel is located rather close to the lid in this region. The NCT vehicle side surface dose rates are presented in Table 5.6.1-12. The maximum dose rate on the vehicle side occurs at axial Location 7 with a value of 21.6 mrem/hr. NCT vehicle end dose rates are presented in Table 5.6.1-14. The maximum vehicle surface dose rate occurs on the impact limiter surface over the port. This dose rate is 84.5 mrem/hr, which bounds the vehicle surface dose rates on the underside, side, and bottom ends. This dose rate is less than the limit of 200 mrem/hr.

2 m from vehicle surface: The NCT dose rates 2 m from the side surface of the vehicle are presented in Table 5.6.1-13. The maximum dose rate of 6.75 mrem/hr occurs at axial Location 14. This dose rate is less than the limit of 10 mrem/hr and bounds the dose rates 2 m from the ends of the vehicle presented in Table 5.6.1-14.

HAC: The applicable HAC dose rate limit from 10CFR71.51(a)(2) is 1000 mrem/hr 1 m from the package surface.

In the HAC models, the neutron shield resin and impact limiter wood is replaced with air, and 1.2 in. of lead slump is modeled at both the top and bottom ends. The tally surfaces are located 1 m from the outer surfaces of the cask. The dose rates at the ends of the package are divided into three segments, and the dose rates at the side of the package are divided in 25 segments of equal width. The tally locations are shown on Figure 5.6.1-11. HAC dose rate results are presented in Table 5.6.1-2. The maximum HAC dose rate of 148 mrem/hr occurs 1 m from the side of the package near the lead slump region. This dose rate is significantly less than the limit of 1000 mrem/hr.

5.6.1.5 Appendices

5.6.1.5.1 References

1. MCNP5, "MCNP – A General Monte Carlo N-Particle Transport Code, Version 5; Volume II: User's Guide," LA-CP-03-0245, Los Alamos National Laboratory, April 2003
2. SCALE: A Modular Code System for Performing Standardized Computer Analyses for Licensing Evaluations, ORNL/TM-2005/39, Version 6, Vols. I-III, January 2009
3. ANL/RERTR/TM-25, Rev. 1, Photon Dose Rates from Spent Fuel Assemblies with Relation to Self-Protection, Argonne National Laboratory, February 1996.

Proprietary Information Withheld Pursuant to 10 CFR 2.390.

Proprietary Information on Pages 5.6.1-13 through 5.6.1-27
Withheld Pursuant to 10 CFR 2.390.

Table 5.6.1-1
Summary of TN-LC-MTR NCT Dose Rates

(Exclusive Use Package for Transportation)

Package Surface (mrem/hr), Limit = 1000 mrem/hr				
	Top End	**Side**	**Bottom End**	
Gamma	82.5	65.5	32.3	
Neutron	1.98	5.89	0.922	
(n,g)	3.59E-02	8.48E-02	2.08E-02	
Total	84.5	71.5	33.3	
Vehicle Surface (mrem/hr), Limit = 200 mrem/hr				
	Top End	**Side**	**Bottom End**	**Underside**
Gamma	82.5	21.2	32.3	46.6
Neutron	1.98	0.364	0.922	0.792
(n,g)	3.59E-02	1.51E-02	2.08E-02	2.71E-02
Total	84.5	21.6	33.3	47.5
2 m from Vehicle Surface (mrem/hr), Limit = 10 mrem/hr				
	Top End	**Side**	**Bottom End**	
Gamma	3.43	6.62	2.02	
Neutron	8.62E-02	0.119	4.86E-02	
(n,g)	1.64E-03	7.61E-3	1.11E-03	
Total	3.52	6.75	2.07	

Table 5.6.1-2
Summary of TN-LC-MTR HAC Dose Rates

	1 m from Package Surface (mrem/hr), Limit = 1000 mrem/hr		
	Top End	**Side**	**Bottom End**
Gamma	18.8	146	10.8
Neutron	0.903	1.90	0.554
(n,g)	1.54E-03	2.92E-03	1.07E-03
Total	19.7	148	11.3

Table 5.6.1-3
MTR Fuel Data

Parameter	HEU1	HEU2	MEU	LEU
U-235 enrichment (%)	90	90	40	19
U-235 mass (g)	380	460	380	470
U mass (g)	422.2	511.1	950.0	2473.7
U-238 mass (g)	42.2	51.1	570.0	2003.7
Wt.% U	30	30	50	75
Al-U mass (g)	1407.4	1703.7	1900.0	3298.2
Al mass (g)	985.2	1192.6	950.0	824.6
Power density (MW/kg U-235)	2.857	2.857	2.857	2.857
Element power (MW)	1.086	1.314	1.086	1.343
Maximum Burnup (MWD/MTU)	660,000	577,500	293,300	139,300
MTU	4.2222E-04	5.1111E-04	9.5000E-04	2.4737E-03
Specific Power (MW/MTU)	2571.3	2571.3	1142.8	542.8
Irradiation time (D)	256.7	224.6	256.7	256.6
Channel width (cm)	0.219	0.219	0.219	0.219
Fuel meat thickness (cm)	0.0508	0.0508	0.0508	0.0508
Fuel meat width (cm)	6.35	6.35	6.35	6.35
Fuel meat height (cm)	60.96	60.96	60.96	60.96
Number of plates	23	23	23	23
Moderator/coolant	Light water	Light water	Light water	Light water
Moderator/coolant density (g/cm^3)	0.9786	0.9786	0.9786	0.9786
Fuel temperature (K)	447	447	447	447
Cladding temperature (K)	446	446	446	446
Moderator/coolant temperature (K)	325	325	325	325
U-235 number den. (atoms/b-cm)	2.1526E-03	2.6058E-03	2.1526E-03	2.6624E-03
U-238 number den. (atoms/b-cm)	2.3616E-04	2.8588E-04	3.1881E-03	1.1207E-02
Al number den. (atoms/b-cm)	4.8616E-02	5.8851E-02	4.6880E-02	4.0690E-02
Total number den. (atoms/b-cm)	5.1005E-02	6.1743E-02	5.2221E-02	5.4559E-02

Table 5.6.1-4
MTR Fuel Qualification

Type	Burnup (MWD/MTU)	Decay Time (days)	Decay Heat (watts)	NCT Response Function Dose Rate (mrem/hr)[1]
HEU1 $E \geq 90\%$ $M_{U235} \leq 380$ g	66,000	740	5.8	7.11
	165,000	1120	7.4	7.14
	330,000	1440	10.0	7.12
	495,000	1680	12.5	7.14
	660,000	1950	15.0	7.09
HEU2 $E \geq 90\%$ $M_{U235} \leq 460$ g	57,750	770	5.8	7.04
	144,375	1150	7.5	7.10
	288,750	1470	10.3	7.15
	433,125	1710	13.0	7.16
	577,500	1950	15.6	7.17
MEU $40\% \leq E < 90\%$ $M_{U235} \leq 380$ g	29,330	740	5.8	7.11
	73,325	1120	7.4	7.16
	146,650	1440	10.0	7.18
	219,975	1690	12.5	7.10
	293,300	1940	15.0	7.19
LEU $19\% \leq E < 40\%$ $M_{U235} \leq 470$ g	13,930	830	6.0	7.09
	34,825	1220	8.0	7.11
	69,650	1560	11.3	7.18
	104,475	1850	14.2	7.08
	139,300	2150	16.9	7.14

Notes:
1. This dose rate represents the total NCT dose rate 2 m from the side of the vehicle using a response function developed by MCNP. This dose rate is used only to select the bounding NCT source term. The dose rates 2 m from the side of the vehicle listed in Table 5.6.1-13 are the dose rates for licensing purposes and are slightly smaller. This difference is due to the increased detail in the final MCNP models.

Table 5.6.1-5
MTR Gamma Response Function

Upper Energy (MeV)	Response Function (mrem/hr)*
0.05	0.000E+00
0.10	0.000E+00
0.20	0.000E+00
0.30	0.000E+00
0.40	0.000E+00
0.60	1.511E-16
0.80	6.159E-15
1.00	1.134E-13
1.33	1.334E-12
1.66	6.941E-12
2.00	1.934E-11
2.50	4.355E-11
3.00	7.936E-11
4.00	1.338E-10
5.00	1.924E-10
6.50	2.387E-10
8.00	2.678E-10
10.00	2.909E-10

* - Multiply an entry of the response function corresponding to a particular energy range by an intensity of a gamma radiation source from a single fuel element in that energy range to get a dose rate due the source in that energy range. The resulting dose rate is per 54 fuel elements.

Table 5.6.1-6
MTR Bounding Gamma Source per Fuel Element

Upper Energy (MeV)	Gamma Source (γ/s)
0.05	2.440E+13
0.10	7.205E+12
0.20	5.922E+12
0.30	1.620E+12
0.40	1.160E+12
0.60	9.728E+12
0.80	3.431E+13
1.00	4.288E+12
1.33	8.927E+11
1.66	3.450E+11
2.00	1.254E+10
2.50	5.712E+10
3.00	6.095E+08
4.00	5.263E+07
5.00	1.012E+04
6.50	4.060E+03
8.00	7.962E+02
10.00	1.690E+02
Total	8.994E+13

Table 5.6.1-7
MTR Neutron Response Function

Upper Energy (MeV)	Response Function (mrem/hr)
3.00E-03	1.128E-07
1.70E-02	8.728E-08
1.00E-01	4.860E-08
4.00E-01	4.731E-08
9.00E-01	1.030E-07
1.40E+00	1.955E-07
1.85E+00	2.419E-07
3.00E+00	3.200E-07
6.43E+00	3.495E-07
2.00E+01	6.000E-07

Table 5.6.1-8
MTR Bounding Neutron Source per Fuel Element

Upper Energy (MeV)	Neutron Source (n/s)
1.00E-08	1.549E-07
3.00E-08	4.891E-07
5.00E-08	6.716E-07
1.00E-07	2.256E-06
2.25E-07	8.201E-06
3.25E-07	8.544E-06
4.00E-07	7.355E-06
8.00E-07	5.017E-05
1.00E-06	3.083E-05
1.13E-06	2.179E-05
1.30E-06	3.044E-05
1.77E-06	9.479E-05
3.05E-06	3.227E-04
1.00E-05	2.901E-03
3.00E-05	2.621E-02
1.00E-04	1.552E-01
5.50E-04	2.139E+00
3.00E-03	2.795E+01
1.70E-02	4.012E+02
1.00E-01	7.054E+03
4.00E-01	5.357E+04
9.00E-01	1.181E+05
1.40E+00	1.131E+05
1.85E+00	8.933E+04
3.00E+00	9.966E+04
6.43E+00	6.085E+04
2.00E+01	5.873E+03
Total	5.479E+05

Table 5.6.1-9
Important TN-LC-MTR Basket Model Dimensions

Proprietary Information Withheld Pursuant to 10 CFR 2.390.

Table 5.6.1-10
TN-LC-MTR NCT Side Surface Dose Rates between Impact Limiters (mrem/hr)

Location	Gamma	σ	Neutron	σ	(n,g)	σ	Total	σ
8	6.55E+01	1.4%	2.57E+00	0.5%	8.48E-02	0.5%	6.82E+01	1.3%
9	5.49E+01	0.8%	1.08E+00	0.5%	9.63E-02	0.4%	5.61E+01	0.8%
10	5.03E+01	0.9%	9.94E-01	0.5%	9.41E-02	0.4%	5.14E+01	0.9%
11	6.52E+01	0.7%	1.10E+00	0.5%	9.93E-02	0.4%	6.64E+01	0.7%
12	4.43E+01	0.8%	9.40E-01	0.6%	9.29E-02	0.4%	4.54E+01	0.8%
13	5.97E+01	0.5%	1.05E+00	0.5%	9.86E-02	0.4%	6.08E+01	0.5%
14	5.86E+01	0.6%	1.14E+00	0.5%	1.01E-01	0.4%	5.99E+01	0.6%
15	4.59E+01	0.9%	1.77E+00	0.5%	9.01E-02	0.5%	4.78E+01	0.9%
16	6.59E+01	0.8%	1.19E+00	0.5%	1.02E-01	0.4%	6.72E+01	0.7%
17	4.85E+01	0.8%	9.58E-01	0.5%	9.47E-02	0.4%	4.96E+01	0.8%
18	5.49E+01	0.8%	1.01E+00	0.5%	9.56E-02	0.4%	5.60E+01	0.8%
19	6.37E+01	0.8%	1.08E+00	0.5%	9.81E-02	0.4%	6.49E+01	0.8%
20	4.36E+01	0.8%	9.18E-01	0.6%	9.11E-02	0.4%	4.46E+01	0.8%
21	6.43E+01	0.8%	1.08E+00	0.5%	9.16E-02	0.4%	6.54E+01	0.8%
22	4.88E+01	0.7%	1.28E+00	0.6%	7.26E-02	0.5%	5.02E+01	0.7%
IL Attach.	**6.55E+01**	**1.4%**	**5.89E+00**	**2.3%**	**8.48E-02**	**0.5%**	**7.15E+01**	**1.3%**
Shear Key	4.59E+01	0.9%	6.42E+00	1.4%	9.01E-02	0.5%	5.24E+01	0.8%

Table 5.6.1-11
TN-LC-MTR NCT Vehicle Underside Dose Rates (mrem/hr)

Location	Gamma	σ	Neutron	σ	(n,g)	σ	Total	σ
6[1]	2.57E+01	2.4%	4.25E-01	0.5%	2.02E-02	0.6%	2.61E+01	2.3%
7[1]	**4.66E+01**	**2.2%**	**7.92E-01**	**0.4%**	**2.71E-02**	**0.6%**	**4.75E+01**	**2.2%**
8	3.39E+01	1.2%	9.80E-01	0.4%	3.44E-02	0.5%	3.50E+01	1.2%
9	3.06E+01	1.3%	6.99E-01	0.4%	4.07E-02	0.4%	3.14E+01	1.3%
10	2.91E+01	0.8%	5.61E-01	0.4%	4.34E-02	0.4%	2.97E+01	0.7%
11	3.07E+01	0.7%	5.29E-01	0.4%	4.49E-02	0.4%	3.12E+01	0.7%
12	2.79E+01	0.6%	5.08E-01	0.4%	4.48E-02	0.4%	2.84E+01	0.6%
13	2.96E+01	0.6%	5.32E-01	0.4%	4.53E-02	0.4%	3.01E+01	0.6%
14	2.97E+01	0.7%	5.96E-01	0.4%	4.51E-02	0.4%	3.03E+01	0.7%
15	2.82E+01	0.7%	6.48E-01	0.4%	4.47E-02	0.4%	2.89E+01	0.7%
16	3.04E+01	0.7%	5.94E-01	0.4%	4.48E-02	0.4%	3.10E+01	0.6%
17	2.85E+01	0.6%	5.20E-01	0.4%	4.49E-02	0.4%	2.91E+01	0.6%
18	2.88E+01	0.6%	4.98E-01	0.4%	4.49E-02	0.4%	2.94E+01	0.6%
19	3.03E+01	1.0%	5.01E-01	0.4%	4.38E-02	0.4%	3.08E+01	1.0%
20	2.75E+01	0.8%	4.92E-01	0.4%	4.17E-02	0.4%	2.80E+01	0.8%
21	2.85E+01	0.7%	5.26E-01	0.4%	3.79E-02	0.4%	2.90E+01	0.6%
22	2.23E+01	0.9%	5.98E-01	0.4%	3.02E-02	0.5%	2.29E+01	0.8%
23①	8.73E+00	1.9%	4.58E-01	0.5%	2.02E-02	0.7%	9.21E+00	1.8%
24①	4.44E+00	3.0%	2.45E-01	0.6%	1.38E-02	0.8%	4.70E+00	2.9%
IL Attach.	3.39E+01	1.2%	1.30E+00	2.3%	3.44E-02	0.5%	3.53E+01	1.2%
Shear Key	2.82E+01	0.7%	1.32E+00	1.6%	4.47E-02	0.4%	2.96E+01	0.7%

Notes:
1. Locations 6, 7, 23, and 24 represent the side of the impact limiters.

Table 5.6.1-12
TN-LC-MTR NCT Vehicle Side Dose Rates (mrem/hr)

Location	Gamma	σ	Neutron	σ	(n,g)	σ	Total	σ
6	1.68E+01	2.2%	2.45E-01	0.4%	1.02E-02	0.6%	1.70E+01	2.1%
7	**2.12E+01**	**1.9%**	**3.64E-01**	**0.4%**	**1.51E-02**	**0.5%**	**2.16E+01**	**1.8%**
8	2.01E+01	1.3%	4.62E-01	0.4%	2.02E-02	0.5%	2.06E+01	1.3%
9	2.05E+01	1.0%	4.60E-01	0.4%	2.41E-02	0.4%	2.09E+01	1.0%
10	1.98E+01	0.7%	4.05E-01	0.4%	2.68E-02	0.4%	2.03E+01	0.7%
11	2.03E+01	1.1%	3.75E-01	0.4%	2.81E-02	0.4%	2.07E+01	1.0%
12	1.98E+01	0.8%	3.66E-01	0.4%	2.89E-02	0.4%	2.02E+01	0.7%
13	1.96E+01	0.6%	3.74E-01	0.4%	2.93E-02	0.4%	2.00E+01	0.6%
14	1.97E+01	0.6%	3.88E-01	0.4%	2.95E-02	0.4%	2.01E+01	0.6%
15	1.96E+01	0.6%	3.98E-01	0.4%	2.91E-02	0.4%	2.00E+01	0.6%
16	1.98E+01	0.7%	3.83E-01	0.4%	2.93E-02	0.4%	2.02E+01	0.6%
17	1.94E+01	0.6%	3.60E-01	0.4%	2.91E-02	0.4%	1.98E+01	0.6%
18	1.93E+01	0.6%	3.46E-01	0.4%	2.84E-02	0.4%	1.97E+01	0.6%
19	1.95E+01	0.7%	3.39E-01	0.4%	2.73E-02	0.4%	1.98E+01	0.7%
20	1.84E+01	0.7%	3.37E-01	0.4%	2.56E-02	0.4%	1.88E+01	0.7%
21	1.70E+01	0.7%	3.39E-01	0.4%	2.23E-02	0.4%	1.73E+01	0.7%
22	1.34E+01	0.8%	3.10E-01	0.4%	1.83E-02	0.5%	1.37E+01	0.8%
23	7.60E+00	1.5%	2.31E-01	0.4%	1.31E-02	0.6%	7.84E+00	1.4%
24	3.73E+00	2.2%	1.55E-01	0.5%	8.20E-03	0.7%	3.90E+00	2.1%

Table 5.6.1-13
TN-LC-MTR NCT 2 m from Vehicle Side Dose Rates (mrem/hr)

Location	Gamma	σ	Neutron	σ	(n,g)	σ	Total	σ
1	1.14E+00	3.4%	2.95E-02	0.6%	1.72E-03	0.8%	1.18E+00	3.3%
2	1.64E+00	3.7%	3.49E-02	0.5%	2.12E-03	0.7%	1.68E+00	3.6%
3	2.13E+00	2.7%	4.24E-02	0.5%	2.59E-03	0.7%	2.17E+00	2.6%
4	2.84E+00	2.0%	5.15E-02	0.5%	3.15E-03	0.6%	2.89E+00	2.0%
5	3.70E+00	2.1%	6.26E-02	0.4%	3.78E-03	0.5%	3.77E+00	2.0%
6	4.46E+00	1.6%	7.48E-02	0.4%	4.44E-03	0.5%	4.54E+00	1.6%
7	4.78E+00	1.3%	8.63E-02	0.4%	5.08E-03	0.5%	4.87E+00	1.3%
8	5.29E+00	1.5%	9.50E-02	0.4%	5.66E-03	0.5%	5.39E+00	1.4%
9	5.67E+00	1.1%	1.04E-01	0.4%	6.12E-03	0.5%	5.78E+00	1.1%
10	5.96E+00	1.0%	1.11E-01	0.4%	6.56E-03	0.5%	6.08E+00	1.0%
11	6.12E+00	0.8%	1.16E-01	0.4%	7.03E-03	0.4%	6.25E+00	0.8%
12	6.40E+00	0.8%	1.19E-01	0.4%	7.30E-03	0.4%	6.53E+00	0.7%
13	6.41E+00	0.6%	1.20E-01	0.4%	7.50E-03	0.4%	6.54E+00	0.6%
14	**6.62E+00**	**0.8%**	**1.19E-01**	**0.4%**	**7.61E-03**	**0.4%**	**6.75E+00**	**0.8%**
15	6.53E+00	0.7%	1.18E-01	0.4%	7.69E-03	0.4%	6.66E+00	0.7%
16	6.43E+00	0.8%	1.16E-01	0.4%	7.57E-03	0.4%	6.56E+00	0.8%
17	6.31E+00	0.8%	1.13E-01	0.4%	7.43E-03	0.4%	6.43E+00	0.7%
18	6.00E+00	0.7%	1.09E-01	0.4%	7.25E-03	0.4%	6.12E+00	0.7%
19	5.67E+00	0.8%	1.04E-01	0.4%	6.81E-03	0.4%	5.78E+00	0.8%
20	5.32E+00	1.6%	9.71E-02	0.4%	6.40E-03	0.5%	5.42E+00	1.5%
21	4.64E+00	0.8%	8.89E-02	0.4%	5.98E-03	0.5%	4.73E+00	0.7%
22	4.05E+00	0.8%	7.94E-02	0.4%	5.45E-03	0.5%	4.14E+00	0.8%
23	3.41E+00	0.9%	7.06E-02	0.5%	4.85E-03	0.5%	3.49E+00	0.9%
24	2.62E+00	1.0%	6.06E-02	0.4%	4.20E-03	0.5%	2.68E+00	1.0%
25	1.92E+00	1.5%	5.03E-02	0.5%	3.54E-03	0.6%	1.98E+00	1.5%
26	1.38E+00	2.7%	4.06E-02	0.5%	2.94E-03	0.6%	1.43E+00	2.7%
27	1.02E+00	2.4%	3.28E-02	0.6%	2.36E-03	0.7%	1.05E+00	2.3%
28	7.74E-01	2.8%	2.73E-02	0.6%	1.93E-03	0.8%	8.03E-01	2.7%
29	5.64E-01	2.7%	2.26E-02	0.7%	1.56E-03	0.9%	5.88E-01	2.6%

Table 5.6.1-14
TN-LC-MTR NCT End Dose Rates (mrem/hr)

Location	Gamma	σ	Neutron	σ	(n,g)	σ	Total	σ
Bottom End at Impact Limiter Surface/Vehicle End Surface								
1	2.93E+01	7.3%	1.02E+00	3.4%	2.50E-02	9.3%	3.04E+01	7.0%
2	**3.23E+01**	**8.4%**	**9.22E-01**	**1.2%**	**2.08E-02**	**2.6%**	**3.33E+01**	**8.1%**
3	1.80E+01	4.9%	6.66E-01	0.9%	1.87E-02	1.7%	1.87E+01	4.7%
4	5.40E+00	4.1%	2.57E-01	0.6%	1.31E-02	0.9%	5.67E+00	3.9%
5	2.45E+00	3.5%	1.12E-01	0.7%	6.25E-03	1.1%	2.56E+00	3.3%
6	2.61E+00	2.7%	9.60E-02	0.5%	5.73E-03	0.6%	2.71E+00	2.6%
7	2.46E+00	1.6%	7.57E-02	0.5%	5.05E-03	0.6%	2.54E+00	1.5%
8	2.37E+00	1.6%	6.08E-02	0.5%	4.21E-03	0.6%	2.44E+00	1.5%
Bottom End 2 m from Impact Limiter Surface/Vehicle End Surface								
1,2,3	**2.02E+00**	**7.7%**	**4.86E-02**	**1.8%**	**1.11E-03**	**4.4%**	**2.07E+00**	**7.5%**
4,5	1.47E+00	4.8%	4.06E-02	0.8%	1.05E-03	1.6%	1.51E+00	4.7%
6	8.12E-01	4.6%	3.07E-02	0.6%	1.14E-03	1.2%	8.44E-01	4.4%
7	5.53E-01	4.1%	2.42E-02	0.6%	1.26E-03	0.9%	5.78E-01	3.9%
8	4.82E-01	3.1%	2.15E-02	0.5%	1.38E-03	0.7%	5.05E-01	3.0%
Top End at Impact Limiter Surface/Vehicle End Surface								
1	3.71E+01	5.7%	1.85E+00	2.7%	2.87E-02	7.8%	3.90E+01	5.4%
2	4.23E+01	4.7%	1.72E+00	0.9%	3.49E-02	2.0%	4.40E+01	4.5%
3	3.11E+01	4.2%	1.21E+00	0.7%	3.01E-02	1.4%	3.23E+01	4.1%
4	1.37E+01	3.2%	4.59E-01	0.5%	1.96E-02	0.8%	1.42E+01	3.1%
5	1.09E+01	3.4%	1.86E-01	0.6%	8.59E-03	0.9%	1.11E+01	3.3%
6	9.07E+00	2.4%	1.45E-01	0.4%	6.78E-03	0.6%	9.23E+00	2.4%
7	6.40E+00	2.9%	1.03E-01	0.5%	5.52E-03	0.6%	6.51E+00	2.8%
8	4.79E+00	3.1%	7.78E-02	0.5%	4.50E-03	0.6%	4.88E+00	3.0%
Port	**8.25E+01**	**7.8%**	**1.98E+00**	**5.5%**	**3.59E-02**	**14.7%**	**8.45E+01**	**7.6%**
Top End 2 m from Impact Limiter Surface/Vehicle End Surface								
1,2,3	**3.43E+00**	**7.1%**	**8.62E-02**	**1.4%**	**1.64E-03**	**3.6%**	**3.52E+00**	**6.9%**
4,5	2.56E+00	4.1%	7.12E-02	0.6%	1.56E-03	1.3%	2.63E+00	4.0%
6	1.49E+00	2.7%	5.04E-02	0.5%	1.50E-03	1.0%	1.54E+00	2.6%
7	1.09E+00	3.0%	3.67E-02	0.5%	1.56E-03	0.8%	1.13E+00	2.9%
8	9.73E-01	2.9%	2.96E-02	0.5%	1.59E-03	0.7%	1.00E+00	2.8%

Table 5.6.1-15
TN-LC-MTR HAC Dose Rates (mrem/hr)

Location	Gamma	σ	Neutron	σ	(n,g)	σ	Total	σ
Side								
1	2.07E+01	3.8%	7.41E-01	0.4%	1.23E-03	2.4%	2.14E+01	3.7%
2	4.24E+01	4.0%	9.98E-01	0.4%	1.64E-03	2.0%	4.34E+01	3.9%
3	8.37E+01	3.3%	1.37E+00	0.3%	2.19E-03	1.6%	8.50E+01	3.2%
4	**1.46E+02**	**3.5%**	**1.90E+00**	**0.2%**	**2.92E-03**	**1.3%**	**1.48E+02**	**3.4%**
5	1.23E+02	3.5%	2.57E+00	0.2%	3.79E-03	1.1%	1.26E+02	3.4%
6	6.74E+01	2.4%	3.24E+00	0.2%	4.59E-03	1.0%	7.06E+01	2.3%
7	5.53E+01	1.9%	3.80E+00	0.2%	5.33E-03	0.9%	5.91E+01	1.8%
8	4.40E+01	1.3%	4.18E+00	0.1%	5.81E-03	0.9%	4.82E+01	1.2%
9	4.00E+01	1.1%	4.42E+00	0.1%	6.17E-03	0.8%	4.45E+01	1.0%
10	3.80E+01	0.9%	4.57E+00	0.1%	6.39E-03	0.8%	4.26E+01	0.8%
11	3.79E+01	0.9%	4.64E+00	0.1%	6.47E-03	0.8%	4.25E+01	0.8%
12	3.73E+01	0.8%	4.66E+00	0.1%	6.64E-03	0.8%	4.19E+01	0.7%
13	3.69E+01	0.8%	4.66E+00	0.1%	6.66E-03	0.8%	4.16E+01	0.7%
14	3.71E+01	1.1%	4.65E+00	0.1%	6.65E-03	0.8%	4.18E+01	1.0%
15	3.69E+01	0.9%	4.61E+00	0.1%	6.48E-03	0.8%	4.16E+01	0.8%
16	3.68E+01	1.1%	4.51E+00	0.1%	6.27E-03	0.8%	4.13E+01	1.0%
17	3.60E+01	0.9%	4.34E+00	0.1%	6.05E-03	0.9%	4.03E+01	0.8%
18	3.45E+01	0.8%	4.08E+00	0.2%	5.52E-03	0.9%	3.85E+01	0.7%
19	3.34E+01	1.3%	3.65E+00	0.2%	4.90E-03	0.9%	3.70E+01	1.2%
20	2.87E+01	1.6%	3.05E+00	0.2%	4.33E-03	1.0%	3.17E+01	1.5%
21	2.41E+01	3.4%	2.37E+00	0.2%	3.41E-03	1.2%	2.65E+01	3.1%
22	1.63E+01	6.1%	1.69E+00	0.3%	2.64E-03	1.5%	1.80E+01	5.6%
23	1.16E+01	6.7%	1.17E+00	0.3%	1.85E-03	1.8%	1.28E+01	6.1%
24	6.58E+00	5.5%	8.38E-01	0.4%	1.35E-03	2.2%	7.42E+00	4.9%
25	3.41E+00	4.8%	6.05E-01	0.5%	1.01E-03	2.8%	4.02E+00	4.0%
Bottom End								
1	**1.08E+01**	**10.9%**	**5.54E-01**	**0.9%**	**1.07E-03**	**4.4%**	**1.13E+01**	**10.4%**
2	5.92E+00	6.1%	4.96E-01	0.5%	9.68E-04	2.5%	6.42E+00	5.7%
3	3.19E+00	5.5%	4.91E-01	0.4%	8.64E-04	1.9%	3.69E+00	4.8%
Top End								
1	**1.88E+01**	**6.4%**	**9.03E-01**	**0.7%**	**1.54E-03**	**3.6%**	**1.97E+01**	**6.1%**
2	1.48E+01	4.3%	7.60E-01	0.4%	1.37E-03	2.1%	1.56E+01	4.1%
3	1.40E+01	3.2%	6.58E-01	0.3%	1.10E-03	1.6%	1.46E+01	3.1%

Table 5.6.1-16
Parameters of Linear Equations for Calculation of Cooling Times to Qualify MTR Fuel Assemblies at Various Burn-ups for Loading.

Type	Burnup Ranges, (MWD/MTU)		Parameters of Linear Equations $KX+L$, where X is a burnup in MWD/MTU	
	From	To	K	L
HEU1: $E \geq 90\%$ $M_{U235} \leq 380$ g	66,000	165,000	0.0038	486.7
	165,000	330,000	0.0019	800.0
	330,000	495,000	0.0015	960.0
	495,000	660,000	0.0016	870.0
HEU2: $E \geq 90\%$ $M_{U235} \leq 460$ g	57,750	144,375	0.0044	516.7
	144,375	288,750	0.0022	830.0
	288,750	433,125	0.0017	990.0
	433,125	577,500	0.0017	990.0
MEU: $40\% \leq E < 90\%$ $M_{U235} \leq 380$ g	29,330	73,325	0.0086	486.7
	73,325	146,650	0.0044	800.0
	146,650	219,975	0.0034	940.0
	219,975	293,300	0.0034	940.0
LEU: $19\% \leq E < 40\%$ $M_{U235} \leq 470$ g	13,930	34,825	0.0187	570.0
	34,825	69,650	0.0098	880.0
	69,650	104,475	0.0083	980.0
	104,475	139,300	0.0086	950.0

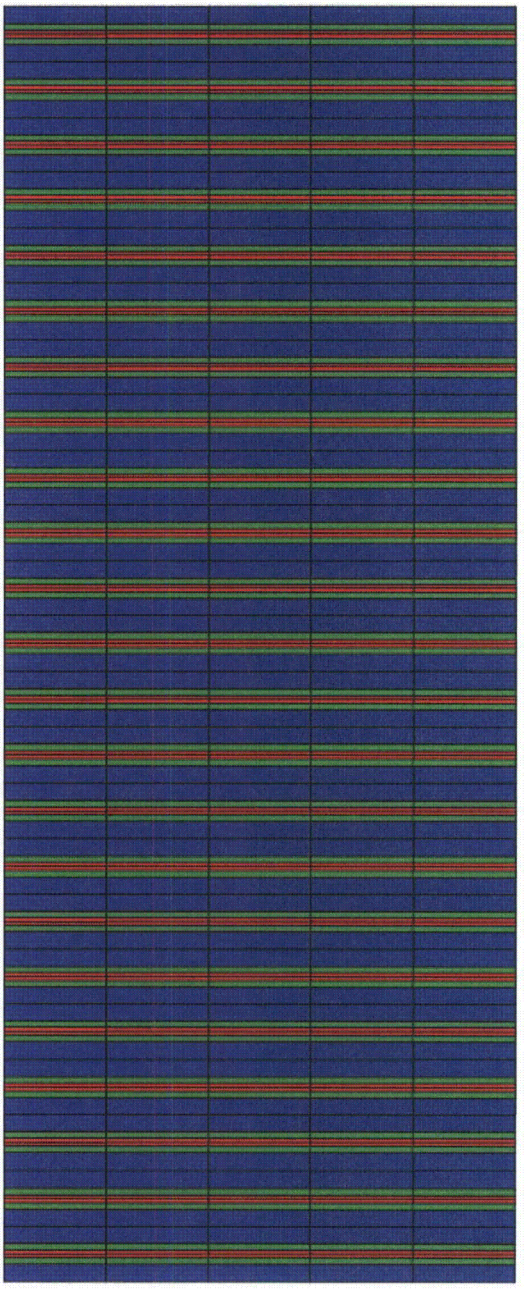

Figure 5.6.1-1
TRITON MTR Element Model

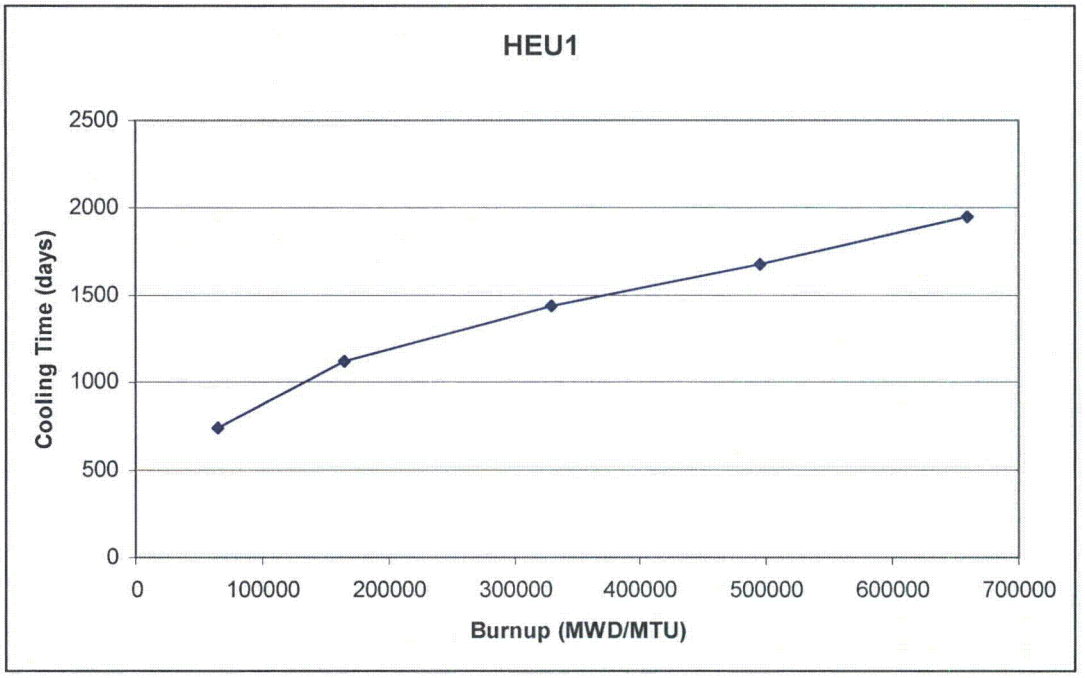

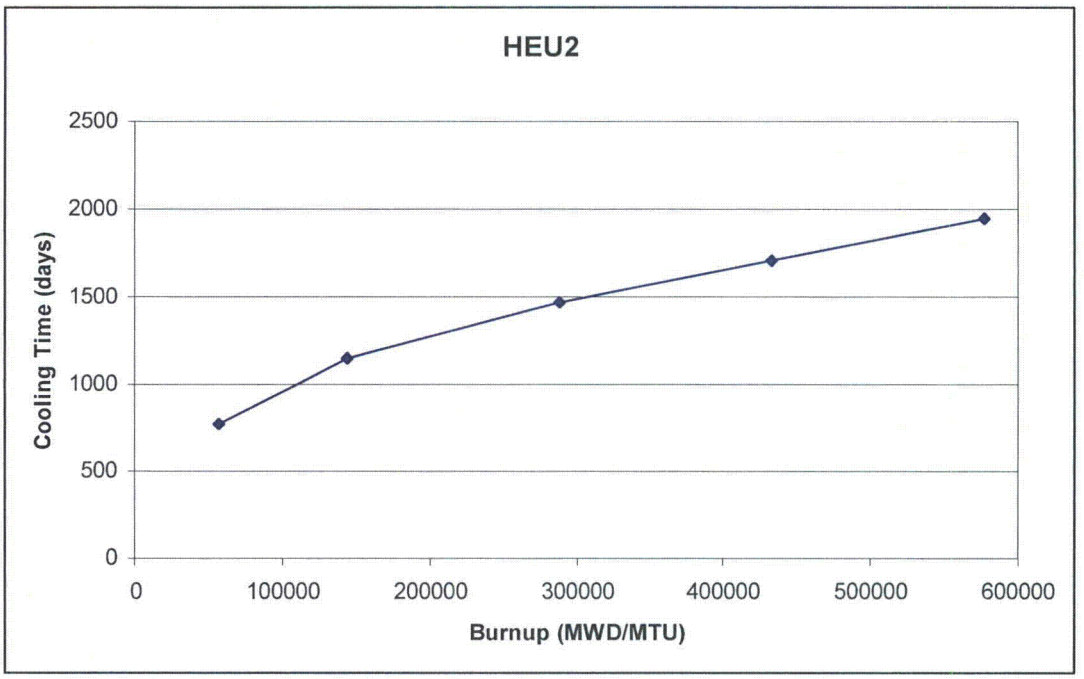

Figure 5.6.1-2
Cooling Time Plots (HEU1 and HEU2)

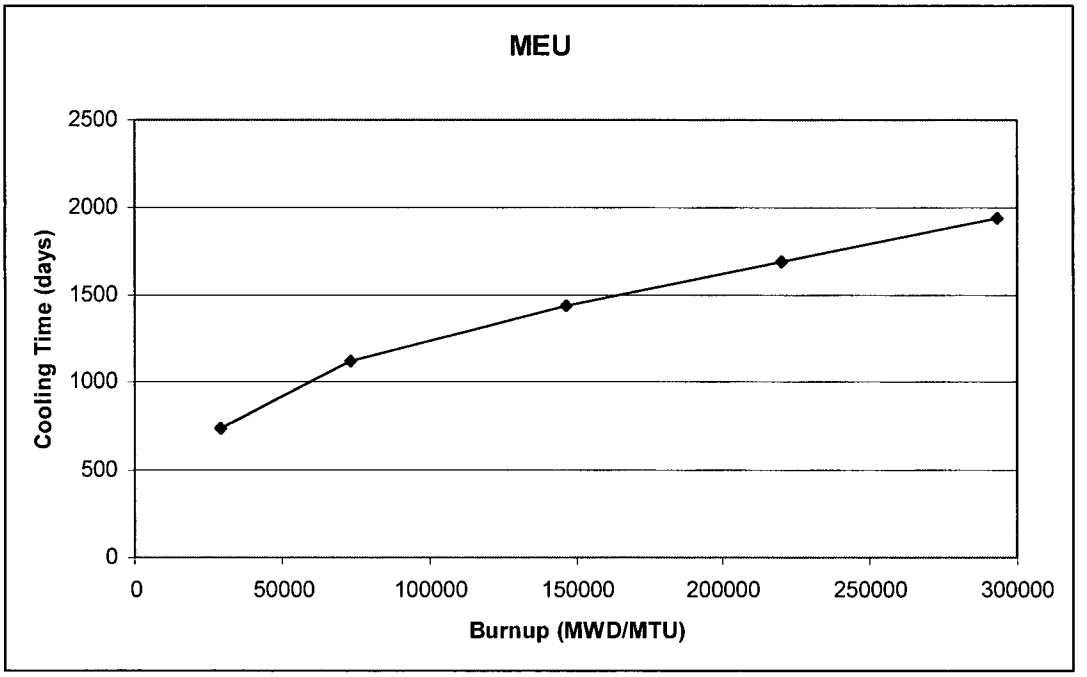

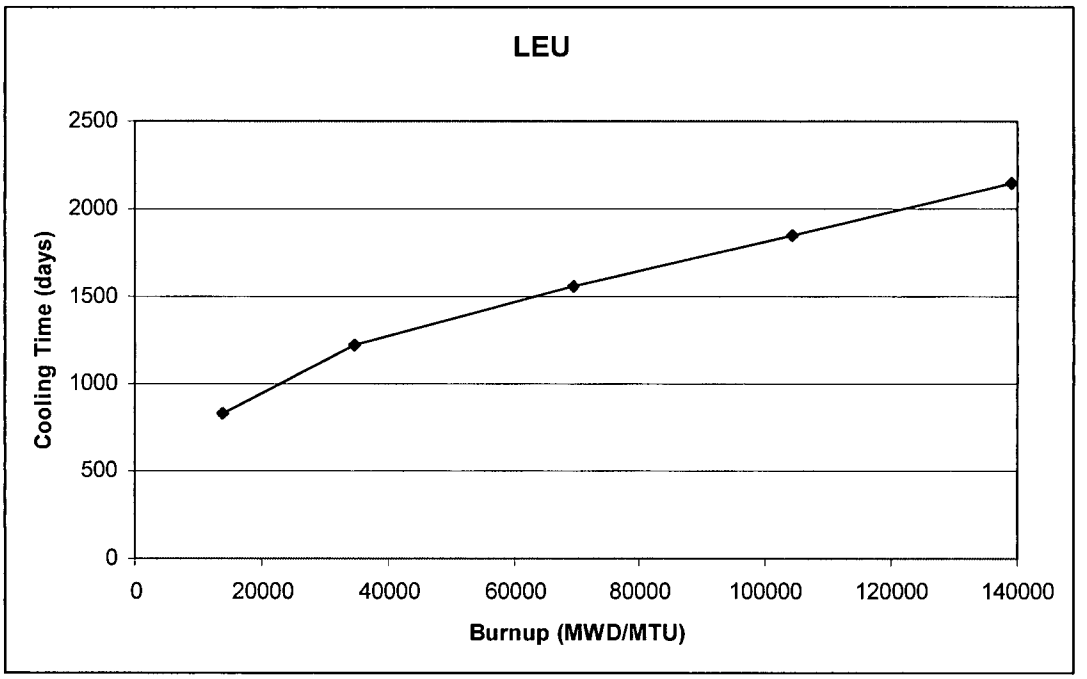

Figure 5.6.1-3
Cooling Time Plots (MEU and LEU)

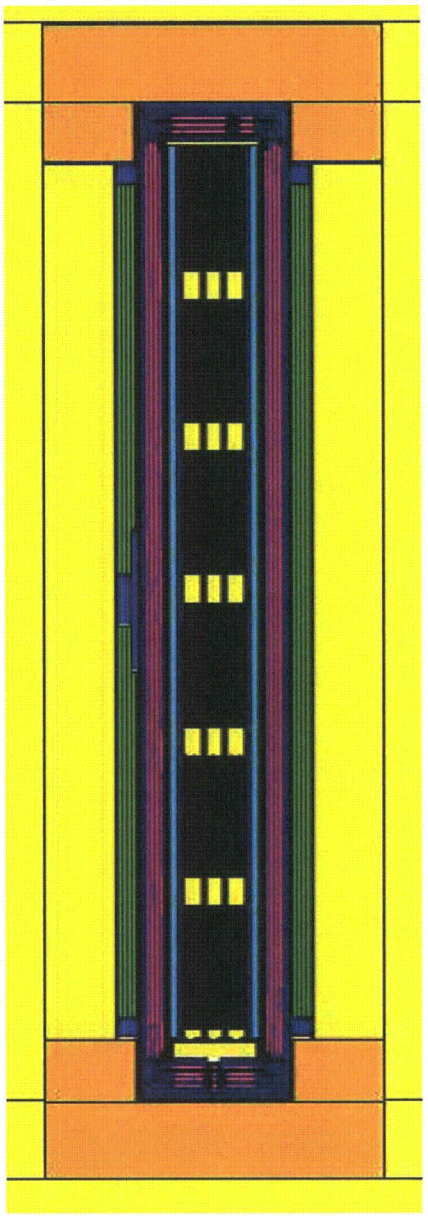

Figure 5.6.1-4
TN-LC-MTR MCNP Model, y-z View

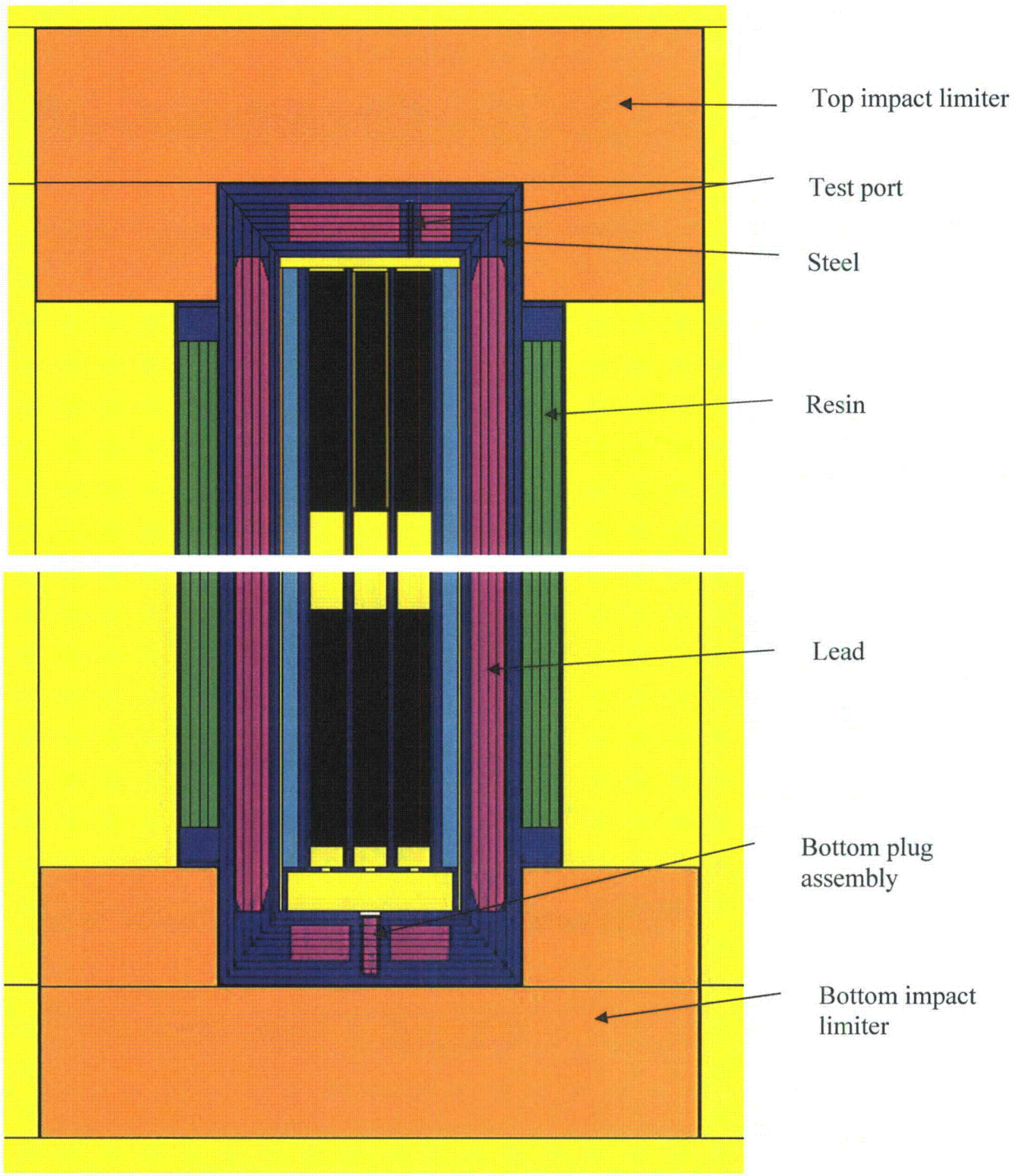

Figure 5.6.1-5
TN-LC-MTR MCNP Model, Close-Up y-z View

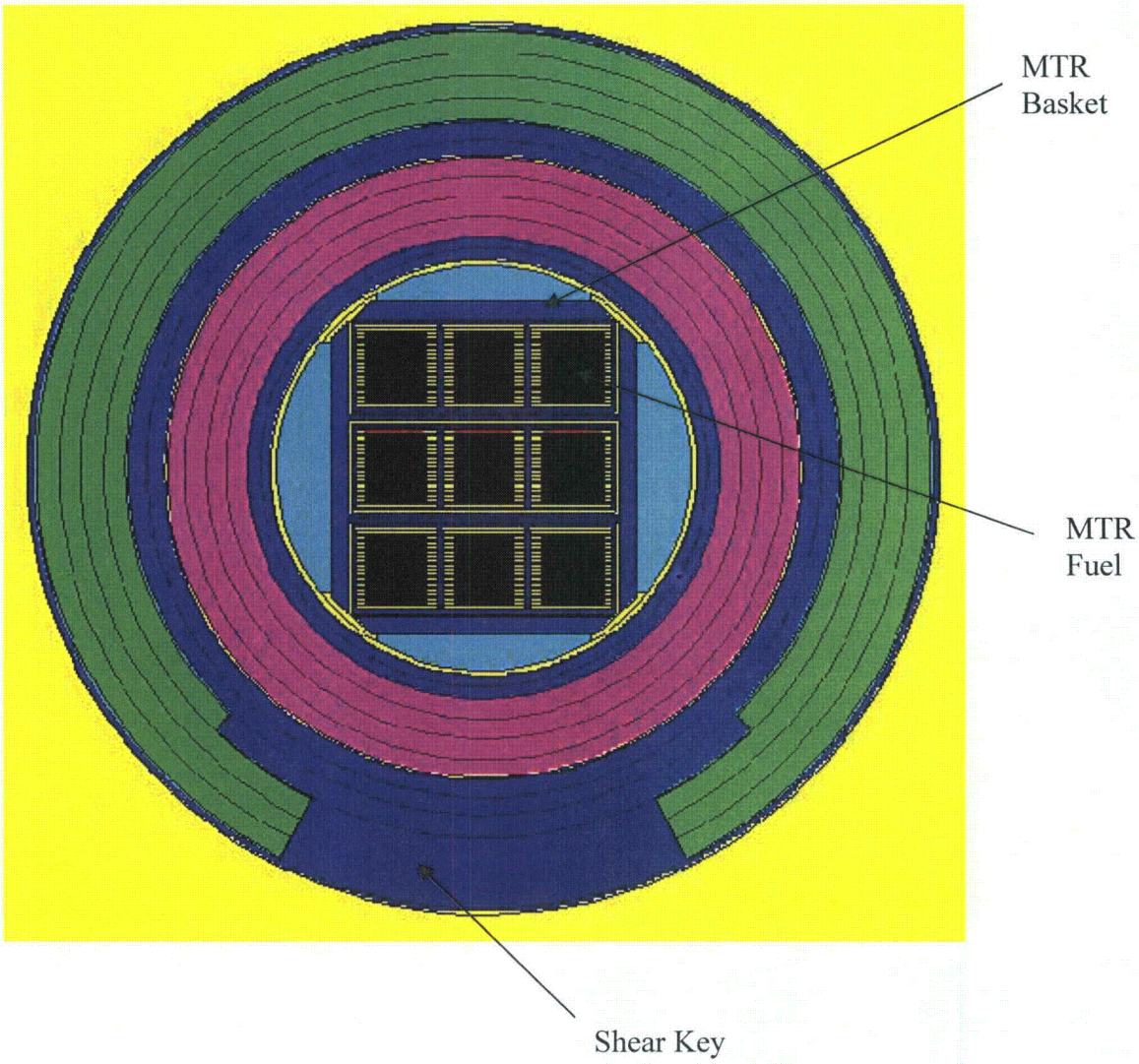

Figure 5.6.1-6
TN-LC-MTR MCNP Model, x-y View through Shear Key

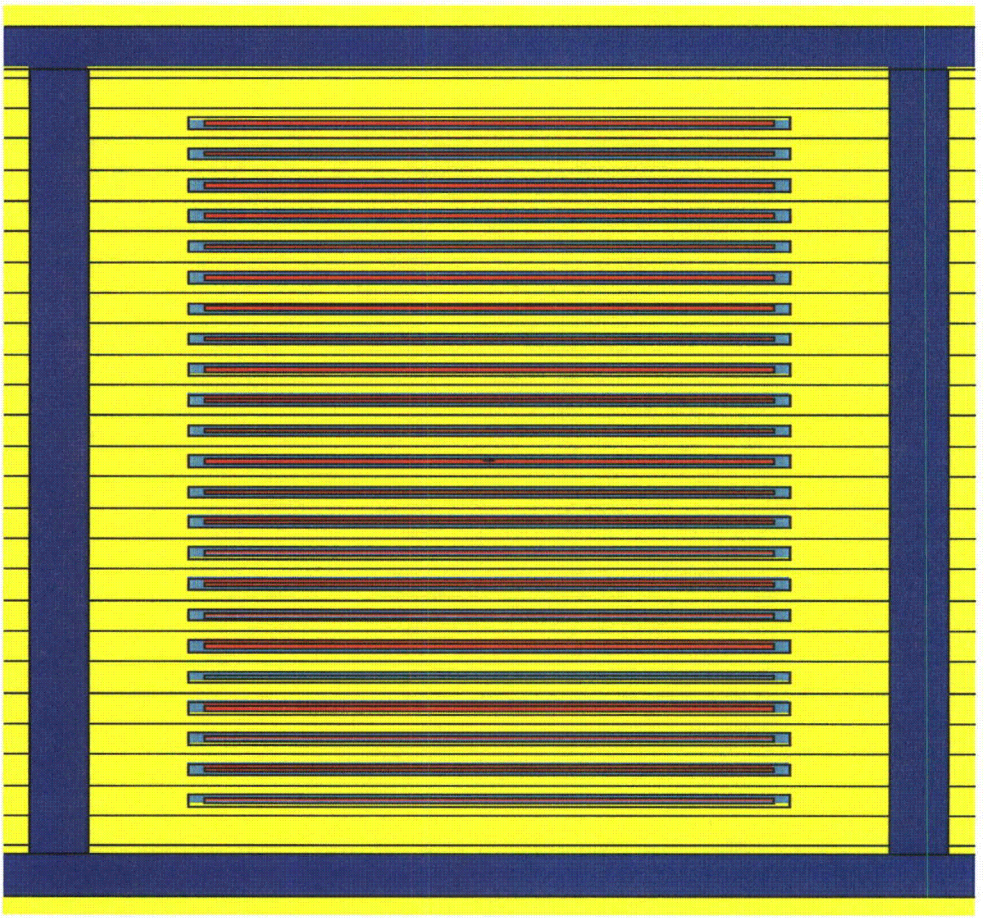

Figure 5.6.1-7
MTR Fuel Model

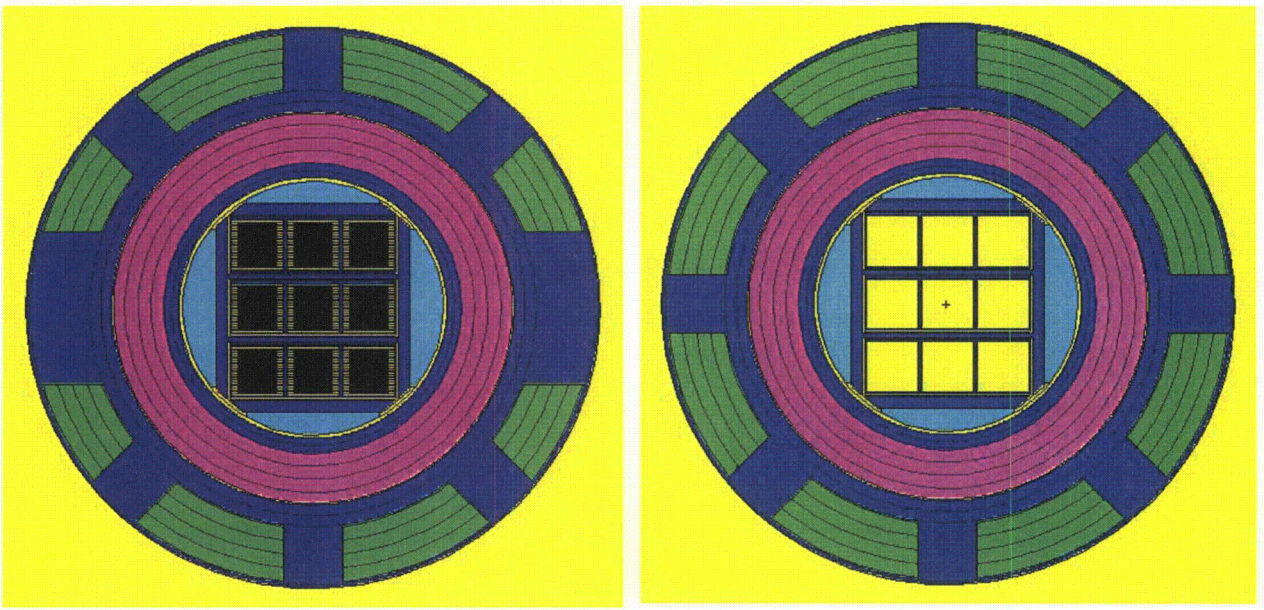

Top of Cask

Bottom of Cask

Figure 5.6.1-8
TN-LC-MTR MCNP Model, x-y View through Impact Limiter Attachment Blocks

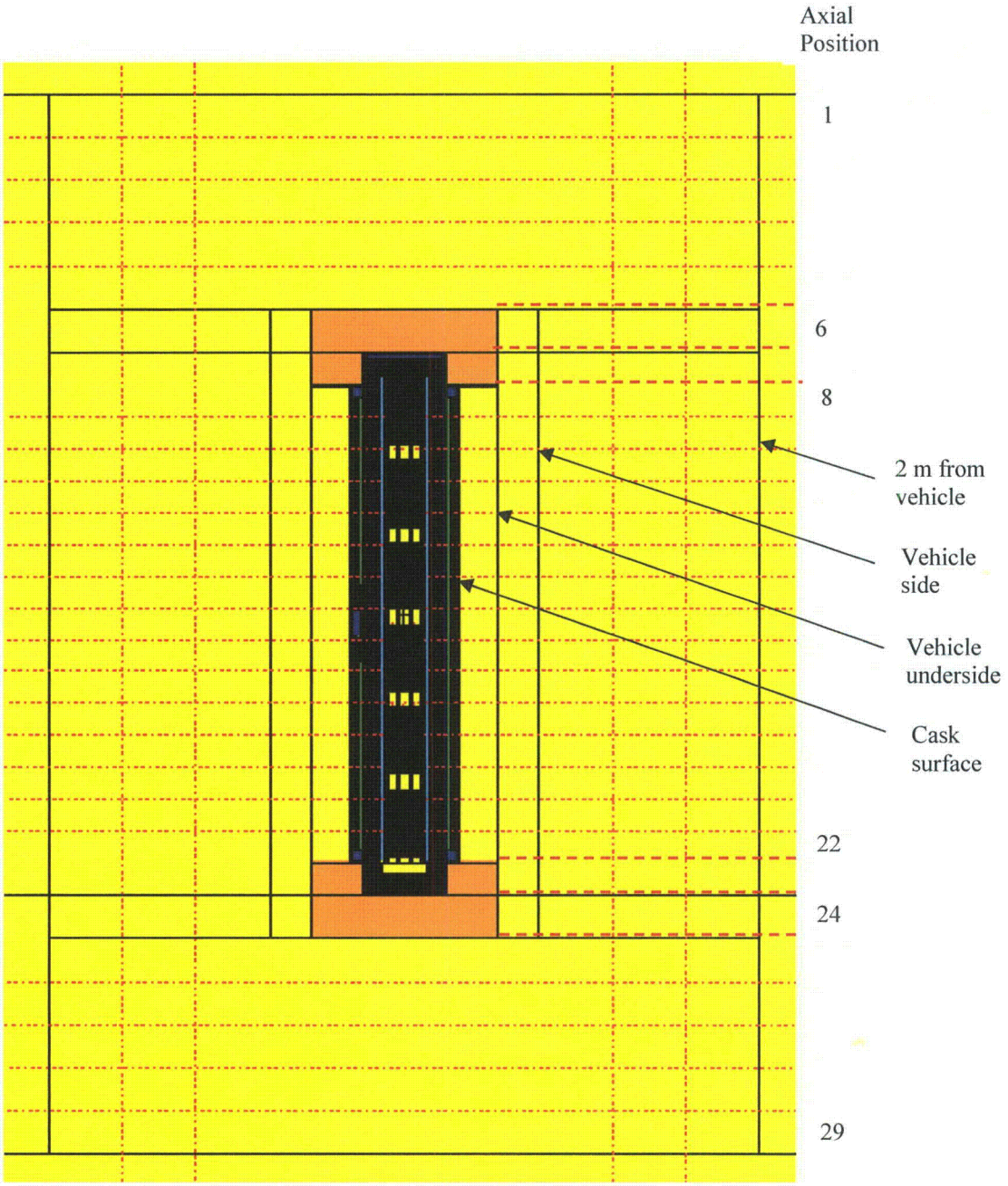

Figure 5.6.1-9
TN-LC-MTR NCT Radial Surface Tallies

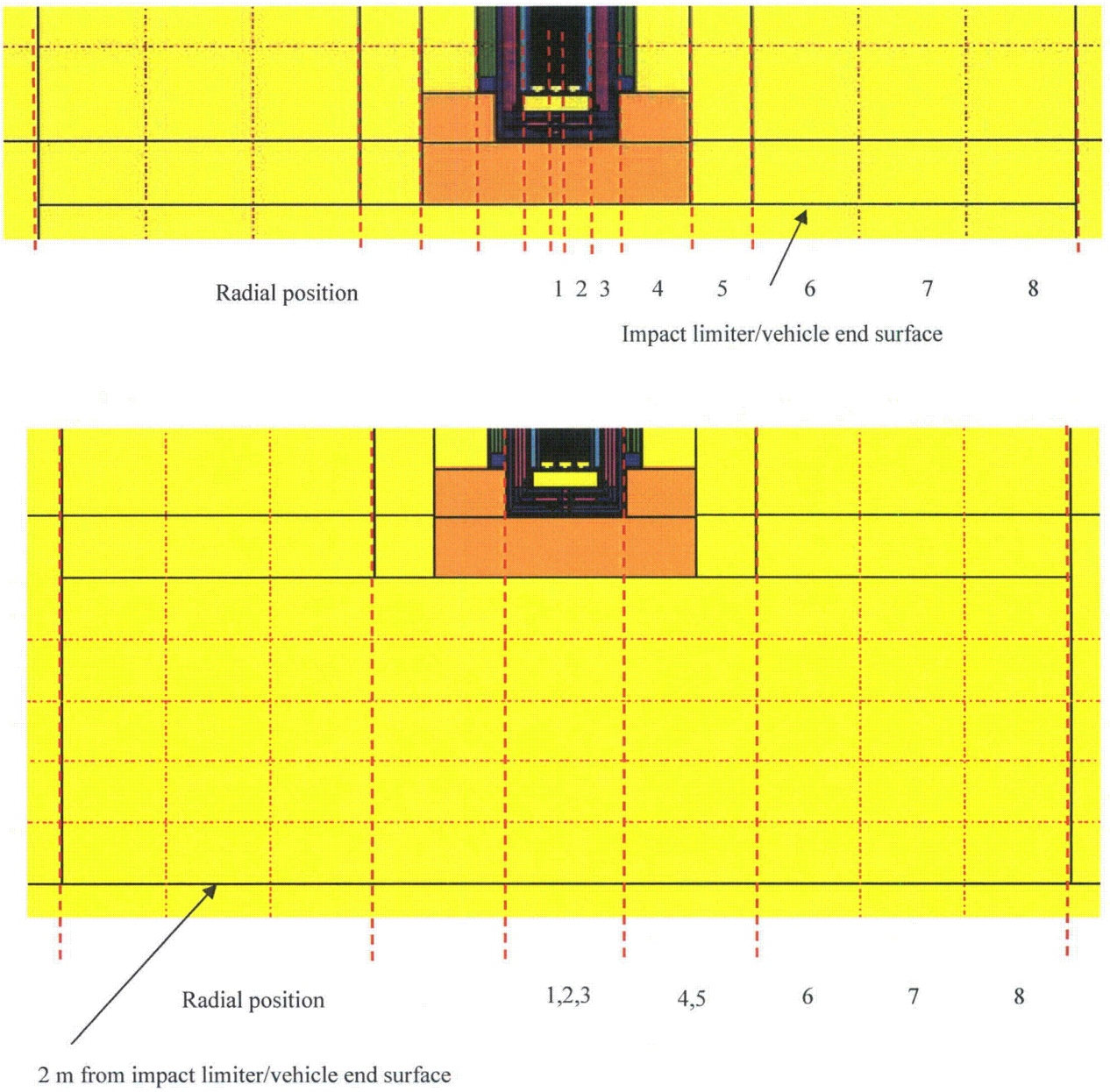

Figure 5.6.1-10
TN-LC-MTR NCT End Surface Tallies

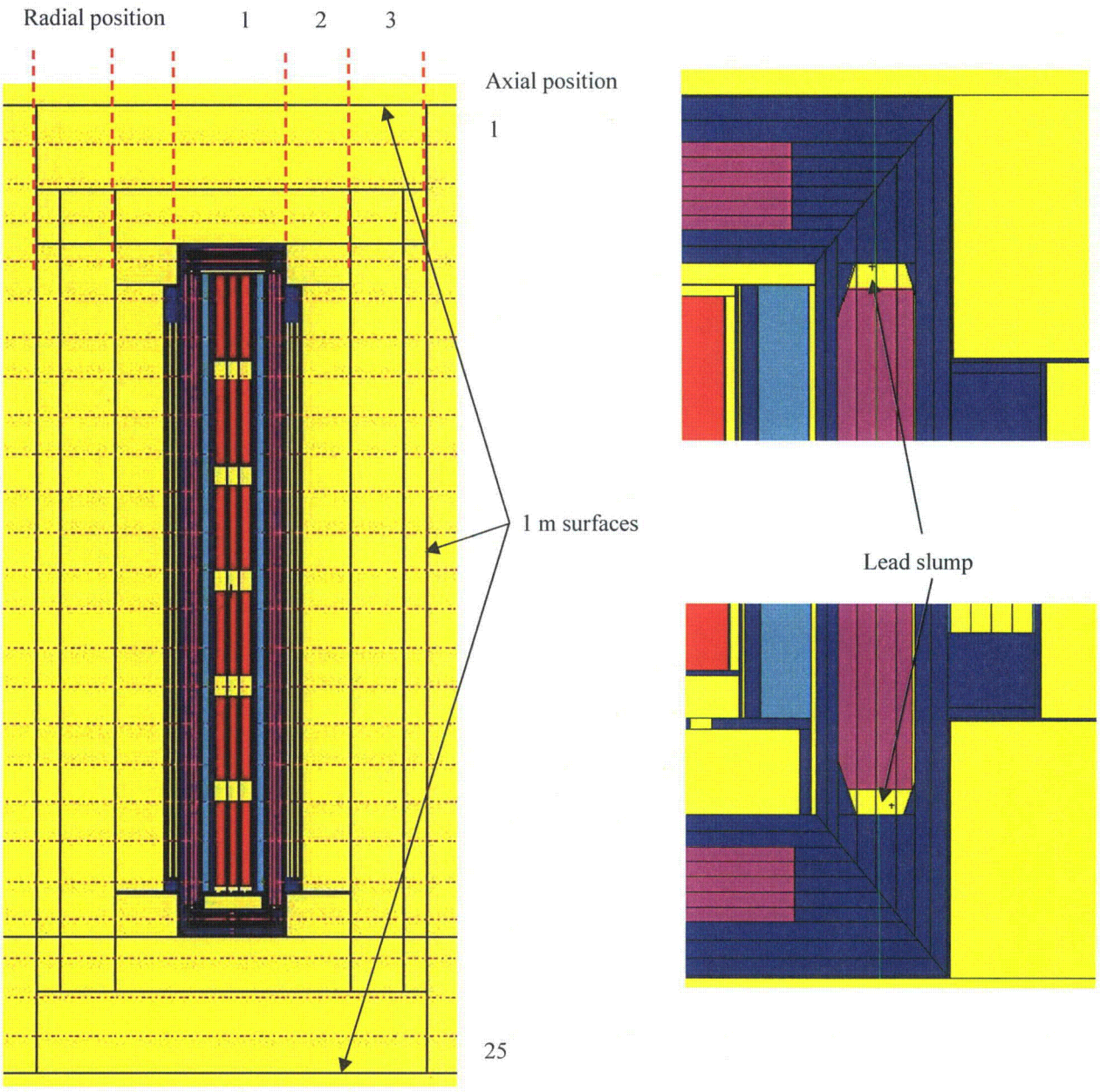

Figure 5.6.1-11
TN-LC-MTR HAC 1 m Tallies

Appendix 5.6.2
TN-LC-NRUX Basket Shielding Evaluation

TABLE OF CONTENTS

Proprietary Information Withheld Pursuant to 10 CFR 2.390.

LIST OF TABLES

LIST OF FIGURES

Appendix 5.6.2
TN-LC-NRUX Basket Shielding Evaluation

NOTE: References in this Appendix are shown as [1], [2], etc. and refer to the reference list in Section 5.6.2.5.1.

This Appendix presents the shielding evaluation of the TN-LC transportation package containing the TN-LC-NRUX basket. The MCNP computer program [1] is used to calculate the dose rates using a detailed three-dimensional model. The dose rates are evaluated per the requirements of 10CFR71.47 and 71.51 for exclusive use transportation in a closed transport vehicle.

5.6.2.1 Description of the Shielding Design

5.6.2.1.1 Design Features

The shielding design of the cask is described in Section 5.1.1.

Proprietary Information Withheld Pursuant to 10 CFR 2.390.

5.6.2.1.2 Summary Tables of Maximum Radiation Levels

Normal conditions of transport (NCT) dose rates are computed for exclusive use transport in a closed transport vehicle. These dose rate limits are as follows:

- Surface of the package: 1000 mrem/hr
- Surface of the transport vehicle: 200 mrem/hr
- 2 m from the surface of the transport vehicle: 10 mrem/hr

The transport vehicle is assumed to be 8 ft wide. Because the TN-LC is a long package, the ends of the transport vehicle are conservatively assumed to be at the ends of the impact limiters. The underside (floor) of the vehicle is conservatively assumed to correspond to the radius of the impact limiters. The dose rates on the vehicle roof are not computed as these dose rates are bounded by the dose rates on the underside of the vehicle. Dose rates are also computed 2 m from the sides and ends of the vehicle. The NCT dose rates for the TN-LC-NRUX basket payload are summarized in Table 5.6.2-1.

The maximum package surface dose rate of 57.3 mrem/hr occurs at the shear key on the side of the package. In the transportation configuration, the shear key mates with equipment attached to the transport vehicle and, hence, is not accessible. This dose rate is significantly less than the limit of 1000 mrem/hr on the package surface in a closed transport vehicle.

The maximum vehicle surface dose rate of 35.2 mrem/hr occurs at the top end of the vehicle (which also corresponds to the top surface of the impact limiter). This dose rate occurs over the port in the lid, and is significantly less than the limit of 200 mrem/hr on the vehicle surface.

The maximum dose rate 2 m from the vehicle surface of 2.79 mrem/hr occurs at the side of the vehicle. This dose rate is less than the limit of 10 mrem/hr at 2 m from the vehicle surface.

If it is assumed that the normally occupied space is 2 m from the ends of the impact limiters, then the dose rate limit of 2 mrem/hr is not exceeded.

Under hypothetical accident conditions (HAC), it is assumed that the neutron shield resin and impact limiter wood is replaced with air, and 1.2 in. of lead slump is modeled at both the top and bottom ends. Dose rates are computed 1 m from the surface of the cask body to bound any impact limiter or neutron shield crush damage. The maximum HAC dose rates are provided in Table 5.6.2-2. The maximum dose rate of 38.7 mrem/hr occurs at the side of the package, which is well below the limit of 1000 mrem/hr.

5.6.2.2 Source Specification

5.6.2.2.1 Gamma Source

The gamma source for NRU and NRX fuel is computed by the TRITON module of the SCALE6 code package [2]. TRITON allows for a two-dimensional representation of the fuel elements. Because the input is two dimensional, all input is for a basis of 1 metric ton of uranium (MTU). All TRITON output is also per 1 MTU, so the results must be scaled by the MTU of the fuel element.

Proprietary Information Withheld Pursuant to 10 CFR 2.390.

Proprietary Information Withheld Pursuant to 10 CFR 2.390.

5.6.2.2.2 Neutron Source

The neutron source is generated using the same TRITON models from which the gamma source is generated. The neutron source is comprised of both spontaneous fission and (α,n) reactions with the aluminum in the fuel matrix. The neutron source is provided in Table 5.6.2-6 for both NRU (586 g uranium) and NRX with either heavy or light water. The NRX with heavy water source is the bounding source used in the dose rate calculations.

5.6.2.2.3 Fuel Qualification

Fuel is limited to high-enriched NRU and NRX fuels decayed at least 10 years. Also, the fuels must be bounded by the U-235 mass limits utilized in the source term calculations (545 g U-235 for NRU, and 488.6 g U-235 for NRX).

5.6.2.3 Shielding Model

5.6.2.3.1 Configuration of Source and Shielding

The fuel, basket, and packaging are modeled explicitly in the MCNP computer program. The cask model is described in Section 5.3.1. The details of the model specific to the TN-LC-NRUX basket are described in this section.

The NRX fuel element type is used for the source geometry, as the self-shielding differences between the two fuel types are negligible due to the similarity between the fuels. The source is evenly distributed throughout the fuel pellet material, which is modeled with an active length of 8 ft. Only the active fuel region of the NRX element is modeled, and it is assumed that any flow tubes are removed. The end regions and flow tubes are aluminum and provide negligible source. Because the end regions and flow tubes would provide some shielding, it is conservative to neglect them.

The important shielding dimensions for the TN-LC-NRUX basket are provided in Table 5.6.2-7. The overall model geometry is illustrated in Figure 5.6.2-3. A close-up view of the model ends is illustrated in Figure 5.6.2-4. A view showing the basket is illustrated in Figure 5.6.2-5. A view through the impact limiter attachment blocks is illustrated in Figure 5.6.2-6.

Proprietary Information Withheld Pursuant to 10 CFR 2.390.

Under hypothetical accident conditions (HAC), the impact limiter wood and neutron shield resin are replaced with air. This bounds any postulated fire or crush damage. In addition, 1.2 in. of lead slump is modeled at both the top and bottom ends of the cask as a result of an end drop. This bounds the maximum lead slump value of 1.129 in. from Appendix 2.13.3. The radial lead slump at the cask ends due to a side drop is negligible (<0.2 in.) and has been neglected. HAC dose rates are conservatively computed 1 m from the cask body surface.

5.6.2.3.2 Material Properties

The material and physical parameters of the fuel are provided in Table 5.6.2-4. The NRX fuel has aluminum cladding with a density of 2.7 g/cm^3. The aluminum is modeled as pure. Material properties for the cask and basket structural materials are provided in Section 5.3.2.

5.6.2.4 Shielding Evaluation

5.6.2.4.1 Methods

MCNP5 v1.40 is used for the shielding analysis [1]. MCNP5 is a standard, well-accepted shielding program utilized to compute dose rates for shielding licenses. A three-dimensional model is developed that captures all of the relevant design parameters of the cask and internals. Dose rates are calculated by tallying the neutron and gamma fluxes over surfaces of interest and converting these fluxes to dose rates using flux-to-dose rate conversion factors. Secondary gammas resulting from neutron capture are also tallied. Subcritical neutron multiplication is also performed by the program.

Separate models are developed for neutron and gamma source terms. Geometry splitting and simple Russian roulette are used as a variance reduction technique for most tallies. The importance of the particles increases as the particles traverse the shielding materials. When necessary, DXTRAN spheres are used to accelerate program convergence above the lid port.

5.6.2.4.2 Input and Output Data

A number of input/output cases are used to generate the results, as listed below. A sample input file is provided in Section 5.6.2.5.3.

Radiological sources are determined with TRITON\NEWT models.

MCNP models are used to calculate response function due to neutron and gamma radiation source as well as for a determination of radiation fields at various distances around the cask at NCT and HAC.

Convergence is good (<10 percent) for all limiting dose rates. A separate gamma model is developed to compute the dose rate on the impact limiter surface over the lid port.

5.6.2.4.3 Flux-to-Dose-Rate Conversion

The flux-to-dose rate conversion factors are provided in Section 5.4.3.

5.6.2.4.4 External Radiation Levels

Tally locations are selected to be consistent with exclusive use transportation in a closed transport vehicle. Therefore, the applicable NCT dose rate limits from 10CFR71.47(b)(1), (2) and (3) are:

- 1000 mrem/hr on the package surface. This includes the surface of the cask between the impact limiters, and the impact limiter surfaces.
- 200 mrem/hr on the vehicle surface. The vehicle has six surfaces (2 sides, 2 ends, roof, and underside). The two sides of the vehicle are assumed to be 8 ft apart with the package in the center. The underside (floor) of the vehicle is conservatively assumed to be at the impact limiter radius, and the dose rates at the underside of the vehicle bound the dose rates at the

roof of the vehicle, which is farther away from the package. The ends of the vehicle are conservatively assumed to be at the impact limiter end surfaces.

- 10 mrem/hr 2 m from the vehicle surface. This dose rate does not apply 2 m from the roof of the vehicle or 2 m from the underside of the vehicle.

Circumferential tallies are placed around the packaging. Twenty-nine (29) axial locations are utilized, as illustrated in Figure 5.6.2-7. Locations 8 through 22 are utilized on the side of the cask between the impact limiters, Locations 6 though 24 are utilized on the side of the package at the impact limiter radius (underside of vehicle) and the side of the vehicle, and Locations 1 through 29 are utilized 2 m from the side of the vehicle.

At the ends of the packaging, dose rates are tallied on the impact limiter surfaces and 2 m from the impact limiter surfaces. Eight radial locations are utilized for the surface tallies, as illustrated in Figure 5.6.2-8. Location 1 captures any streaming effects from the bottom plug assembly. An off-center tally is used directly over the lid port to capture any streaming effects on the top impact limiter surface. For the dose rates 2 m from the ends, five radial locations are utilized by combining Locations 1,2,3 and 4,5 as shown on Figure 5.6.2-8. Any streaming effects are generally negligible 2 m from the ends and are not investigated for the TN-LC-NRUX basket. Because the bounding end dose rates are for the 1FA basket, the end streaming effects at 2 m are examined in more detail in the 1FA shielding calculation (See Appendix 5.6.4).

With the exception of neutron streaming through the shear key, the circumferential dose rates are relatively uniform. A mesh tally is used at the shear key to capture the neutron streaming effects in this region, as this location will have the maximum neutron dose rate. The axial heights of the mesh are chosen to correspond to the heights of the regions of interest. The mesh is 1 cm thick, and consists of 18 angular regions (20° each).

The shear key faces downward and results in a higher than average neutron dose rate on the surface of the package and the underside of the vehicle. The shear key does not result in gamma streaming because neutron shielding material is replaced with steel, which is a superior gamma shield. For this reason, the shear key is conservatively ignored in the gamma models, and neutron mesh tally results for the shear key are added to the average gamma results at axial Location 15. The mesh tally is used only at the cask surface and vehicle underside/impact limiter radius because any streaming effects will be essentially washed out beyond this distance, and also because it is not required to calculate dose rates 2 m from the underside of the vehicle. The reported dose rates 2 m from the side of the vehicle are circumferential tallies and, hence, include the contribution due to neutron streaming through the shear key.

Package surface: The NCT side surface dose rates are presented in Table 5.6.2-8. Dose rates on the side surfaces of the impact limiters are presented in Table 5.6.2-9 at axial locations 6, 7, 23, and 24. Dose rates on the external flat surfaces of the impact limiters are presented in Table 5.6.2-12. The maximum package surface dose rate occurs at the location of the shear key with a dose rate of 57.3 mrem/hr. Note that this location is not accessible when the package is in the transportation configuration. This dose rate is less than the limit of 1000 mrem/hr.

Vehicle surface: The NCT vehicle underside/impact limiter radius dose rates are presented in Table 5.6.2-9. The maximum dose rate on the vehicle underside occurs at the location of the shear key with a dose rate of 18.0 mrem/hr. The NCT vehicle side surface dose rates are presented in Table 5.6.2-10. The maximum dose rate on the vehicle side occurs at axial Locations 11 and 12 with a value of 11.4 mrem/hr. NCT vehicle end dose rates are presented in Table 5.6.2-12. The dose rate at the top end of the vehicle surface is 35.2 mrem/hr over the port, which bounds the vehicle surface dose rates on the underside, side, and bottom ends. This dose rate is significantly less than the limit of 200 mrem/hr.

2 m from vehicle surface: The NCT dose rates 2 m from the side surface of the vehicle are presented in Table 5.6.2-11. The maximum dose rate of 2.79 mrem/hr occurs at axial Locations 11 and 12. This dose rate is less than the limit of 10 mrem/hr and bounds the dose rates 2 m from the ends of the vehicle presented in Table 5.6.2-12.

Normally Occupied Space: If it is assumed that the normally occupied space is 2 m from the ends of the impact limiters, then the dose rate limit of 2 mrem/hr is not exceeded.

HAC: The applicable HAC dose rate limit from 10CFR71.51(a)(2) is 1000 mrem/hr 1 m from the package surface.

In the HAC models, the neutron shield resin and impact limiter wood is replaced with air, and 1.2 in. of lead slump is modeled at both the top and bottom ends. The tally surfaces are located 1 m from the outer surfaces of the cask. The dose rates at the ends of the package are divided into three segments, and the dose rates at the side of the package are divided in 25 segments of equal width. The tally locations are shown on Figure 5.6.2-9. HAC dose rate results are presented in Table 5.6.2-13. The maximum HAC dose rate of 38.7 mrem/hr occurs 1 m from the side of the package. This dose rate is significantly less than the limit of 1000 mrem/hr.

5.6.2.5 Appendix

5.6.2.5.1 References

1. MCNP5, "MCNP – A General Monte Carlo N-Particle Transport Code, Version 5; Volume II: User's Guide," LA-CP-03-0245, Los Alamos National Laboratory, April 2003
2. SCALE: A Modular Code System for Performing Standardized Computer Analyses for Licensing Evaluations, ORNL/TM-2005/39, Version 6, Vols. I-III, January 2009

Proprietary Information on Pages 5.6.2-10 through 5.6.2-26
Withheld Pursuant to 10 CFR 2.390.

Table 5.6.2-1
Summary of TN-LC-NRUX NCT Dose Rates

(Exclusive Use Package for Transportation)

Package Surface (mrem/hr), Limit = 1000 mrem/hr				
	Top End	**Side**	**Bottom End**	
Gamma	30.7	27.4	17.7	
Neutron	4.40	29.6	0.112	
(n,g)	7.46E-02	0.311	3.86E-03	
Total	35.2	57.3	18.8	
Vehicle Surface (mrem/hr), Limit = 200 mrem/hr				
	Top End	**Side**	**Bottom End**	**Underside**
Gamma	30.7	9.61	17.7	12.2
Neutron	4.40	1.72	0.112	5.71
(n,g)	7.46E-02	0.109	3.86E-03	0.132
Total	35.2	11.4	18.8	18.0
2 m from Vehicle Surface (mrem/hr), Limit = 10 mrem/hr				
	Top End	**Side**	**Bottom End**	
Gamma	0.983	2.36	0.104	
Neutron	0.225	0.413	1.09E-02	
(n,g)	4.16E-03	2.03E-02	2.13E-04	
Total	1.21	2.79	0.115	

Table 5.6.2-2
Summary of TN-LC-NRUX HAC Dose Rates

	1 m from Package Surface (mrem/hr), Limit = 1000 mrem/hr		
	Top End	**Side**	**Bottom End**
Gamma	4.92	18.8	1.02
Neutron	2.43	19.9	0.136
(n,g)	3.52E-03	2.08E-02	1.95E-04
Total	7.35	38.7	1.15

Table 5.6.2-3
NRU Fuel Data

Proprietary Information Withheld Pursuant to 10 CFR 2.390.

Table 5.6.2-4
NRX Fuel Data

Proprietary Information Withheld Pursuant to 10 CFR 2.390.

Table 5.6.2-5
NRU/NRX Bounding Gamma Source per Fuel Element

Upper Energy (MeV)	NRU (γ/s)	NRX Heavy Water (γ/s)	NRX Light Water (γ/s)	Hybrid (γ/s)
0.045	**1.892E+13**	1.720E+13	1.711E+13	1.892E+13
0.10	**6.469E+12**	5.825E+12	5.881E+12	6.469E+12
0.20	**3.978E+12**	3.640E+12	3.548E+12	3.978E+12
0.30	**1.210E+12**	1.099E+12	1.091E+12	1.210E+12
0.40	**8.306E+11**	7.436E+11	7.598E+11	8.306E+11
0.60	3.358E+12	**4.568E+12**	1.916E+12	4.568E+12
0.80	**2.949E+13**	2.831E+13	2.557E+13	2.949E+13
1.00	1.600E+12	**2.229E+12**	8.499E+11	2.229E+12
1.33	5.854E+11	**6.857E+11**	3.688E+11	6.857E+11
1.66	1.277E+11	**1.715E+11**	7.132E+10	1.715E+11
2.00	**2.442E+09**	2.221E+09	2.207E+09	2.442E+09
2.50	**1.517E+09**	1.381E+09	1.373E+09	1.517E+09
3.00	2.297E+07	**2.500E+07**	1.890E+07	2.500E+07
4.00	2.000E+06	**2.166E+06**	1.617E+06	2.166E+06
5.00	9.094E+03	**4.374E+04**	4.561E+02	4.374E+04
6.50	3.646E+03	**1.755E+04**	1.822E+02	1.755E+04
8.00	7.146E+02	**3.441E+03**	3.559E+01	3.441E+03
10.00	1.564E+02	**7.535E+02**	7.772E+00	7.535E+02
Total	6.657E+13	6.448E+13	5.717E+13	6.855E+13

Table 5.6.2-6
NRU/NRX Bounding Neutron Source per Fuel Element

Upper Energy (MeV)	NRU (n/s)	NRX Heavy Water (n/s)	NRX Light Water (n/s)
1.00E-08	1.402E-07	7.193E-07	7.216E-09
3.00E-08	4.405E-07	2.210E-06	2.174E-08
5.00E-08	6.042E-07	3.024E-06	2.964E-08
1.00E-07	2.029E-06	1.014E-05	9.923E-08
2.25E-07	7.373E-06	3.683E-05	3.600E-07
3.25E-07	7.681E-06	3.836E-05	3.747E-07
4.14E-07	7.918E-06	3.954E-05	3.862E-07
8.00E-07	4.379E-05	2.187E-04	2.135E-06
1.00E-06	2.771E-05	1.383E-04	1.351E-06
1.13E-06	1.887E-05	9.419E-05	9.197E-07
1.30E-06	2.809E-05	1.402E-04	1.369E-06
1.86E-06	1.017E-04	5.079E-04	4.961E-06
3.06E-06	2.747E-04	1.371E-03	1.339E-05
1.07E-05	2.952E-03	1.446E-02	1.630E-04
2.90E-05	3.828E-02	1.188E-01	5.858E-03
1.01E-04	2.514E-01	7.996E-01	3.727E-02
5.83E-04	3.341E+00	1.136E+01	4.544E-01
3.04E-03	4.046E+01	1.366E+02	5.542E+00
1.50E-02	4.775E+02	1.579E+03	6.720E+01
1.11E-01	1.368E+04	4.205E+04	2.097E+03
4.08E-01	8.603E+04	2.668E+05	1.296E+04
9.07E-01	1.917E+05	5.840E+05	2.946E+04
1.42E+00	1.879E+05	5.715E+05	2.898E+04
1.83E+00	1.302E+05	3.966E+05	1.998E+04
3.01E+00	1.337E+05	4.909E+05	1.559E+04
6.38E+00	5.404E+04	2.632E+05	2.607E+03
2.00E+01	5.526E+03	2.687E+04	2.633E+02
Total	8.033E+05	2.644E+06	1.120E+05

Table 5.6.2-7
Important TN-LC-NRUX Basket Model Dimensions

Proprietary Information Withheld Pursuant to 10 CFR 2.390.

Table 5.6.2-8
TN-LC-NRUX NCT Side Surface Dose Rates between Impact Limiters (mrem/hr)

Location	Gamma	σ	Neutron	σ	(n,g)	σ	Total	σ
8	2.18E+01	0.4%	8.89E+00	0.3%	2.63E-01	0.4%	3.09E+01	0.3%
9	2.85E+01	0.3%	5.25E+00	0.3%	3.75E-01	0.3%	3.41E+01	0.3%
10	2.88E+01	0.4%	5.38E+00	0.3%	4.03E-01	0.3%	3.46E+01	0.3%
11	2.87E+01	0.3%	5.42E+00	0.3%	4.14E-01	0.3%	3.45E+01	0.3%
12	2.86E+01	0.3%	5.41E+00	0.3%	4.15E-01	0.3%	3.44E+01	0.3%
13	2.86E+01	0.3%	5.38E+00	0.3%	4.11E-01	0.3%	3.44E+01	0.3%
14	2.84E+01	0.3%	5.70E+00	0.3%	3.99E-01	0.3%	3.44E+01	0.3%
15	2.74E+01	0.3%	8.32E+00	0.3%	3.11E-01	0.3%	3.60E+01	0.3%
16	1.28E+01	0.5%	2.81E+00	0.4%	2.01E-01	0.4%	1.58E+01	0.4%
17	7.83E-01	1.5%	6.81E-01	0.8%	7.78E-02	0.6%	1.54E+00	0.8%
18	2.95E-02	6.7%	1.82E-01	1.4%	2.81E-02	1.0%	2.40E-01	1.4%
19	1.08E-02	5.0%	8.51E-02	2.0%	1.41E-02	1.5%	1.10E-01	1.7%
20	1.36E-02	31.0%	4.63E-02	2.5%	8.36E-03	1.9%	6.83E-02	6.4%
21	8.38E-03	7.6%	3.50E-02	2.9%	5.58E-03	2.2%	4.90E-02	2.4%
22	1.00E-02	12.9%	5.36E-02	3.3%	5.12E-03	2.8%	6.87E-02	3.2%
Shear Key	**2.74E+01**	**0.3%**	**2.96E+01**	**0.9%**	**3.11E-01**	**0.3%**	**5.73E+01**	**0.5%**

Table 5.6.2-9
TN-LC-NRUX NCT Vehicle Underside Dose Rates (mrem/hr)

Location	Gamma	σ	Neutron	σ	(n,g)	σ	Total	σ
6[1]	3.18E+00	1.3%	1.18E+00	0.3%	5.50E-02	0.5%	4.42E+00	0.9%
7[1]	5.69E+00	0.9%	2.35E+00	0.3%	7.90E-02	0.4%	8.12E+00	0.7%
8	1.04E+01	0.4%	3.35E+00	0.3%	1.16E-01	0.3%	1.39E+01	0.3%
9	1.37E+01	0.3%	2.89E+00	0.2%	1.53E-01	0.3%	1.67E+01	0.2%
10	1.46E+01	0.3%	2.65E+00	0.2%	1.74E-01	0.2%	1.74E+01	0.2%
11	1.49E+01	0.3%	2.60E+00	0.2%	1.84E-01	0.2%	1.77E+01	0.3%
12	1.47E+01	0.3%	2.57E+00	0.2%	1.85E-01	0.2%	1.75E+01	0.2%
13	1.46E+01	0.3%	2.61E+00	0.2%	1.79E-01	0.2%	1.74E+01	0.2%
14	1.42E+01	0.3%	2.74E+00	0.2%	1.63E-01	0.3%	1.71E+01	0.2%
15	1.22E+01	0.3%	2.63E+00	0.3%	1.32E-01	0.3%	1.49E+01	0.2%
16	7.06E+00	0.4%	1.67E+00	0.3%	9.27E-02	0.3%	8.82E+00	0.3%
17	2.29E+00	0.7%	7.42E-01	0.5%	5.43E-02	0.5%	3.08E+00	0.5%
18	6.08E-01	1.5%	3.21E-01	0.7%	2.83E-02	0.6%	9.58E-01	1.0%
19	2.10E-01	3.0%	1.55E-01	1.0%	1.51E-02	0.9%	3.80E-01	1.7%
20	1.01E-01	2.9%	9.67E-02	1.4%	8.59E-03	1.1%	2.06E-01	1.6%
21	6.52E-02	4.3%	6.76E-02	1.6%	5.56E-03	1.4%	1.38E-01	2.2%
22	5.67E-02	11.7%	6.47E-02	1.7%	3.93E-03	1.8%	1.25E-01	5.4%
23①	2.36E-02	20.4%	4.20E-02	1.9%	2.79E-03	2.2%	6.83E-02	7.1%
24①	2.43E-02	3.8%	2.33E-02	2.0%	1.99E-03	2.4%	4.96E-02	2.1%
Shear Key	**1.22E+01**	**0.3%**	**5.71E+00**	**1.0%**	**1.32E-01**	**0.3%**	**1.80E+01**	**0.4%**

Notes:
1. Locations 6, 7, 23, and 24 represent the side of the impact limiters.

Table 5.6.2-10
TN-LC-NRUX NCT Vehicle Side Dose Rates (mrem/hr)

Location	Gamma	σ	Neutron	σ	(n,g)	σ	Total	σ
6	2.32E+00	0.9%	7.55E-01	0.3%	3.18E-02	0.4%	3.11E+00	0.7%
7	4.02E+00	0.6%	1.22E+00	0.3%	5.07E-02	0.4%	5.29E+00	0.5%
8	6.45E+00	0.4%	1.67E+00	0.3%	7.12E-02	0.3%	8.19E+00	0.3%
9	8.37E+00	0.3%	1.81E+00	0.2%	8.93E-02	0.3%	1.03E+01	0.2%
10	9.28E+00	0.3%	1.76E+00	0.2%	1.02E-01	0.3%	1.11E+01	0.2%
11	**9.61E+00**	**0.3%**	**1.72E+00**	**0.2%**	**1.09E-01**	**0.2%**	**1.14E+01**	**0.2%**
12	**9.60E+00**	**0.3%**	**1.70E+00**	**0.2%**	**1.10E-01**	**0.2%**	**1.14E+01**	**0.2%**
13	9.42E+00	0.3%	1.68E+00	0.2%	1.06E-01	0.2%	1.12E+01	0.2%
14	8.76E+00	0.3%	1.63E+00	0.2%	9.56E-02	0.3%	1.05E+01	0.2%
15	7.22E+00	0.3%	1.44E+00	0.3%	8.00E-02	0.3%	8.74E+00	0.2%
16	4.84E+00	0.4%	1.08E+00	0.3%	6.19E-02	0.3%	5.99E+00	0.3%
17	2.49E+00	0.5%	6.83E-01	0.4%	4.34E-02	0.4%	3.22E+00	0.4%
18	1.12E+00	0.8%	3.92E-01	0.5%	2.87E-02	0.5%	1.54E+00	0.6%
19	5.33E-01	1.9%	2.29E-01	0.6%	1.84E-02	0.6%	7.81E-01	1.3%
20	2.70E-01	1.7%	1.47E-01	0.8%	1.19E-02	0.8%	4.29E-01	1.1%
21	1.61E-01	2.6%	1.01E-01	0.9%	7.81E-03	0.9%	2.70E-01	1.6%
22	1.04E-01	2.7%	7.49E-02	1.1%	5.48E-03	1.1%	1.84E-01	1.6%
23	7.92E-02	4.1%	5.78E-02	1.3%	3.78E-03	1.3%	1.41E-01	2.4%
24	6.18E-02	5.5%	4.43E-02	1.2%	2.57E-03	1.4%	1.09E-01	3.2%

Table 5.6.2-11
TN-LC-NRUX NCT 2 m from Vehicle Side Dose Rates (mrem/hr)

Location	Gamma	σ	Neutron	σ	(n,g)	σ	Total	σ
1	2.65E-01	1.2%	9.25E-02	0.4%	5.32E-03	0.6%	3.63E-01	0.9%
2	3.50E-01	1.0%	1.12E-01	0.4%	6.48E-03	0.5%	4.68E-01	0.8%
3	4.84E-01	0.9%	1.40E-01	0.3%	8.00E-03	0.5%	6.32E-01	0.7%
4	6.57E-01	0.7%	1.76E-01	0.3%	9.74E-03	0.4%	8.43E-01	0.5%
5	8.95E-01	0.6%	2.20E-01	0.3%	1.17E-02	0.4%	1.13E+00	0.4%
6	1.22E+00	0.4%	2.69E-01	0.3%	1.38E-02	0.3%	1.50E+00	0.4%
7	1.55E+00	0.4%	3.13E-01	0.3%	1.58E-02	0.4%	1.88E+00	0.3%
8	1.82E+00	0.4%	3.50E-01	0.3%	1.75E-02	0.3%	2.18E+00	0.3%
9	2.06E+00	0.4%	3.78E-01	0.3%	1.88E-02	0.3%	2.45E+00	0.3%
10	2.24E+00	0.3%	4.02E-01	0.3%	1.99E-02	0.3%	2.66E+00	0.3%
11	**2.36E+00**	**0.3%**	**4.13E-01**	**0.3%**	**2.03E-02**	**0.3%**	**2.79E+00**	**0.3%**
12	**2.35E+00**	**0.3%**	**4.13E-01**	**0.3%**	**2.06E-02**	**0.3%**	**2.79E+00**	**0.3%**
13	2.30E+00	0.3%	4.00E-01	0.3%	2.03E-02	0.3%	2.72E+00	0.3%
14	2.13E+00	0.3%	3.77E-01	0.3%	1.95E-02	0.3%	2.53E+00	0.3%
15	1.91E+00	0.3%	3.49E-01	0.3%	1.84E-02	0.3%	2.27E+00	0.3%
16	1.62E+00	0.4%	3.13E-01	0.3%	1.70E-02	0.4%	1.95E+00	0.3%
17	1.34E+00	0.4%	2.76E-01	0.3%	1.54E-02	0.4%	1.63E+00	0.3%
18	1.07E+00	0.4%	2.36E-01	0.3%	1.38E-02	0.4%	1.32E+00	0.4%
19	8.31E-01	0.5%	2.02E-01	0.4%	1.19E-02	0.4%	1.04E+00	0.4%
20	6.36E-01	0.6%	1.69E-01	0.4%	1.05E-02	0.5%	8.15E-01	0.5%
21	4.81E-01	0.7%	1.41E-01	0.4%	9.16E-03	0.5%	6.31E-01	0.5%
22	3.68E-01	0.8%	1.15E-01	0.5%	7.84E-03	0.5%	4.91E-01	0.6%
23	2.83E-01	0.9%	9.61E-02	0.5%	6.58E-03	0.6%	3.86E-01	0.7%
24	2.11E-01	1.0%	7.72E-02	0.5%	5.37E-03	0.6%	2.93E-01	0.7%
25	1.51E-01	1.1%	6.19E-02	0.6%	4.33E-03	0.6%	2.18E-01	0.8%
26	1.16E-01	1.4%	4.89E-02	0.7%	3.44E-03	0.7%	1.69E-01	1.0%
27	8.57E-02	1.3%	3.96E-02	0.7%	2.77E-03	0.8%	1.28E-01	0.9%
28	7.10E-02	2.0%	3.28E-02	0.8%	2.25E-03	0.9%	1.06E-01	1.3%
29	5.75E-02	4.1%	2.77E-02	0.9%	1.82E-03	1.0%	8.70E-02	2.7%

Table 5.6.2-12
TN-LC-NRUX NCT End Dose Rates (mrem/hr)

Location	Gamma	σ	Neutron	σ	(n,g)	σ	Total	σ
Bottom End at Impact Limiter Surface/Vehicle End Surface								
1	**1.77E+00**	**9.3%**	**1.12E-01**	**11.8%**	**3.86E-03**	**26.9%**	**1.88E+00**	**8.7%**
2	8.01E-01	3.8%	1.20E-01	4.5%	3.23E-03	8.4%	9.25E-01	3.3%
3	5.49E-01	3.5%	7.79E-02	3.1%	2.59E-03	6.1%	6.29E-01	3.0%
4	8.54E-02	3.4%	2.56E-02	2.3%	1.80E-03	2.9%	1.13E-01	2.6%
5	4.07E-02	2.7%	2.97E-02	1.1%	1.57E-03	1.6%	7.20E-02	1.6%
6	7.16E-02	1.3%	4.55E-02	0.6%	2.84E-03	0.7%	1.20E-01	0.8%
7	1.19E-01	1.3%	5.82E-02	0.5%	4.10E-03	0.5%	1.81E-01	0.8%
8	1.60E-01	0.8%	6.63E-02	0.4%	4.72E-03	0.5%	2.31E-01	0.6%
Bottom End 2 m from Impact Limiter Surface/Vehicle End Surface								
1,2,3	**1.04E-01**	**4.1%**	**1.09E-02**	**5.7%**	**2.13E-04**	**10.4%**	**1.15E-01**	**3.7%**
4,5	4.01E-02	2.9%	9.52E-03	1.6%	2.83E-04	2.8%	4.99E-02	2.3%
6	3.10E-02	2.1%	1.65E-02	0.8%	6.72E-04	1.1%	4.81E-02	1.4%
7	3.54E-02	1.6%	2.04E-02	0.6%	1.09E-03	0.8%	5.69E-02	1.0%
8	4.45E-02	1.2%	2.36E-02	0.5%	1.48E-03	0.6%	6.96E-02	0.8%
Top End at Impact Limiter Surface/Vehicle End Surface								
1	1.05E+01	8.8%	4.66E+00	2.3%	9.17E-02	5.9%	1.53E+01	6.1%
2	1.03E+01	3.5%	4.15E+00	0.7%	8.32E-02	1.6%	1.46E+01	2.5%
3	8.23E+00	2.0%	3.01E+00	0.5%	7.55E-02	1.1%	1.13E+01	1.5%
4	3.01E+00	1.6%	1.19E+00	0.4%	5.15E-02	0.6%	4.24E+00	1.1%
5	1.55E+00	1.6%	5.31E-01	0.4%	2.43E-02	0.7%	2.11E+00	1.2%
6	1.50E+00	1.0%	4.59E-01	0.3%	2.18E-02	0.4%	1.98E+00	0.8%
7	1.30E+00	0.8%	3.56E-01	0.3%	1.81E-02	0.4%	1.67E+00	0.6%
8	1.12E+00	0.7%	2.75E-01	0.3%	1.44E-02	0.4%	1.40E+00	0.6%
Port	**3.07E+01**	**5.2%**	**4.40E+00**	**4.3%**	**7.46E-02**	**10.4%**	**3.52E+01**	**4.5%**
Top End 2 m from Impact Limiter Surface/Vehicle End Surface								
1,2,3	**9.83E-01**	**7.6%**	**2.25E-01**	**1.1%**	**4.16E-03**	**2.8%**	**1.21E+00**	**6.2%**
4,5	6.26E-01	1.7%	1.83E-01	0.5%	3.92E-03	1.0%	8.14E-01	1.3%
6	3.70E-01	1.7%	1.30E-01	0.4%	4.02E-03	0.8%	5.05E-01	1.2%
7	2.50E-01	1.4%	1.01E-01	0.4%	4.40E-03	0.6%	3.55E-01	1.0%
8	2.27E-01	1.2%	8.72E-02	0.3%	4.70E-03	0.5%	3.19E-01	0.9%

Table 5.6.2-13
TN-LC-NRUX HAC Dose Rates (mrem/hr)

Location	Gamma	σ	Neutron	σ	(n,g)	σ	Total	σ
Side								
1	3.10E+00	1.4%	2.61E+00	0.2%	3.51E-03	1.3%	5.71E+00	0.7%
2	6.05E+00	1.6%	3.66E+00	0.2%	4.78E-03	1.1%	9.71E+00	1.0%
3	1.09E+01	1.2%	5.23E+00	0.2%	6.61E-03	0.8%	1.62E+01	0.8%
4	1.52E+01	1.2%	7.56E+00	0.1%	9.19E-03	0.7%	2.28E+01	0.8%
5	1.79E+01	1.2%	1.07E+01	0.1%	1.25E-02	0.6%	2.86E+01	0.8%
6	1.68E+01	0.8%	1.39E+01	0.1%	1.54E-02	0.5%	3.08E+01	0.4%
7	1.84E+01	0.3%	1.68E+01	0.1%	1.82E-02	0.4%	3.52E+01	0.2%
8	1.88E+01	0.3%	1.88E+01	0.1%	2.00E-02	0.4%	3.77E+01	0.2%
9	1.88E+01	0.3%	1.98E+01	0.1%	2.08E-02	0.4%	3.86E+01	0.1%
10	**1.88E+01**	**0.3%**	**1.99E+01**	**0.1%**	**2.08E-02**	**0.4%**	**3.87E+01**	**0.1%**
11	1.81E+01	0.3%	1.90E+01	0.1%	2.02E-02	0.4%	3.72E+01	0.1%
12	1.67E+01	0.3%	1.73E+01	0.1%	1.87E-02	0.4%	3.40E+01	0.1%
13	1.40E+01	0.3%	1.47E+01	0.1%	1.60E-02	0.5%	2.87E+01	0.2%
14	9.91E+00	0.4%	1.18E+01	0.1%	1.31E-02	0.5%	2.17E+01	0.2%
15	5.97E+00	0.8%	8.83E+00	0.1%	1.00E-02	0.6%	1.48E+01	0.3%
16	3.13E+00	0.7%	6.31E+00	0.1%	7.43E-03	0.8%	9.45E+00	0.2%
17	1.66E+00	0.9%	4.40E+00	0.2%	5.38E-03	1.0%	6.06E+00	0.3%
18	9.47E-01	1.2%	3.04E+00	0.2%	3.95E-03	1.2%	3.99E+00	0.3%
19	5.82E-01	1.7%	2.14E+00	0.3%	2.76E-03	1.5%	2.73E+00	0.4%
20	3.97E-01	2.3%	1.54E+00	0.3%	2.04E-03	1.9%	1.93E+00	0.5%
21	2.87E-01	3.0%	1.12E+00	0.4%	1.62E-03	2.2%	1.41E+00	0.7%
22	2.22E-01	3.8%	8.37E-01	0.5%	1.14E-03	2.8%	1.06E+00	0.9%
23	1.54E-01	4.6%	6.40E-01	0.6%	9.14E-04	3.2%	7.95E-01	1.0%
24	1.53E-01	5.4%	4.97E-01	0.7%	6.97E-04	3.9%	6.51E-01	1.4%
25	1.31E-01	8.5%	4.07E-01	0.8%	5.56E-04	4.5%	5.38E-01	2.2%
Bottom End								
1[1]	**1.02E+00**	**52.9%**	**1.36E-01**	**1.8%**	**1.95E-04**	**10.4%**	**1.15E+00**	**46.6%**
2[1]	1.98E-01	24.8%	1.57E-01	0.9%	1.89E-04	5.3%	3.56E-01	13.8%
3	1.01E-01	13.2%	2.66E-01	0.5%	3.55E-04	2.6%	3.68E-01	3.6%
Top End								
1	**4.92E+00**	**5.5%**	**2.43E+00**	**0.4%**	**3.52E-03**	**2.3%**	**7.35E+00**	**3.7%**
2	3.21E+00	1.6%	2.17E+00	0.2%	3.16E-03	1.3%	5.39E+00	0.9%
3	2.33E+00	1.4%	2.14E+00	0.2%	2.96E-03	1.0%	4.47E+00	0.7%

Notes:
1. The uncertainty is higher than 10 percent, but the dose rate is sufficiently far from the limit that it is acceptable.

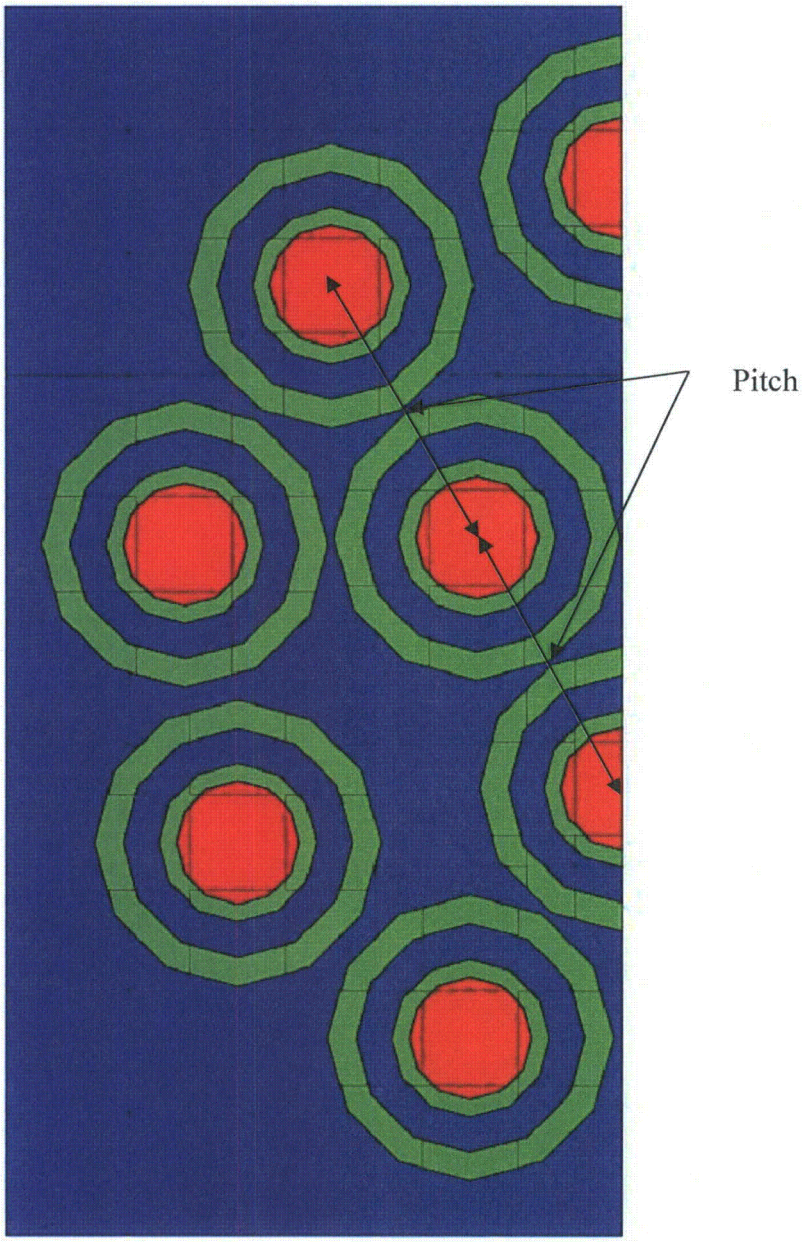

Figure 5.6.2-1
TRITON NRU Element Model

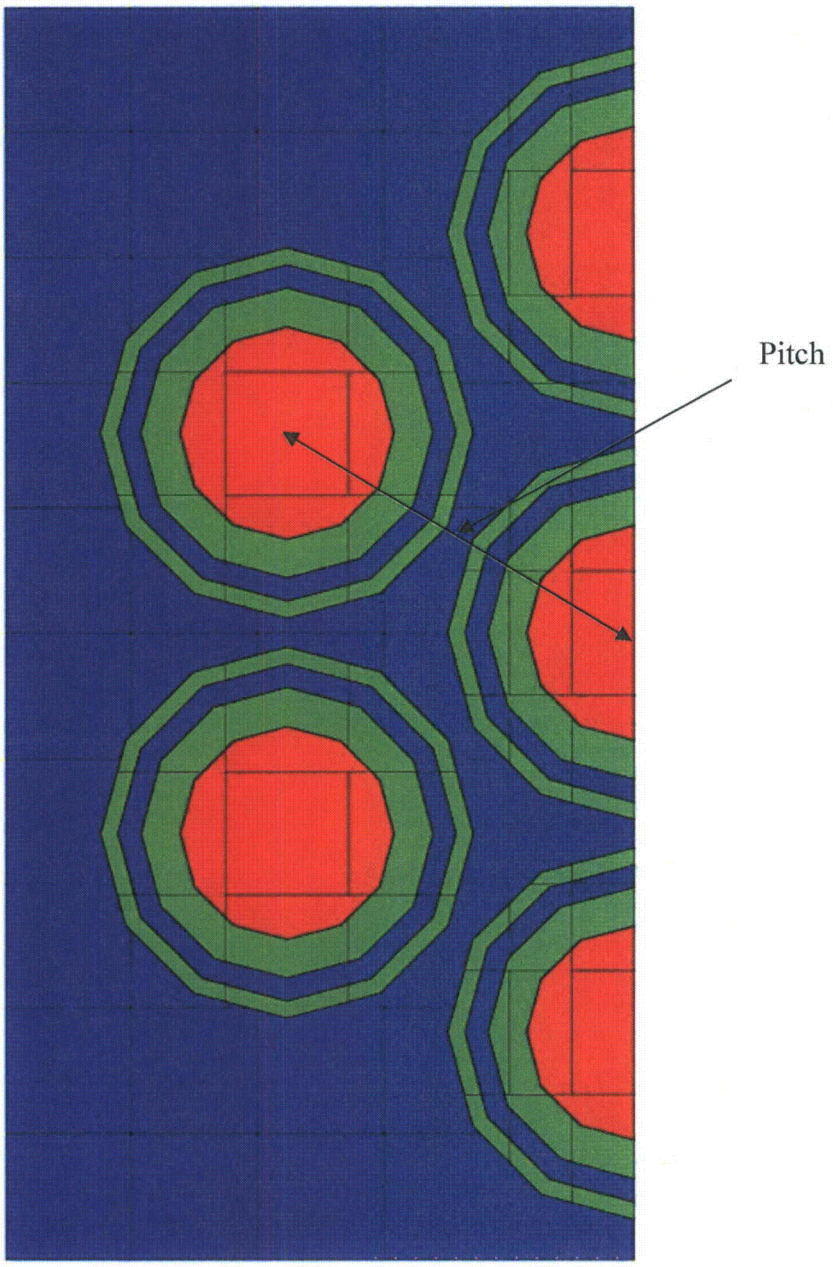

Figure 5.6.2-2
TRITON NRX Element Model

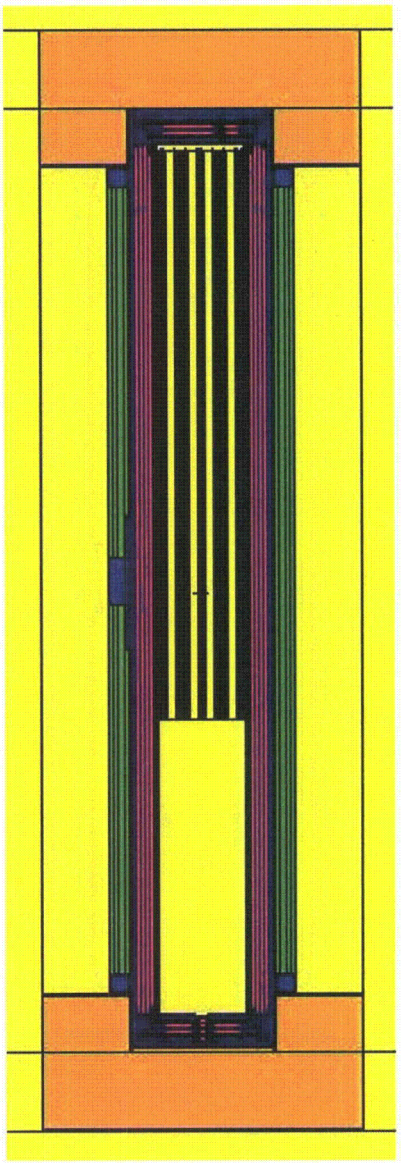

Figure 5.6.2-3
TN-LC-NRUX MCNP Model, y-z View

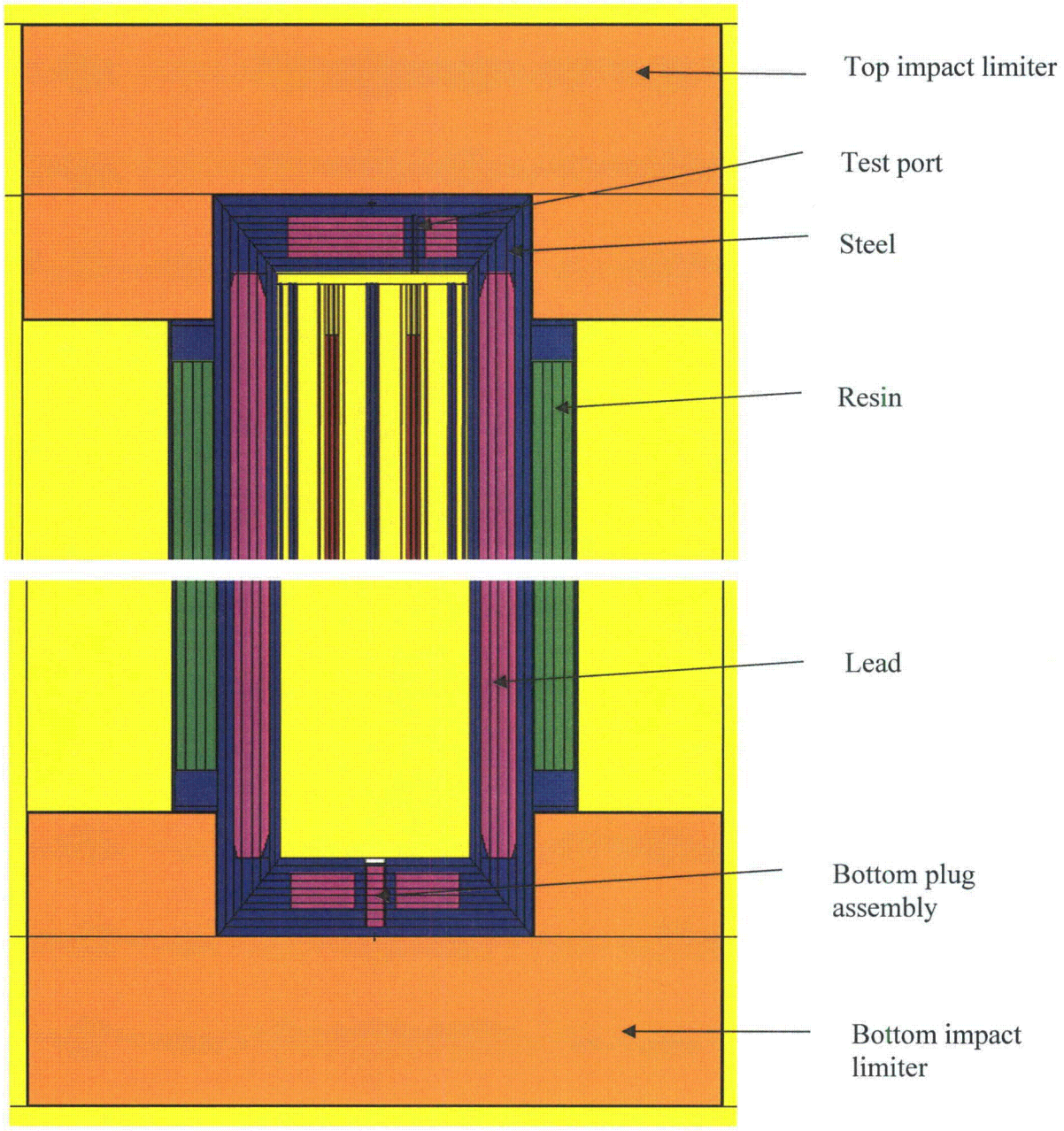

Figure 5.6.2-4
TN-LC-NRUX MCNP Model, Close-Up y-z View

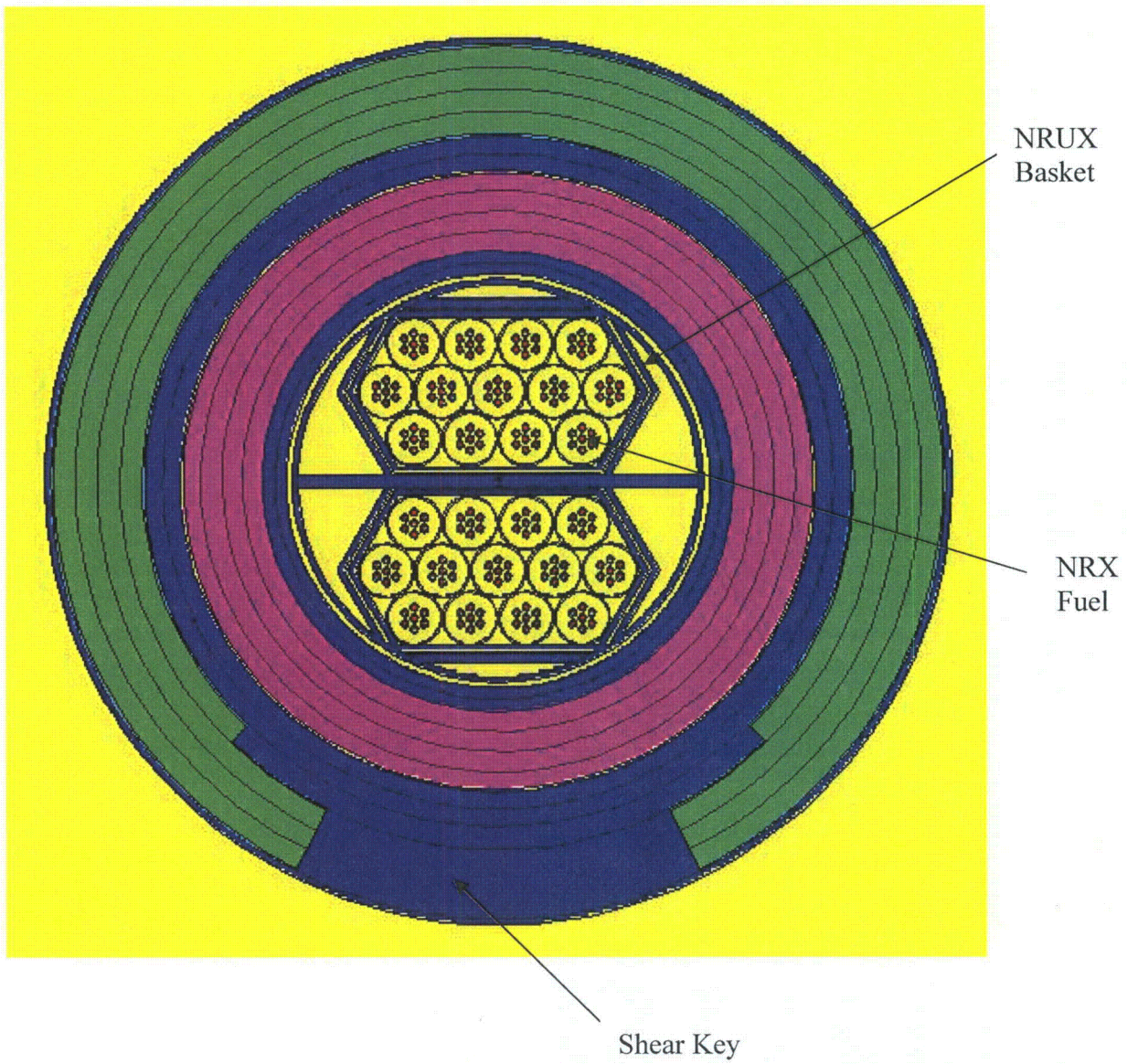

Figure 5.6.2-5
TN-LC-NRUX MCNP Model, x-y View through Shear Key

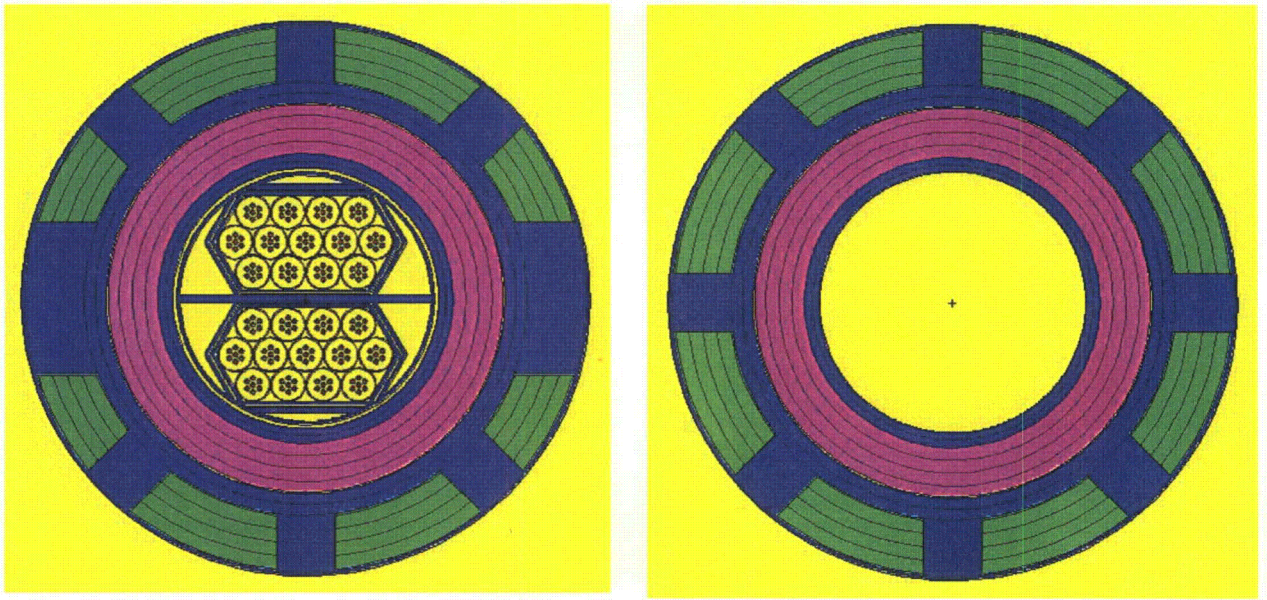

Top of Cask

Bottom of Cask

Figure 5.6.2-6
TN-LC-NRUX MCNP Model, x-y View through Impact Limiter Attachment Blocks

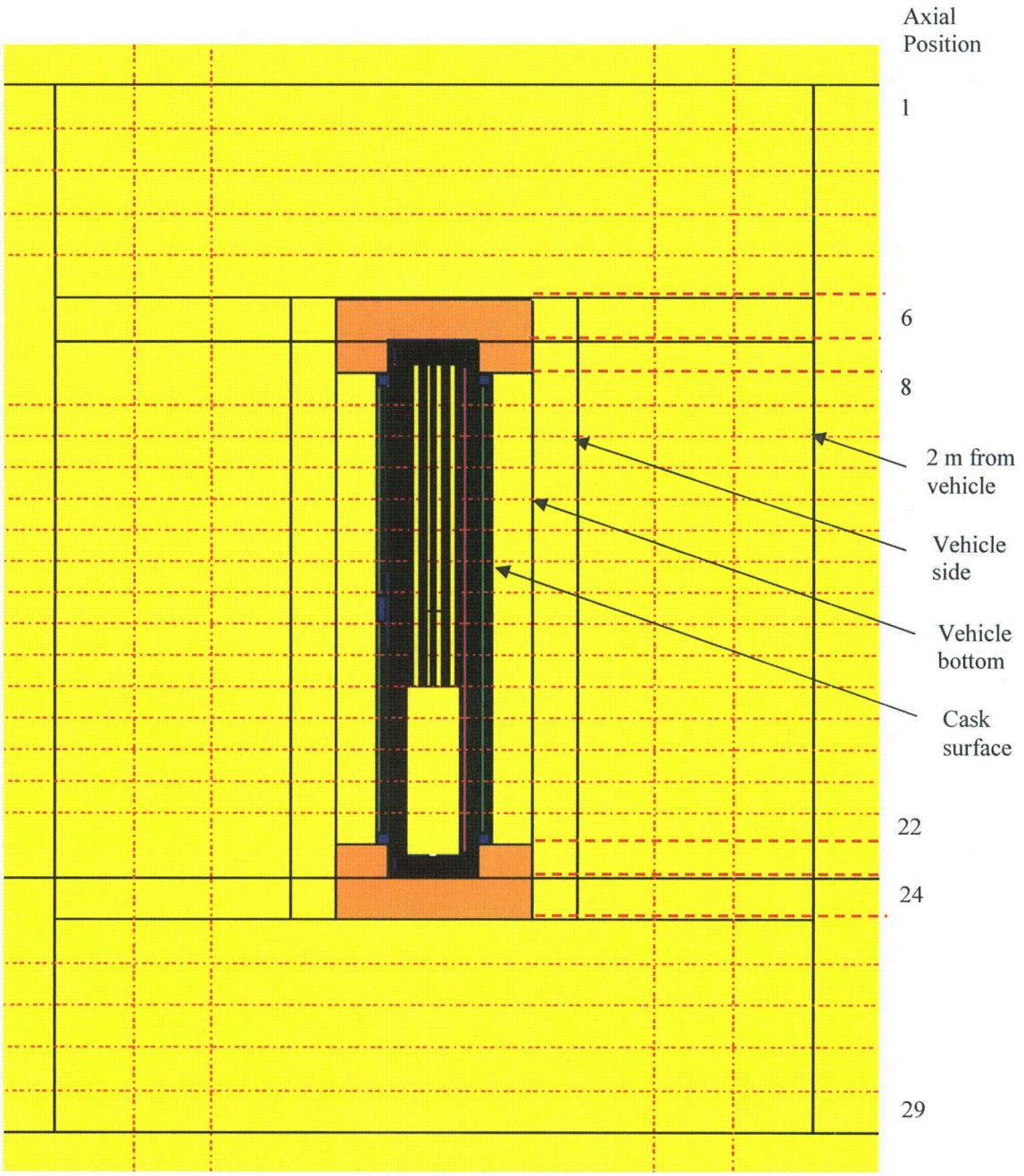

Figure 5.6.2-7
TN-LC-NRUX NCT Radial Surface Tallies

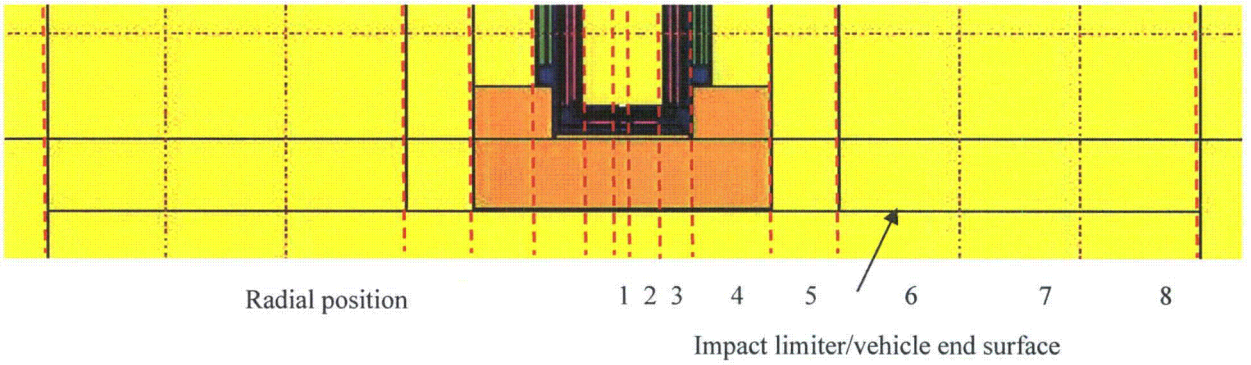

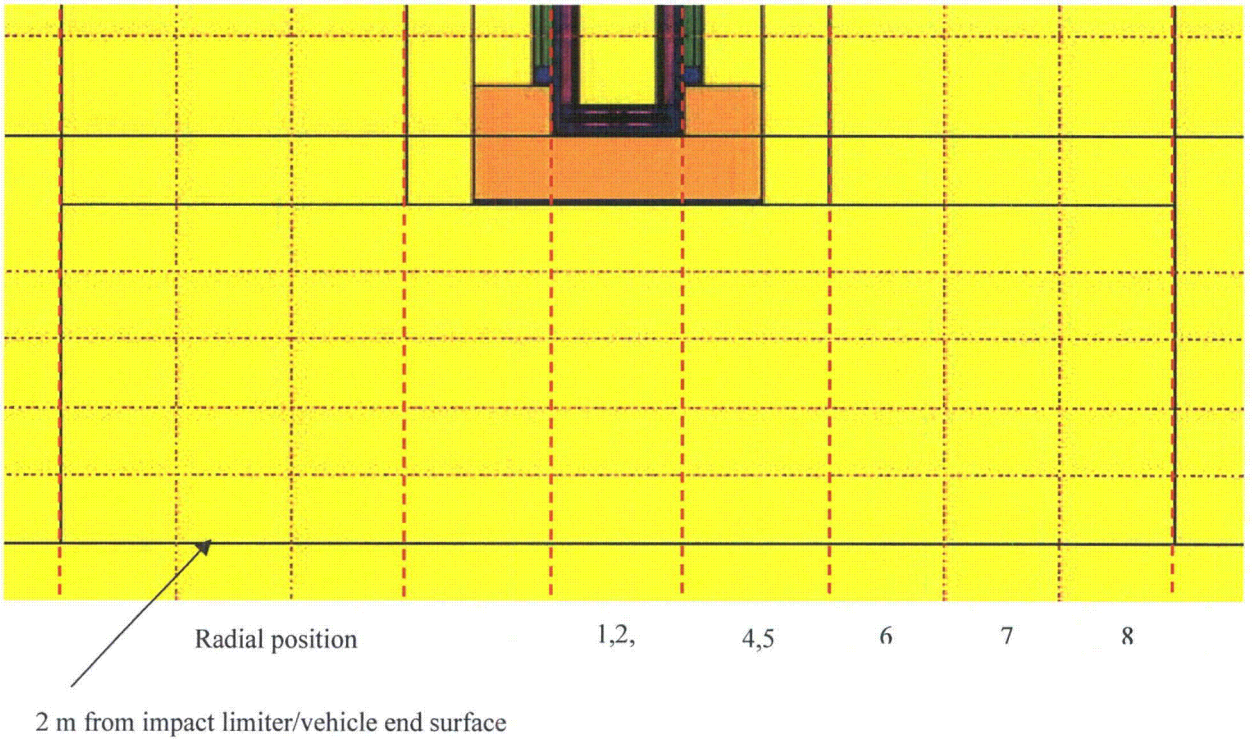

Figure 5.6.2-8
TN-LC-NRUX NCT End Surface Tallies

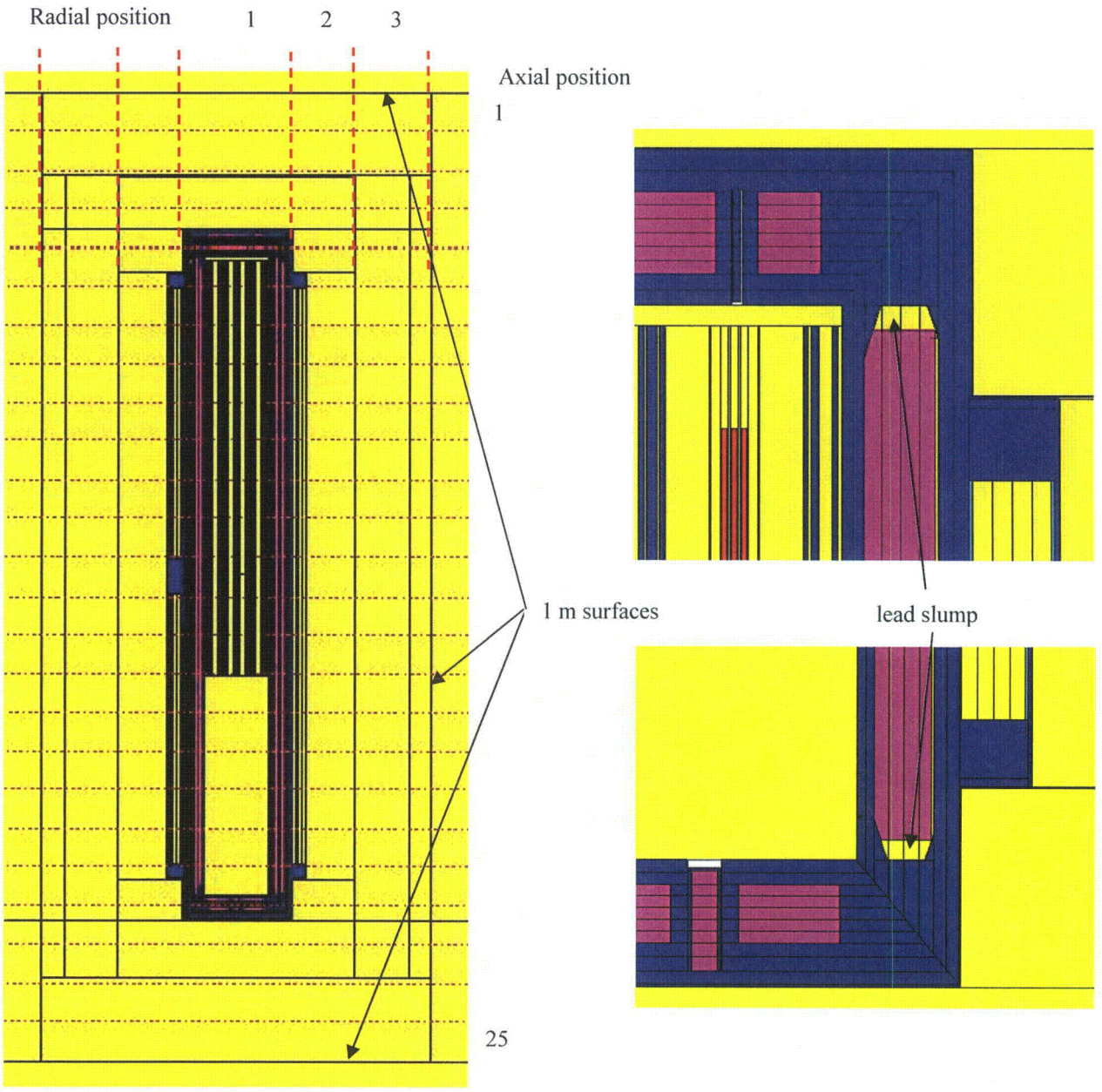

Figure 5.6.2-9
TN-LC-NRUX HAC 1 m Tallies

Appendix 5.6.3
TN-LC-TRIGA Basket Shielding Evaluation

TABLE OF CONTENTS

Proprietary Information Withheld Pursuant to 10 CFR 2.390.

LIST OF TABLES

LIST OF FIGURES

Appendix 5.6.3
TN-LC-TRIGA Basket Shielding Evaluation

NOTE: References in this Appendix are shown as [1], [2], etc. and refer to the reference list in Section 5.6.3.5.1.

This Appendix presents the shielding evaluation of the TN-LC transportation package containing the TN-LC-TRIGA basket. The MCNP computer program [1] is used to calculate the dose rates using a detailed three-dimensional model. The dose rates are evaluated per the requirements of 10CFR71.47 and 71.51 for exclusive use transportation in a closed transport vehicle.

5.6.3.1 Description of the Shielding Design

5.6.3.1.1 Design Features

The shielding design of the cask is described in Section 5.1.1.

Proprietary Information Withheld Pursuant to 10 CFR 2.390.

5.6.3.1.2 Summary Tables of Maximum Radiation Levels

Normal conditions of transport (NCT) dose rates are computed for exclusive use transport in a closed transport vehicle. These dose rate limits are as follows:

- Surface of the package: 1000 mrem/hr
- Surface of the transport vehicle: 200 mrem/hr
- 2 m from the surface of the transport vehicle: 10 mrem/hr

The transport vehicle is assumed to be 8 ft wide. Because the TN-LC is a long package, the ends of the transport vehicle are conservatively assumed to be at the ends of the impact limiters. The underside (floor) of the vehicle is conservatively assumed to correspond to the radius of the impact limiters. The dose rates on the vehicle roof are not computed as these dose rates are bounded by the dose rates on the underside of the vehicle. Dose rates are also computed 2 m from the sides and ends of the vehicle. The NCT dose rates for the TN-LC-TRIGA basket payload are summarized in Table 5.6.3-1.

The maximum package surface dose rate of 95.8 mrem/hr occurs on the side of the package. This dose rate is less than the limit of 1000 mrem/hr on the package surface in a closed transport vehicle.

The maximum vehicle surface dose rate of 49.8 mrem/hr occurs at the top end of the vehicle (which also corresponds to the top surface of the impact limiter). This dose rate occurs over the port in the lid and is less than the limit of 200 mrem/hr on the vehicle surface. The maximum dose rate 2 m from the vehicle surface of 8.27 mrem/hr occurs at the side of the vehicle. This dose rate is less than the limit of 10 mrem/hr at 2 m from the vehicle surface.

Per 10CFR71.47(b)(4), dose rate limits in any normally occupied space do not apply if the carrier is private and exposed personnel wear dosimetry devices. If it is assumed that the normally occupied space is 2 m from the ends of the vehicle, then the dose rate limit of 2 mrem/hr is exceeded. Therefore, personnel in any normally occupied space shall wear dosimetry devices.

Hypothetical accident condition (HAC) dose rates are computed. Under HAC, it is conservatively assumed that both the neutron shield and impact limiter wood are replaced with air, and 1.2 in. of lead slump is modeled at both the top and bottom ends. Dose rates are computed 1 m from the surface of the cask body. The HAC dose rates for the TN-LC-TRIGA basket are summarized in Table 5.6.3-2. The maximum dose rate of 79.8 mrem/hr occurs at the side of the package, which is well below the limit of 1000 mrem/hr.

5.6.3.2 Source Specification

5.6.3.2.1 Gamma Source

The gamma source for TRIGA fuel is computed by the TRITON module of the SCALE6 code package [2]. TRITON allows for a two-dimensional representation of the fuel assemblies. Because the input is two dimensional, all input is for a basis of 1 metric ton of uranium (MTU). All TRITON output is also per 1 MTU, so the results must be scaled by the MTU of the fuel assembly.

Proprietary Information Withheld Pursuant to 10 CFR 2.390.

A summary of the data used to develop the TRITON models is presented in Table 5.6.3-3. Given the H/Zr atom ratio, maximum uranium mass in the U-ZrH fuel matrix, and mass of U-235 and U-238, the mass of hydrogen and zirconium may be computed for each fuel type. These masses and the known fuel volumes are then used to compute number densities for input to TRITON.

Proprietary Information Withheld Pursuant to 10 CFR 2.390.

The cooling times needed to meet dose rate limits for the maximum burnup values are long. Therefore, TRITON models for intermediate burnup values are also developed. These burnup values correspond to 1/4, 1/2, and 3/4 of the maximum burnup values, for a total of four TRITON models for each fuel type. The lower burnups are achieved by reducing the irradiation time.

The TRITON model for ACPR fuel is shown in Figure 5.6.3-1. A separate TRITON model is not developed for each TRIGA fuel type listed in Table 5.6.3-3.

Proprietary Information Withheld Pursuant to 10 CFR 2.390.

Proprietary Information Withheld Pursuant to 10 CFR 2.390.

Proprietary Information Withheld Pursuant to 10 CFR 2.390. Cobalt is present in stainless steel at 0.8 g/kg (800 ppm). Therefore, the cobalt density in steel is 0.8/1000*7.94 = 6.352E-03 g/cm^3. The stainless steel portion is then input as 7.94 – 6.352E-03 = 7.9336 g/cm^3 to give the standard SCALE stainless steel density.

From these source terms, a bounding NCT source term is selected for detailed dose rate calculations. Selecting the bounding NCT source term involves the following methodology:

1. Run TRITON for the desired TRIGA fuel type and burnup. Save the TRITON "F71" output file.

2. The limiting dose rate for transportation is usually the dose rate at a distance of 2 m from the side of the vehicle, which has a limit of 10 mrem/hr. Therefore, the total (i.e., gamma and neutron) dose rate at this location for each of the source terms is computed. To allow sufficient margin, a dose rate of approximately 8.2 mrem/hr is targeted. The source term is determined using trial and error by using the TRITON "F71" output file as an input to an ORIGEN-S decay calculation and adjusting the cooling times as-needed.

Proprietary Information Withheld Pursuant to 10 CFR 2.390. A sample TRITON input file and ORIGEN-S restart file are provided in Section 5.6.3.5.2.

The decay times to meet dose rate limits, the decay heat, as well as the NCT dose rate value used to select the bounding source, are provided in Table 5.6.3-4. Based on these results, the bounding source term for NCT dose rate calculations is for ACPR fuel at the maximum burnup and a decay time of 1870 days. The design basis gamma source term is provided in Table 5.6.3-5.

The dose rate calculations in Step 2 are performed using a response function developed by MCNP. A relatively detailed MCNP model of the TRIGA fuel, basket, and TN-LC package is developed. This model is very similar to the final MCNP model of the package. The only dose rate location in the response function model is the dose rate 2 m from the surface of the vehicle.

Proprietary Information Withheld Pursuant to 10 CFR 2.390.

The NCT gamma response functions are provided in Table 5.6.3-6. The NCT neutron response function is developed in a similar manner and is discussed in Section 5.6.3.2.2.

Proprietary Information Withheld Pursuant to 10 CFR 2.390.

In general, the bounding source term may be different for NCT and HAC analysis. For HAC, it is assumed that the neutron shield resin and impact limiter wood is replaced with air. Therefore, sources with a large neutron source may become bounding because the neutron dose rate will increase greater than the gamma dose rate when the neutron shield is lost. However, the neutron dose rates for TRIGA fuel are a small fraction of the total dose rate (<4 percent), and the HAC dose rates will be approximately the same for any of the NCT source terms. Therefore, the NCT source term is also used in the HAC dose rate calculations.

5.6.3.2.2 Neutron Source

The neutron source is generated using the same TRITON models from which the gamma source is generated. The neutron source is primarily from spontaneous fission because there are few (α,n) target nuclei in the fuel matrix.

Proprietary Information Withheld Pursuant to 10 CFR 2.390.

The neutron NCT response function is provided in Table 5.6.3-8. The neutron source is provided in Table 5.6.3-9. The neutron source is for ACPR fuel at maximum burnup.

5.6.3.2.3 Fuel Qualification

The information in Table 5.6.3-4 is used to determine the minimum cooling time required for the fuel based on the fuel burnup. Fuel is limited to the fuel types listed in the table. The fuel types imply the enrichments and maximum uranium loadings given in Table 5.6.3-3. The cooling times in Table 5.6.3-4 are plotted in Figure 5.6.3-2. Because only a limited number of burnup points are investigated, burnups may be either rounded up to the next higher burnup in Table 5.6.3-4, or linear interpolation may be used in conjunction with Table 5.6.3-17 to determine the minimum cooling time. Although the plots are reasonably linear, to ensure a conservative cooling time, add an additional 30 days to the linearly interpolated value. If the burnup is less than the minimum value shown in Table 5.6.3-4, use the cooling time listed for the minimum burnup. Fuel with a burnup that exceeds the maximum values listed in Table 5.6.3-4 cannot be shipped.

Examples are provided to illustrate the method.

Example 1: An ACPR fuel assembly has a burnup of 75,000 MWD/MTU. The minimum cooling time based on linear interpolation is 1003 days plus an additional 30 days, or 1033 days.

Example 2: A standard stainless steel clad fuel assembly has a burnup of 10,000 MWD/MTU. The minimum cooling time is 520 days, based on the lowest burnup listed for this fuel type in Table 5.6.3-4.

5.6.3.3 Shielding Model

5.6.3.3.1 Configuration of Source and Shielding

The fuel, basket, and packaging are modeled explicitly in the MCNP computer program. The cask model is described in Section 5.3.1.

Proprietary Information Withheld Pursuant to 10 CFR 2.390.

The sources used in the models are summarized in Table 5.6.3-5, Table 5.6.3-7, and Table 5.6.3-9.

Proprietary Information Withheld Pursuant to 10 CFR 2.390.

Important dimensions of the TN-LC-TRIGA basket model are summarized in Table 5.6.3-10. An example of the overall model geometry with the TN-LC-TRIGA basket is shown in Figure 5.6.3-3 through Figure 5.6.3-7. The overall model geometry is illustrated in Figure 5.6.3-3. A close-up view of the model ends is illustrated in Figure 5.6.3-4. A view perpendicular to the cask axis is illustrated in Figure 5.6.3-5. The model geometry of the fuel assembly is illustrated in Figure 5.6.3-6. A view through the impact limiter attachment blocks is illustrated in Figure 5.6.3-7.

Proprietary Information Withheld Pursuant to 10 CFR 2.390.

Under hypothetical accident conditions (HAC), the impact limiter wood and neutron shield resin are replaced with air. This bounds any postulated fire or crush damage. In addition, 1.2 in. of lead slump is modeled at both the top and bottom ends of the cask as a result of an end drop. This bounds the maximum lead slump value of 1.129 in. from Appendix 2.13.3. The radial lead slump at the cask ends due to a side drop is negligible (<0.2 in.) and has been neglected. HAC dose rates are conservatively computed 1 m from the cask body surface.

5.6.3.3.2 Material properties

Material properties for the cask and basket structural materials are provided in Section 5.3.2.

Proprietary Information Withheld Pursuant to 10 CFR 2.390.

The fuel meat number densities for TRIGA fuel are provided in Table 5.6.3-3.

Proprietary Information Withheld Pursuant to 10 CFR 2.390.

5.6.3.4 Shielding Evaluation

5.6.3.4.1 Methods

MCNP5 v1.40 is used for the shielding analysis [1]. MCNP5 is a standard, well-accepted shielding program utilized to compute dose rates for shielding licenses. A three-dimensional model is developed that captures all of the relevant design parameters of the cask and internals. Dose rates are calculated by tallying the neutron and gamma fluxes over surfaces of interest and converting these fluxes to dose rates using flux-to-dose rate conversion factors. Secondary gammas resulting from neutron capture are also tallied. Subcritical neutron multiplication is also performed by the program.

Separate models are developed for neutron and gamma source terms. Simple Russian roulette is used as a variance reduction technique for most tallies. The importance of the particles increases as the particles traverse the shielding materials. When necessary, DXTRAN spheres are used to accelerate program convergence above the lid port or below the bottom plug assembly.

5.6.3.4.2 Input and Output Data

A number of input/output cases are used to generate the results, as listed below. A sample input file is provided in Section 5.6.3.5.3.

Convergence is good (<10 percent) for all total dose rates of interest. Separate gamma models are developed to compute the dose rate on the impact limiter surface over the lid port and bottom plug assembly.

5.6.3.4.3 Flux-to-Dose-Rate Conversion

The flux-to-dose rate conversion factors are provided in Section 5.4.3.

5.6.3.4.4 External Radiation Levels

Tally locations are selected to be consistent with exclusive use transportation in a closed transport vehicle. Therefore, the applicable NCT dose rate limits from 10CFR71.47(b) (1), (2) and (3) are:

- 1000 mrem/hr on the package surface. This includes the surface of the cask between the impact limiters, and the impact limiter surfaces.
- 200 mrem/hr on the vehicle surface. The vehicle has six surfaces (2 sides, 2 ends, roof, and underside). The two sides of the vehicle are assumed to be 8 ft apart with the package in the center. The underside (floor) of the vehicle is conservatively assumed to be at the impact limiter radius, and the dose rates at the underside of the vehicle bound the dose rates at the roof of the vehicle, which is farther away from the package. The ends of the vehicle are conservatively assumed to be at the impact limiter end surfaces.
- 10 mrem/hr 2 m from the vehicle surface. This dose rate does not apply 2 m from the roof of the vehicle or 2 m from the underside of the vehicle.

Circumferential tallies are placed around the packaging. Twenty-nine (29) axial locations are utilized, as illustrated in Figure 5.6.3-8. Locations 8 through 22 correspond to the side of the cask between the impact limiters, Locations 6 though 24 correspond to the side of the package at the impact limiter radius (underside of vehicle) and the side of the vehicle, and Locations 1 through 29 are utilized 2 m from the side of the vehicle.

At the ends of the packaging, dose rates are tallied on the impact limiter surfaces and 2 m from the impact limiter surfaces. Eight radial locations are utilized for the surface tallies, as illustrated in Figure 5.6.3-9. Location 1 captures any streaming effects from the bottom plug assembly. An off-center tally is used directly over the lid port to capture any streaming effects on the top impact limiter surface. For the dose rates 2 m from the ends, five radial locations are utilized by combining Locations 1,2,3 and 4,5 as shown in Figure 5.6.3-9. Any streaming effects are generally negligible 2 m from the ends and are not investigated for the TN-LC-TRIGA basket. Because the bounding end dose rates are for the 1FA basket, the end streaming effects at 2 m are examined in more detail in the 1FA shielding calculation (see Appendix 5.6.4).

Because the basket design is not circumferentially symmetric, the dose rate will vary around the perimeter of the package. This effect is most pronounced close to the package surface, and diminishes with distance. Close to the surface of the package, this variation is less than 15 percent from the average. At 2 m from the surface of the vehicle, this variation is negligible (~5 percent). Because the radial dose rates are significantly below the dose rate limits, a detailed tally to capture these angular effects is not warranted. Therefore, circumferential average tallies are reported in the radial direction for most dose rate locations.

However, because the impact limiter attachments and the shear key penetrate the neutron shield and displace neutron shielding material, there will be neutron streaming at these locations. This effect is captured explicitly using angular mesh tallies. The axial heights of the mesh are chosen to correspond to the heights of the regions of interest. The mesh is 1 cm thick, and consists of 18 angular regions (20° each). For the case of TRIGA fuel, which has a very low neutron source, this streaming effect may be quantified, although it has little effect on the total dose rates.

The shear key faces downward and results in a higher than average neutron dose rate on the surface of the package and the underside of the vehicle. The shear key and impact limiter attachments do not result in gamma streaming because neutron shielding material is replaced with steel, which is a superior gamma shield. For this reason, these features are conservatively ignored in the gamma models, and neutron mesh tally results for the shear key are added to the average gamma results at axial Location 15. Because the neutron dose rate is low at the shear key, an equivalent result is not provided for the impact limiter attachments. The mesh tally is used only at the cask surface and vehicle underside/impact limiter radius because any streaming effects will be essentially washed out beyond this distance and also because it is not required to calculate dose rates 2 m from the underside of the vehicle. The reported dose rates 2 m from the side of the vehicle are circumferential tallies and, hence, include the contribution due to neutron streaming through the shear key.

Dose rate models are developed for Configuration 1 (long spacer) and Configuration 2 (short spacer). The maximum dose rates are essentially the same in the radial direction for both Configurations 1 and 2. Therefore, all radial dose rates are reported for Configuration 1 only.

Dose rates at the top end are reported for Configuration 1 only, and dose rates at the bottom end are reported for Configuration 2 only.

Package surface: The NCT side surface dose rates are presented in Table 5.6.3-11. Dose rates on the side surfaces of the impact limiters are presented in Table 5.6.3-12 at axial locations 6, 7, 23, and 24. Dose rates on the external flat surfaces of the impact limiters are presented in Table 5.6.3-15. The maximum package surface dose rate occurs on the side of the cask with a dose rate of 95.8 mrem/hr. This dose rate is less than the limit of 1000 mrem/hr.

The gamma dose rate for the top vent on the top impact limiter surface is computed in a separate file using a DXTRAN sphere to assist in tally convergence. Likewise, the bottom center dose rate on the bottom impact limiter surface is also computed in a separate file using a DXTRAN sphere to assist in tally convergence.

Vehicle surface: The NCT vehicle underside/impact limiter radius dose rates are presented in Table 5.6.3-12. The maximum dose rate on the vehicle underside occurs at axial Location 14 with a dose rate of 42.0 mrem/hr. The NCT vehicle side surface dose rates are presented in Table 5.6.3-13. The maximum dose rate on the vehicle side occurs at axial Location 14 with a value of 26.9 mrem/hr. NCT vehicle end dose rates are presented in Table 5.6.3-15. The maximum vehicle surface dose rate occurs on the impact limiter surface over the port. This dose rate is 49.8 mrem/hr, which bounds the vehicle surface dose rates on the underside, side, and bottom ends. This dose rate is less than the limit of 200 mrem/hr.

2 m from vehicle surface: The NCT dose rates 2 m from the side surface of the vehicle are presented in Table 5.6.3-14. The maximum dose rate of 8.27 mrem/hr occurs at axial Location 14. This dose rate is less than the limit of 10 mrem/hr and bounds the dose rates 2 m from the ends of the vehicle presented in Table 5.6.3-15.

HAC: The applicable HAC dose rate limit from 10CFR71.51(a)(2) is 1000 mrem/hr 1 m from the package surface.

In the HAC models, the neutron shield resin and impact limiter wood are replaced with air, and 1.2 in. of lead slump is modeled at both the top and bottom ends. The tally surfaces are located 1 m from the outer surfaces of the cask. The dose rates at the ends of the package are divided into three segments, and the dose rates at the side of the package are divided in 25 segments of equal width. The tally locations are shown on Figure 5.6.3-10. HAC dose rate results are presented in Table 5.6.3-16. The maximum HAC dose rate of 79.8 mrem/hr occurs 1 m from the side of the package near the lead slump region. This dose rate is significantly less than the limit of 1000 mrem/hr. The HAC calculations are performed only for Configuration 1 because the HAC dose rates are a maximum in the radial direction, and the dose rates are far from the limit.

5.6.3.5 Appendices

5.6.3.5.1 References

1. MCNP5, "MCNP – A General Monte Carlo N-Particle Transport Code, Version 5; Volume II: User's Guide," LA-CP-03-0245, Los Alamos National Laboratory, April 2003
2. SCALE: A Modular Code System for Performing Standardized Computer Analyses for Licensing Evaluations, ORNL/TM-2005/39, Version 6, Vols. I-III, January 2009
3. JW Sterbentz, Radionuclide Mass Inventory, Activity, Decay Heat, and Dose Rate Parametric Data for TRIGA Spent Nuclear Fuels, INEL-96/0482, Idaho National Engineering Laboratory, March 1997.

5.6.3.5.2 **Proprietary Information Withheld Pursuant to 10 CFR 2.390.**

Proprietary Information Withheld Pursuant to 10 CFR 2.390.

Proprietary Information on Pages 5.6.3-13 through 5.6.3-27
Withheld Pursuant to 10 CFR 2.390.

Table 5.6.3-1
Summary of TN-LC-TRIGA NCT Dose Rates

(Exclusive Use Package for Transportation)

Package Surface (mrem/hr), Limit = 1000 mrem/hr				
	Top End	**Side**	**Bottom End**	
Gamma	49.7	95.6	3.90	
Neutron	7.73E-02	0.182	4.36E-02	
(n,g)	1.93E-03	1.28E-02	1.78E-03	
Total	49.8	95.8	3.94	
Vehicle Surface (mrem/hr), Limit = 200 mrem/hr				
	Top End	**Side**	**Bottom End**	**Underside**
Gamma	49.7	26.8	3.90	42.0
Neutron	7.73E-02	4.64E-02	4.36E-02	7.47E-02
(n,g)	1.93E-03	3.38E-03	1.78E-03	5.29E-03
Total	49.8	26.9	3.94	42.0
2 m from Vehicle Surface (mrem/hr), Limit = 10 mrem/hr				
	Top End	**Side**	**Bottom End**	
Gamma	2.63	8.25	0.415	
Neutron	4.26E-03	1.25E-02	1.69E-03	
(n,g)	1.06E-04	8.28E-04	1.37E-04	
Total	2.63	8.27	0.417	

Table 5.6.3-2
Summary of TN-LC-TRIGA HAC Dose Rates

	1 m from Package Surface (mrem/hr), Limit = 1000 mrem/hr		
	Top End	**Side**	**Bottom End**
Gamma	12.9	79.6	0.512
Neutron	4.65E-02	0.166	1.04E-02
(n,g)	1.61E-04	6.01E-04	2.94E-05
Total	13.0	79.8	0.523

Table 5.6.3-3
TRIGA Fuel Data

(Part 1 of 2)

Proprietary Information Withheld Pursuant to 10 CFR 2.390.

Table 5.6.3-3
TRIGA Fuel Data
(Part 2 of 2)

Proprietary Information Withheld Pursuant to 10 CFR 2.390.

Table 5.6.3-4
TRIGA Fuel Qualification

Type	Burnup (MWD/MTU)	Decay Time (days)	Decay Heat (watts)	NCT Response Function Dose Rate (mrem/hr)[1]
ACPR	35,750	650	1.91	8.12
	71,500	970	1.91	8.15
	107,250	1310	1.90	8.15
	143,000	1870	1.88	**8.20**
AL14, AL15	35,750	400	2.48	8.05
	71,500	560	2.58	8.08
	107,250	640	2.88	8.06
	143,000	710	3.21	8.07
ST1, ST2, ST3	35,750	520	1.84	8.11
	71,500	840	1.69	8.10
	107,250	1170	1.58	8.13
	143,000	1730	1.49	8.18
FLIP-HEU	112,500	1000	2.34	8.16
	225,000	1380	2.76	8.13
	337,500	1820	3.16	8.15
	450,000	2520	3.54	8.19
FLIP-LEU-I	35,750	920	2.17	8.10
	71,500	1290	2.46	8.14
	107,250	1710	2.72	8.16
	143,000	2360	2.97	8.17
FLIP-LEU-II	36,500	1190	2.61	8.19
	73,000	1690	3.25	8.12
	109,500	2320	3.90	8.17
	146,000	3170	4.57	8.19
FFCR ACPR	35,750	670	1.84	8.11
	71,500	1020	1.80	8.16
	107,250	1420	1.75	8.15
	143,000	2100	1.74	8.16
FFCR ST1, ST2, ST3	35,750	540	1.76	8.10
	71,500	890	1.57	8.11
	107,250	1280	1.44	8.15
	143,000	1960	1.36	8.17
FFCR FLIP-LEU-I	35,750	940	2.11	8.13
	71,500	1350	2.33	8.12
	107,250	1840	2.56	8.14
	143,000	2580	2.82	8.17

Notes:
1. This dose rate represents the total NCT dose rate 2 m from the side of the vehicle using a response function developed by MCNP. This dose rate is used only to select the bounding NCT source term. The dose rates 2 m from the side of the vehicle listed in Table 5.6.3-14 are the dose rates for licensing purposes.

Table 5.6.3-5
TRIGA Bounding Gamma Source per Fuel Assembly

Upper Energy (MeV)	Fuel (γ/s)	Cladding and End Fittings (γ/s)[1]
0.045	2.839E+12	1.071E+10
0.10	9.817E+11	2.578E+09
0.20	6.465E+11	5.206E+08
0.30	1.853E+11	2.554E+07
0.40	1.305E+11	3.330E+07
0.60	9.150E+11	2.274E+06
0.80	4.304E+12	8.808E+05
1.00	4.049E+11	2.997E+09
1.33	1.004E+11	6.170E+11
1.66	3.237E+10	1.742E+11
2.00	1.115E+09	1.227E+01
2.50	3.612E+09	4.171E+06
3.00	5.550E+07	3.562E+03
4.00	4.936E+06	3.042E-14
5.00	6.390E+02	0.000E+00
6.50	2.561E+02	0.000E+00
8.00	5.020E+01	0.000E+00
10.00	1.065E+01	0.000E+00
Total	1.054E+13	8.081E+11

Notes:
1. The cladding and end fitting source includes the 1.4 factor to account for steel outside the active fuel region.

Table 5.6.3-6
TRIGA Gamma NCT Response Functions

Upper Energy (MeV)	Fuel (mrem/hr)	Cladding (mrem/hr)
0.045	0	0
0.10	0	0
0.20	0	0
0.30	0	0
0.40	0	0
0.60	3.074E-16	0
0.80	1.816E-14	0
1.00	3.125E-13	0
1.33	3.650E-12	4.334E-12
1.66	1.915E-11	2.194E-11
2.00	5.323E-11	0
2.50	1.196E-10	0
3.00	2.162E-10	0
4.00	3.634E-10	0
5.00	5.197E-10	0
6.50	6.333E-10	0
8.00	7.061E-10	0
10.00	7.605E-10	0

Table 5.6.3-7
TRIGA Total Gamma Source Strengths, per Region

Region	Steel mass (g) (A)	Flux factor (B)	Effective Steel Mass (g) (AxB)	Source Strength (1 assembly)	Source Strength (180 assemblies)
Top fitting	265	0.1	26.5	8.559E+10	1.541E+13
Top plenum	45.5	0.2	9.1	2.939E+10	5.291E+12
In-core cladding	179	1.0	179	5.781E+11	1.041E+14
Bottom plenum	45.5	0.2	9.1	2.939E+10	5.291E+12
Bottom fitting	265	0.1	26.5	8.559E+10	1.541E+13
Subtotal cladding	800	na	250	8.081E+11	1.455E+14
Fuel region	na	na	N/A	1.054E+13	1.898E+15
Total	na	na	N/A	1.135E+13	2.043E+15

Table 5.6.3-8
TRIGA Neutron Response Function

Upper Energy (MeV)	Response Function (mrem/hr)
3.04E-03	4.953E-07
1.50E-02	4.721E-07
1.11E-01	4.384E-07
4.08E-01	4.152E-07
9.07E-01	4.437E-07
1.42E+00	5.862E-07
1.83E+00	6.555E-07
3.01E+00	8.475E-07
6.38E+00	1.040E-06
2.00E+01	1.879E-06

Table 5.6.3-9
TRIGA Bounding Neutron Source per Fuel Assembly

Upper Energy (MeV)	Neutron Source (n/s)
1.00E-08	9.766E-09
3.00E-08	3.060E-08
5.00E-08	4.200E-08
1.00E-07	1.411E-07
2.25E-07	5.130E-07
3.25E-07	5.342E-07
4.14E-07	5.508E-07
8.00E-07	3.046E-06
1.00E-06	1.928E-06
1.13E-06	1.309E-06
1.30E-06	1.957E-06
1.86E-06	7.073E-06
3.06E-06	1.912E-05
1.07E-05	2.000E-04
2.90E-05	8.215E-04
1.01E-04	5.841E-03
5.83E-04	8.831E-02
3.04E-03	1.035E+00
1.50E-02	1.128E+01
1.11E-01	2.300E+02
4.08E-01	1.314E+03
9.07E-01	2.859E+03
1.42E+00	2.926E+03
1.83E+00	2.029E+03
3.01E+00	4.276E+03
6.38E+00	3.721E+03
2.00E+01	3.766E+02
Total	1.774E+04

Table 5.6.3-10
Important TN-LC-TRIGA Basket Model Dimensions

Proprietary Information Withheld Pursuant to 10 CFR 2.390.

Table 5.6.3-11
TN-LC-TRIGA NCT Side Surface Dose Rates between Impact Limiters (mrem/hr)

Location	Gamma	σ	Neutron	σ	(n,g)	σ	Total	σ
8	6.62E+01	0.3%	2.21E-01	0.5%	8.31E-03	0.6%	6.64E+01	0.3%
9	9.23E+01	0.3%	1.67E-01	0.4%	1.19E-02	0.4%	9.25E+01	0.3%
10	5.69E+01	0.3%	9.49E-02	0.5%	9.64E-03	0.5%	5.70E+01	0.3%
11	8.59E+01	0.4%	1.52E-01	0.4%	1.18E-02	0.4%	8.61E+01	0.4%
12	7.99E+01	0.4%	1.43E-01	0.5%	1.14E-02	0.4%	8.01E+01	0.4%
13	5.86E+01	0.3%	9.81E-02	0.5%	9.90E-03	0.5%	5.87E+01	0.3%
14	**9.56E+01**	**0.4%**	**1.82E-01**	**0.4%**	**1.28E-02**	**0.4%**	**9.58E+01**	**0.4%**
15	6.67E+01	0.4%	1.93E-01	0.5%	1.01E-02	0.5%	6.69E+01	0.4%
16	6.75E+01	0.3%	1.24E-01	0.5%	1.08E-02	0.4%	6.77E+01	0.3%
17	9.42E+01	0.4%	1.69E-01	0.4%	1.26E-02	0.4%	9.43E+01	0.3%
18	5.79E+01	0.3%	9.63E-02	0.5%	9.66E-03	0.5%	5.80E+01	0.3%
19	8.09E+01	0.4%	1.40E-01	0.5%	1.11E-02	0.4%	8.11E+01	0.4%
20	8.25E+01	0.4%	1.40E-01	0.5%	1.00E-02	0.4%	8.26E+01	0.4%
21	2.27E+01	0.4%	3.85E-02	0.8%	4.07E-03	0.7%	2.28E+01	0.4%
22	9.72E-01	1.6%	1.34E-02	1.6%	1.44E-03	1.3%	9.87E-01	1.6%
Shear Key	6.67E+01	0.4%	6.09E-01	1.5%	1.01E-02	0.5%	6.73E+01	0.4%

Table 5.6.3-12
TN-LC-TRIGA NCT Vehicle Underside Dose Rates (mrem/hr)

Location	Gamma	σ	Neutron	σ	(n,g)	σ	Total	σ
6[1]	2.20E+01	0.4%	2.29E-02	0.6%	1.42E-03	0.8%	2.20E+01	0.4%
7[1]	3.35E+01	0.3%	4.79E-02	0.5%	2.23E-03	0.7%	3.36E+01	0.3%
8	3.51E+01	0.3%	8.02E-02	0.4%	3.59E-03	0.5%	3.52E+01	0.3%
9	4.07E+01	0.3%	7.37E-02	0.4%	4.57E-03	0.4%	4.08E+01	0.3%
10	3.70E+01	0.3%	6.26E-02	0.3%	4.92E-03	0.4%	3.70E+01	0.3%
11	4.08E+01	0.3%	6.53E-02	0.3%	5.17E-03	0.4%	4.09E+01	0.3%
12	4.01E+01	0.3%	6.49E-02	0.3%	5.27E-03	0.4%	4.02E+01	0.3%
13	3.75E+01	0.3%	6.36E-02	0.3%	5.22E-03	0.4%	3.75E+01	0.3%
14	**4.20E+01**	**0.3%**	**7.47E-02**	**0.3%**	**5.29E-03**	**0.4%**	**4.20E+01**	**0.3%**
15	3.83E+01	0.3%	7.63E-02	0.4%	5.17E-03	0.4%	3.84E+01	0.3%
16	3.86E+01	0.3%	7.02E-02	0.4%	5.20E-03	0.4%	3.87E+01	0.3%
17	4.14E+01	0.3%	6.70E-02	0.3%	5.24E-03	0.4%	4.15E+01	0.3%
18	3.67E+01	0.3%	5.85E-02	0.3%	4.93E-03	0.4%	3.68E+01	0.3%
19	3.86E+01	0.3%	5.85E-02	0.4%	4.63E-03	0.4%	3.87E+01	0.3%
20	3.43E+01	0.4%	5.04E-02	0.4%	3.84E-03	0.5%	3.43E+01	0.4%
21	1.66E+01	0.4%	2.86E-02	0.5%	2.43E-03	0.6%	1.67E+01	0.4%
22	4.95E+00	0.6%	1.46E-02	0.7%	1.29E-03	0.8%	4.97E+00	0.6%
23[1]	8.22E-01	1.1%	7.01E-03	1.1%	5.90E-04	1.2%	8.29E-01	1.1%
24[1]	2.23E-01	1.9%	3.19E-03	1.4%	3.31E-04	1.6%	2.27E-01	1.9%
Shear Key	3.83E+01	0.3%	1.37E-01	1.5%	5.17E-03	0.4%	3.84E+01	0.3%

Notes:
1. Locations 6, 7, 23, and 24 represent the side of the impact limiters.

Table 5.6.3-13
TN-LC-TRIGA NCT Vehicle Side Dose Rates (mrem/hr)

Location	Gamma	σ	Neutron	σ	(n,g)	σ	Total	σ
6	1.42E+01	0.3%	1.58E-02	0.5%	9.08E-04	0.7%	1.42E+01	0.3%
7	1.83E+01	0.4%	2.80E-02	0.4%	1.50E-03	0.6%	1.83E+01	0.4%
8	2.12E+01	0.3%	4.03E-02	0.4%	2.16E-03	0.5%	2.12E+01	0.3%
9	2.49E+01	0.3%	4.44E-02	0.4%	2.68E-03	0.4%	2.49E+01	0.3%
10	2.55E+01	0.3%	4.34E-02	0.3%	3.01E-03	0.4%	2.55E+01	0.3%
11	2.63E+01	0.3%	4.33E-02	0.3%	3.21E-03	0.4%	2.64E+01	0.3%
12	2.66E+01	0.3%	4.37E-02	0.3%	3.34E-03	0.4%	2.66E+01	0.3%
13	2.62E+01	0.3%	4.44E-02	0.3%	3.39E-03	0.4%	2.63E+01	0.3%
14	**2.68E+01**	**0.3%**	**4.64E-02**	**0.3%**	**3.38E-03**	**0.4%**	**2.69E+01**	**0.3%**
15	2.64E+01	0.3%	4.70E-02	0.3%	3.36E-03	0.4%	2.64E+01	0.3%
16	2.62E+01	0.3%	4.56E-02	0.3%	3.33E-03	0.4%	2.62E+01	0.3%
17	2.61E+01	0.3%	4.27E-02	0.3%	3.25E-03	0.4%	2.62E+01	0.3%
18	2.51E+01	0.3%	3.92E-02	0.3%	3.05E-03	0.4%	2.51E+01	0.3%
19	2.37E+01	0.3%	3.58E-02	0.3%	2.74E-03	0.4%	2.37E+01	0.3%
20	1.97E+01	0.4%	2.96E-02	0.4%	2.30E-03	0.5%	1.97E+01	0.4%
21	1.25E+01	0.4%	2.12E-02	0.4%	1.70E-03	0.5%	1.25E+01	0.4%
22	6.16E+00	0.5%	1.33E-02	0.5%	1.15E-03	0.7%	6.17E+00	0.5%
23	2.69E+00	0.9%	7.92E-03	0.7%	7.06E-04	0.8%	2.70E+00	0.9%
24	1.07E+00	0.7%	4.57E-03	0.8%	3.98E-04	1.0%	1.07E+00	0.7%

Table 5.6.3-14
TN-LC-TRIGA NCT 2 m from Vehicle Side Dose Rates (mrem/hr)

Location	Gamma	σ	Neutron	σ	(n,g)	σ	Total	σ
1	1.14E+00	0.4%	2.26E-03	0.7%	1.69E-04	0.9%	1.14E+00	0.4%
2	1.59E+00	0.7%	2.80E-03	0.6%	2.12E-04	0.8%	1.59E+00	0.7%
3	2.19E+00	0.4%	3.52E-03	0.5%	2.61E-04	0.7%	2.19E+00	0.4%
4	2.98E+00	0.5%	4.50E-03	0.5%	3.25E-04	0.6%	2.99E+00	0.4%
5	3.67E+00	0.3%	5.70E-03	0.4%	3.92E-04	0.6%	3.68E+00	0.3%
6	4.53E+00	0.3%	7.07E-03	0.4%	4.77E-04	0.5%	4.54E+00	0.3%
7	5.31E+00	0.3%	8.46E-03	0.4%	5.46E-04	0.5%	5.32E+00	0.3%
8	5.99E+00	0.3%	9.42E-03	0.4%	6.15E-04	0.5%	6.00E+00	0.3%
9	6.63E+00	0.3%	1.04E-02	0.4%	6.70E-04	0.5%	6.64E+00	0.3%
10	7.20E+00	0.3%	1.12E-02	0.4%	7.24E-04	0.5%	7.21E+00	0.3%
11	7.66E+00	0.3%	1.19E-02	0.4%	7.58E-04	0.5%	7.67E+00	0.3%
12	8.03E+00	0.3%	1.24E-02	0.3%	8.00E-04	0.4%	8.04E+00	0.3%
13	8.21E+00	0.3%	1.26E-02	0.3%	8.18E-04	0.4%	8.22E+00	0.3%
14	**8.25E+00**	**0.3%**	**1.25E-02**	**0.3%**	**8.28E-04**	**0.4%**	**8.27E+00**	**0.3%**
15	8.18E+00	0.3%	1.24E-02	0.3%	8.26E-04	0.4%	8.20E+00	0.3%
16	7.93E+00	0.3%	1.20E-02	0.3%	8.06E-04	0.4%	7.94E+00	0.3%
17	7.58E+00	0.3%	1.14E-02	0.3%	7.78E-04	0.5%	7.59E+00	0.3%
18	7.05E+00	0.3%	1.07E-02	0.4%	7.34E-04	0.5%	7.06E+00	0.3%
19	6.38E+00	0.4%	9.81E-03	0.4%	6.93E-04	0.5%	6.39E+00	0.4%
20	5.59E+00	0.4%	8.84E-03	0.4%	6.32E-04	0.5%	5.60E+00	0.4%
21	4.69E+00	0.3%	7.81E-03	0.4%	5.78E-04	0.5%	4.69E+00	0.3%
22	3.86E+00	0.4%	6.65E-03	0.4%	5.07E-04	0.6%	3.87E+00	0.4%
23	3.08E+00	0.6%	5.68E-03	0.5%	4.44E-04	0.6%	3.09E+00	0.6%
24	2.26E+00	0.5%	4.65E-03	0.5%	3.75E-04	0.6%	2.26E+00	0.4%
25	1.56E+00	0.6%	3.61E-03	0.5%	3.03E-04	0.6%	1.57E+00	0.6%
26	1.08E+00	0.5%	2.81E-03	0.6%	2.44E-04	0.7%	1.08E+00	0.5%
27	7.72E-01	0.7%	2.18E-03	0.6%	1.94E-04	0.8%	7.74E-01	0.6%
28	5.59E-01	1.3%	1.74E-03	0.7%	1.54E-04	0.9%	5.61E-01	1.3%
29	4.12E-01	1.4%	1.38E-03	0.8%	1.23E-04	1.0%	4.13E-01	1.4%

Table 5.6.3-15
TN-LC-TRIGA NCT End Dose Rates (mrem/hr)

Location	Gamma	σ	Neutron	σ	(n,g)	σ	Total	σ
Bottom End at Impact Limiter Surface/Vehicle End Surface								
1	**3.90E+00**	**2.9%**	**4.36E-02**	**5.1%**	**1.78E-03**	**12.3%**	**3.94E+00**	**2.8%**
2	3.17E+00	1.1%	4.01E-02	1.7%	1.44E-03	3.4%	3.21E+00	1.0%
3	2.30E+00	0.9%	2.96E-02	1.2%	1.26E-03	2.2%	2.33E+00	0.9%
4	1.39E+00	0.6%	1.35E-02	0.8%	9.53E-04	1.1%	1.41E+00	0.6%
5	1.63E+00	0.7%	7.62E-03	0.8%	5.73E-04	1.1%	1.64E+00	0.7%
6	2.53E+00	0.6%	8.20E-03	0.5%	5.88E-04	0.6%	2.54E+00	0.6%
7	2.94E+00	0.5%	7.29E-03	0.4%	5.45E-04	0.6%	2.95E+00	0.4%
8	2.94E+00	0.7%	6.15E-03	0.4%	4.67E-04	0.6%	2.94E+00	0.7%
Bottom End 2 m from Impact Limiter Surface/Vehicle End Surface								
1,2,3	3.30E-01	3.0%	2.45E-03	2.2%	7.63E-05	5.2%	3.32E-01	2.9%
4,5	2.58E-01	0.6%	2.04E-03	1.0%	8.18E-05	1.8%	2.60E-01	0.6%
6	2.42E-01	1.0%	1.75E-03	0.8%	9.54E-05	1.3%	2.44E-01	1.0%
7	3.12E-01	0.5%	1.65E-03	0.6%	1.18E-04	0.9%	3.14E-01	0.5%
8	**4.15E-01**	**0.5%**	**1.69E-03**	**0.5%**	**1.37E-04**	**0.8%**	**4.17E-01**	**0.5%**
Top End at Impact Limiter Surface/Vehicle End Surface								
1	3.04E+01	2.5%	8.44E-02	4.0%	2.48E-03	10.3%	3.04E+01	2.5%
2	2.93E+01	1.6%	7.89E-02	1.4%	2.26E-03	2.7%	2.94E+01	1.6%
3	2.42E+01	1.5%	5.57E-02	1.0%	1.91E-03	1.8%	2.43E+01	1.5%
4	1.17E+01	0.9%	2.27E-02	0.7%	1.31E-03	1.0%	1.17E+01	0.9%
5	9.43E+00	0.4%	1.08E-02	0.7%	6.73E-04	1.1%	9.45E+00	0.4%
6	8.56E+00	0.4%	1.01E-02	0.5%	6.39E-04	0.7%	8.57E+00	0.4%
7	6.08E+00	0.4%	8.60E-03	0.5%	5.76E-04	0.6%	6.09E+00	0.4%
8	4.54E+00	0.4%	7.04E-03	0.5%	4.73E-04	0.6%	4.55E+00	0.4%
Port	**4.97E+01**	**1.6%**	**7.73E-02**	**8.3%**	**1.93E-03**	**19.1%**	**4.98E+01**	**1.6%**
Top End 2 m from Impact Limiter Surface/Vehicle End Surface								
1,2,3	**2.63E+00**	**2.4%**	**4.26E-03**	**2.0%**	**1.06E-04**	**4.7%**	**2.63E+00**	**2.4%**
4,5	2.00E+00	1.3%	3.53E-03	0.8%	1.09E-04	1.7%	2.01E+00	1.3%
6	1.32E+00	1.0%	2.67E-03	0.7%	1.16E-04	1.2%	1.32E+00	1.0%
7	9.94E-01	0.8%	2.24E-03	0.6%	1.31E-04	0.9%	9.96E-01	0.8%
8	9.43E-01	0.6%	2.09E-03	0.5%	1.48E-04	0.8%	9.45E-01	0.5%

Table 5.6.3-16
TN-LC-TRIGA HAC Dose Rates (mrem/hr)

Location	Gamma	σ	Neutron	σ	(n,g)	σ	Total	σ
Side								
1	1.37E+01	0.5%	5.65E-02	0.5%	2.17E-04	2.1%	1.38E+01	0.5%
2	2.80E+01	0.5%	7.93E-02	0.4%	3.02E-04	1.7%	2.81E+01	0.5%
3	6.30E+01	0.5%	1.13E-01	0.3%	4.36E-04	1.3%	6.31E+01	0.4%
4	**7.96E+01**	**0.5%**	**1.66E-01**	**0.3%**	**6.01E-04**	**1.0%**	**7.98E+01**	**0.5%**
5	6.32E+01	0.4%	2.38E-01	0.2%	8.44E-04	0.8%	6.34E+01	0.4%
6	5.14E+01	0.3%	3.09E-01	0.2%	1.07E-03	0.7%	5.17E+01	0.3%
7	5.23E+01	0.3%	3.69E-01	0.2%	1.25E-03	0.7%	5.27E+01	0.3%
8	5.10E+01	0.3%	4.11E-01	0.2%	1.41E-03	0.6%	5.14E+01	0.3%
9	5.10E+01	0.3%	4.38E-01	0.2%	1.49E-03	0.6%	5.15E+01	0.3%
10	5.10E+01	0.3%	4.53E-01	0.1%	1.55E-03	0.6%	5.15E+01	0.3%
11	5.05E+01	0.3%	4.59E-01	0.1%	1.58E-03	0.6%	5.10E+01	0.3%
12	5.12E+01	0.3%	4.59E-01	0.1%	1.57E-03	0.6%	5.16E+01	0.3%
13	5.06E+01	0.3%	4.55E-01	0.1%	1.57E-03	0.6%	5.11E+01	0.3%
14	5.01E+01	0.3%	4.49E-01	0.1%	1.55E-03	0.6%	5.06E+01	0.3%
15	4.96E+01	0.3%	4.37E-01	0.1%	1.49E-03	0.6%	5.00E+01	0.3%
16	4.77E+01	0.3%	4.15E-01	0.2%	1.42E-03	0.6%	4.81E+01	0.3%
17	4.47E+01	0.3%	3.80E-01	0.2%	1.27E-03	0.7%	4.51E+01	0.3%
18	3.85E+01	0.4%	3.27E-01	0.2%	1.11E-03	0.7%	3.88E+01	0.4%
19	2.75E+01	0.4%	2.63E-01	0.2%	9.03E-04	0.8%	2.78E+01	0.4%
20	1.67E+01	0.5%	1.95E-01	0.2%	6.93E-04	1.0%	1.69E+01	0.4%
21	9.00E+00	0.8%	1.38E-01	0.3%	4.98E-04	1.2%	9.14E+00	0.8%
22	4.72E+00	0.9%	9.37E-02	0.4%	3.54E-04	1.5%	4.81E+00	0.9%
23	2.52E+00	1.1%	6.36E-02	0.5%	2.41E-04	1.9%	2.58E+00	1.1%
24	1.46E+00	0.9%	4.32E-02	0.6%	1.68E-04	2.5%	1.50E+00	0.9%
25	9.14E-01	1.2%	3.04E-02	0.8%	1.26E-04	3.1%	9.45E-01	1.2%
Bottom End								
1	**5.12E-01**	**5.7%**	**1.04E-02**	**2.0%**	**2.94E-05**	**8.9%**	**5.23E-01**	**5.6%**
2	3.85E-01	2.6%	1.28E-02	1.0%	4.28E-05	4.0%	3.97E-01	2.5%
3	4.95E-01	1.2%	2.01E-02	0.5%	7.13E-05	2.2%	5.15E-01	1.2%
Top End								
1	**1.29E+01**	**2.7%**	**4.65E-02**	**1.0%**	**1.61E-04**	**4.0%**	**1.30E+01**	**2.7%**
2	9.87E+00	1.1%	4.29E-02	0.5%	1.58E-04	2.1%	9.91E+00	1.1%
3	9.05E+00	0.5%	4.48E-02	0.4%	1.69E-04	1.4%	9.10E+00	0.5%

Table 5.6.3-17
TRIGA Fuel Qualification Linear Interpolation Factors

Type	Burnup (MWd/MTU)	Cooling time (d)	Linear Interpolation (y=Kx+L)	
			K	L
ACPR	35,750-71,500	650-970	0.0090	330
	71,500-107,250	970-1310	0.0095	290
	107,250-143,000	1310-1870	0.0157	-370
AL14, AL15	35,750-71,500	400-560	0.0045	240
	71,500-107,250	560-640	0.0022	400
	107,250-143,000	640-710	0.0020	430
ST1, ST2, ST3	35,750-71,500	520-840	0.0090	200
	71,500-107,250	840-1170	0.0092	180
	107,250-143,000	1170-1730	0.0157	-510
FLIP-HEU	112,500-225,000	1000-1380	0.0034	620
	225,000-337,000	1380-1820	0.0039	496
	337,000-450,000	1820-2520	0.0062	-268
FLIP-LEU-I	35,750-71,500	920-1290	0.0103	550
	71,500-107,250	1290-1710	0.0117	450
	107,250-143,000	1710-2360	0.0182	-240
FLIP-LEU-II	36,500-73,000	1190-1690	0.0140	690
	73,000-109,500	1690-2320	0.0176	430
	109,500-146,000	2320-3170	0.0238	-230
FFCR ACPR	35,750-71,500	670-1020	0.0098	320
	71,500-107,250	1020-1420	0.0112	220
	107,250-143,000	1420-2100	0.0190	-620
FFCR ST1, ST2, ST3	35,750-71,500	540-890	0.0098	190
	71,500-107,250	890-1280	0.0109	110
	107,250-143,000	1280-1960	0.0190	-760
FFCR FLIP-LEU-I	35,750-71,500	940-1350	0.0115	530
	71,500-107,250	1350-1840	0.0137	370
	107,250-143,000	1840-2580	0.0207	-380

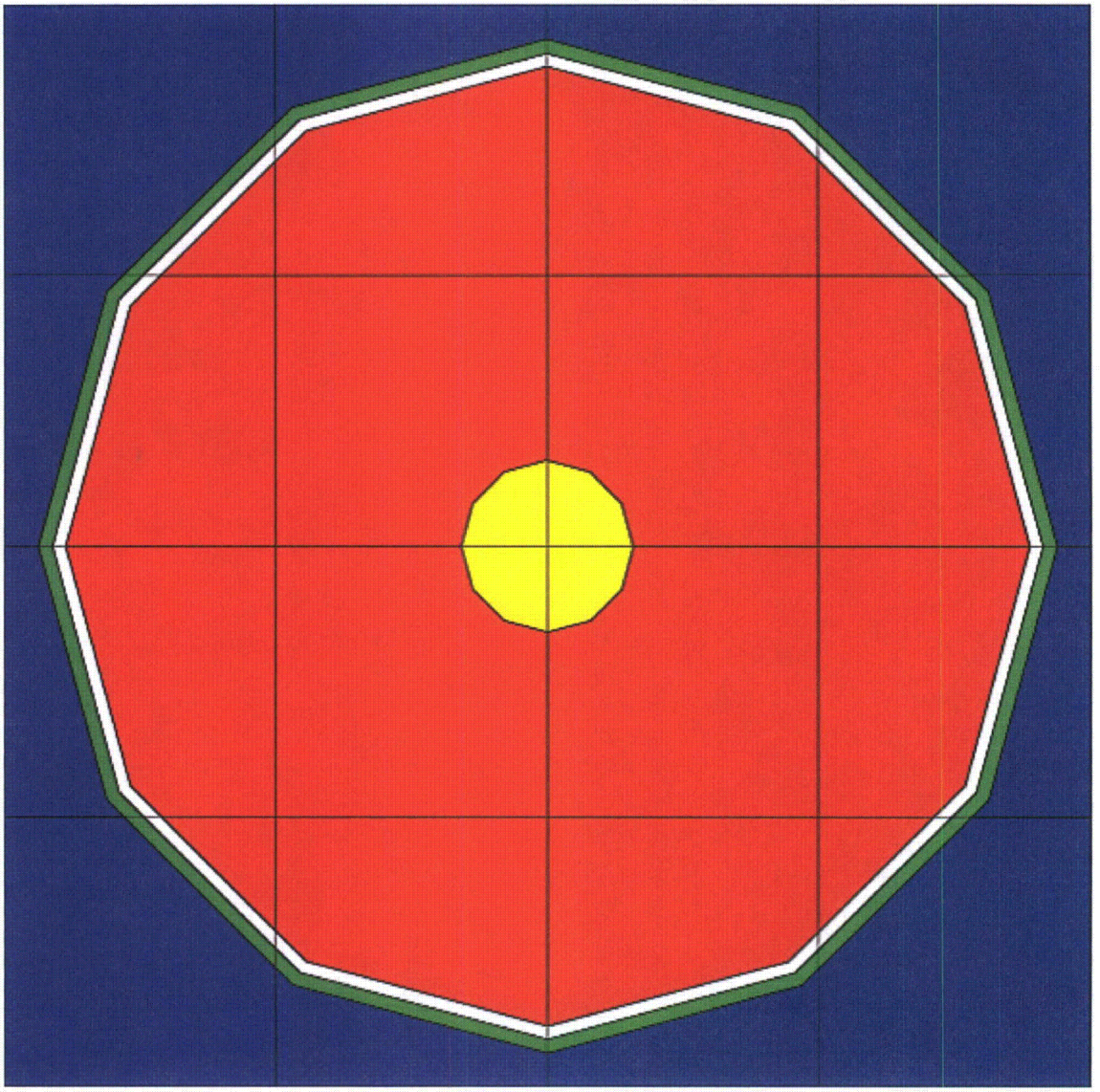

Figure 5.6.3-1
TRITON ACPR TRIGA Assembly Model

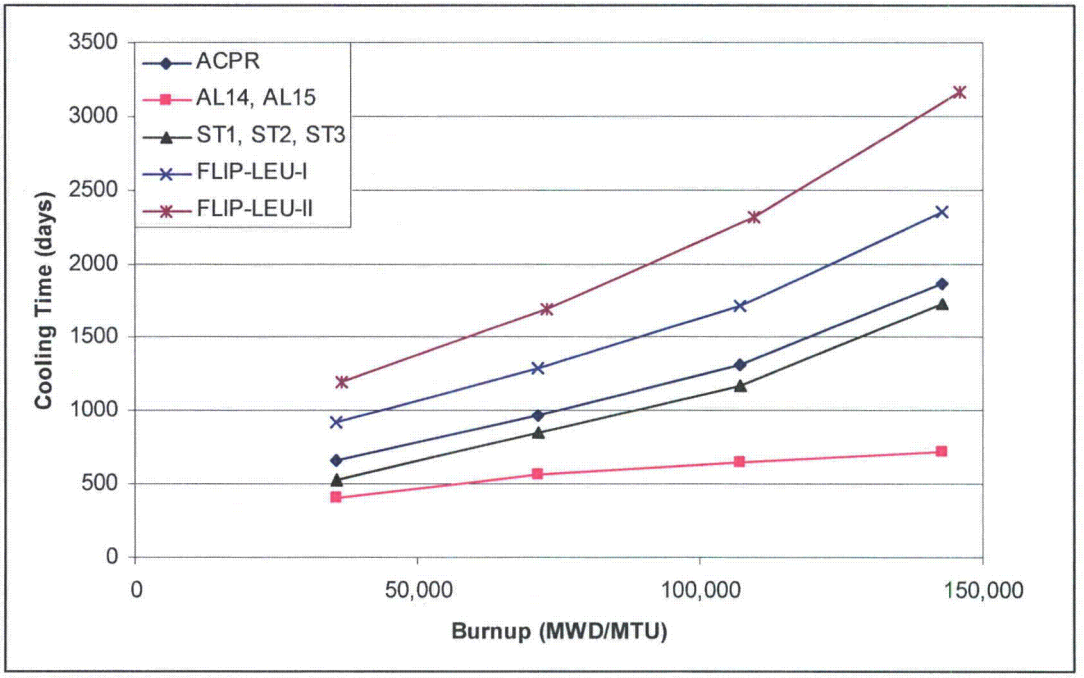

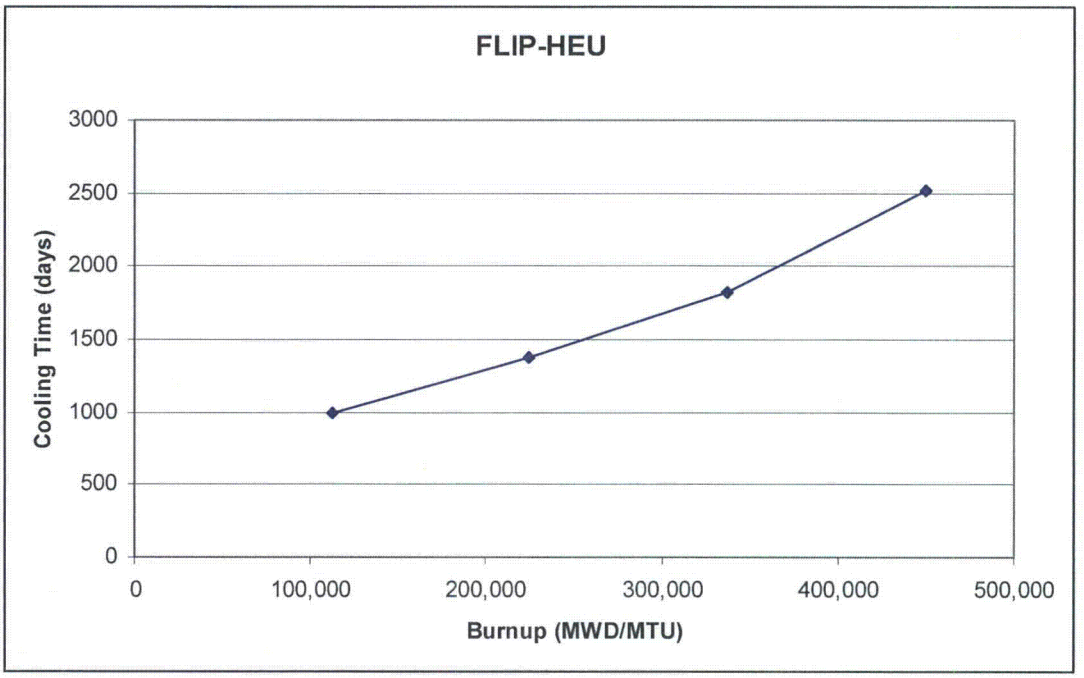

Figure 5.6.3-2
TRIGA Cooling Time Plots

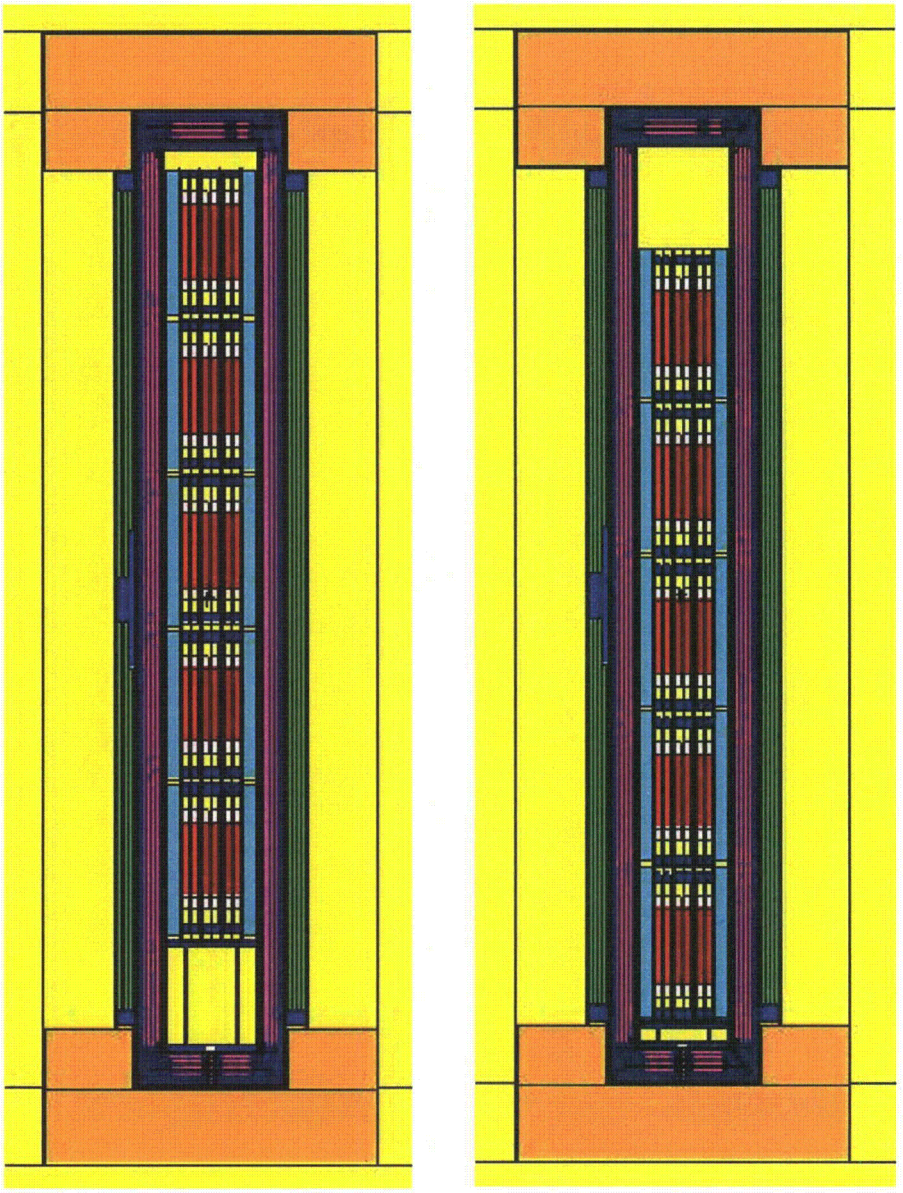

Configuration 1 Configuration 2

Figure 5.6.3-3
TN-LC-TRIGA MCNP Model, y-z View

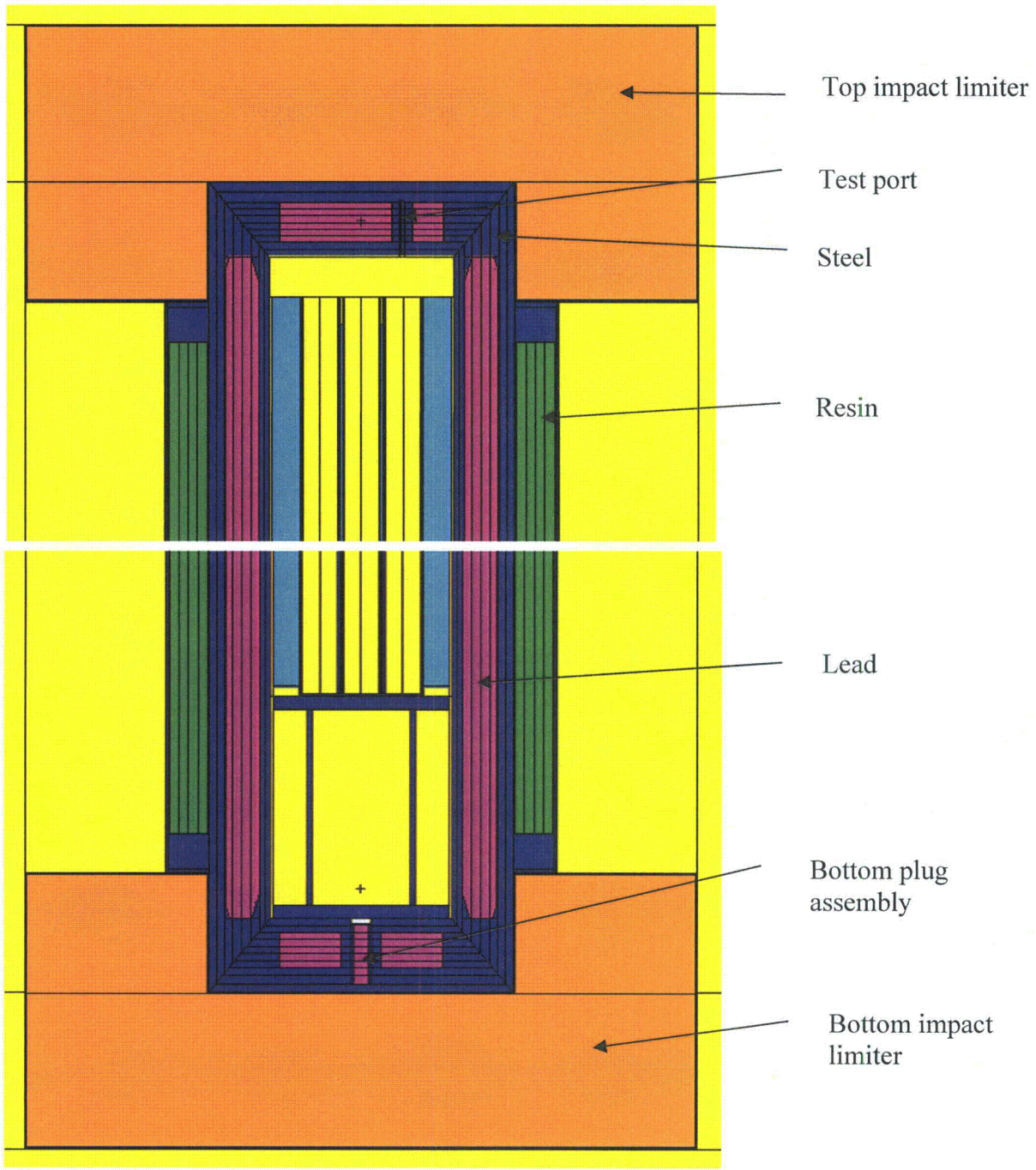

Figure 5.6.3-4
TN-LC-TRIGA MCNP Model, Close-up y-z View

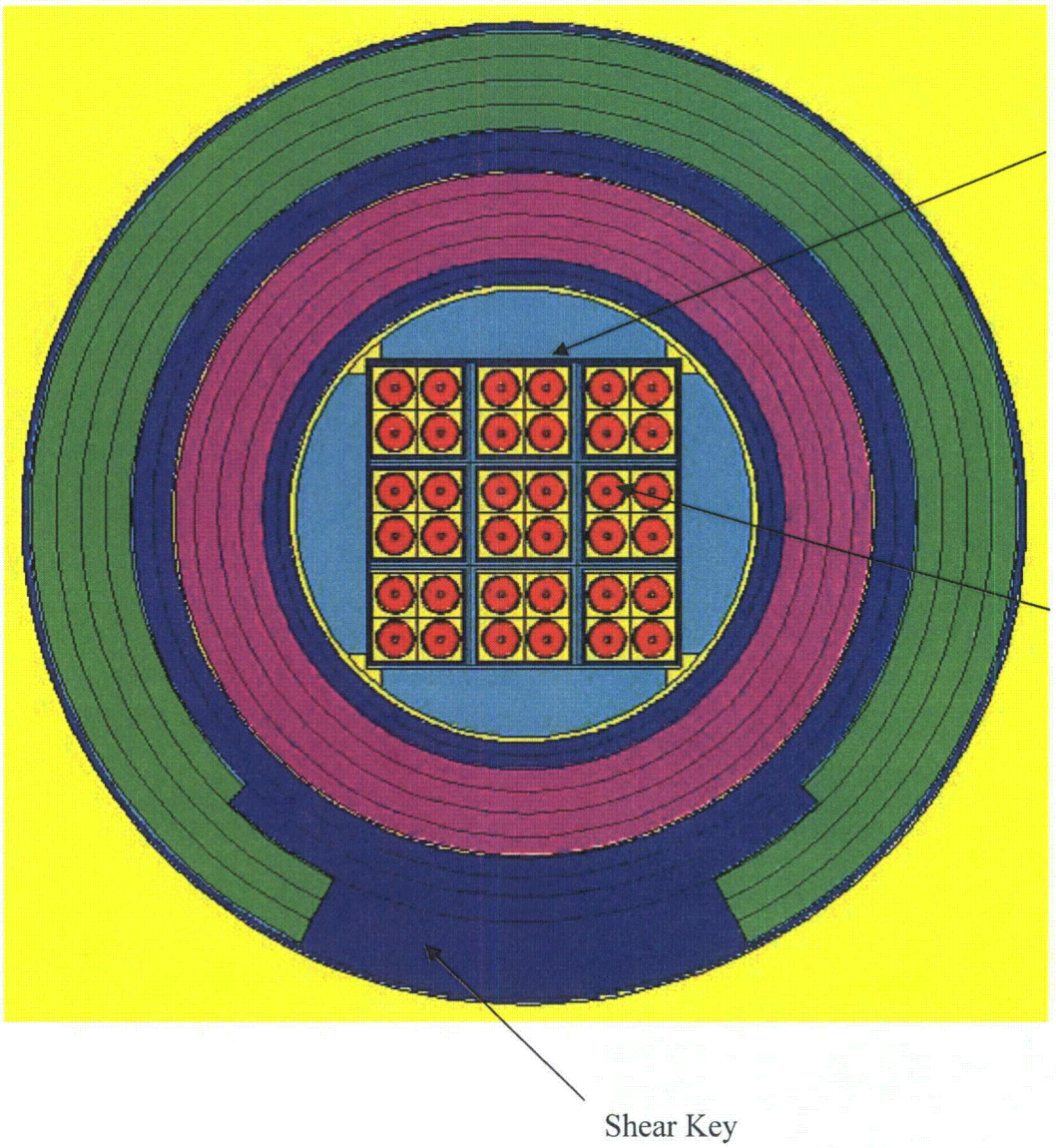

Figure 5.6.3-5
TN-LC-TRIGA MCNP Model, x-y View through Shear Key

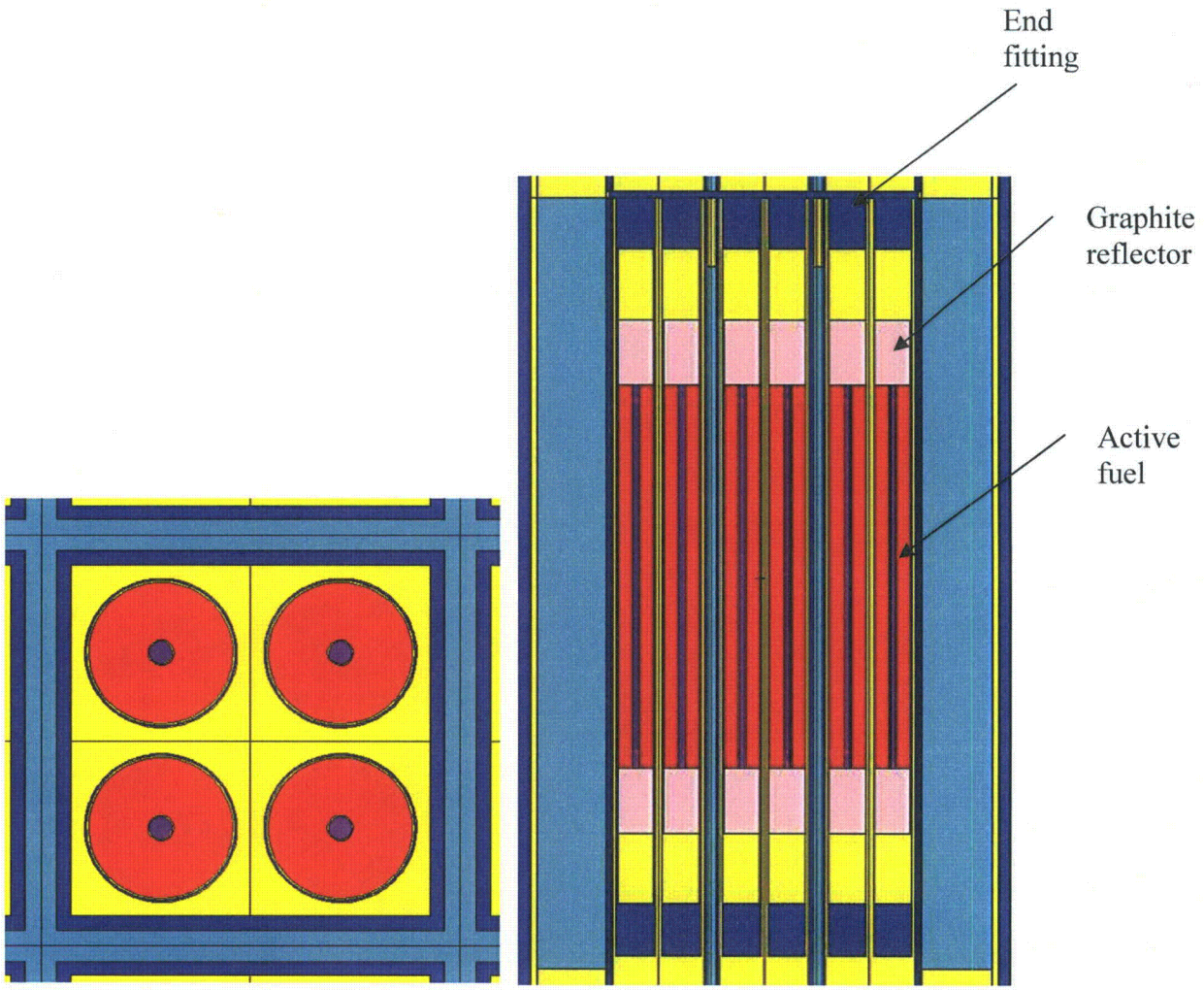

Figure 5.6.3-6
TRIGA Fuel Model

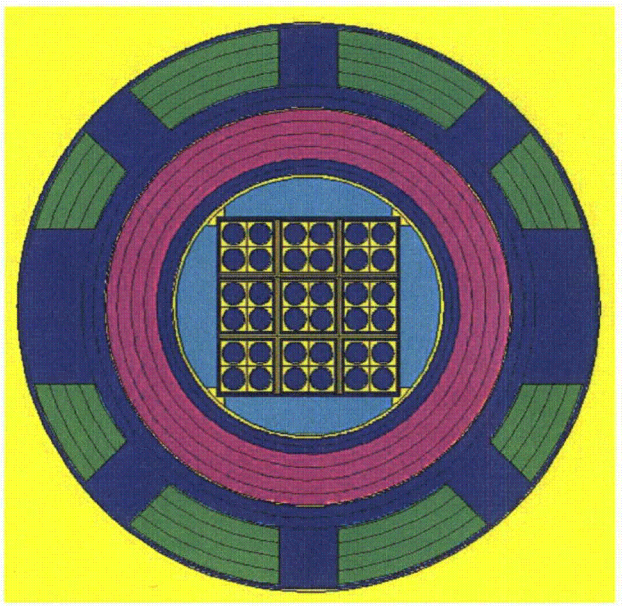

Top of Cask

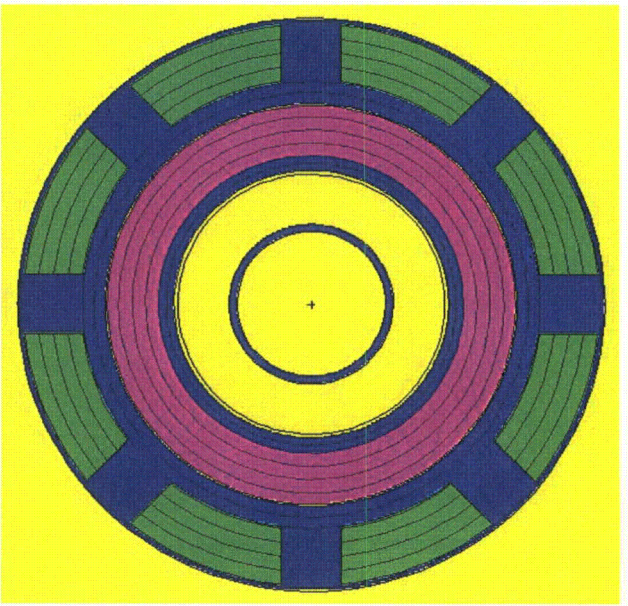

Bottom of Cask

Figure 5.6.3-7
TN-LC-TRIGA MCNP Model, x-y View through Impact Limiter Attachment Blocks

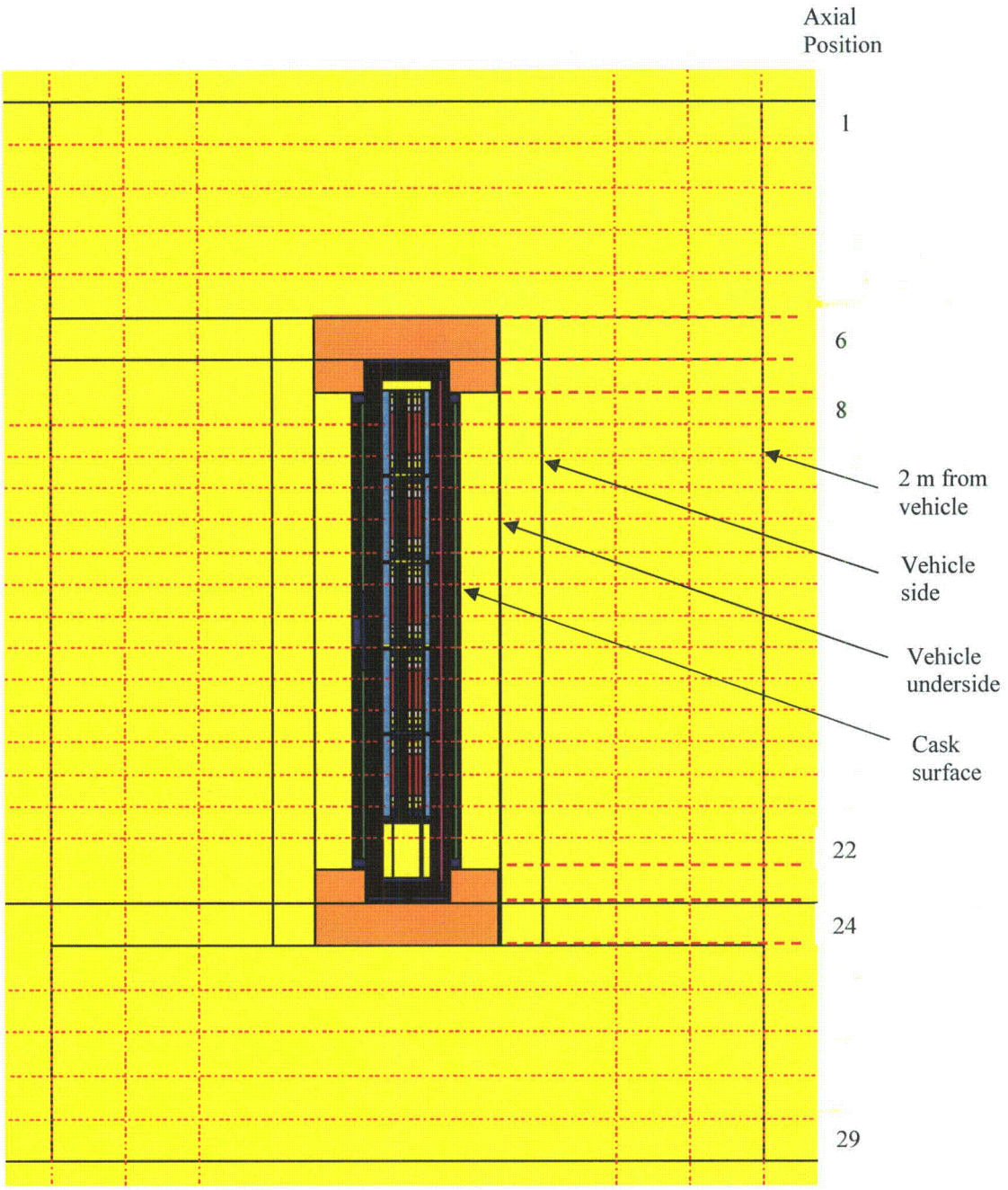

Figure 5.6.3-8
TN-LC-TRIGA NCT Radial Surface Tallies

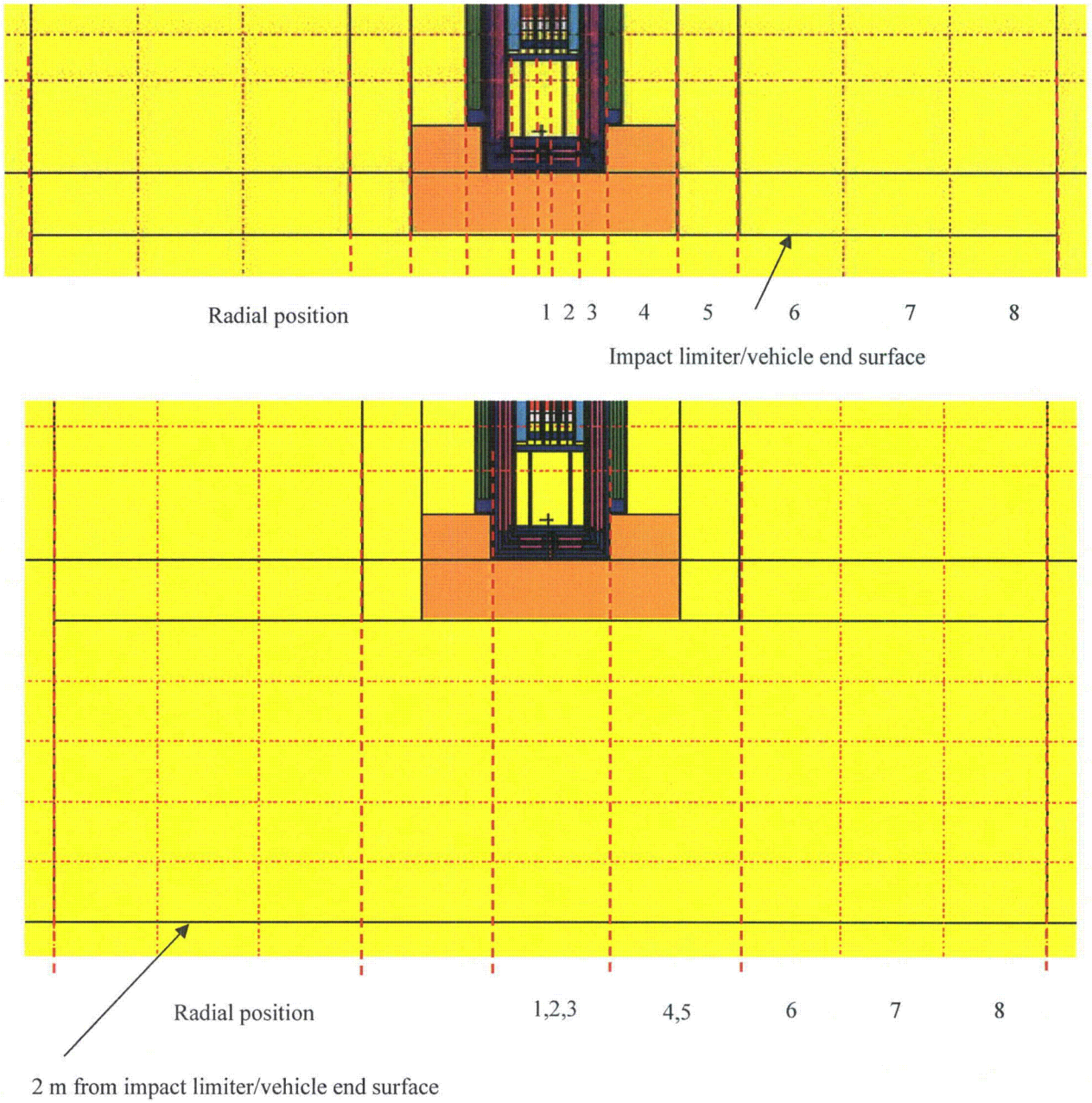

Figure 5.6.3-9
TN-LC-TRIGA NCT End Surface Tallies

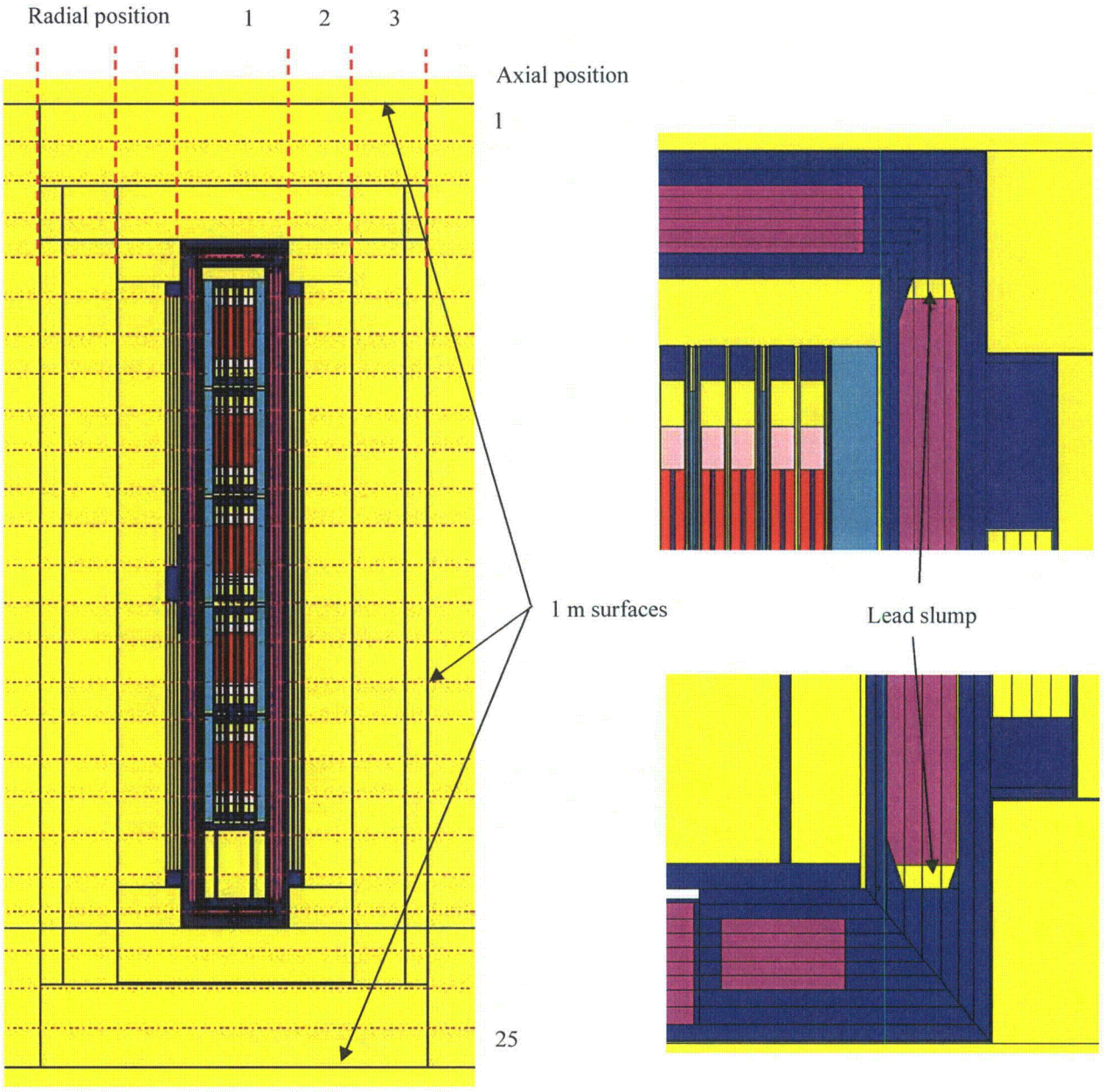

Figure 5.6.3-10
TN-LC-TRIGA HAC 1 m Tallies